National Chiao-Tung University PhD Dissertation

國立交通大學博士學位論文

Regulation of Two-component Systems in the Polymyxin B Resistance and Capsular Polysaccharide Biosynthesis in *Klebsiella pneumoniae* CG43

克雷白氏肺炎桿菌 CG43 雙分子系統與多黏菌素 B 抗性及莢膜多醣體生合成之調控

生物科技學系

博士班

學生：鄭新耀（9229506）

Student：Hsin-Yao Cheng

指導教授：彭慧玲博士

Advisor：Hwei-Ling Peng, Ph. D.

中華民國九十九年九月

September, 2010

謝誌 (Acknowledgement)

博士班生涯結束的此刻，並沒有預期的喜悅，也許稍稍被迎接未來挑戰的壓力沖淡了，但我想更多是內心深處的捨不得。這個結束象徵著另一個開始，在我跨步邁進之前，僅以生澀已久的字語，為這段永難磨滅的記憶寫下註腳。

研究的過程往往幽暗未知，而無數良師益友們的鼓勵與支持，讓我有繼續走下去的勇氣。這些年來始終最感激的，還是指導教授彭慧玲老師。學識上，彭老師提供豐富的資源與寬廣的空間，使我彷彿感到自己沒有極限；彭老師更替我留心相關研討會訊息，使我有機會認識許多同領域甚至不同領域的學者，拓展研究思考的觀點。生活上，彭老師親切地帶我度過研究生涯的適應期，躊躇時指引我研究的方向，犯錯時不吝寬容的原諒，心情低落時帶我走出悲傷的氛圍。彭老師在經濟方面的協助，使我可以心無旁騖的進行研究，學術論文與研究計畫書撰寫上，更是仔細引導，讓駑頓的我逐步摸索，修正錯誤。在學術與生活上，我何其幸運可以接受彭老師的指導，老師謝謝您！

感謝清大分醫所的張晃猷老師，張老師淵博的學識與豐富研究經驗，一直在我的研究生涯中扮演不可或缺的助力，論文及計畫書寫作的指導更讓我獲益良多，擔任資格考、非論文資格考及畢業口試委員時，總能確切地指出我的不足之處，讓我在深入探討課題時能有適當的反思，張老師學者的風範將是我研究生涯努力的目標。此外更要感謝張老師實驗室學姊與學弟妹持續的關心與支持。謝謝在中山醫學大學任教的怡琪學姊，提供實驗設計與論文寫作上的最佳楷模，感謝親切與我討論實驗並熱心提供協助的婕琳、莉芳與韻如學姊，此外實驗室學弟妹蕙如、Manish、幸瑜、漢聲與欣瑜，你們的陪伴使我獲得堅持的勇氣。

感謝生科所楊昀良老師，大學時修習楊老師的課程，便感受到楊老師深厚的學識與獨特的親和力。直至研究所資格考、非論文資格考及畢業口試，這份親和力伴隨深入中肯的見解，不僅消弭報告的緊張感，更使我融入學術討論的樂趣。論文的仔細修改與列舉的小問題，使我體認楊老師細心嚴謹的治學態度，並對往後的生涯有更高的期許。

感謝生科所林志生老師，林老師的課程自大學起就使我獲益良多，研究所時互動的上課模式與課堂中的腦力激盪，使我無形中增長許多知識。研究所資格考、非論文資格考及畢業口試，林老師以各種觀點給予的寶貴建議，不僅豐富論文，更拓展研究的格局。林老師鉅細靡遺地閱讀論文，並對於資料呈現的格式提供許多建議，使我得以改善論文中諸多錯誤，對此深表感謝。除此之外，林老師對於學術環境現實面的懇切提醒，也讓我對未來的挑戰有更深入的體認與心理準備。我瞭解並會永遠珍惜老師的諄諄教誨，老師謝謝您！

感謝中興大學鄧文玲老師，除豐富的微生物學與分子技術的背景外，鄧老師在討論時讓我感覺更像親切的實驗室學姊。在口試場合對於實驗結果的討論，往往讓我學得比報告前更多，特別是爽朗的笑聲與機敏的反應，在談笑風生之間增長我的見聞。鄧老師熱情與謹慎並存的態度，與論文修改的貼心提醒，讓我體會懂得並享受研究的樂趣。

感謝中研院陳金榜老師，陳老師在蛋白質結構的豐富研究成果，讓我獲益良多。同時也感謝陳老師實驗室的博士班研究生羅世奇，在多次的討論中，使我對 PmrD 蛋白質結構與功能相關性有更進一步的

認識，並激發許多研究的靈感。

在新竹的實驗室曾幾何時成了我第二個家，感謝這難得的緣分讓我認識實驗室的大家。感謝盈璁學長，認真細心地指導還是專題生、懵懂的我，為我的研究生活鋪下第一塊磚；感謝定宇、平輝學長在剛進入實驗室的初期，耐心教導我實驗技巧；感謝靖婷學姊帶領我進入雙分子系統的研究領域，也讓我熟悉分子生物學的工具；感謝盈蓉學姊看著我完成大學部專題到博士班畢業，無論實驗技巧、思考邏輯、寫作要領，都在學姊身上學到很多，學姊散發的活力與熱情，總是能讓四周的人快樂起來；婉君學姊爽朗的笑聲與熱心的指導；珮瑄學姊美妙的歌喉、好吃的義大利麵料理與驚人的工作量；騰逸學長，怡欣、巧韻、致翔學姊等親切的照顧，都是我充滿感恩的記憶；從大學開始就是同學的祐俊，那黝黑外表下的細心讓我記憶深刻；認識十一年的健誠，除了驚人歌喉、細緻的陶藝巧手，更在許多實驗討論中與我分享嶄新的想法，在實驗設計操作上的嚴謹態度與整理報告的功力令我望塵莫及；聰明努力的智凱，與我分享許多小說心得、認真踏實的育聖、兼具美貌與智慧的心瑋；酷酷的南台灣帥哥格維、與我一起展開暑假游泳減肥計畫的登魁、內向的朝陽；溫柔中帶著堅強的實驗室生力軍靜柔、外表粗獷做起實驗又格外細心的秉熹、運動型的正妹研究生嘉怡、氣質彬彬頗有骨感的承哲；剛進實驗室時幾乎被我拎在身上的顗峰與雅雯，看著你們成長進步，身為直屬學長的我倍感欣慰；努力學習的志桓，你認真的態度是每個人的榜樣、優雅如貴婦的純珊，讓我知道新竹有很多好吃的簡餐店；甜美中帶點鄉土味的佩君、剛柔並濟認真負責的家華，直升博班的哲充；網拍美少女品瑄與崴云、看起來總是有實驗後疲態的豪君；眼神中帶點憂鬱的舉豪、譽為彭家趙又廷的帥哥力成、圓圓肚子漸漸消失的郁勝；專題生佳融、宗穎、冠維、Stephanie (You'll become really somebody!)，你們都是我難以割捨的回憶。

謝謝吳東昆老師實驗室的程翔學長、媛婷學姊在實驗上的照顧與幫忙，以及最後論文撰寫的建議；謝謝晉豪、晉源，實驗上慷慨的協助。謝謝廖光文老師實驗室的昱丞學弟，畢業的志豪、國領學長陪我打球聊天，感謝同樣身為博士班研究生的存操、羿喬，彼此互相的鼓勵打氣。謝謝所辦小姐淑卿、佳文、聖鈴、珍佑長久以來的幫忙。

謝謝我的十幾年來的好朋友仕賢、建宏、威任、佳穎、佩芳、佳翰、柄宏，在我失意的時候陪我喝酒聊天，看電影吃美食抒發情緒，讓我可以適當轉換心情，繼續進行研究。

最後要感謝我的家人，在天堂的奶奶與外婆，我多麼希望與妳們分享這份喜悅；感謝我的老爸老媽，還有可愛活潑的妹妹伊芳，如果沒有你們的全力支持，我想我無法走到這裡。你們的支持像一股不滅的能量，使我努力的小小火花化為燦爛的光芒。僅以這微小的榮耀，獻給永遠難以替代的你們。

新耀

2010/9/28

論文摘要

克雷白氏肺炎桿菌是臨床上一種重要的病原菌，常造成伺機性感染，包含尿道感染、肺炎、化膿性感染、原發性肝膿瘍及敗血症等。隨著多重抗藥菌株的產生與散佈，改善目前治療方式，並深入瞭解其致病機轉顯得刻不容緩。為適應環境改變，病原菌常藉由雙分子系統調控並適當表現其毒性因子。雙分子系統 (two-component system; 2CS) 由位於細胞內膜的感應蛋白及細胞質內的反應調控蛋白組成。本論文著重探討克雷白氏菌中雙分子系統 PhoP/PhoQ、PmrA/PmrB、RstA/RstB 及 RcsCDB 於其毒性因子的調控。

多黏菌素為近年重新評估使用的藥物之一，沙門氏菌中 PhoP/PhoQ, PmrA/PmrB 及 PmrD 蛋白質共同調控多黏菌素 B 之抗性，為瞭解克雷白氏菌中多黏菌素 B 抗性的機轉，我們對可能參與的基因進行突變。結果顯示，相對於參與莢膜多醣體生合成基因，合成 PmrF、PhoP、PmrA、PmrD 等參與脂多醣修飾及調控蛋白之基因缺損，會使克雷白氏菌多黏菌素 B 抗性有較顯著的降低。藉由 LacZ 報導基因及 DNA 電泳遲滯實驗 (electrophoretic mobility shift assay)，我們發現 *pmrD* 基因表現受到 PhoP 的直接活化，細菌雙雜合實驗 (bacterial two-hybrid analysis) 也證明 PmrD 與 PmrA 在細菌體內的交互作用，另外藉由磷酸根傳遞分析 (phosphotransfer assay) 與激酶/去磷酸酶實驗 (kinase/phosphatase assay) 更指出，此交互作用可防止感應蛋白 PmrB 對 PmrA 的去磷酸化。這些結果顯示克雷白氏菌 PmrD 扮演了連結雙分子系統 PhoP/PhoQ 及 PmrA/PmrB 的角色。進一步藉由點突變方式，我們在 15 個所選擇的 PmrD 殘基中，發現 9 個改變為丙氨酸後對多黏菌素抗性有顯著影響，顯示這些氨基酸序列可能在 PmrD 與 PmrA 交互作用扮演重要角色。

為瞭解克雷白氏菌 RstA/RstB 之調控，我們利用 LacZ 報導基因證明 PhoP 及 RstA 可正向調控 *rstA* 基因表現。此外利用克雷白氏菌野生株與 *rstA* 基因缺損株 cDNA 進行刪除雜交法 (subtractive cDNA hybridization)，我們搜尋到 11 個可能受到 RstA 活化及 19 個可能受到 RstA 抑制的基因，結果顯示 RstA/RstB 可能參與調控鐵分子的運送、攝取以及重金屬鉛之抗性；然而針對野生株、*rstA*、*rstB* 以及 *rstArstB* 基因缺損突變株進行表型比較，顯示 *rstA* 或 *rstB* 基因缺損對於細菌在含鐵或缺鐵環境的生長、螯鐵分子生合成 (siderophore biosynthesis)、重金屬鉛抗性、酸性環境適應性或膽鹽抗性均沒有顯著影響，顯示克雷白氏菌中 RstA/RstB 的功能仍待釐清。

除雙分子系統 RcsCDB 之外，克雷白氏菌 K2 莢膜多醣體生合成亦受到轉錄因子

RmpA2 的調控。在克雷白氏菌 CG43 大型毒性質體 pLVPK 序列中，我們發現另一個黏性分子基因 *rmpA*。分析 *rmpA* 基因缺損株與 *rmpA* 回補菌株，我們發現 RmpA 可能與 RcsB 共同活化莢膜多醣體生合成。藉由細菌雙雜合實驗及免疫共沈澱分析，顯示 RmpA 與可與 RcsB 交互作用。此外藉由 LacZ 報導基因、DNA 電泳遲滯實驗、有限稀釋反轉錄聚合酶連鎖反應 (limiting-dilution RT-PCR) 及 *fur* 基因缺損株表型的分析，我們發現 *rmpA* 基因表現受到鐵離子攝取調控蛋白 Fur 抑制，顯示莢膜多醣體生合成與鐵離子攝取在克雷白氏菌致病過程中可能存在交互作用。

綜合以上所述，本論文探討克雷白氏菌雙分子系統兩種調控方式：一種可藉由連結蛋白 PmrD 與反應調控蛋白 PmrA 相互作用，達成其轉譯後修飾來活化下游多黏菌素 B 抗性基因表現；另一種則包含反應調控蛋白 RcsB 與其協助分子 RmpA 之共同作用，藉以活化莢膜多醣體生合成。這些結果暗示在不同環境下，克雷白氏菌可藉由許多有彈性及效率的方式調控其致病因子表現。

Thesis Abstract

Klebsiella pneumoniae, an important opportunistic pathogen, causes urinary tract infections, pneumonia, purulent infections, primary liver abscess and septicemia. The emergence and wide-spread of multiresistant strains has urged the improvement of current therapeutic strategies and a deeper understanding of its pathogenesis. Pathogenic bacteria usually utilize two-component systems (2CSs), consisting of an inner membrane sensor kinase and a cytoplasmic response regulator, to modulate the expression of virulence factors in response to environmental stimuli. The objectives of this dissertation were to investigate the functional role and regulation of 2CSs PhoP/PhoQ, PmrA/PmrB, RstA/RstB and RcsCDB in *K. pneumoniae* virulence determinants.

The 2CSs PhoP/PhoQ, PmrA/PmrB and a small protein PmrD regulated *Salmonella enterica* resistance to polymyxin B, one of the reevaluated antimicrobial agents. To investigate the regulation of polymyxin B resistance in *K. pneumoniae*, mutation effects of the genetic determinants likely involved in the resistance were investigated. Compared with the deletion of the genes involved in capsular polysaccharide (CPS) biosynthesis, the deletion of *pmrF*, *phoP*, *pmrA* or *pmrD* encoding the proteins participated in the lipopolysaccharide modifications or regulation resulted in a significantly reduced resistance. Through LacZ reporter assay and DNA electrophoretic mobility shift assay (EMSA), we have found that the expression of *pmrD* was directly activated by PhoP. Bacterial two-hybrid analysis has indicated an *in vivo* interaction between PmrD and PmrA. As illustrated by *in vitro* phosphotransfer assay and kinase/phosphatase assay, such an interaction could protect PmrA from the dephosphorylation by its cognate sensor protein PmrB. The results suggest a role of *Klebsiella* PmrD in connecting 2CSs PhoP/PhoQ and PmrA/PmrB. By point mutation strategy, 9 of the 15 selected residues on PmrD were shown to be critically involved in the polymyxin B resistance implying these residues are required for PmrD/PmrA interaction.

To characterize the 2CS RstA/RstB in *K. pneumoniae*, LacZ reporter assay conducted indicated a positive regulatory role of PhoP and RstA on the expression of *rstA*. Subtractive hybridization of the cDNA from the parental strain and isogenic Δ*rstA* mutant has led to the identification of 11 RstA-activated genes and 19 RstA-repressed genes involved in various cellular functions, such as iron transport/uptake and lead resistance. Comparative phenotype analysis of the wild-type strain, Δ*rstA*, Δ*rstB* and Δ*rstA*Δ*rstB* mutants, however, showed that the deletion of *rstA* or *rstB* had no apparent effects on the growth under iron-depletion or

-repletion conditions, siderophore biosynthesis, lead resistance, acid stress response or the resistance to bile salts, indicating that the functional role of RstA/RstB in *K. pneumoniae* remained to be clarified.

In addition to the 2CS RcsCDB, *K. pneumoniae* K2 CPS biosynthesis was also regulated by the transcription factor RmpA2. Sequence analysis of pLVPK in *K. pneumoniae* CG43 has revealed *rmpA*, another mucoid factor encoding gene. Phenotype analysis of the *rmpA* deletion mutant and the complemented strain has implied that RmpA activated K2 CPS biosynthesis through an cooperation with RcsB. Both bacterial two-hybrid analysis and co-immunoprecipitation have further confirmed RmpA/RcsB interaction. Besides, through LacZ reporter assay, DNA EMSA, limiting-dilution PCR and phenotype analysis of Δ*fur* mutant strain, we have shown that the expression of *rmpA* was negatively regulated by Fur, the global ferric ion uptake regulator. The results indicated the interplay between capsular polysaccharide biosynthesis and iron uptake in *K. pneumoniae* pathogenesis.

In summary, two modes of 2CS regulation in *K. pneumoniae* were investigated in this dissertation: one regarding the interaction between the connector protein PmrD and PmrA, resulting in a post-translational modification to enhance the expression of downstream genes involved in polymyxin B resistance; the other comprising the cooperation between the response regulator RcsB and its accessory factor RmpA for the activation of the K2 CPS biosynthesis. The findings indicated that under different environmental conditions, *K. pneumoniae* could regulate the expression of its virulence determinants in a versatile and efficient manner.

Table of Contents

List of Tables

List of Figures

Abbreviations

2CS(s)	two-component system(s)
bp(s)	base pair(s)
AMV	avian myeloblastosis virus
AP(s)	antimicrobial peptide(s)
CPS	capsular polysaccharide
CFU	colony forming unit
EDTA	ethylenediaminetetraacetic acid
ESBL	extended-spectrum β-lactamase
EMSA	electrophoretic mobility shift assay
HDTMA	hexadecyltrimethylammonium bromide
Hpt	histidine-containing phosphotransfer
HV	hypermucoviscosity
IPTG	isopropyl 1-thio-β-$_D$-galactopyranoside
kb	kilobase(s)
kDa	kilodalton(s)
LB	Luria-Bertani
μg	microgram
mL	mililiter
μL	microliter
mM	milimolar
μM	micromolar
MOPS	3-(N-morpholino)hpropanesulfonic acid
ng	nanogram
OD	optical density
ONPG	o-nitrophenyl-β-$_D$-galactopyranoside
PAGE	polyacrylamide gel electrophoresis
PAI	pathogenecity island
PIPES	piperazine-N,N'-bis(2-ethanesulfonic acid)
PLA	pyogenic liver abscess
rpm	revolutions per minutes
RT	reverse transcriptase
SDS	sodium dodecyl sulfate
X-gal	5-bromo-4-chloro-3-indolyl-β-$_D$-galactopyranoside

CHAPTER 1

General Introduction

1.1 *Klebsiella pneumoniae*

Klebsiella pneumoniae is a rod-shaped, non-motile, heavily-encapsulated gram-negative bacterium belonging to the *Enterobacteriaceae*. The *Klebsiella* spp. are ubiquitous in nature, with two plausible habitats: one is the surface water, soil, sewage and the plants (9, 25, 58, 157, 212), and other is the mucosal surfaces of animal hosts including humans, whereas two common habitats in humans are nasopharynx and the intestinal tract (196).

1.1.1 Virulence factors of *K. pneumoniae*

The factors contributing to *K. pneumoniae* pathogenesis include capsular polysaccharide (CPS), lipopolysaccharide (LPS), iron acquisition systems and adhesion factors. Clinically isolated *K. pneumoniae* usually produces large amounts of capsular polysaccharide (CPS) and therefore forms large glistering colonies with viscid consistency. As a major virulence factor, CPS acts to protect the bacteria from phagocytosis, from killing by polymorphonuclear granulocytes and from killing by bactericidal serum factors (62, 70, 143). Besides the physical hindrance to fimbrial binding, the role of *Klebsiella* CPS in mediating the bacterial resistance to antimicrobial peptides has also been reported (30, 150). *K. pneumoniae* strains expressing K1 and K2 CPS are the most virulent to mice (167). In addition to the 77 serotypes distinguished, a new K serotype has been identified recently (186). Most recently, the hypermucoviscosity (HV) phenotype of *K. pneumoniae* isolates resulting from a profound expression of CPS has also been correlated with the development of invasive syndrome (137).

The LPS O-antigen and the lipid A are responsible for the resistance to serum factors and the establishment of septic shock (62, 160). The adhesion factors, including the type 1 (223, 225, 226) and 3 pilus (107, 131, 222) and the non-fimbrial adhesion CF29K (50) and KPF28 (51, 52), were associated with the initial attachment and subsequent colonization of *K. pneumoniae* in the respiratory and urinary tract. The aerobactin-mediated iron uptake system, which has been reported to be located in a large resident plasmid, also contributed to the virulence of *K. pneumoniae* (48, 177, 237).

1.1.2 Characteristics of *K. pneumoniae* infections

As an opportunistic pathogen, the vast majority of *K. pneumoniae* infections were found in immuno-compromised individuals who are hospitalized and suffered from severe underlying diseases, such as diabetes mellitus or chronic pulmonary obstruction. In respect of

bacteremia caused by nosocomial gram-negative pathogens, *Klebsiella* is second only to *Escherichia coli* (270). Reported carrier rates in hospitalized patients are 77% in the stool, 19% in the pharynx and 42% on the hands of patients (47, 213). Such high rates of nosocomial colonization, however, were likely due to the use of antibiotics rather than the factors with delivery of care in the hospital (198, 207). The widespread use of antimicrobial therapy has been implicated to be responsible for the occurrence of multiresistant strains of *K. pneumoniae* in hospitals (213, 242) during outbreaks of nosocomial infections since 1980s (6, 75, 81, 252). The most common site of infection caused by *K. pneumoniae* is the urinary tract, which accounts for 6 to 17% of all nosocomial infections and shows an even higher incidence in patients with neuropathic bladders or with diabetes mellitus (15, 153).

Compared with other primary pathogens such as *E. coli* and *Salmonella* spp., *K. pneumoniae* has drawn less attention due to its opportunistic nature. However, with the extensive use of antibiotics and the widespread of multiresistant strain, especially the extended-spectrum β-lactamase (ESBL)-producing strains emerged since 1982 (71, 75, 159, 161), there has been renewed interest in *K. pneumoniae* infections. The resistance of *K. pneumoniae* to third-generation cephalosporins was usually conferred via the biosynthesis of ESBLs to hydrolyze broad-spectrum cephalosporins, monobactans and penicillins. In addition to increased frequency of β-lactam resistance, variations in the class of β-lactamase have emerged recently. The previously prevailing SHV and TEM enzymes were replaced by CTX, and strains producing CTX-ESBLs often showed resistance to fluoroquinolones and ciprofloxacin (22). The notion that ESBLs are often plasmid-mediated and that multiresistant *K. pneumoniae* strains usually harbor a relatively stable plasmid encoding ESBL have rendered *K. pneumoniae* a major threat to the ever-increasing number of susceptible individuals. Initially started from Argentina, the strains have now also been observed in areas other than Latin America (172, 197, 201), including Europe and Asia (148, 181). ESBL-producing *K. pneumoniae* strains have thus become more important due to the associations with treatment failure, prolonged stay in the hospital, increased health expense and a possible increase in mortality (189). With the unusual pattern of antibiotic resistance of the organism, physicians were forced to use unconventional agents such as tigecycline, polymyxin, colistin and inhalatory aminoglycosides with limited success (124).

The community-acquired *K. pneumoniae* infections were often treated empirically according to the prevalence of antimicrobial resistance. Risk factors for ESBL-producing *K. pneumoniae* included previous hospitalization, antimicrobial used in the 3 months, age over

60, male gender and diabetes mellitus (124). Although varied from country to country, the emergence of infections from ESBL-producing strains has been reported in Europe, Asia, and South and North America (17, 44, 195). Though most strains produced TEM type ESBL, an increase in occurrence of CTX has been reported (152). Carbapenems are considered to be the preferred agents for the treatment of serious infections caused by ESBL-producing *K. pneumoniae* strains due to their stability to β-lactamase hydrolysis. However, strains capable of express carbapenemases of the KPC variety in nosocomial infections have been reported recently in America (178), Brazil (168), the United Kingdom (259) and Greek (240). Many are only susceptible to tigecycline and colistin while some have developed resistant as well (138), imposing a major challenge for public health.

During the last decade, *K. pneumoniae* infections causing community-acquired primary pyogenic liver abscess (PLA) have also become an emerging disease receiving increasing attention. Distinct from the classical PLA, which is a complication of intra-abdominal or biliary tract infections resulting from multiple aerobic and anaerobic bacterial strains (158), PLA caused by primary infection of *K. pneumoniae* as a single pathogen is often cryptogenic and often complicated with metastatic lesions (135, 147, 248). The strains belonging to K1 serotype was predominant, and most cases have been reported from Taiwan (42), which were associated with a distinct invasive syndrome in liver abscess, meningitis and endophthalmitis. Other cases have also been reported from other parts of Asia including Korea (43) and Singapore (236, 268) while there are also reports in other parts of the world including North America (68, 133, 199), Australia (243) and Europe (34, 115). The geographical diversity may have been due to interaction between bacterial and host variables, socio-economic factors and genetic susceptibility varied across racial groups (124).

Attempts have been made to identify the risk factors for *K. pneumoniae* infections associated with abscess-formation. As listed in Table 1.1, diabetes mellitus is the most tightly associated with *K. pneumoniae* PLA among the host factors. With respect to *K. pneumoniae* associated risk factors, phenotypic attributes like hypermucoviscosity, K1/K2 capsule serotype, and genetic factors such as *magA* and *rmpA* are the most frequently reported. To date, the correlation between HV phenotype and *K. pneumoniae* PLA, community-acquired urinary tract infections (146) and bacteremia (137, 271) has been generally accepted while he relationship between a specific K serotype, especially K1, and *K. pneumoniae* PLA was still debatable. The gene *rmpA*, which was originally isolated from a large resident plasmid in *K. pneumoniae* strains of K2 serotype (175), has been reported to encode the ability to enhance

the biosynthesis of exopolysaccharides in *E. coli* (176). RmpA2, encoded by a gene homologous to *rmpA*, has been shown to activate *Klebsiella* K2 CPS biosynthesis at the transcriptional level (130). The *magA* gene was originally identified from a tissue-invasive K1 strain NTUH-K2044 and was found to be present in all isolates of K1 serotype (65). Toll-like receptor 4 recognition has been implicated in the infection by *K. pneumoniae* strains carrying *magA* (263). Most recent finding indicated that *magA* should be renamed as wzy_{K1}, encoding the polymerase for K1 CPS biosynthesis (66, 269). In addition, the loci derived from pLVPK, a 219,385-bp plasmid of an invasive K2 strain CG43 (241), has also been implicated in the abscess formation during *K. pneumoniae* infections (237). A search in the genetic requirements of PLA in a mice oral infection model by *K. pneumoniae* has identified a set of regulatory genes suggesting the prerequisite formation of a regulatory network during the infection process (241). Despite these findings, the existence of other bacterial factors mediating *K. pneumoniae* pathogenesis, especially in PLA, remained elusive. Also, the widespread of multiresistant *K. pneumoniae* strains has urged the demands for the prevention of infections, rapid detection of infections and efficient treatments more urgent than before. As a result, a deeper understanding of the regulatory mechanisms of *K. pneumoniae* virulence factors would be required for future advances in the new therapeutic strategies.

1.2 Two-component systems (2CSs)

Bacteria must be able to sense and respond to their environment in order to survive. One major way microbes accomplish this is using signal transduction machinery such as two-component systems (2CSs). 2CSs are distributed widely throughout the prokaryotes and eukaryotes, with the exception of animals, rendering them as a target for the development of novel antimicrobial agents (85, 86).

As the most prevailing signal transduction mechanisms to control gene expression in bacteria, a typical 2CS consists of a membrane-associated sensor kinase and a cytoplasmic response regulator. In response to an external stimulus, the sensor protein undergoes auto-phosphorylation at a conserved histidine residue, and the signal is subsequently relayed to the cytosol via phosphorylation at the aspartic acid in the receiver domain of the response regulator (27). The signal transduction cascade may thus activate genes required for bacterial virulence during infections or survival in hostile environments (12). As is widely believed, 2CS proteins function as components of a signal transduction network, enabling bacteria to respond to complex environmental stimuli (5).

1.2.1 Classification of 2CSs

The 2CSs were classified into three major types by virtue of their functional domains: the classical system, the unorthodox system, and the hybrid system (204). Mostly, a 2CS sensor kinase carrying one input domain and one transmitter domain was called a classical (IT-type) sensors kinase. The others contain both the sensor kinase signature and a receiver domain of the response regulator, which were referred to as hybrid (ITR-type) sensors kinases. A small fraction of the hybrid sensors possesses an additional output domain at the carboxyl terminus and were referred to as unorthodox (ITRO-type) sensor kinases. For example, in *P. aeruginosa* PAO1, there are 42 IT-type sensor kinases, 12 ITR-type senor kinases, and 5 ITRO-type sensor kinases. Only three Hpt (histidine-containing phosphotransfer) modules had been observed (204). With the increasing number of bacterial 2CS identified, an emerging theme is the discovery of auxiliary factors, which are capable of influencing phosphotransfer but distinct from sensor kinases and response regulators. As the number of auxiliary factors increases, the members of a 2CS would surely increase, forming a three (and more) component system (27). Auxiliary factors could either exert its function by targeting the response regulator, as in the case of the unorthodox 2CS response regulators RcsB and its auxiliary factor RcsA (122, 155, 251). Auxiliary factors could also target on the sensor protein. One of the examples in a multiple component system is the Rap and Spo0E family phosphatases that interact with, and stimulate the auto-phosphatase activity of, the Spo0F and Spo0A response regulators respectively (219).

1.2.2 The sensor kinase

Each sensor kinase contains a variable input domain that is adapted for the detection of a specific stimulus, typically a chemical ligand, and a conserved transmitter domain that transfers the signal to its cognate response regulator through a phosphorylation cascade (57). A prototype sensor kinase is a homodimeric integral membrane domain in which the sensor domain is depicted as an extracellular loop within two membrane-spanning segments. The transmitter domain is localized within the cytoplasm. Recently the domains adapted by sensor proteins have been classified as extracellular sensor domains such as PDC (PhoQ-DcuS-CitA) (39, 40, 215), or membrane-embedded sensor domain similar to the phototaxis sensory rhodopsin II-transducer complex HtrII-SrII (84) and cytoplasmic sensor domains such as PAS (7, 123), GAF (102) or PHY (266). Although there is an apparent lack of uniformity between the specific conformational changes that take place within sensor domains upon changes in stimulus, the recent structural evidence suggests that the communication between

sensor and transmitter domains in sensor protein signaling is mediated by subtle structural changes along the dimmer interface and that related aspects of symmetry and asymmetry may also exist.

Signal termination in 2CSs usually occurs via the loss of the phosphoryl group from the response regulator. For example, the Spo0E family phosphatases (56, 88), which catalyze the dephosphorylation of the response regulator Spo0A involved in the initiation of endospore formation not only in *Bacillus subtilis* but also in other gram-positive bacteria, contain sequence and structural features similar to the chemotaxis phosphatases of CheZ (126, 275) and CheC/CheX/FliY families (188, 191, 230).

1.2.3 The response regulator

Consisted of a receiver domain and an output domain, the response regulator typically acts as the effector of 2CS. The input or receiver domain, which is usually conserved among regulators, received signals transferred from the sensor kinase and in some case from small phosphor donors such as phosphoramidates and acyl phosphates (258). Phosphorylation of the receiver domain is usually followed by a conformational change of the response regulator, which subsequently results in dimerization of the protein.

In contrast to the input domain, the output domain was rather diverse. Though most response regulators act as transcriptional regulators with various DNA-binding domains, the output domains of response regulators covered effector domains with a wide range of cellular functions, including RNA-binding, chemotaxis, two-component phosphorelay, cyclic di-GMP signaling, cAMP signaling and protein Ser/Thr phosphorylation (76). The properties that no restriction was applied on the variety of domains fused with the receiver domain and many 2CSs were able to interfere with the functioning of other signal transduction systems put 2CSs at the top of the bacterial signaling hierarchy.

1.2.4 The 2CS network

The increasing knowledge of 2CSs has revealed a diversity of designs controlling the flow of information within and between circuits. As a result, a 2CS network could be expected from two aspects, either the control of phosphorylation/dephosphorylation, or the signal integration and distribution among phosphotransfer pathways.

The control of phosphorylation/dephosphorylation covers single-step phosphotransfer, in which the sensor kinase exerts only its kinase activity, like the histidine kinase CheA in chemotaxis circuits (126), or exerts both kinase and phosphatase activity, as exemplified by

the *E. coli* 2CSs OmpR/EnvZ (11), PhoP/PhoQ (166) and CpxR/CpxA (217). In the latter case, a high expression level of the histidine kinase will increase the complex formation of the kinase/response regulator pair, with a commitment decrease in the response regulator phosphorylation.

The occurrence of phosphorelay in a 2CS could be found either in separate components, as in the sporulation phosphorelay of *B. subtilis* (180), or in hybrid proteins which usually contain reversible phosphorylation (4, 80) as also observed in RcsCDB phosphorelay regulating *E. coli* group I CPS biosynthesis (155). Possibly, the evolution of such complex phosphorelay machinery in 2CS signaling could provide additional points of control.

Finally, the autoregulation, which is resulted from a positive feedback from the 2CS itself, probably modulates the sensitivity to the applied stimulus, as explored in the BvgA/BvgS in *Bordetella bronchiseptica* (255). This may also create a short-term "learning" behavior, as shown in 2CS PhoB/PhoR in *E. coli* (103). A negative autoregulation could even give rise to an oscillatory behavior in the expression of downstream genes, as observed in the 2CS CovS/CovR in *Streptococcus pyogenes* (93).

In view of signal integration and distribution among phosphotransfer pathways, the 2CS network contains branched pathways of either "one-to-many" in the chemotaxis regulatory system (126), "many-to one" in the quorum sensing network of *Vibrio harveyi* (151), or "cross-regulation" via auxiliary proteins in *S. enterica* PmrD connector-mediated circuit (117, 119). Though much has been investigated in the complex 2CS network, a need remains for better understanding towards the properties of different circuit architectures to identify potential drug targets.

1.3 Thesis objectives

The prevalent presence of 2CS encoding genes in the bacterial genome as well as the wide spectrum of physiological functions governed by different 2CSs, such as virulence properties, have aroused our interest in studying the 2CSs in *K. pneumoniae*. Based on the available *E. coli* 2CSs listed in the KEGG database (http://www.genome.ad.jp/kegg/pathway/), a previous search of the homologous 2CS-coding genes in the genome sequence of *K. pneumoniae* MGH78578 (http://genome.wustl.edu/) has been performed. Among the 29 sensor kinase coding genes and 26 response regulator coding genes identified, the 2CSs PhoP/PhoQ, PmrA/PmrB, RstA/RstB and RcsCDB coding genes were also included. The role of 2CSs PhoP/PhoQ, PmrA/PmrB in *S. enterica* pathogenesis has been well documented (2, 13, 78, 205,

260). A novel mechanism connecting 2CSs PhoP/PhoQ and PmrA/PmrB by a small protein PmrD has shed light on the complex and versatile regulation of 2CS target genes (59, 117). RstA/RstB has been identified as a member of magnesium stimulon governed by the master 2CS PhoP/PhoQ (164). Recent studies have shed light its functional role in bacterial acid resistance (214), iron transport (111) and the survival against stressed encountered in the digestive tract (69). Despite these findings, the function of RstA/RstB remained rather limited. In addition, the RcsCDB phosphorelay has been reported to regulate *E. coli* group I CPS (87) and *K. pneumoniae* K2 CPS biosynthesis (245). In *K. pneumoniae*, in addition to RmpA2 which activated K2 *cps* expression independently to RcsB (130), another mucoid factor encoding gene *rmpA* was also indentified in pLVPK (37). Based on the critical role of CPS in *K. pneumoniae* pathogenesis, it would be of importance to investigate the mode of regulation of RmpA as well as its interplay with the RcsCDB phosphorelay. The objectives of this thesis are to investigate the functional role of PhoP/PhoQ, PmrA/PmrB, RstA/RstB and RcsCDB in the regulation of *K. pneumoniae* virulence determinants, and an overview is listed as follows:

Chapter 2 described the functional role of bacterial CPS as well as 2CSs PhoP/PhoQ and PmrA/PmrB in the regulation of polymyxin B resistance in *K. pneumoniae* CG43. In addition to the characterization of the PmrD connector-mediated pathway in *K. pneumoniae* at both genetic and the molecular level, the residues implicated in PmrD functioning were also explored via a mutagenesis approach.

Chapter 3 presents the characterization of the 2CS RstA/RstB in *K. pneumoniae* CG43. The involvement of PhoP and RstA on the expression of *rstA* was investigated, and RstA-regulated genes were identified by subtractive cDNA hybridization. Based on the results from cDNA subtraction and recent findings in RstA/RstB, phenotype analysis was conducted to explore the possible biological functions of RstA/RstB in *K. pneumoniae*.

Chapter 4 reports RmpA regulation of *K. pneumoniae* K2 CPS biosynthesis. The cooperation of RmpA and the RcsCDB phosphorelay was implicated from phenotype analysis and was demonstrated through both *in vivo* and *in vitro* approaches. A comparative analysis of RmpA and RmpA2 has further led to the identification of Fur, a global iron uptake regulator, in *Klebsiella* K2 CPS biosynthesis as well as the interplay of iron uptake and capsule biosynthesis in *K. pneumoniae* pathogenesis.

Chapter 5 concludes the entire thesis from a comprehensive point of view and provides perspectives regarding further investigations on the regulatory mechanisms and biological functions of the 2CSs herein investigated.

Table 1.1. Risk factors associated with abscess formations in *K. pneumoniae* infections

Risk factor	Description	Reference
K. pneumoniae associated factor		
Phenotype attributes	Hypermucoviscosity (HV)	(136, 237, 272)
	Extended spectrum β-lactamase (ESBL) production[a]	(136)
	Capsular serotype (K1 or K2)	(43, 67, 136, 143, 243, 267, 268)
Genetic factors		
K1-specific gene	*magA*, *allS*	(42, 68, 136, 154)
HV regulatory gene	*rmpA*, *rmpA2*	(136, 272)
Integrative and conjugative element	ICE*Kp1* (Homologue of *Yersinia* high-pathogenecity island (HPI))	(145)
Iron acquisition system	*iucABCEiutA*, *iroAiroNDCB*, *kfu*	(68, 272)
pLVPK derived loci	$terW^{+}iutA^{+}rmpA^{+}silS^{+}$	(237)
Host factor		
Underlying disease	Diabetes mellitus	(134, 237, 239)
	Urinary tract obstruction	(239)
	Malignancy	(239)
Association with focal infections	Pneumonia	(239)
	Urinary tract infections	(239)
Therapeutic treatments	Poor glycemic control	(144)
Disease acquisition	Community acquisition	(237)

[a.] Negatively correlated.

CHAPTER 2

Molecular Characterization of the PhoPQ-PmrD-PmrAB Mediated Pathway Regulating Polymyxin B Resistance in *Klebsiella pneumoniae* CG43

2.1 Abstract

The cationic peptide antibiotic polymyxin has recently been reevaluated in the treatment of severe infections caused by gram negative bacteria. In this study, the genetic determinants for capsular polysaccharide level and lipopolysaccharide modification involved in polymyxin B resistance of the opportunistic pathogen *Klebsiella pneumoniae* were characterized. The expressional control of the genes responsible for the resistance was assessed by a LacZ reporter system. The PmrD connector-mediated regulation for the expression of *pmr* genes involved in polymyxin B resistance was also demonstrated by DNA EMSA, two-hybrid analysis and *in vitro* phosphor-transfer assay. Deletion of the *rcsB*, which encoded an activator for the production of capsular polysaccharide, had a minor effect on *K. pneumoniae* resistance to polymyxin B. On the other hand, deletion of *ugd* or *pmrF* gene resulted in a drastic reduction of the resistance. The polymyxin B resistance was shown to be regulated by the two-component response regulators PhoP and PmrA at low magnesium and high iron, respectively. Similar to the control identified in *Salmonella*, expression of *pmrD* in *K. pneumoniae* was dependent on PhoP, the activated PmrD would then bind to PmrA to prolong the phosphorylation state of the PmrA, and eventually turn on the expression of *pmr* for the resistance to polymyxin B. The study reports a role of the capsular polysaccharide level and the *pmr* genes for *K. pneumoniae* resistance to polymyxin B. The PmrD connector-mediated pathway in governing the regulation of *pmr* expression was demonstrated. In comparison to the *pmr* regulation in *Salmonella*, PhoP in *K. pneumoniae* plays a major regulatory role in polymyxin B resistance.[a]

[a] A part of this chapter has been published:

1. **Cheng, H. Y., Y. F. Chen, and H. L. Peng.** 2010. Molecular characterization of the PhoPQ-PmrD-PmrAB mediated pathway regulating polymyxin B resistance in *Klebsiella pneumoniae* CG43. *J Biomed Sci* 17:60-75.
2. **Luo, S. C., Y. C. Lou, H. Y. Cheng, Y. R. Pan, H. L. Peng, and C. Chen.** 2010. Solution structure and phospho-PmrA recognition mode of PmrD from *Klebsiella pneumoniae*. *J Struct Biol.* (In press)

2.2 Introduction

Klebsiella pneumoniae, an important nosocomial pathogen, causes a wide range of infections including pneumonia, bacteremia, urinary tract infection, and sometimes even life-threatening septic shock (196). The emergence of multiresistant *K. pneumoniae* has reduced the efficacy of antibiotic treatments and prompted the reevaluation of previously but not currently applied antibiotics (63, 64) or a combined therapy (116). Polymyxins, originally isolated from *Bacillus polymyxa*, have emerged as promising candidates for the treatment of infections (274). As a member of antimicrobial peptides (APs), the bactericidal agent exerts its effects by interacting with the lipopolysaccharide (LPS) of gram-negative bacteria. The polycationic peptide ring on polymyxin competes for and substitutes the calcium and magnesium bridges that stabilize LPS, thus disrupting the integrity of the outer membrane leading to cell death (95, 274).

The *Klebsiella* capsular polysaccharide (CPS), which enables the organism to escape from complement-mediated serum killing and phagocytosis (53, 113), has been shown to physically hinder the binding of C3 complement (45) or polymyxin B (30). The assembly and transport of *Klebsiella* CPS followed the *E. coli* Wzy-dependent pathway (253), in which mutations at *wza* encoding the translocon protein forming the complex responsible for CPS polymer translocation and export resulted in an inability to assemble a capsular layer on the cell surface (55). The CPS biosynthesis in *K. pneumoniae* was transcriptionally regulated by the two-component system (2CS) RcsCDB (155) where the deletion of the response regulator encoding gene *rcsB* in *K. pneumoniae* caused a loss of mucoid phenotype and reduction in CPS production (130).

In *Escherichia coli* and *Salmonella enterica* serovar Typhimurium, polymyxin B resistance is achieved mainly through the expression of LPS modification enzymes, including PmrC, an aminotransferase for the decoration of the LPS with phosphoethanolamine (125) and the *pmrHFIJKLM* operon (92, 260) (also called *pbgP* or *arn* operon (20, 265)) encoding enzymes. Mutations at *pmrF*, which encoded a transferase for the addition of 4-aminoarabinose on bactoprenol phosphate, rendered *S. enterica* and *Yersinia pseudotuberculosis* more susceptible to polymyxin B (92, 156). The *S. enterica ugd* gene encodes an enzyme responsible for the supply of the amino sugar precursor $_{L}$-aminoarabinose for LPS modifications and hence the Ugd activity is essential for the resistance to polymyxin B (235). On the other hand, the *E. coli ugd* mutant with an impaired capsule also became

highly susceptible to polymyxin B (128).

The 2CS PmrA/PmrB, consisting of the response regulator PmrA and its cognate sensor kinase PmrB, has been identified as a major regulatory system in polymyxin B resistance (91, 261). The resistance in *S. enterica* or *E. coli* has been shown to be inducible by the extracellular iron (256). In addition to acidic pH (193), the role of ferric ions as a triggering signal for the expression of PmrA/PmrB has been demonstrated (261). The 2CS PhoP/PhoQ which regulates the magnesium regulon (120) could also activate polymyxin B resistance under low magnesium in *S. enterica*, in which the PhoP/PhoQ-dependent control is connected by the small basic protein PmrD. The expression of *pmrD* could be activated by PhoP while repressed by PmrA forming a feedback loop (118, 127). The activated PmrD could then bind to the phosphorylated PmrA leading to a persistent expression of the PmrA-activated genes (117).

The PmrD encoding gene was also identified in *E. coli* and *K. pneumoniae*. However, *pmrD* deletion in *E. coli* had no effect on the bacterial susceptibility to polymyxin B (256). Recently, the PhoP-dependent expression of *pmrD* has also been demonstrated in *K. pneumoniae*. According to the predicted semi-conserved PhoP box in the *pmrD* upstream region, a direct binding of PhoP to the *pmrD* promoter for the regulation was speculated (165).

In this study, specific deletions of genetic loci involved in CPS biosynthesis and LPS modifications were introduced into *K. pneumoniae* CG43, a highly virulent clinical isolate of K2 serotype (36). Involvement of the genetic determinants in polymyxin B resistance was investigated.

2.3 Results

2.3.1 Reduced production of capsular polysaccharide had minor effect on the polymyxin B resistance in *K. pneumoniae*

K. pneumoniae CG43 is a highly encapsulated virulent strain (36). In order to verify the role of CPS in polymyxin B resistance, the Δ*ugd* and Δ*wza* mutants were generated by allelic exchange strategy, and their phenotype as well as the amount of CPS produced were compared with the parental strain CG43S3 and Δ*rcsB* mutant (130). As shown in Fig. 2.1A, the Δ*ugd* and Δ*wza* mutants formed apparently smaller colonies on LB agar plate compared with the glistering colony of the parental strain CG43S3. Although the colony morphology of the Δ*rcsB* mutant was indistinguishable from CG43S3, the CPS-deficient phenotype was evident as assessed using sedimentation assay and the amount of K2 CPS produced (Fig. 2.1B). Deletion of *rcsB* resulted in an approximately 50% reduction of the CPS, while the Δ*wza* mutant produced less than 20% of that of its parental strain CG43S3. The CPS biosynthesis in Δ*ugd* mutant was almost abolished, indicating an indispensible role of Ugd in CPS biosynthesis. To investigate how the CPS level was associated with polymyxin B resistance, the survival rates of the strains challenged with polymyxin B were compared. The Δ*ugd* mutant producing the lowest amount of CPS was extremely sensitive to the treatment of polymyxin B (Fig. 2.1C). Although the Δ*ugd* mutant was CPS-deficient, the impaired polymyxin resistance may have been largely attributed to the defect in LPS biosynthesis since the survival rates of Δ*wza* and Δ*rcsB* mutants appeared to be comparable with the parental strain CG43S3. This argues against the notion that the level of polymyxin B resistance is positively correlated to the amount of CPS (30). Nevertheless, the possibility that a higher amount of CPS was required for the resistance could not be ruled out. As shown in Fig. 2.1D, the introduction of pRK415-RcsB (38) resulted in a significantly higher resistance to polymyxin B in both Δ*rcsB* mutant and its parental strain. This indicated a protective effect of large amounts of CPS in polymyxin resistance.

2.3.2 PmrF is involved in polymyxin B resistance and survival within macrophage

To investigate if the *K. pneumoniae pmr* homologues played a role in polymyxin B resistance, a *pmrF* deletion mutant strain and a plasmid pRK415-PmrF were generated. As shown in Fig. 2.2A, when the strains were grown in LB medium, a low magnesium condition (89), differences in the survival rates were not apparent. When the strains were grown in LB

supplemented with 1 mM $FeCl_3$, an apparent deleting effect of *pmrF* in polymyxin B resistance was observed, and the survival rate could be restored by the introduction of pRK415-PmrF. The results indicated a role of PmrF in the polymyxin B resistance in high iron condition. In addition to the mucosa surfaces, antimicrobial peptides and proteins play important roles in the microbicidal activity of phagosome (14). To investigate the effect of *pmrF* deletion in the bacterial survival within phagosome, phagocytosis assay was carried out. Since *K. pneumoniae* CG43S3 was highly resistant to engulfment by phagocytes in our initial experiments, the Δ*rcsB* mutant which produced less CPS was used as the parental strain to generate Δ*pmrF*Δ*rcsB* mutant. As shown in Fig. 2.2B, deletion of *pmrF* resulted in an approximately four-fold reduction in the recovery rate, which was restored after the introduction of pRK415-PmrF. This indicated an important role of *pmrF* not only in polymyxin B resistance but also in bacterial survival within macrophage.

2.3.3 Deletion effect of *Klebsiella pmrA, pmrD* or *phoP* on polymyxin B resistance

To investigate how PmrA, PhoP and PmrD were involved in the regulation of polymyxin B resistance in *K. pneumoniae*, Δ*pmrA*, Δ*phoP* and Δ*pmrD* mutant strains were generated. Deletion of either one of these genes resulted in a dramatic reduction of resistance to polymyxin B when the strains were grown in LB medium (Fig. 2.3A). The deleting effects were no longer observed when the strains grown in LB supplemented with 10 mM magnesium, implying an involvement of the PhoP-dependent regulation in LB, a low magnesium environment. Under high-iron conditions, the deletion of *pmrA* caused the greatest reduction in the survival rate. Introduction of pRK415-PmrA or pRK415-PhoP into the Δ*pmrA*Δ*phoP* double mutant strain not only restored but also enhanced the bacterial resistance to polymyxin B (Fig. 2.3B), which is likely due to an over-expression level of *phoP* or *pmrA* by the multicopy plasmid. Finally, whether the deletion of *pmrA*, *phoP* or *pmrD* affected the survival rate in phagosomes was also investigated. Interestingly, deletion of *phoP* resulted in most apparent effect while the *pmrA* deletion had less effect on the bacterial survival in macrophages. This was probably due to low iron concentration in the phagosomes (89). The introduction of pRK415-PhoP or pRK415-PmrD could restore the recovery rates of Δ*phoP*Δ*rcsB* and Δ*pmrD*Δ*rcsB*, although not to the extent displayed by the parental strain. Taken together, our results indicate the presence of two independent pathways in the regulation of polymyxin B resistance and the bacterial survival within macrophage phagosomes.

2.3.4 Effect of *pmrA*, *phoP* or *pmrD* deletion on P_{pmrH}::*lacZ* and P_{pmrD}::*lacZ* expression

As the functional role of the structural gene *pmrF* and the regulator genes *phoP*, *pmrD* and *pmrA* was verified, it would be of importance to investigate the regulatory network govern by PhoPQ-PmrD-PmrAB on the expression of *pmr* genes. Sequence analysis has revealed PhoP and PmrA box consensus in the upstream region of *pmrH* and PhoP box consensus in the upstream region of *pmrD* (Fig. 2.4A). To investigate the interplay of PhoP, PmrA, and PmrD on the expression of *pmr* and *pmrD* genes, the reporter plasmids placZ15-PpmrH and placZ15-PpmrD were constructed and mobilized into *K. pneumoniae* CG43S3Δ*lacZ* and its derived Δ*pmrA*Δ*lacZ*, Δ*pmrD*Δ*lacZ* or Δ*phoP*Δ*lacZ* isogenic strains, respectively. The β-galactosidase activities of *K. pneumoniae* transformants under different environmental conditions were determined. In the wild-type strain CG43S3Δ*lacZ*, the P_{pmrH}::*lacZ* activity was repressed in the presence of high magnesium but enhanced in high ferric ion (Fig. 2.4B). Such iron-inducible activity was abolished after the addition of iron scavenger deferoxamine. As shown in Fig. 2.4B, deleting effect of *pmrA* or *phoP* on the activity of P_{pmrH}::*lacZ* could be observed in LB or LB supplemented with ferric iron. The negative effect of *pmrD* deletion was also apparent at high iron condition but was abolished after the addition of deferoxamine. The results clearly demonstrate the involvement of PmrA, PhoP and PmrD in the regulation of the expression of *pmr* genes, particularly in the presence of high ferric irons. As shown in Fig. 2.4C, the P_{pmrD}::*lacZ* activity was significantly reduced in high-magnesium conditions or upon the deletion of *phoP*. Interestingly, the deletion of *pmrA* or high ferric irons had little effect on the activity of P_{pmrD}::*lacZ*. The results suggest that the expression of *K. pneumoniae pmrD* is regulated in a PhoP-dependent but PmrA-independent manner.

2.3.5 Analysis of EMSA indicates a direct binding of the recombinant PhoP to P_{pmrD}

The binding of PhoP or PmrA to P_{pmrH} has been determined recently (165). In order to determine whether PhoP binds directly to P_{pmrD}, EMSA was performed. As shown in Fig. 2.5A, binding of the recombinant His-PhoP protein to P_{pmrD} was evident by the formation of a protein/DNA complex with a slower mobility. The binding specificity was also examined by the addition of specific competitor (P_{pmrD} DNA) or non-specific competitor (*pmrD* gene or pUC19 DNA). The formation of the complex was gradually reduced with the increasing ratios of unlabeled to labeled P_{pmrD} DNA fragments and completely diminished at the highest ratio investigated. In the presence of unspecific competitor DNA, the formation of

protein/DNA complexes could also be observed although a portion of free probe was still noted, possibly due to the high amounts of DNA added. As shown in Fig. 2.5B, the formation of protein/DNA complex diminished when His-PhoP$_{N149}$, in which the carboxyl-terminal helix-turn-helix domain has been truncated, was used instead of His-PhoP. The results strongly suggest the PhoP binds via its C-terminal domain to the promoter of *pmrD* for the activation of the *pmrD* expression in *K. pneumoniae*.

2.3.6 Two-hybrid analysis of the *in vivo* interaction between *Klebsiella* PmrD and PmrA

The interaction between *Klebsiella* PmrD and PmrA has been shown as a prerequisite for the connector-mediated pathway (165). To demonstrate *in vivo* interaction, a bacterial two-hybrid assay was performed. The plasmid pBT-PmrA carrying the RNAPα-PmrA coding region and the plasmid pTRG-PmrD carrying the λ-cI-PmrD coding sequence were generated. *In vivo* interaction between the two reporter strains allowed the binding of λ-cI to the operator region as well as the recruitment of α-RNAP for the expression of the *ampR* and *lacZ* reporter genes. The bacteria harboring the positive control plasmids pTRG-Gal11^{P} and pBT-LGF2 showed a vigorous growth on the indicator plate, as reflected by the apparent colony formation when the culture was diluted serially (Fig. 2.6A). In contrast, the strain carrying the negative control vectors pBT and pTRG revealed impaired colony formation. As shown in Fig. 2.6A, a profound growth pattern of the *E. coli* cells harboring pBT-PmrA and pTRG-PmrD was observed indicating an interaction between the PmrD and PmrA.

2.3.7 PmrD prevents the dephosphorylation of PmrA catalyzed by PmrB

In *S. enterica*, the phosphorylation of PmrA by the cognate sensor protein PmrB has been demonstrated to enhance its affinity in binding to its target promoter. The subsequent dephosphorylation of PmrA by PmrB helped to relieve from over-activation of this system (1). In *Salmonella*, PmrD has been shown to be able to protect PmrA from both intrinsic and PmrB-mediated dephosphorylation (22). To verify if *Klebsiella* PmrD also participates in the phosphorylation, *in vitro* phosphotransfer assay was carried out with the recombinant proteins His-PmrA, His-PmrD and His-PmrB$_{C276}$. As shown in Fig. 2.6B, the His-PmrA was rapidly phosphorylated upon addition of the autophosphorylated His-PmrB$_{C276}$ and then gradually dephosphorylated. Addition of His-PmrD apparently prolong the phosphorylation state of the His-PmrA, which could be maintained for at least 60 min (Fig. 2.6B). As shown in Fig. 2.6C, the specificity of the interaction between His-PmrD and His-PmrA was also demonstrated since the phosphorylation state of His-PmrA could not be detected when incubated with the

small cationic proteins RNase A or cytochrome C (117). Similar levels of phospho-PmrB$_{C276}$ were observed in the presence or absence of PmrD (Fig. 2.6D), suggesting the His-PmrD had no effect on the phorphorylation state of His-PmrB$_{C276}$. The above findings have indicated that the reduced polymyxin B resistance in Δ*pmrD* mutant (Fig. 2.3A) could be due to the insufficient expression level of *pmr* genes (Fig. 2.4B) resulting from rapid dephosphorylation of PmrA by PmrB in the absence of PmrD. Accordingly, the PmrD connector-mediated pathway also played a role in *K. pneumoniae* resistance to polymyxin B.

2.3.8 Identification of residues critical for PmrD functionality

Since the PmrD homologues from *K. pneumoniae*, *E. coli* and *S. enterica* shared a lower sequence identity (30.3%) compared to the respective PmrA (74.9%) or PmrB (58.5%) counterparts, it was likely that differences in PmrD rather than PmrA sequences would alter their interaction properties and the subsequent polymyxin B resistance. To provide insights into how *K. pneumoniae* PmrD exert its function and to explore how PmrD sequence variation during the evolution could result in functional divergences, multiple sequence alignment of PmrD homologues was performed (Fig. 2.7A). Of all the amino acids aligned, the residues that may exhibit charge-charge interaction properties or conserved among the PmrD proteins were selected and individually changed to Alanine. The ability of the altered *pmrD* alleles encoding different PmrD proteins with point mutations to restore the polymyxin B resistance in Δ*pmrD* mutant was then investigated.

As shown in Fig. 2.7B, the polymyxin B resistance of Δ*pmrD* mutant strains carrying pRK415 or the derived plasmids encoding either the wild-type PmrD or PmrD with each point mutation was determined. Compared with the strain carrying a wild-type allele, the survival rates of Δ*pmrD* mutants carrying plasmids encoding PmrDK6A, PmrDS23A, PmrDE31A, PmrDG24A, PmrDL26A, PmrDM28A, PmrDT46A, PmrDY53A or PmrDY71A were reduced, indicative of an important role of these residues in PmrD functionality. In contrast, Δ*pmrD* strains carrying PmrDQ9A, PmrDD10A, PmrDT69A, PmrDT77A, PmrDT78A, PmrDD80A encoding plasmids were almost as resistant as the strain harboring pRK415-PmrD. The results suggested that some of the charged residues, such as Lysine at position 6 and Glutamate at position 31, may play an important role in the local charge-charge interactions with the charged domains on PmrA, such as the receiver domain with a negatively charged aspartic acid. In addition, some of the well-conserved residues may have maintained the overall stability of PmrD including Serine at position 23, Glycine at position 24, Leucine at position 26, Methionine at position 28, Threonine at position 46,

Tyrosine at positions 53 and 71. Whether the alteration of these residues would affect the turnover of PmrD protein remained to be verified. Since the residues involved PmrD functionality have been identified, it would be important to explore their roles in PmrD/PmrA interaction in order to elucidate the mode of action between these proteins.

In addition to the residues selected above, it was found that PmrDC35S could protect PmrA from dephosphorylation as PmrD (Fig. 2.7C). The alteration in Cysteine at position 54 seemed to affect the overall stability of PmrD since the protein was mostly present at the insoluble fraction indicating the importance of disulfide bond formation in PmrD structure. Recently our collaborators have determined the solution structure of *Klebsiella* PmrD and conducted amide chemical shift perturbations as well as saturation transfer assays using PmrDC54S to reveal the recognition surface of PmrD by the dimerized receiver domain of PmrA. The interface contained a contiguous patch involving Tryptophan at positions 3 and 4, Serine at positions 23 and 73, Leucine at position 26, Glutamate at positions 27 and 74, Methionine at position 28, Threonine at positions 46 and 69, Leucine at position 48, Alanine at positions 49, 51 and 68, Aspartic acid at position 50, Arginine at position 52, Isoleucine at position 65, Asparagine at position 67, Histidine at position 70 and Tyrosine at position 71. The findings have provided a structural basis of our results in polymyxin B resistance assay shown in Fig. 2.7B and a rational explanation for the critical role of residues at positions 23, 26, 28, 46 and 71 in PmrD/PmrA recognition process.

2.4 Discussion

Although the amount of CPS produced by Δ*rcsB* mutant was more than twice of that produced by Δ*wza* mutant, no apparent difference between the wild type strain CG43S3, Δ*wza* mutant, and Δ*rcsB* mutant in polymyxin B resistance could be observed. This is different from the previous finding that *K. pneumoniae* CPS was an important physical barrier for the APs (30). This discrepancy may be attributed to some of the *K. pneumoniae* strains used for comparison in the previous study produced extremely low level of the CPS. Nevertheless, a higher amount of CPS was protective for the bacterial resistance to polymyxin B.

On the other hand, the deletion of *ugd* resulted in the loss of resistance to polymyxin B. Sequence analysis of the available *K. pneumoniae* genome NTHU-K2044 (262), MGH78578 (http://genome.wustl.edu/) and 342 (74) revealed no PmrA (260) or PhoP box (120) in the upstream region of the *manC-manB-ugd* genes (42). This implies the involvement of a regulatory mechanism different from that for *S. enterica ugd*, which was positively regulated by the three 2CS regulators PhoP, PmrA and RcsB (170).

Consistent with the reported findings (165), deletion of *Klebsiella pmrF* which encodes one of the enzymes required for synthesis and incorporation of aminoarabinose in LPS resulted in decreased resistance to polymyxin B and survival within macrophages. The *pmr* expression has been shown to be directly regulated by PhoP under low magnesium or by PmrA in high ferric ions, or by the connector-mediated pathway reported for *Salmonella*,(165). Similar to the observations in *E. coli*, *S. enterica* (256), *Yersinia pestis* (257), and *Pseudomonas aeruginosa* (169), a positive regulatory role of PmrA and PhoP in polymyxin B resistance in *K. pneumoniae* was also demonstrated.

The deletion of *phoP* resulted in more drastic effect on the bacterial survival in macrophage than the *pmrA* deletion, implying a different level of control between PhoP and PmrA in *K. pneumoniae* resistance to phagocytosis. During phagocytosis, phagosomal maturation and phagolysosomes formation are accompanied by progressive acidification and acquisition of various hydrolases, reactive oxygen, nitrogen species, and APs (70). Low pH and low-magnesium have been shown to be able to stimulate expression of the PhoP-activated genes (89, 90). Apart from its microbicidal activity, the APs inside phagosomes has even been reported as an inducing signal for the activation of the PhoP/PhoQ system (185). The deletion of *pmrF* or *phoP* caused a significant reduction in

intra-macrophage survival of the bacteria, implying a role of the AP resistance regulation in the bacterial pathogenesis.

Until now, PmrD was only found in *E. coli*, *Shigella flexneri*, *S. enterica* and *K. pneumoniae*. Although PmrD in *Klebsiella* appeared to act in a way similar to the PmrD in *S. enterica*, they share only about 40% sequence identity. The expression of *K. pneumoniae pmrD* was shown to be PhoP-dependent and the regulation was achieved through a direct binding of PhoP to the putative *pmrD* promoter. In addition, the binding of PmrD was shown to efficiently protect the PmrA from dephosphorylation. The *in vivo* interaction between PmrD and PmrA demonstrated using bacterial two-hybrid analysis further supported the presence of the connector-mediated pathway in *K. pneumoniae*. Although the level of interaction between PmrD and PmrA appears to be similar to the positive control (Fig. 2.5A), it still awaits quantitative analysis to validate the strength of *Klebsiella* PmrD/PmrA interaction. It was also noted that the level of the detected signals was reduced after PmrA phosphorylation by PmrB (Fig. 2.5B, lanes 2 and 8 compared with lanes 1 and 7). The finding was reminiscence of the phosphatase activity of the sensor protein PmrB, which exerted it effect as soon as PmrA was phosphorylated and rapidly exceeded the kinase activity on PmrB in the absence of PmrD. Nevertheless, the ratio of the proteins used in the assay may have also led to the phosphorylation dynamics observed.

In summary, involvement of *Klebsiella pmr* genes in polymyxin B resistance and the regulation for the expression of *pmr* genes were analyzed. As shown in Fig. 2.8, the regulatory network for the expression of the *pmr* genes is comprised of 2CS response regulators PhoP and PmrA, and the connector protein PmrD. In low magnesium environments, PhoP could activate the expression of *pmrD* and *pmr* genes independently to promote polymyxin B resistance. In the presence of high levels of ferric ions, the PmrA protein was phosphorylated by PmrB, the PmrD protein could interact with PmrA to prolong its phosphorylation state and a continuous expression of *pmr* genes subsequently, which also led to the bacterial resistance to polymyxin B. The findings here also provided a molecular basis of the connector-mediated pathway in *K. pneumoniae*. The complexity in the control of *pmr* genes expression may provide ecological niches for *K. pneumoniae* in response to a variety of environmental clues, for example, in the process of infection.

2.5 Figure

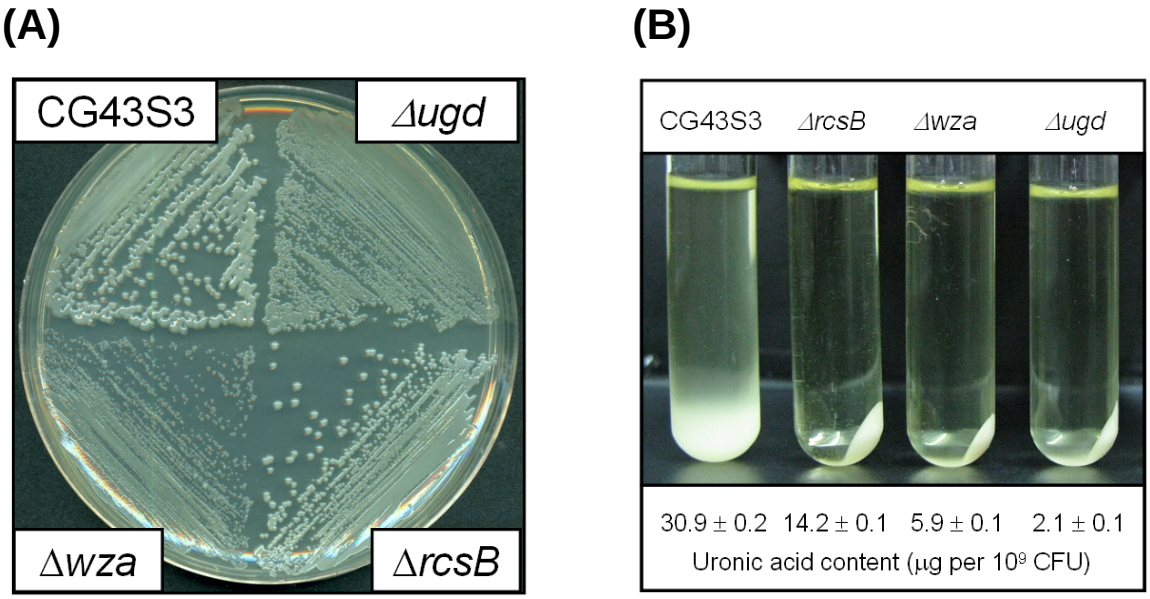
(A)
CG43S3
Δugd
Δwza
ΔrcsB
(B)
CG43S3
ΔrcsB
Δwza
Δugd
30.9 ± 0.2
14.2 ± 0.1
5.9 ± 0.1
2.1 ± 0.1
Uronic acid content (μg per 10⁹ CFU)

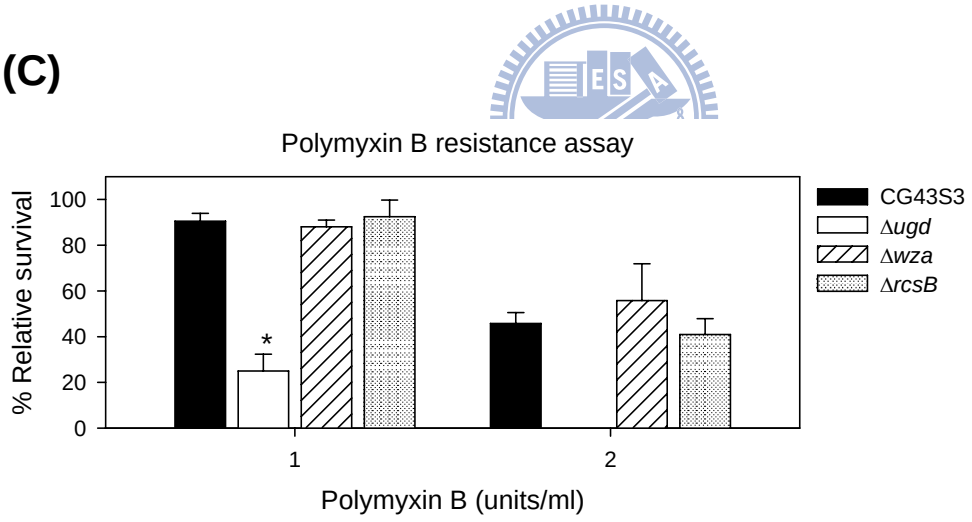
(C)
Polymyxin B resistance assay
% Relative survival
100
80
60
40
20
0
*
1
2
Polymyxin B (units/ml)
CG43S3
Δugd
Δwza
ΔrcsB

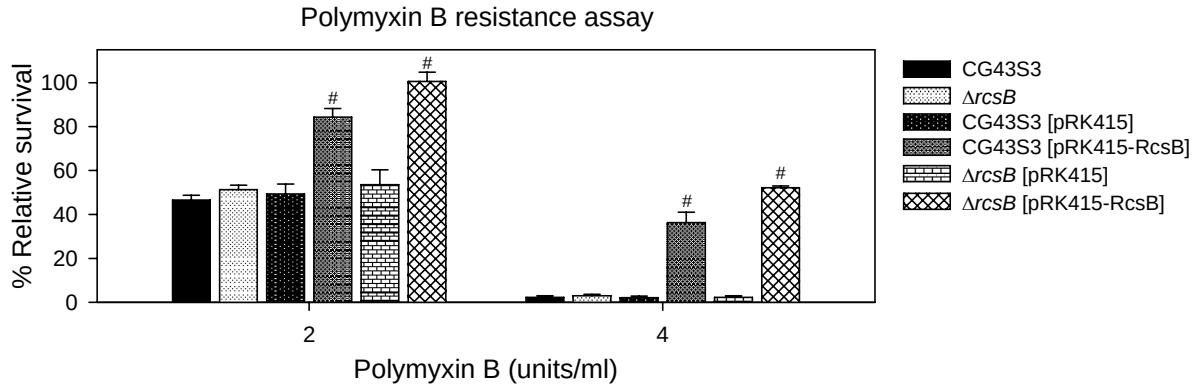
(D)
Polymyxin B resistance assay
% Relative survival
100
80
60
40
20
0
#
2
4
Polymyxin B (units/ml)
CG43S3
ΔrcsB
CG43S3 [pRK415]
CG43S3 [pRK415-RcsB]
ΔrcsB [pRK415]
ΔrcsB [pRK415-RcsB]

Fig. 2.1. Deletion effects of *ugd*, *wza* and *rcsB* genes on *K. pneumoniae* K2 CPS production and resistance to polymyxin B

(A) Comparison of colony morphology. The *K. pneumoniae* strains were streaked on an LB agar plate, incubated at 37℃ overnight and photographed. (B) Sedimentation test. The strains were cultured overnight in LB broth at 37 ℃ and subjected to centrifugation at 4,000 ×*g* for 5 min. Quantification of K2 CPS amounts of each strain is shown below the figure. Values are shown as averages ± standard deviations from triplicate samples. (C) Polymyxin resistance assay. The log-phased cultures of *K. pneumoniae* CG43S3, Δ*ugd*, Δ*wza* or Δ*rcsB* mutants were challenged with 1 or 2 units/mL of polymyxin B. (D) Polymyxin resistance assay. The log-phased culture of *K. pneumoniae* strains were challenged with 2 or 4 units/mL of polymyxin B. The survival rates are shown as the average ± standard deviations from triplicate samples. *, $P < 0.01$ compared with the parental strain CG43S3. #, $P < 0.01$ compared with each strain carrying pRK415.

(A)

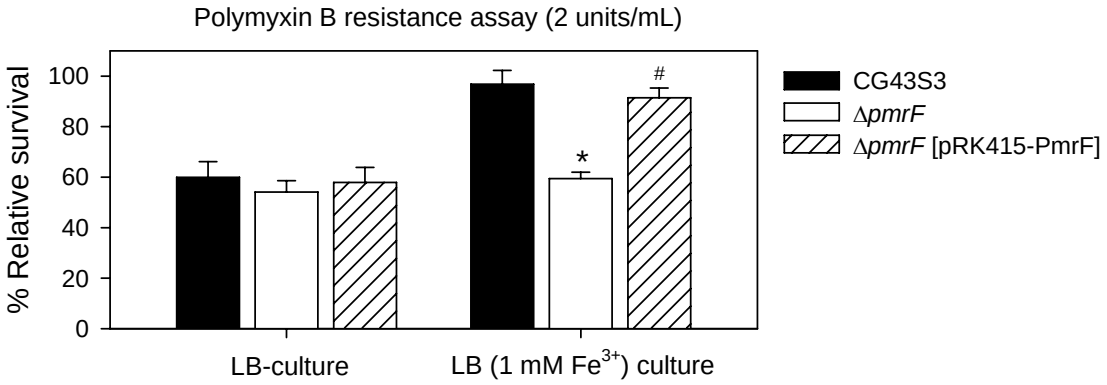

(B)

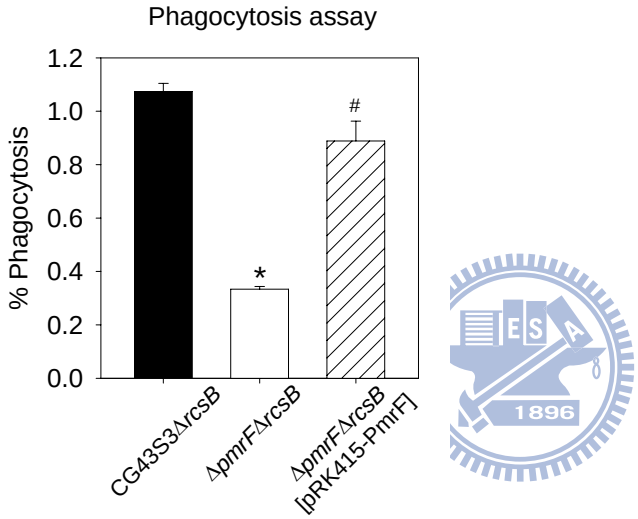

Fig. 2.2. Involvement of *K. pneumoniae pmrF* gene in polymyxin B resistance and intra-macrophage survival

(A) The log-phased cultures of *K. pneumoniae* CG43S3, the Δ*pmrF* mutant or Δ*pmrF* carrying pRK415-PmrF were grown in LB or LB supplemented with 1mM Fe^{3+} and then challenged with 2 units/mL of polymyxin B. The survival rates are shown as the average ± standard deviations from triplicate samples. (B) The survival rates of *K. pneumoniae* CG43S3Δ*rcsB*, the isogenic Δ*pmrF*Δ*rcsB* mutant, and Δ*pmrF*Δ*rcsB* mutant strain carrying the complementation plasmid pRK415-PmrF within the mouse macrophage RAW264.7 were determined. The results shown are relative survival rates which were calculated from the viable colony counts of intracellular bacteria divided by individual original inoculums. Values are shown as the average of five replicas. Error bars, standard deviations. *, $P < 0.01$ compared with the parental strain CG43S3. #, $P < 0.01$ compared with Δ*pmrF* mutant strain.

(A)

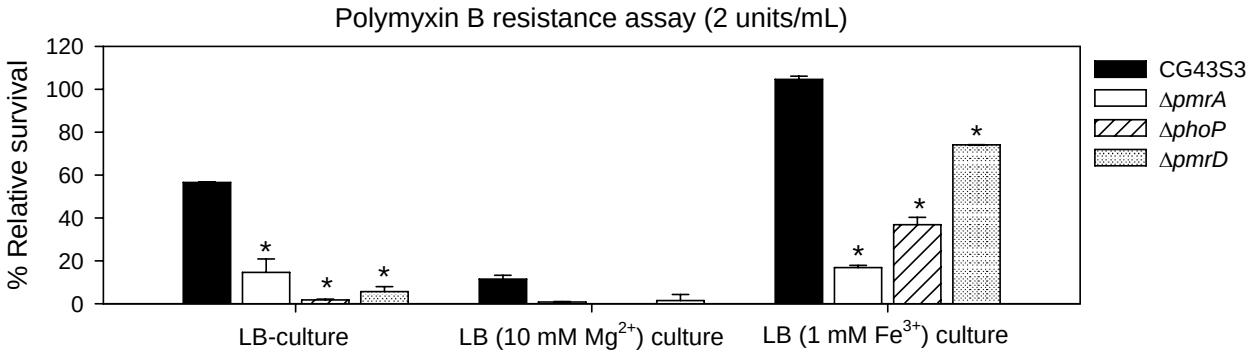
Polymyxin B resistance assay (2 units/mL)
% Relative survival
120
100
80
60
40
20
0
LB-culture
LB (10 mM Mg2+) culture
LB (1 mM Fe3+) culture
CG43S3
ΔpmrA
ΔphoP
ΔpmrD

(B)

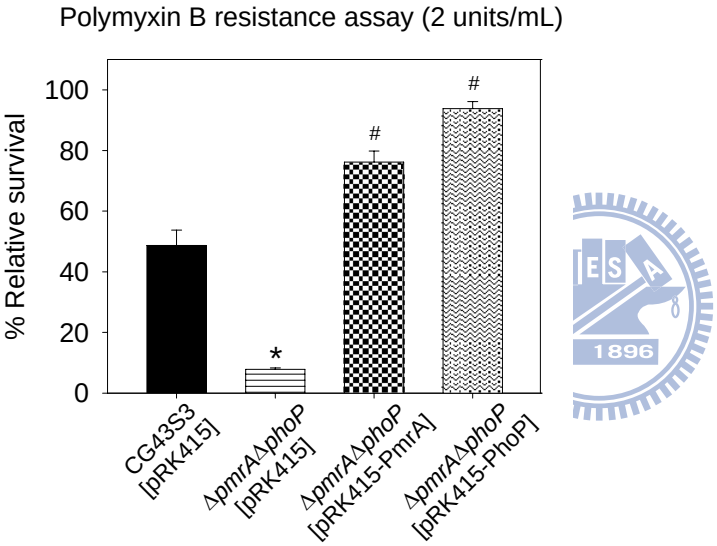
Polymyxin B resistance assay (2 units/mL)
% Relative survival
100
80
60
40
20
0
CG43S3 [pRK415]
ΔpmrAΔphoP [pRK415]
ΔpmrAΔphoP [pRK415-PmrA]
ΔpmrAΔphoP [pRK415-PhoP]

(C)

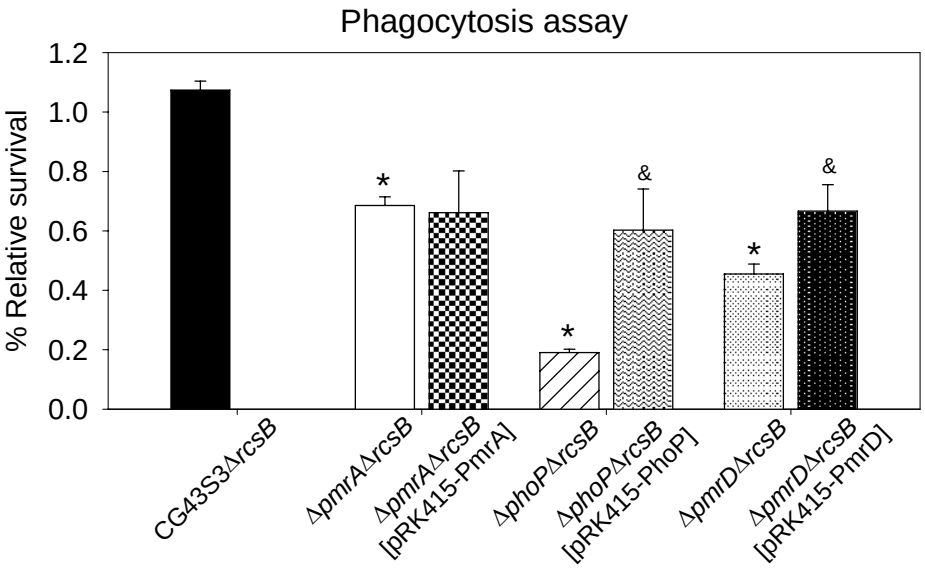
Phagocytosis assay
% Relative survival
1.2
1.0
0.8
0.6
0.4
0.2
0.0
CG43S3ΔrcsB
ΔpmrAΔrcsB
ΔpmrAΔrcsB [pRK415-PmrA]
ΔphoPΔrcsB
ΔphoPΔrcsB [pRK415-PhoP]
ΔpmrDΔrcsB
ΔpmrDΔrcsB [pRK415-PmrD]

Fig. 2.3. Effects of *K. pneumoniae pmrA*, *pmrD* and *phoP* deletion and complementation in polymyxin B resistance and intra-macrophage survival

(A) The log-phased cultures of *K. pneumoniae* CG43S3, the Δ*pmrA*, Δ*pmrD* or Δ*phoP* mutants were grown in LB, LB supplemented with 10 mM Mg^{2+} or LB supplemented with 1mM Fe^{3+} and then challenged with 2 units/mL of polymyxin B. The survival rates are shown as the average ± standard deviations from triplicate samples. (B) The log-phased cultures of *K. pneumoniae* CG43S3 carrying pRK415, the Δ*pmrA*Δ*phoP* mutant strains carrying pRK415, pRK415-PhoP or pRK415-PmrA were grown in LB and challenged with 2 units/mL of polymyxin B. The survival rates are shown as the average ± standard deviations from triplicate samples. (C) The survival rates of *K. pneumoniae* CG43S3Δ*rcsB*, the isogenic Δ*pmrA*Δ*rcsB*, Δ*phoP*Δ*rcsB* and Δ*pmrD*Δ*rcsB* mutants, and each mutant strain carrying the complementation plasmids pRK415-PmrA, pRK415-PhoP or pRK415-PmrD within the mouse macrophage RAW264.7 were determined. The results shown are relative survival rates which were calculated from the viable colony counts of intracellular bacteria divided by individual original inoculums. Values are shown as the average of five replicas. Error bars, standard deviations. *, $P < 0.01$ compared with the parental strain CG43S3 or CG43S3Δ*rcsB*. #, $P < 0.01$ compared with Δ*pmrA*Δ*phoP*[pRK415]. &, $P < 0.01$ compared with Δ*phoP*Δ*rcsB* or Δ*pmrD*Δ*rcsB*.

(A)

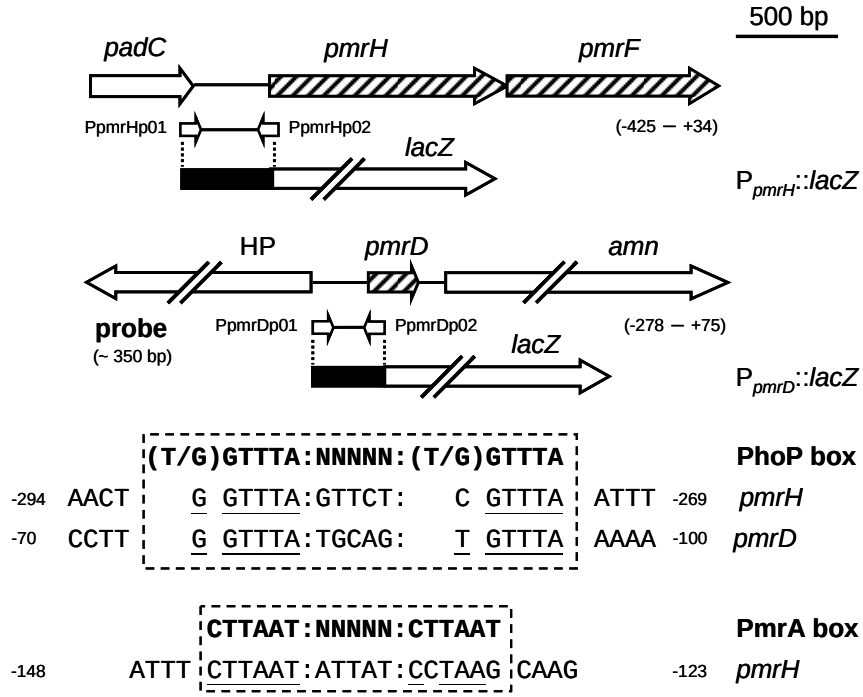
500 bp
padC
pmrH
pmrF
PpmrHp01
PpmrHp02
(-425 – +34)
lacZ
P pmrH ::lacZ
HP
pmrD
amn
probe
(~ 350 bp)
PpmrDp01
PpmrDp02
(-278 – +75)
lacZ
P pmrD ::lacZ
PhoP box
(T/G)GTTTA:NNNNN:(T/G)GTTTA
-294 AACT G GTTTA:GTTCT: C GTTTA ATTT -269 pmrH
-70 CCTT G GTTTA:TGCAG: T GTTTA AAAA -100 pmrD
PmrA box
CTTAAT:NNNNN:CTTAAT
-148 ATTT CTTAAT:ATTAT:CCTAAG CAAG -123 pmrH

(B)

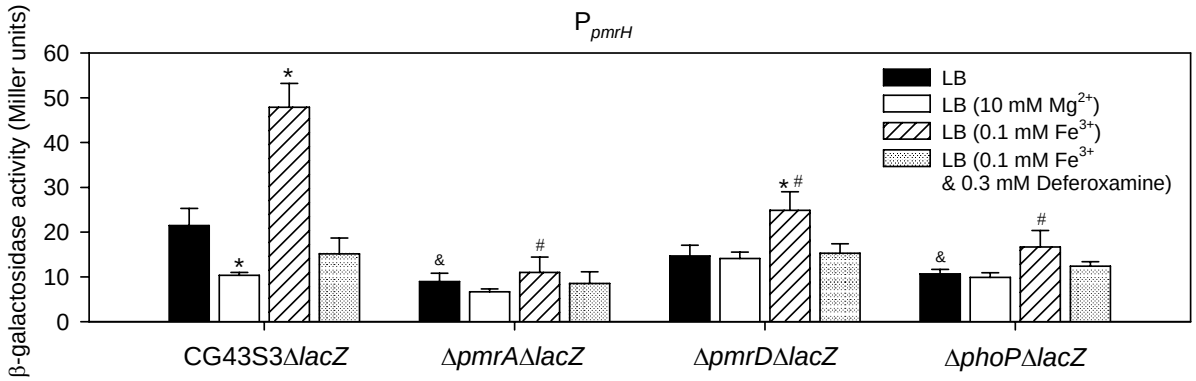
P pmrH
β-galactosidase activity (Miller units)
0
10
20
30
40
50
60
LB
LB (10 mM Mg2+)
LB (0.1 mM Fe3+)
LB (0.1 mM Fe3+ & 0.3 mM Deferoxamine)
CG43S3ΔlacZ
ΔpmrAΔlacZ
ΔpmrDΔlacZ
ΔphoPΔlacZ

(C)

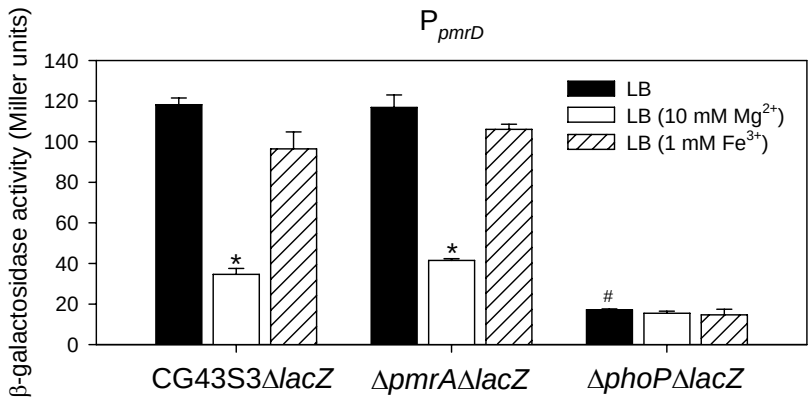
P pmrD
β-galactosidase activity (Miller units)
0
20
40
60
80
100
120
140
LB
LB (10 mM Mg2+)
LB (1 mM Fe3+)
CG43S3ΔlacZ
ΔpmrAΔlacZ
ΔphoPΔlacZ

Fig. 2.4. Schematic representation of *pmrH* and *pmrD* loci and determination of *K. pneumoniae* P_{pmrH}::*lacZ* and P_{pmrD}::*lacZ* activity

(A) Diagrammatic representation of the *pmrH* and *pmrD* loci. The large arrows represent the open reading frames. The relative positions of the primer sets used in PCR-amplification of the DNA fragments encompassing the P_{pmrH} and P_{pmrD} regions are indicated, and the numbers denote the relative positions to the translational start site. The name and approximate size of the DNA probes used in electro-mobility shift assay (EMSA) are shown on the left. The dashed boxes indicate the predicted PhoP and PmrA binding sequences and the alignment result is shown below. The identical nucleotide sequences are underlined. HP, hypothetical protein. (B) The β-galactosidase activities of log-phased cultures of *K. pneumoniae* strains carrying placZ15-PpmrH grown in conditions indicated in the figure were determined and expressed as Miller units. The data shown were the average ± standard deviations from triplicate samples. *, $P < 0.01$ compared with CG43S3Δ*lacZ* or Δ*pmrD*Δ*lacZ* mutant grown in LB medium. #, $P < 0.01$ compared with CG43S3Δ*lacZ* grown in LB medium supplemented with ferric ions. &, $P < 0.01$ compared with CG43S3Δ*lacZ* grown in LB medium. (C) The β-galactosidase activities of log-phased cultures of *K. pneumoniae* strains carrying placZ15-PpmrD grown in conditions indicated in the figure were determined and expressed as Miller units. The data shown were the average ± standard deviations from triplicate samples. *, $P < 0.01$ compared with CG43S3Δ*lacZ* or Δ*pmrA*Δ*lacZ* mutant grown in LB medium. #, $P < 0.01$ compared with CG43S3Δ*lacZ* grown in LB medium.

(A)

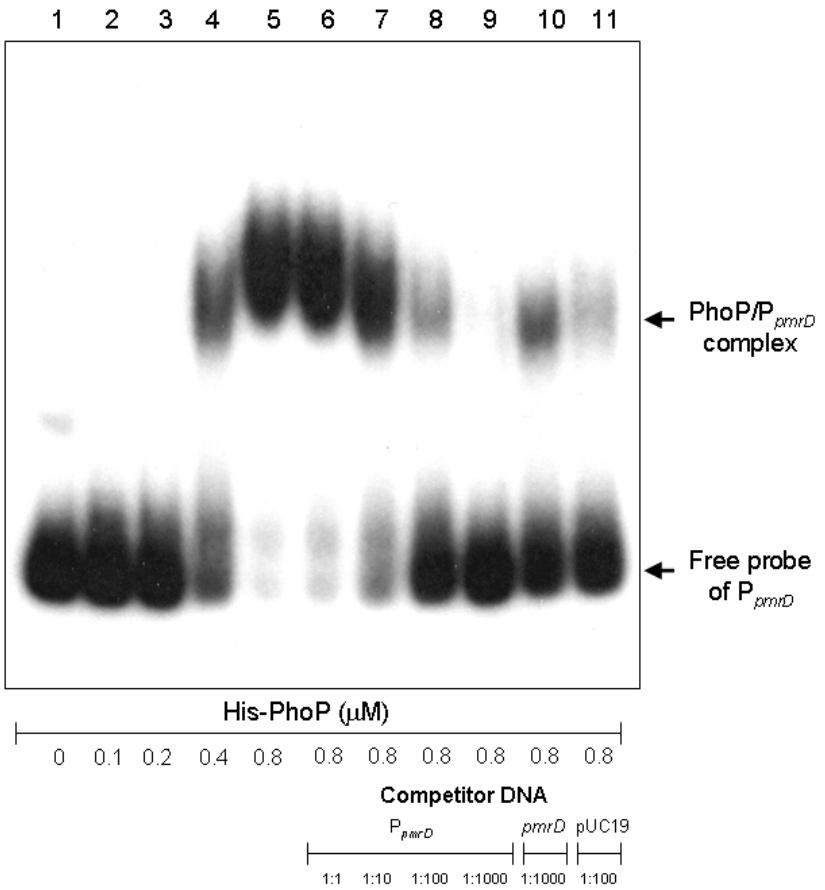
1 2 3 4 5 6 7 8 9 10 11
PhoP/P pmrD complex
Free probe of P pmrD
His-PhoP (μM)
0 0.1 0.2 0.4 0.8 0.8 0.8 0.8 0.8 0.8 0.8
Competitor DNA
P pmrD
pmrD
pUC19
1:1 1:10 1:100 1:1000 1:1000 1:100

(B)

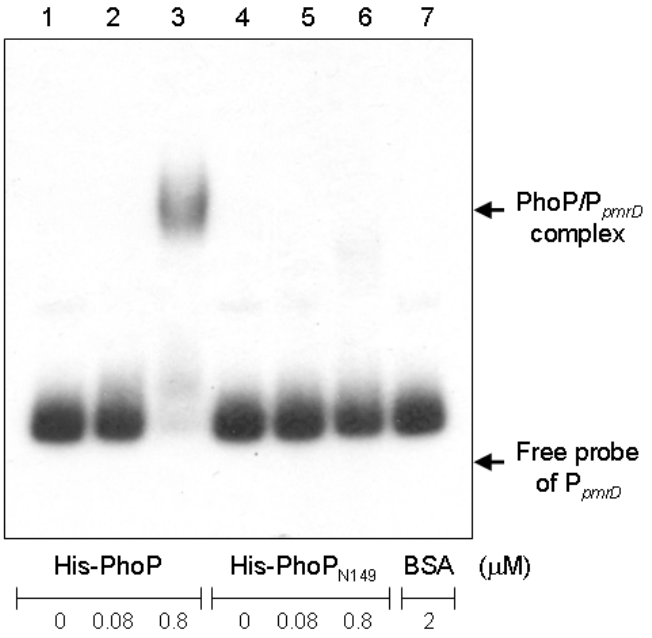
1 2 3 4 5 6 7
PhoP/P pmrD complex
Free probe of P pmrD
His-PhoP
His-PhoP N149
BSA
(μM)
0 0.08 0.8 0 0.08 0.8 2

Fig. 2.5. Binding of His-PhoP and His-PhoP$_{N149}$ to P$_{pmrD}$

(A) Specific binding of recombinant His-PhoP protein to the putative *pmrD* promoter. EMSA was performed by using the ^{32}P-labeled DNA probe of P$_{pmrD}$ incubated with increasing amounts of the His-PhoP (lanes 2 to 5), with 40 pmole of His-PhoP plus increasing amounts of the unlabeled P$_{pmrD}$ DNA (specific competitor, lane 6 to 9), or with excess amounts of non-specific competitor DNA (lane 10 and 11). The amounts of recombinant proteins and DNA probes used are indicated in the figure. (B) EMSA was performed with 0, 4 or 40 pmole of His-PhoP (lanes 1 to 3), His-PhoP$_{N149}$ (lanes 4 to 6) or 100 pmole of BSA (lane 7). The arrows indicate the PhoP/P$_{pmrD}$ complex and free probe of P$_{pmrD}$.

(A)

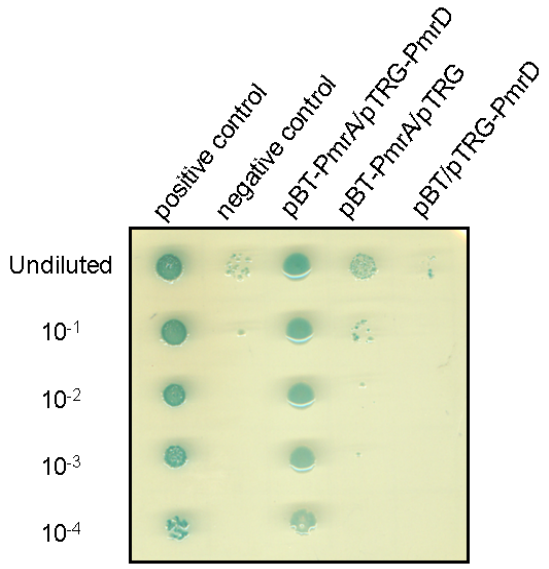
positive control
negative control
pBT-PmrA/pTRG-PmrD
pBT-PmrA/pTRG
pBT/pTRG-PmrD
Undiluted
10-1
10-2
10-3
10-4

(B)

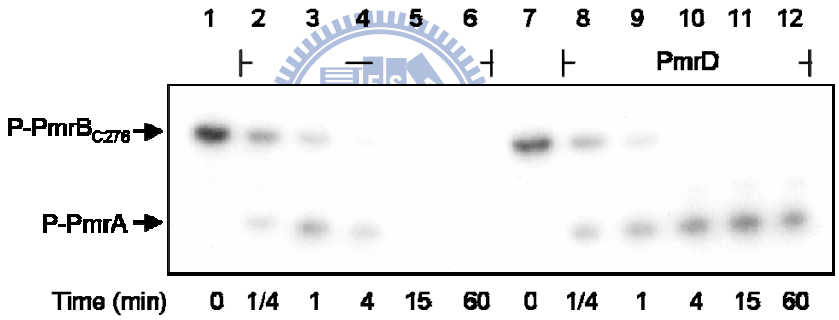
1 2 3 4 5 6 7 8 9 10 11 12
PmrD
P-PmrBC27S
P-PmrA
Time (min) 0 1/4 1 4 15 60 0 1/4 1 4 15 60

(C)

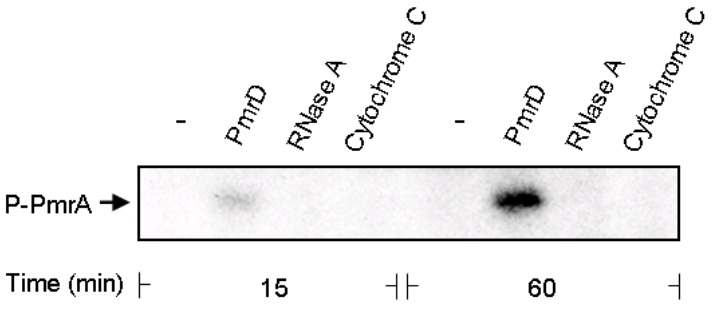
- PmrD RNase A Cytochrome C - PmrD RNase A Cytochrome C
P-PmrA
Time (min) 15 60

(D)

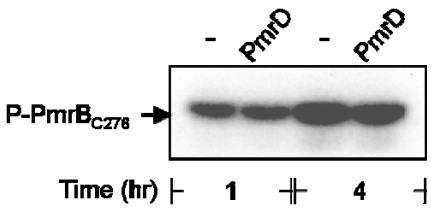
- PmrD - PmrD
P-PmrBC27S
Time (hr) 1 4

Fig. 2.6. *Klebsiella* PmrD interacts with PmrA to prevent dephosphorylation

(A) Bacterial two-hybrid analysis of PmrD/PmrA interaction *in vivo*. The *E. coli* XL1-Blue cells co-transformed with various combinations of pTRG and pBT-derived plasmids were diluted serially and spotted onto the indicator plate. The bacterial growth after 36h was investigated and photographed. Combinations of plasmids carried by each strain were indicated above the figure. (B) *Klebsiella* PmrD prevents the dephosphorylation of PmrA by its cognate sensor protein. The phosphorylation state of the recombinant His-PmrA protein was monitored upon the addition of the sensor protein His-$PmrB_{C276}$ in the presence (PmrD) or absence (-) of purified His-PmrD protein at specific time points as indicated. The arrows indicate phospho-PmrA (P-PmrA) and phospho-$PmrB_{C276}$ (P-$PmrB_{C276}$). (C) Kinase/phosphatase assay was carried out using the recombinant His-PmrA (final concentration 5 μM) and His-$PmrB_{C276}$ (final concentration 2.5 μM) in the presence (PmrD) or absence (-) of the recombintant His-PmrD protein (final concentration 5 μM). The small cationic proteins RNase A and cytochrome C were introduced individually as a negative control at a final concentration of 5 μM. (D) Autokinase assay of the recombinant His-$PmrB_{C276}$ (final concentration 2.5 μM) was performed in the presence (PmrD) or absence (-) of the recombintant His-PmrD protein (final concentration 5 μM).

(A)

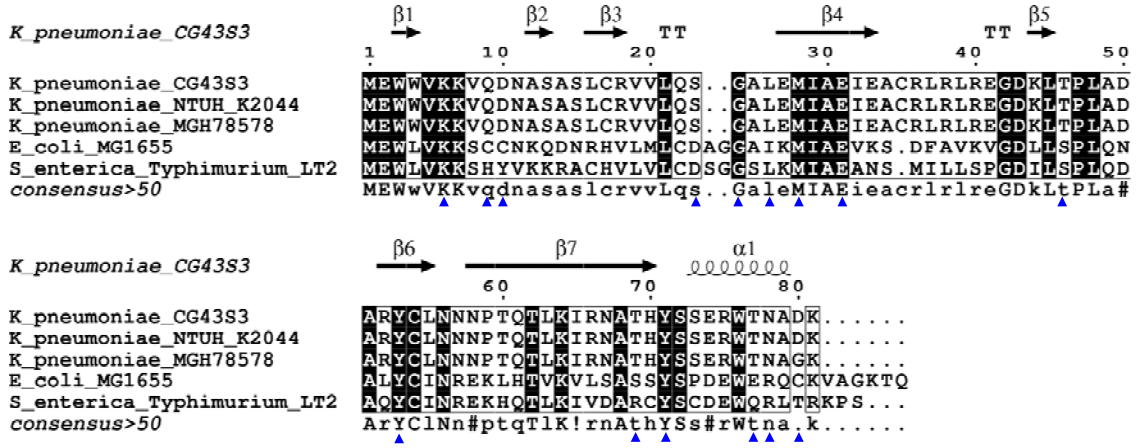
K_pneumoniae_CG43S3
β1 β2 β3 TT β4 TT β5
1 10 20 30 40 50
K_pneumoniae_CG43S3 MEWWVKKVQDNASASLCRVVLQS..GALEMIAEIEACRLRLREGDKLTPLAD
K_pneumoniae_NTUH_K2044 MEWWVKKVQDNASASLCRVVLQS..GALEMIAEIEACRLRLREGDKLTPLAD
K_pneumoniae_MGH78578 MEWWVKKVQDNASASLCRVVLQS..GALEMIAEIEACRLRLREGDKLTPLAD
E_coli_MG1655 MEWLVKKSCCNKQDNRHVLMLCDAGGAIKMIAEVKS.DFAVKVGDLLSPLQN
S_enterica_Typhimurium_LT2 MEWLVKKSHYVKKRACHVLVLCDSGGSLKMIAEANS.MILLSPGDILSPLQD
consensus>50 MEWwVKKvqdnasaslcrvvLqs..GaleMIAEieacrlrlreGDkLtPLa#
K_pneumoniae_CG43S3
β6 β7 α1
60 70 80
K_pneumoniae_CG43S3 ARYCLNNNPTQTLKIRNATHYSSERWTNADK.....
K_pneumoniae_NTUH_K2044 ARYCLNNNPTQTLKIRNATHYSSERWTNADK.....
K_pneumoniae_MGH78578 ARYCLNNNPTQTLKIRNATHYSSERWTNAGK.....
E_coli_MG1655 ALYCINREKLHTVKVLSASSYSPDEWERQCKVAGKTQ
S_enterica_Typhimurium_LT2 AQYCINREKHQTLKIVDARCYSCDEWQRLTRKPS...
consensus>50 ArYClNn#ptqTlK!rnAthYSs#rWtna.k.....

(B)

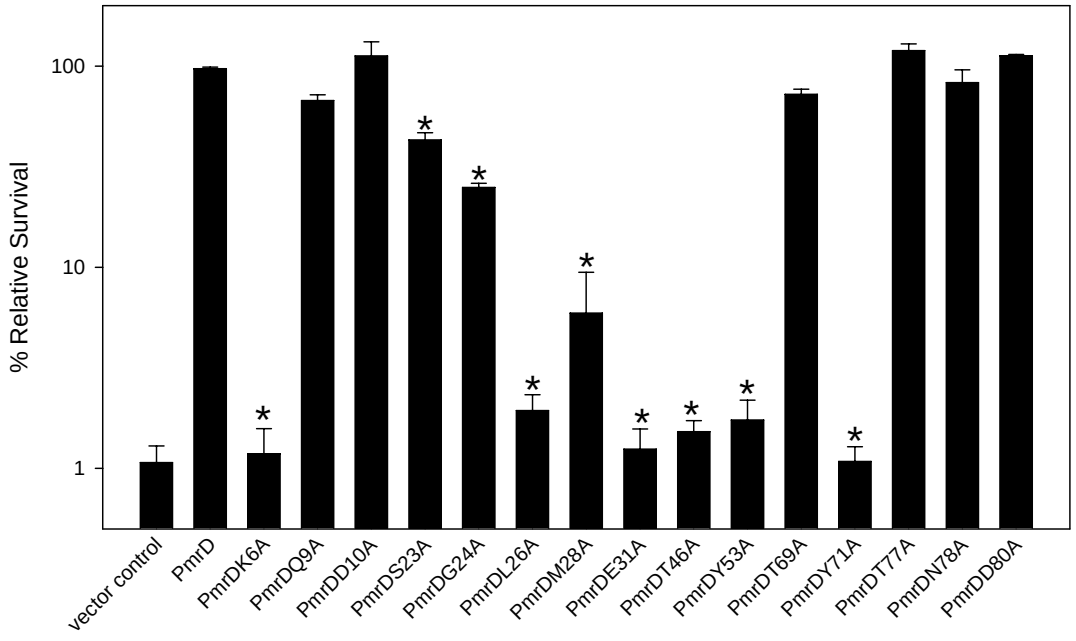
% Relative Survival
100
10
1
*
vector control
PmrD
PmrDK6A
PmrDQ9A
PmrDD10A
PmrDS23A
PmrDG24A
PmrDL26A
PmrDM28A
PmrDE31A
PmrDT46A
PmrDY53A
PmrDT69A
PmrDY71A
PmrDT77A
PmrDN78A
PmrDD80A

(C)

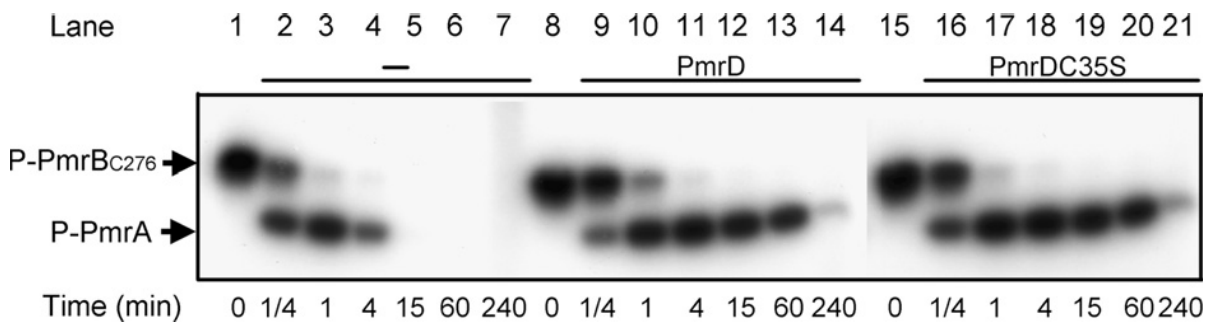
Lane 1 2 3 4 5 6 7 8 9 10 11 12 13 14 15 16 17 18 19 20 21
—
PmrD
PmrDC35S
P-PmrBC276
P-PmrA
Time (min) 0 1/4 1 4 15 60 240 0 1/4 1 4 15 60 240 0 1/4 1 4 15 60 240

Fig. 2.7. Identification of critical residues involved in *Klebsiella* PmrD functioning

(A) Sequence alignment of PmrD homologues from different bacterial species. The predicted secondary structural of *Klebsiella* PmrD was shown above the figure. Residues selected for the construction of plasmids encoding PmrD with point mutations were indicated by arrowheads. (B) The log-phased cultures of *K. pneumoniae* CG43S3Δ*pmrD* mutant strain carrying pRK415 (vector control), pRK415-PmrD (PmrD) or pRK415-PmrD derived plasmid encoding PmrD with each point mutation were grown in LB and then challenged with 4 units/mL of polymyxin B. The survival rates are shown as the average ± standard deviations from triplicate samples. *, $P < 0.01$ compared with each strain carrying pRK415-PmrD. (C) The phosphorylation state of the recombinant His-PmrA protein was monitored upon the addition of the sensor protein His-$PmrB_{C276}$ in the absence (-) or presence (PmrD or PmrDC35S) of purified His-PmrD or His-PmrDC35S proteins at specific time points as indicated. The arrows indicate phospho-PmrA (P-PmrA) and phospho-$PmrB_{C276}$ (P-$PmrB_{C276}$) respectively.

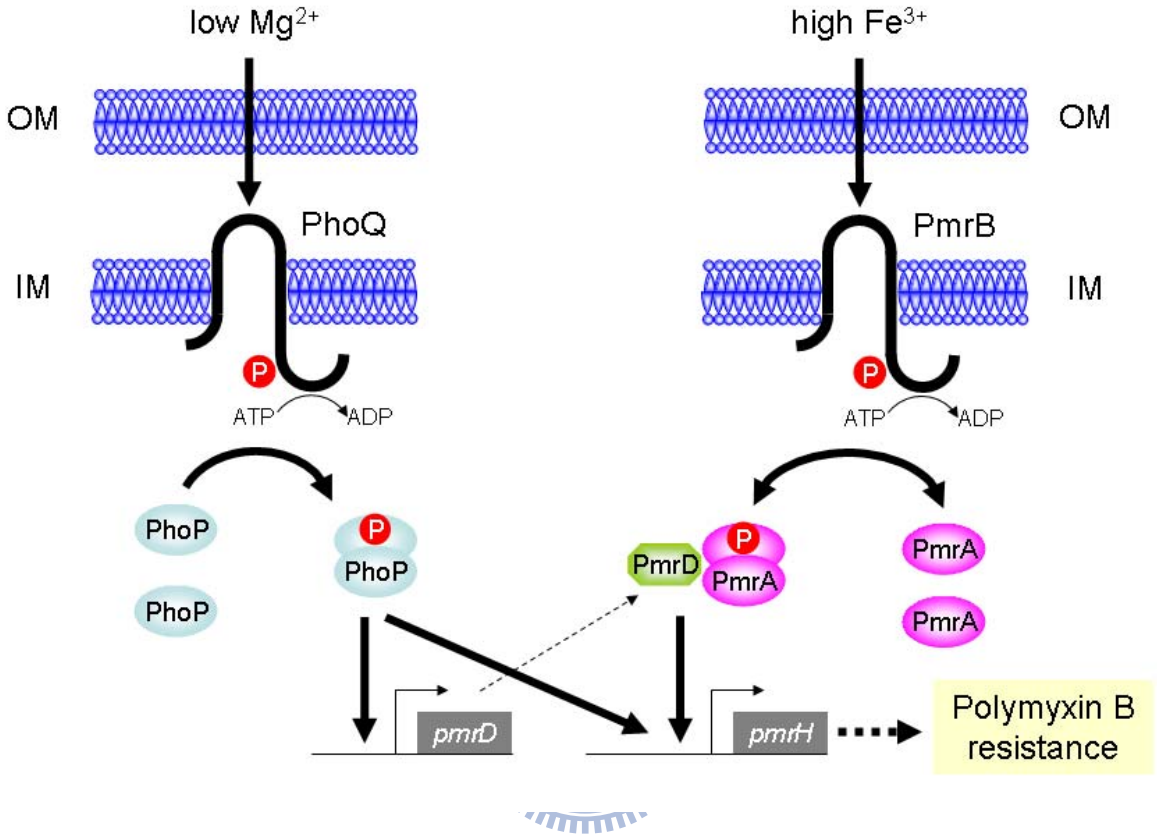

Fig. 2.8. A model illustrating the regulation of polymyxin B resistance in *K. pneumoniae* by PhoP/PhoQ, PmrD and PmrA/PmrB

When environmental magnesium concentrations are low (micro-molar), the PhoP/PhoQ system is turned on, resulting in the expression of *pmrD* through a direct binding of PhoP to P_{pmrD}. The PmrD protein then binds to the phosphorylated form of PmrA, which can also be generated when environmental ferric ion concentrations are high (sub-milimolar). Either PmrA or PhoP can activate the expression of *pmr* genes, eventually rendering the bacteria more resistant to polymyxin B.

CHAPTER 3

Functional Characterization of The Two-component System RstA/RstB in *Klebsiella pneumoniae* CG43

3.1 Abstract

The two component system (2CS) RstA/RstB has been reported as a member of another 2CS PhoP/PhoQ and has been implicated in the regulation of bacterial acid tolerance response, iron transport and the resistance against digestive tract stresses among several enteric bacteria. Firstly, to investigate the regulation of *rstA* expression in *Klebsiella pneumoniae*, the P_{rstA}::*lacZ* transcriptional fusion harboring a DNA fragment encompassing the putative *rstA* promoter region was constructed. Expression of P_{rstA}::*lacZ* was reduced in Δ*phoP* or Δ*rstA* mutant strains, indicating a positive regulatory role of PhoP and RstA. Subsequently, to explore the functional role of RstA/RstB in *K. pneumoniae*, subtractive cDNA hybridization was performed, yielding a total of 11 RstA-activated genes and 19 RstA-repressed genes involved in various cellular functions. Comparative phenotype analyses, including the bacterial growth under iron depletion/repletion conditions, lead resistance, siderophore production, acid stress response and resistance to bile salts, of the wild-type, Δ*rstA*, Δ*rstB* and Δ*rstA*Δ*rstB* mutant strains were carried out. None of the assays yielded results in which the deletion mutants exhibited behaviors apparently different from those observed in the parental strain. This indicates the functional role of RstA/RstB still requires further investigation.

3.2 Introduction

The signal transduction cascade governed by 2CS has been shown to be important in the expression of virulence factors during infections or involved in bacterial survival in hostile environments (12). For example, PhoP/PhoQ, perhaps the most completely characterized 2CS to date, governs the Mg^{2+} regulon and a repertoire of virulence genes in *Salmonella enterica* (8, 90, 164), and is also required for virulence in *Erwinia chrysanthemi* (149), *Neisseria meningitides* (179), *Yersinia pestis* (101), *Pseudomonas aeruginosa* (82, 83) and *Photorhabdus luminescens* (49). In addition to the typical mode of regulation, PhoP-regulated genes can also be expressed when activated by another 2CS PmrA/PmrB through the connector protein PmrD, which in turn activated the bacterial resistance to polymyxin B (59, 117).

Compared with the well-documented characterization of the 2CS PmrA/PmrB, the functional role of RstA/RstB, another 2CS regulated by PhoP/PhoQ, has remained relatively unclear and explored mostly by genome-wide studies (99, 100, 264). Previously, *rstA* was identified as a multicopy suppressor for an essential ATPase encoding gene in *Escherichia coli* K12 (29), and recently a more complex network involving YeaZ and YgiD has implied a functional role of RstA between DNA metabolism and cell division (96). RstA/RstB was also speculated to be involved in bacterial acid resistance since *asr*, which encodes acid shock RNA (214, 228), was identified as one of its downstream targets by genomic SELEX search (183). In *S. enterica*, RstA was found to be able to induce RpoS degradation (28) and modulated Fur activity via the activation of the ferrous iron transporter FeoB (111). More recently, *Salmonella* PhoP/PhoQ was found to either activate iron transporter encoding gene *feoB* through RstA or to induce the expression of *mgtA* encoding the magnesium transporter in response to different environmental signals (41). Moreover, a comprehensive study on mutations of all 2CS response regulator encoding genes in *Yersinia pesudotuberculosis* has indicated the involvement of RstA in bacterial resistance to the stresses encountered in the digestive tract (69).

Sequence analysis of the *rstAB* locus in different bacterial species showed that the gene organization of *K. pneumoniae rstAB* was similar to its counterpart in *S. enterica* in which the two genes were separated rather than physically linked, as was the case in *E. coli*. To search for the downstream genes of RstA/RstB in *K. pneumoniae*, subtractive cDNA hybridization was preformed to identify cDNA fragments specifically present in the wild-type strain or in

the isogenic *rstA* mutant strain lacking the response regulator encoding gene. Phenotypic comparison of the parental strain to the *K. pneumoniae* Δ*rstA*, Δ*rstB* mutant which lacked the sensor kinase encoding gene and the Δ*rstA*Δ*rstB* double mutant strain was performed in order to validate the functional role of RstA/RstB.

3.3 Results

3.3.1 Regulation of *rstA* expression in *K. pneumoniae* CG43

A close examination of the *K. pneumoniae rstAB* region has revealed a PhoP box-like sequence as identified in *E. coli* (120) and *S. enterica* (220). In addition, sequence analysis has indicated the presence of the RstA box recently identified by a genomic SELEX search (183) (Fig. 3.1A). To investigate if the expression of *K. pneumoniae rstA* was subjected to the regulation by PhoP/PhoQ and RstA/RstB, reporter plasmids pHY048, pHY050 and pHY053 each carried a transcriptional fusion of the *rstA* upstream region to a *lacZ* gene were constructed. Results from the reporter assay in Fig. 3.1B indicated that RstA and PhoP were both required in the activation of *rstA* expression, as shown by the reduction of promoter activity in the Δ*rstA*, Δ*phoP* or Δ*rstA*Δ*phoP* mutant strains carrying pHY048 or pHY050. The promoter activity in strains harboring pHY053, which did not contain the PhoP box-like sequence, was largely reduced suggesting a major role of PhoP in *rstA* expression. Nevertheless, the activity in strains carrying pHY053 was not reduced to levels exhibited by strains with vector alone. As a result, the role of other factors such RstA could not be underestimated. The notion that the activities of strain carrying pHY048 or pHY053 was not abolished in Δ*rstA*Δ*phoP* mutant further supported the hypothesis that factors other than PhoP or RstA may still be involved in *rstA* expression in *K. pneumoniae*.

3.3.2 Identification of RstA-regulated genes by subtractive cDNA hybridization

To explore the functional role of RstA/RstB in *K. pneumoniae*, subtractive cDNA hybridization was anticipated to search for genes expressed only in the parental strain or in the Δ*rstA* mutant. Since the promoter activity of strains carrying pHY048 in M9 medium was more than twice as those in LB medium (Fig. 3.2A), it would be conceivable that the a greater number of RstA-regulated genes would be recovered in this condition. Therefore the experiment was performed by using total RNA extracted from M9-grown cultures. The result of second PCR amplification was shown in Fig. 3.2B indicating either the RstA-repressed genes (lane 1) or RstA-activated genes (lane2), each representing differentially-expressed DNA sequences specifically present in the Δ*rstA* mutant or in the parental strain. The distinct PCR-amplicon patterns also indicated a successful hybridization procedure. Subsequently, the DNA fragments were cloned into yT&A, subjected to sequencing determination, and the sequences were compared in the currently available genome sequences of *K. pneumoniae*

NTUH-K2044 (262), MGH78578 (http://genome.wustl.edu/), and 342 (74) by BLAST (http://www.ncbi.nlm.nih.gov). The genes were classified according to their predicted functions as shown in Table 3.1 (for RstA-activated genes) and Table 3.2 (for RstA-repressed genes).

3.3.3 Sequence analysis of RstA-regulated genes

The results from nucleotide sequence determination are shown in Table 3.1 and Table 3.2. A total of 11 RstA-activated genes were identified, and a search in the documents has revealed a wide range of cellular functions involved, including *fecE* encoding an iron dicitrate transport ATP-binding protein (19, 211), *yieP* encoding an ion channel protein, two open reading frames each with a conserved GGDEF or EAL domain involved in cyclic di-GMP metabolism (98, 206, 210, 234), *gabP* encoding an RpoS-dependent γ-aminobutyrate transport protein (21, 208), *yifP* encoding a putative esterase, *ybeF* encoding a LysR family transcriptional regulator, *mnmA* encoding a tRNA methyltransferase involved in *E. coli* tRNA thiolation (114, 182), *tldD* encoding a DNA gyrase modulator involved in the peptide antibiotic microcin processing and antidote degradation (1, 173) and two open reading frames encoding hypothetical proteins with unknown functions.

Sequence analysis of the retrieved 19 DNA fragments representing the RstA-repressed genes has also revealed the involvement of numerous cellular functions such as *iroN* encoding an enterochelin and dihydrobenzoic acid receptor (33, 190, 221), *pbrR* encoding a regulator for the bacterial resistance to heavy metal (16, 112, 194, 232), four genes encoding integral membrane protein or transporter proteins such as *mgtE* encoding a magnesium transporter (3, 97, 110), *hmuR* encoding an outer membrane receptor for hemoglobin uptake (216, 238), an open reading frame encoding a fimbrial protein, an open reading frame encoding a β-lactamase-like protein, an open reading frame encoding a putative glycosyl transferase, *gpmB* encoding a phosphoglycerate mutase (231), *gshB* encoding a glutathione synthetase (141, 184), an open reading frame encoding a putative acetyltransferase, *dnaK* encoding a molecular chaperone (79), *ppk* encoding a polyphosphate kinase (26), *yeaG* encoding an RpoS-dependent serine kinase belonging to the stress response regulon (109, 233, 249) and two open reading frames encoding hypothetical proteins with unknown functions. Based on the findings from cDNA subtraction and previous studies (41, 69, 111, 214), it was of interest to investigate if *K. pneumoniae* RstA/RstB played a role in bacterial growth under iron-depletion/repletion conditions, resistance to lead, siderophore biosynthesis and resistances to stress encountered in the digestive tract.

3.3.4 Effect of iron on the growth of *K. pneumoniae* strains in rich and minimal medium

It has been reported that the two component system RstA/RstB is involved in iron transport in *S. enterica* (111). Furthermore, subtractive cDNA hybridization has revealed that an iron transporter is among RstA-activated genes. Therefore, the growth of *K. pneumoniae* wild type along with Δ*rstA*, Δ*rstB*, and Δ*rstA*Δ*rstB* mutant strains under the iron depletion or repletion conditions was investigated. As shown in Fig. 3.3A, strains grown in LB medium reached an OD_{600} of as high as 1.2 in 6 hours while those grown in LB containing 2',2'-dipyridyl only reached an OD_{600} of 0.7. The addition of 2',2'-dipyridyl resulted in an overall slower bacterial growth in LB medium. To further verify the effect of iron on bacterial growth, strains were grown in M9 minimal medium for the growth curve measurement. As shown in Fig. 3.3B, the strains reach an OD_{600} of 1.0 in 7 hours when grown in M9 medium while the addition of Fe^{2+} to the medium resulted in a higher OD_{600} of 1.2. The growth rates of the strains were similar; neither the iron depletion nor repletion significantly altered bacterial growth.

3.3.5 Effect of lead on the growth of *K. pneumoniae* strains

Initially a disc assay was employed to investigate bacterial resistance to lead; however, when lead nitrate discs were placed on LB, M9 or HMM (heavy metal MOPS) agar plates (132), the lead appeared to react with compounds such as phosphates in the medium and precipitates formed in rings around the discs rapidly. As a result, the growth inhibition assay was performed in HMM broth (132). Results in Fig. 3.4A show that there is evident growth inhibition at and beyond 10 μM Pb^{2+} for *K. pneumoniae* CG43-101, a derivative of *K. pneumoniae* CG43 deprived of a large resident plasmid pLVPK carrying the lead resistance *pbr* gene cluster (37). When the microtiter plate assay was implemented with the wild type strain CG43S3, the Δ*rstA*, Δ*rstB* and Δ*rstA*Δ*rstB* mutants, more gradual growth inhibition patterns were observed (Fig. 3.4B). The four strains, while differing slightly in their growths at the range of lead concentrations tested, did not show as clear and abrupt inhibition patterns as observed in CG43-101. At concentrations below 10 μM Pb^{2+}, several of the strains reach relative growths greater than one, signifying no growth inhibition at these concentrations. Furthermore, the Δ*rstB* mutant strain exhibited growth comparable to that of the wild type, while Δ*rstA* and Δ*rstA*Δ*rstB* mutants displayed slightly lower relative growths in medium supplemented with the same concentrations of lead nitrate. In the presence of 20 μM Pb^{2+}, Δ*rstB* and Δ*rstA*Δ*rstB* mutants exhibited a relative growth generally higher than the parental

strain CG43S3 while in the presence of 40 μM Pb^{2+}, a notable growth inhibition in all strains was observed. At the highest concentration of 80 μM Pb^{2+}, relative growths of around 0.3 were observed. Based on the result of cDNA subtraction, deletion of *rstA* was expected to enhance the bacterial resistance to lead. However, the finding that deletion of *rstA* exerted no apparent effect may have implied a more complicated regulation. Though how RstB exerted it effect and the interplay of RstA still required further investigation, the observation that a slightly higher resistance in Δ*rstB* and Δ*rstA*Δ*rstB* mutants, as exemplified by a higher relative growth at 20 μM Pb^{2+} compared with CG43S3 and Δ*rstA* mutant, has implied a role of RstB in the regulation of bacterial lead resistance.

3.3.6 Siderophore biosynthesis of *K. pneumoniae* strains

To investigate if RstA/RstB was involved in the siderophore biosynthesis, cultures of *K. pneumoniae* strains were spotted on CAS agar plates for phenotype analysis. As shown in Fig. 3.5A, siderophore biosynthesis was evident as shown by the orange zone around the Δ*fur* mutant strain since the global regulator Fur has been shown to repress the expression of aerobactin biosynthesis genes *iucABCD* (18, 229) and enterochelin biosynthesis genes *iroBCDEN* (171, 221). The faint color zones around CG43, CG43S3, and CG43-101 were essentially indistinguishable, indicating low levels of siderophore production. No apparent difference between the Δ*rstA*, Δ*rstB*, Δ*rstA*Δ*rstB* mutants and the parental strain CG43S3 was found, implying that *K. pneumoniae* siderophore biosynthesis was RstA/RstB independent.

3.3.7 Acid tolerance response of *K. pneumoniae* strains

To test if RstA/RstB played a role in *K. pneumoniae* acid tolerance, the survival rates of strains after being acid challenged were determined at different time points. First, a pilot study was performed to determine whether acid resistance of *K. pneumoniae* could be induced after pre-adaptation, as observed in other enteric bacteria such as *S. enterica* (94). As shown in Fig. 3.6A, both the CG43S3 cultures undergoing adaptation at pH 4.5 in LB or M9 medium displayed survivals 10-fold higher than did cultures without the adaptation. Acid resistance of the cultures without pre-adaptation appeared to be higher when grown in M9 rather than when grown in LB, especially at 60 and 90 min post-challenge. Results also indicated that the adaptation resulted in comparable levels of increase in bacterial survival whether strains were grown in LB or in M9 medium. Since the expression of *rstA* appeared to be higher when strains were grown in M9 medium (Fig. 3.2A), the effect of *rstA* and/or *rstB* deletion was investigated in M9-adapted cultures. The results in Fig. 3.6B showed that the

deletion of *rstA*, *rstB*, and *rstArstB* did not considerably affect bacterial survival rates since the strains displayed a similarly close percent survival at the time points investigated. The finding that the deletion of *rcsB* resulted in a slightly lower level of acid tolerance than the parental strain was consistent with the observation in *E. coli* (31, 32). No apparent difference was observed among survival rates of *K. pneumoniae* CG43S3, Δ*rstA*, Δ*rstB* and Δ*rstA*Δ*rstB* mutant, implying that RstA/RstB was not involved in the acid tolerance in *K. pneumoniae*.

3.3.8 Bile salt resistance of *K. pneumoniae* strains

Since the deletion of *rstA* has been shown to affect bacterial resistance to digestive tract stress in *Y. pseudotuberculosis* (69), whether RstA/RstB was involved in *K. pneumoniae* resistance to bile salt, one of the detergent-like bactericidal agent, was investigated. Cultures of *K. pneumoniae* strains were spotted onto LB or M9 agar plates with increasing concentrations of bile salts, and the bacterial growth was observed. As shown in Fig. 3.7, bacterial growth was inhibited as concentrations of bile salt in the medium increased. While the growth inhibition was similar in strains grown in LB or M9 medium, no apparent differences CG43S3, Δ*rstA*, Δ*rstB* and Δ*rstA*Δ*rstB* mutants were observed, suggesting a similar resistance among strains investigated.

3.4 Discussion

The purpose of this study was to investigate the functional role of the 2CS RstA/RstB in *K. pneumoniae* CG43. First, the finding that deletion of *phoP* or *rstA* would result in a reduction of *rstA* expression (Fig. 3.1B) was not surprising since a similar phenomenon has been observed (140, 183). While the precise binding sites of PhoP or RstA required further verification, the possibility of factors other than PhoP and RstA regulating *rstA* expression could not be ruled out since the P_{rstA}::*lacZ* activity was not totally eliminated in Δ*rstA*Δ*phoP* mutant strain (Fig. 3.1B, compared with vector control).

The result from cDNA subtraction has indicated a role of RstA/RstB in the iron metabolism, which has also been reported in *S. enterica* (111). However, there was no apparent difference between the growth rate of these *K. pneumoniae* strains under iron-depletion and repletion conditions (Fig. 3.3) or siderophore biosynthesis (Fig. 3.5). It is speculated that the lack of phenotypic differences between the strains in the conducted assays may be a result of a different, or several different, unknown response regulator(s) influencing downstream genes that control behaviors investigated in this study**.** In *S. enterica* Typhimurium, for example, the gene controlling iron uptake is regulated not only by RstA, but also by the global ferric uptake regulator Fur (111). The results indicated that the interplay of other systems involved in iron homeostasis could not be underestimated.

The results from subtractive cDNA hybridization have also implied a role of RstA in lead resistance. While all strains reflected similar relative growth rates in growth inhibition assay (Fig. 3.4), RstA/RstB may not be directly involved in the regulation. Similar acid tolerance was shown in the survival rates of all tested strains, and even when slight differences in survival appeared at later time points, deviations were never over tenfold (Fig. 3.6). In the bile salt resistance assay, no prominent phenotypic differences were observed between the strains tested in any of the medium, dilutions, or bile salt concentrations (Fig. 3.7). The acid resistance in enteric bacteria was extremely complicated involving at least four regulatory systems (72). Different acid resistance system may regulate a different subset of genes; therefore the acid tolerance response would be a convergence of multiple systems. Moreover, since all the phenotype analysis was conducted by using *in vitro* models, whether RstA/RstB could play a role during *K. pneumoniae* infections still called for investigations *in vivo*. For example, to explore the role of RstA/RstB in bacterial resistance to such stresses related to the gastrointestinal tract, it would be of importance to determine the competitive

index of CG43S3 and Δ*rstA* mutant after oral administration to mice, which would help to verify the role of RstA/RstB in bacterial behavior *in vivo*.

Previous attempts to verify the results from cDNA subtraction using Northern slot blot have failed to distinguish the levels of the transcripts from the CG43S3 and Δ*rstA* mutant strain, which may be due to the relatively low expression levels of the genes identified in comparison with 23S rRNA gene control. As a result, the regulation of RstA on the genes identified by cDNA subtraction would require further investigation via limiting-dilution RT-PCR or more sensitive methods such as real-time RT-PCR to provide a quantitative comparison. The screening of drug resistance in *E. coli* over-expressing of all response regulator encoding genes has indicated a role of RstA in the resistance to fosfomycin and crystal violet (99). A similar screening on the resistance to antimicrobial agents has also been performed by using *E. coli* strains over-producing recombinant RstA proteins or *K. pneumoniae* CG43S3Δ*rstA* mutant carrying an *rstA* expression plasmid via disc assay. However, no apparent increase in the drug resistance was noted in the tested strains. Despite this, the phenotypes implicated from cDNA subtraction or previous studies could be further analyzed by using *K. pneumoniae* strains over-producing RstA.

While this study indicates that the RstA/RstB system may not directly influence the phenotypes tested, the possibility still exists that the 2CS may be indirectly involved with other cascading pathways. Additional study branching from the results and conjectures made in this study can provide further insight into the network built around RstA/RstB and other 2CSs.

3.5 Table

Table 3.1. RstA-activated genes identified by subtractive cDNA hybridization

Predicted function	Homologous gene (Accession no.)	Predicted protein	% Identity (length of comparable amino acid sequence, no. of residues)
Iron transporter	*K. pneumoniae fecE* (BAH63871)	iron(III) dicitrate transport ATP-binding protein	100% (198)
Ion channel	*K. pneumoniae yjeP* (BAH61311)	mechanosensitive ion channel family protein	97% (242)
Cyclic di-GMP metabolism	*K. pneumoniae* KPN_00268 (ABR75721)	cyclic diguanylate phosphodiesterase (EAL) protein	40% (117)
	K. pneumoniae KP1_3652 (BAH64237)	hypothetical protein (GGDEF domain)	97% (44)
Transport proteins	*K. pneumoniae gabP* (BAH61898)	RpoS-dependent gamma-aminobutyrate transport protein	92% (36)
Lipid metabolism	*K. pneumoniae yjfP* (BAH61336)	putative esterase	94% (89)
Regulatory proteins	*K. pneumoniae ybeF* (BAH62363)	putative LysR family transcriptional regulator	97% (131)
tRNA modification	*K. pneumoniae mnmA* (BAH62849)	tRNA (5-methylaminomethyl-2-thiouridylate)-methyltransferase	95% (85)
DNA metabolism	*K. pneumoniae tldD* (BAH65428)	Putative modulator of DNA gyrase	92% (158)
Hypothetical protein	*K. pneumoniae yjcD* (BAH61222)	hypothetical protein	100%(98)
	K. pneumoniae KP1_4995 (BAH65452)	hypothetical protein	92% (38)

48

Table 3.2. RstA-repressed genes identified by subtractive cDNA hybridization

Predicted function	Homologous gene (Accession no.)	Predicted protein	% Identity (length of comparable amino acid sequence, no. of residues)
Iron acquisition	*K. pneumoniae iroN* (BAH64199)	enterochelin and dihydrobenzoic acid receptor	92% (231)
Metal resistance	*K. pneumoniae pbrR* (BAH66039)	metal ion-sensing regulatory protein	99% (132)
Transporter proteins	*K. pneumoniae* KP1_0566 (BAH61430))	putative ABC transporter	98% (177)
	K. pneumoniae ybeX (BAH62385)	putative integral membrane protein	99% (207)
	K. pneumoniae KP1_1781 (BAH62516)	putative general substrate transporter	97% (163)
	K. pneumoniae mgtE (BAH64426)	putative divalent cation transport protein	99% (139)
Receptor proteins	*K. pneumoniae hmuR* (BAF76156)	TonB-dependent outer membrane receptor	100% (42)
Fimbrial proteins	*K. pneumoniae* KP1_4251 (BAH64781)	putative fimbrial-like protein	98% (116)
Antibiotic resistance	*K. pneumoniae* KP1_5391 (BAH65810)	putative beta-lactamase-like protein	98% (218)
Energy metabolism	*K. pneumoniae nuoI* (BAH64467)	NADH dehydrogenase subunit I	97% (132)
Sugar metabolism	*K. pneumoniae* KPN_00998 (ABR76434)	putative glycosyl transferase, group I	93% (103)
	K. pneumoniae gpmB (BAH61648)	phosphoglycerate mutase	97% (146)
Glutathione biosynthesis	*K. pneumoniae gshB* (BAH65148)	glutathione synthetase	95% (132)
Protein modification	*K. pneumoniae* KP1_1405 (BAH62174)	putative GNAT-family acetyltransferase	100% (68)
Protein folding	*K. pneumoniae dnaK* (BAH61668)	molecular chaperone	99% (248)
Regulatory proteins	*K. pneumoniae ppk* (BAH64622)	polyphosphate kinase	99% (119)
	K. pneumoniae yeaG (ABR76626)	RpoS-dependent stress kinase	95% (178)
Hypothetical protein	*K. pneumoniae* KP1_0493 (BAH61369)	hypothetical protein	69% (41)
	K. pneumoniae KP1_4582 (BAH65079)	hypothetical protein	97% (67)

49

3.6 Figure

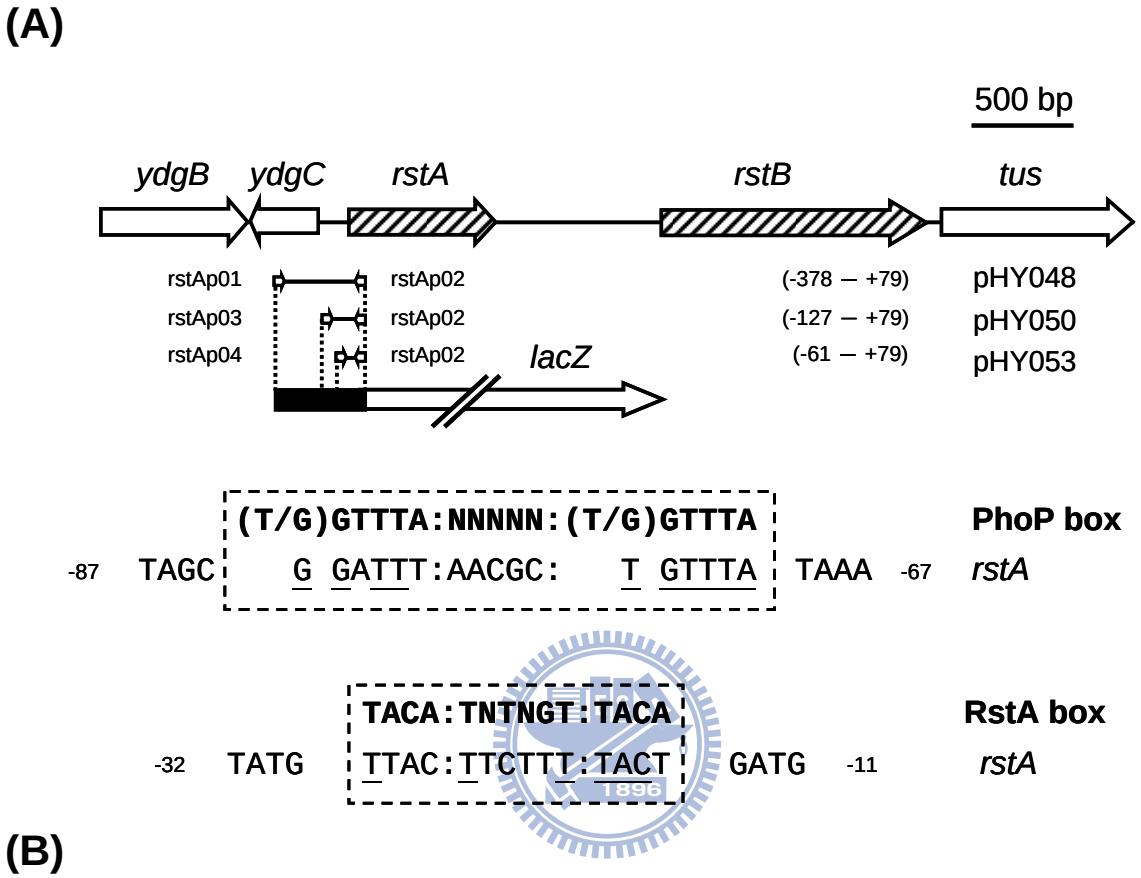
(A)
500 bp
ydgB
ydgC
rstA
rstB
tus
rstAp01
rstAp02
rstAp03
rstAp02
rstAp04
rstAp02
lacZ
(-378 – +79)
(-127 – +79)
(-61 – +79)
pHY048
pHY050
pHY053
(T/G)GTTTA:NNNNN:(T/G)GTTTA
PhoP box
-87 TAGC G GATTT:AACGC: T GTTTA TAAA -67 rstA
TACA:TNTNGT:TACA
RstA box
-32 TATG TTAC:TTCTTT:TACT GATG -11 rstA
(B)
β-galactosidase activity (Miller units)
vector control
pHY048
pHY050
pHY053
CG43S3ΔlacZ
ΔrstAΔlacZ
ΔphoPΔlacZ
ΔrstAΔphoPΔlacZ

Fig. 3.1. Schematic representation of *K. pneumoniae rstA* locus and P_{rstA}::*lacZ* activity measurements

(A) Diagrammatic representation of the *K. pneumoniae rstA* locus. Open reading frames are shown in large arrows. The PCR primers used to amplify DNA fragments harboring different P_{rstA} regions are depicted, and the numbers refer to the positions relative to the translational start site. The dashed boxes indicate the PhoP and RstA binding sequences aligned with the *rstA* upstream region, and identical nucleotides are underlined. (B) The β-galactosidase activities of log-phased cultures of *K. pneumoniae* strains carrying placZ15 (vector control), pHY048, pHY050 or pHY053 grown in LB medium were determined and expressed as Miller units. The data shown were the average ± standard deviations from triplicate samples. *, $P < 0.01$ compared with the same strain carrying pHY048 or pHY050. #, $P < 0.01$ compared with CG43S3Δ*lacZ* harboring the same reporter plasmid.

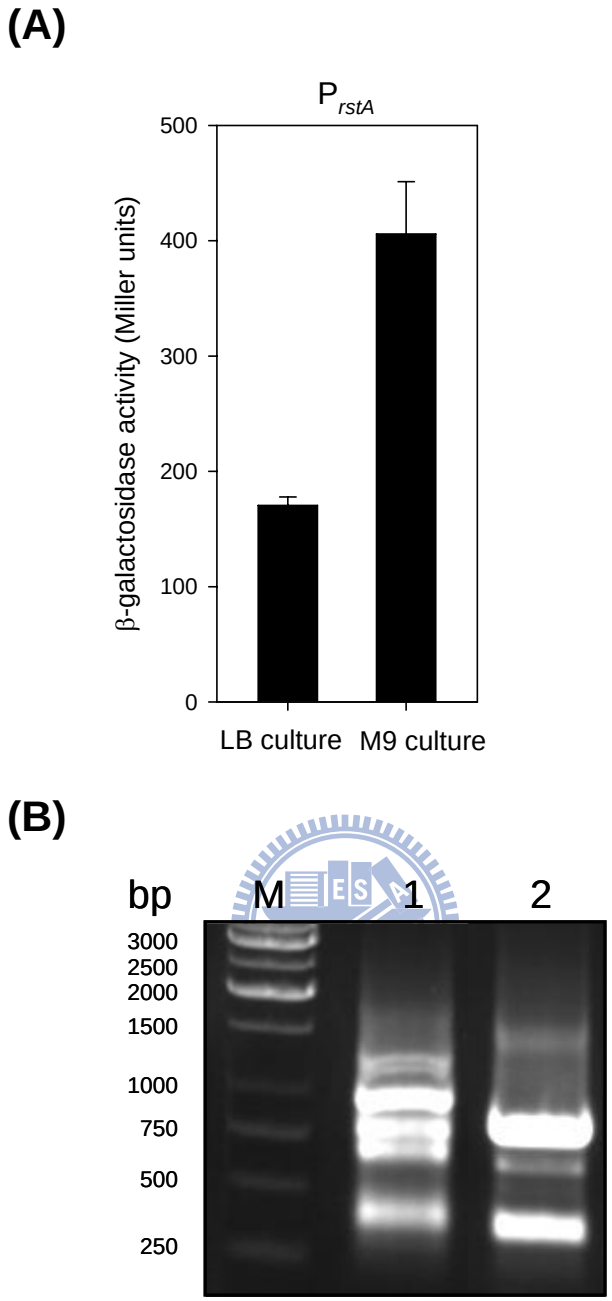

Fig. 3.2. Identification of RstA-regulated genes by subtractive cDNA hybridization

(A) The β-galactosidase activities of log-phased cultures of *K. pneumoniae* CG43S3Δ*lacZ* carrying pHY048 grown in LB or M9 medium were determined and expressed as Miller units. The data shown were the average ± standard deviations from triplicate samples. (B) Gel electrophoresis of the PCR products from the subtractive cDNA hybridization. Lane 1, the RstA-repressed DNA amplicon. Lane 2, the RstA-activated DNA amplicon. M, DNA ladder.

(A)

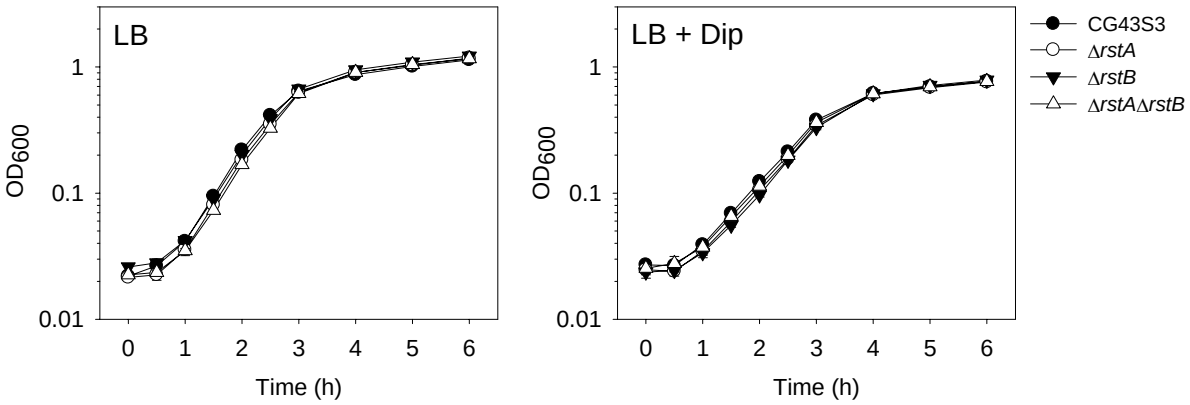

(B)

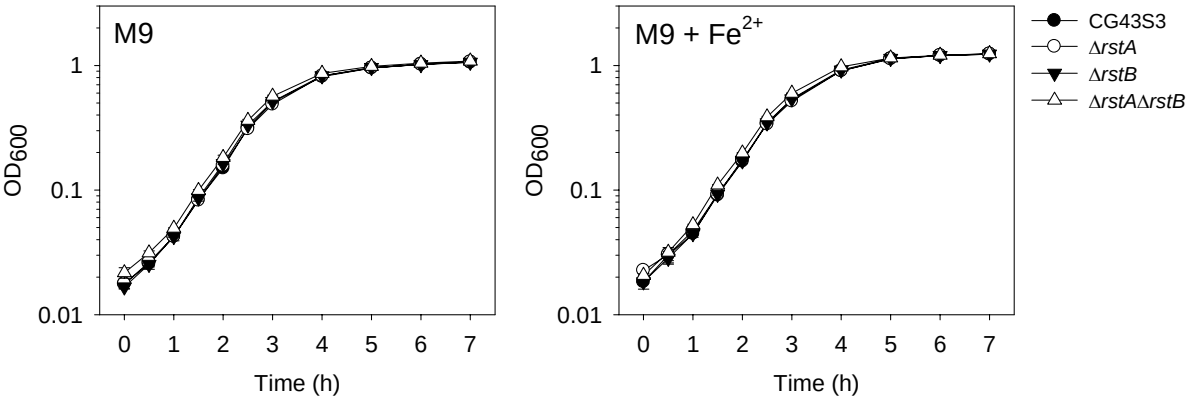

Fig. 3.3. Growth of *K. pneumoniae* strains under iron-depletion/repletion

The Optical density of *K. pneumoniae* strains grown in (A) LB or LB supplemented with 200 μM 2',2'-dipyridyl (LB+Dip) and (B) M9 or M9 supplemented with 20 μM ferrous sulfate (M9+Fe^{2+}) was recorded at the indicated time points and plotted. Error bars, standard deviations from duplicate or triplicate samples.

(A)

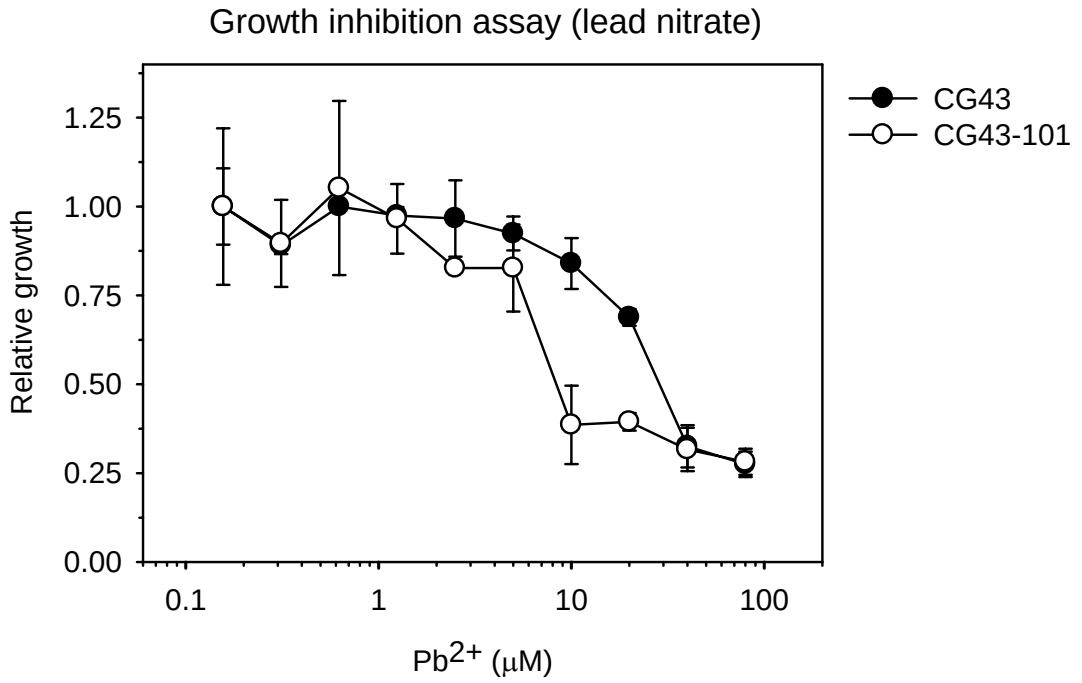

(B)

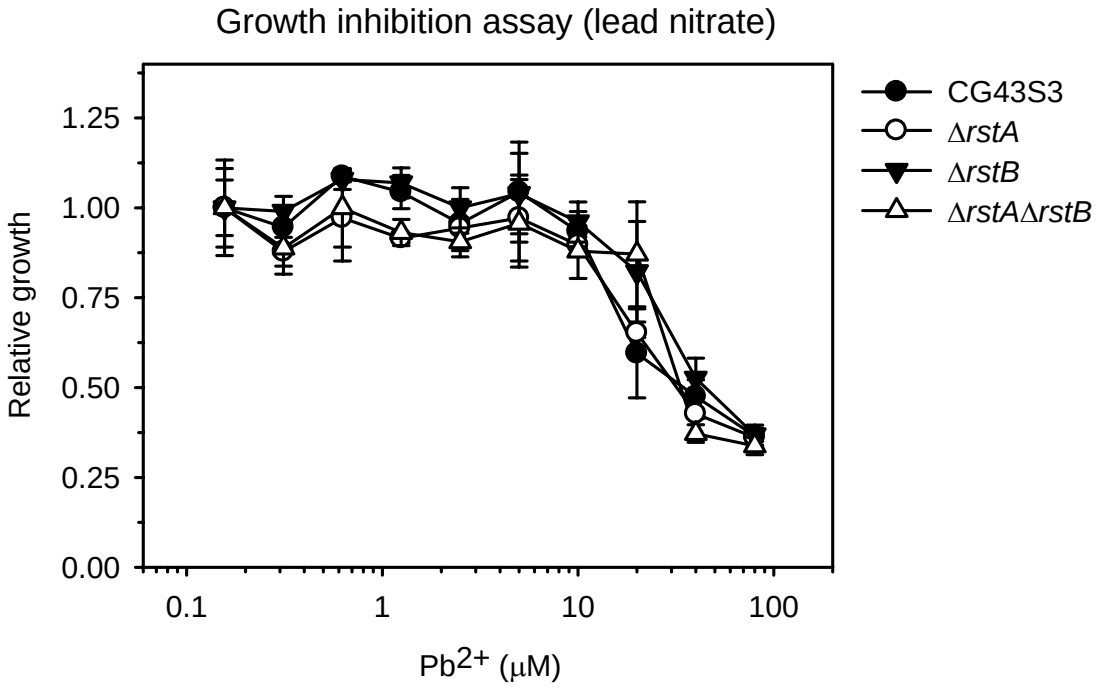

Fig. 3.4. Effect of lead on the relative growth of *K. pneumoniae* strains

A growth inhibition assay was performed to investigate bacterial resistance to lead. Poor lead resistance is demonstrated in strains with reduced relative growths at low lead nitrate concentrations. Error bars, standard deviations from triplicate samples.

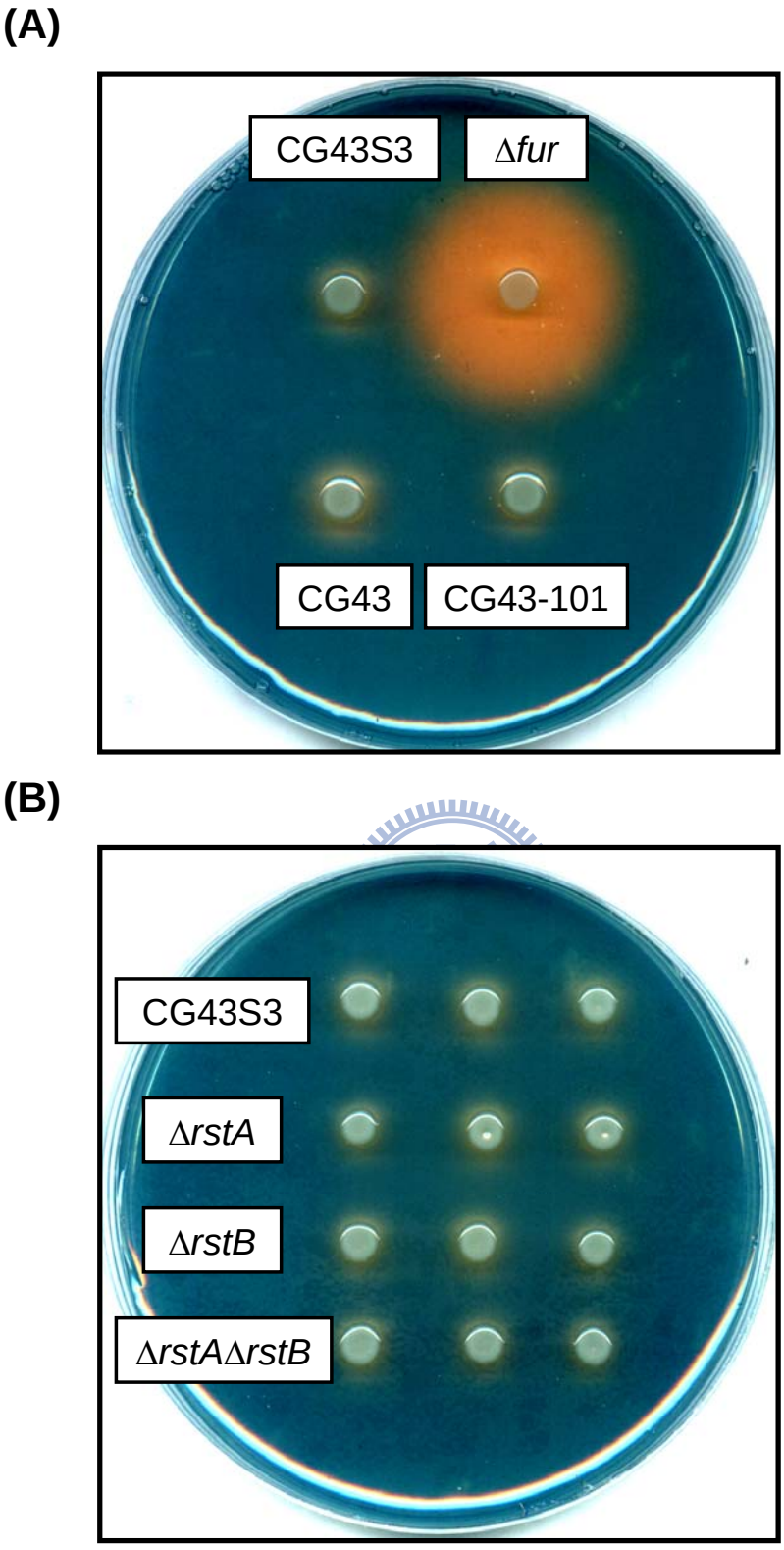

Fig. 3.5. Siderophore production of *K. pneumoniae* strains on CAS agar plates

One microliter of *K. pneumoniae* overnight cultures was spotted onto CAS agar plates (162), incubated at room temperature for 16 h and photographed.

(A)

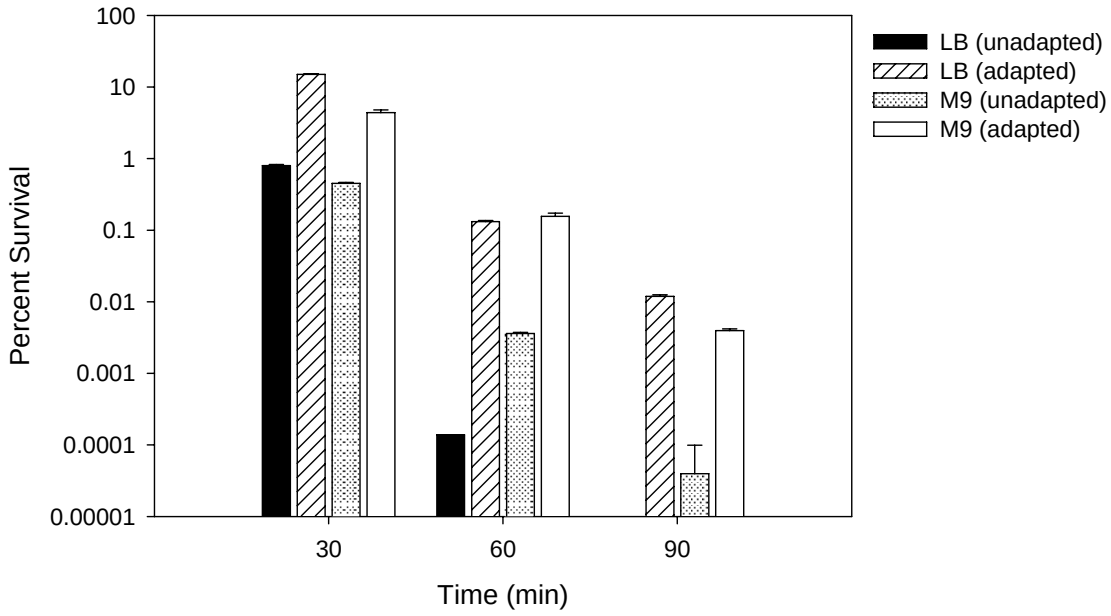

(B)

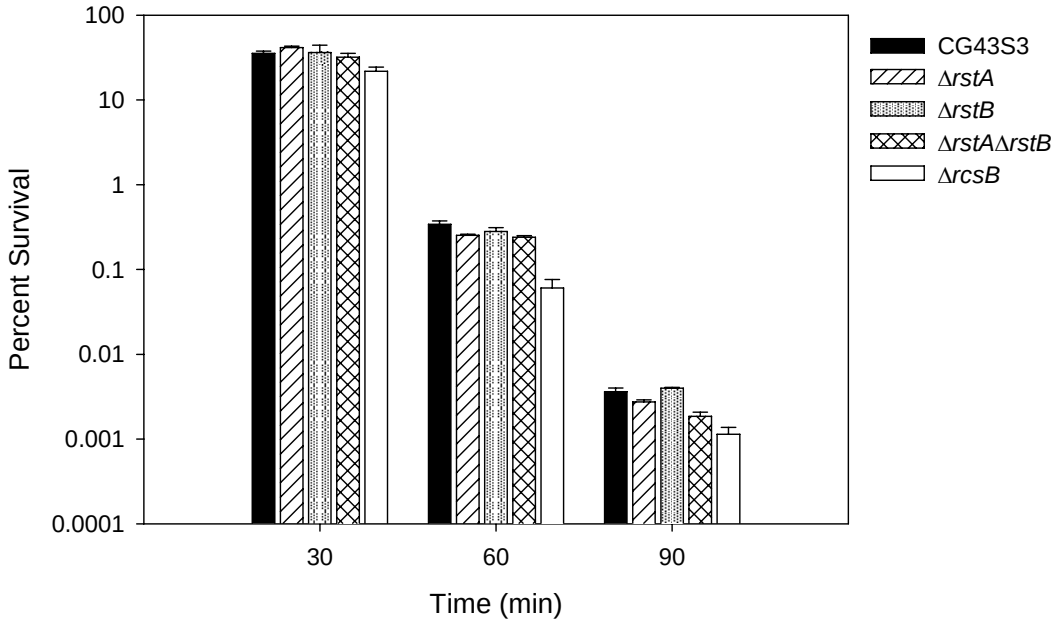

Fig. 3.6. Survival of *K. pneumoniae* strains after acid challenge

(A) The survival of *K. pneumoniae* CG43S3 grown in LB or M9 mediums, either with (adapted) or without (unadapted) pre-adaptation at pH 4.5 was determined at 30, 60 or 90 min after acid challenge at pH 3.0. (B) Strains were grown in M9 medium, adapted at pH 4.5, and the bacterial survival was determined at 30, 60 or 90 min post-challenge at pH 3.0. The survival rates were expressed as the CFU of viable bacteria divided by the CFU before acid challenge. Error bars, standard deviations from triplicate samples.

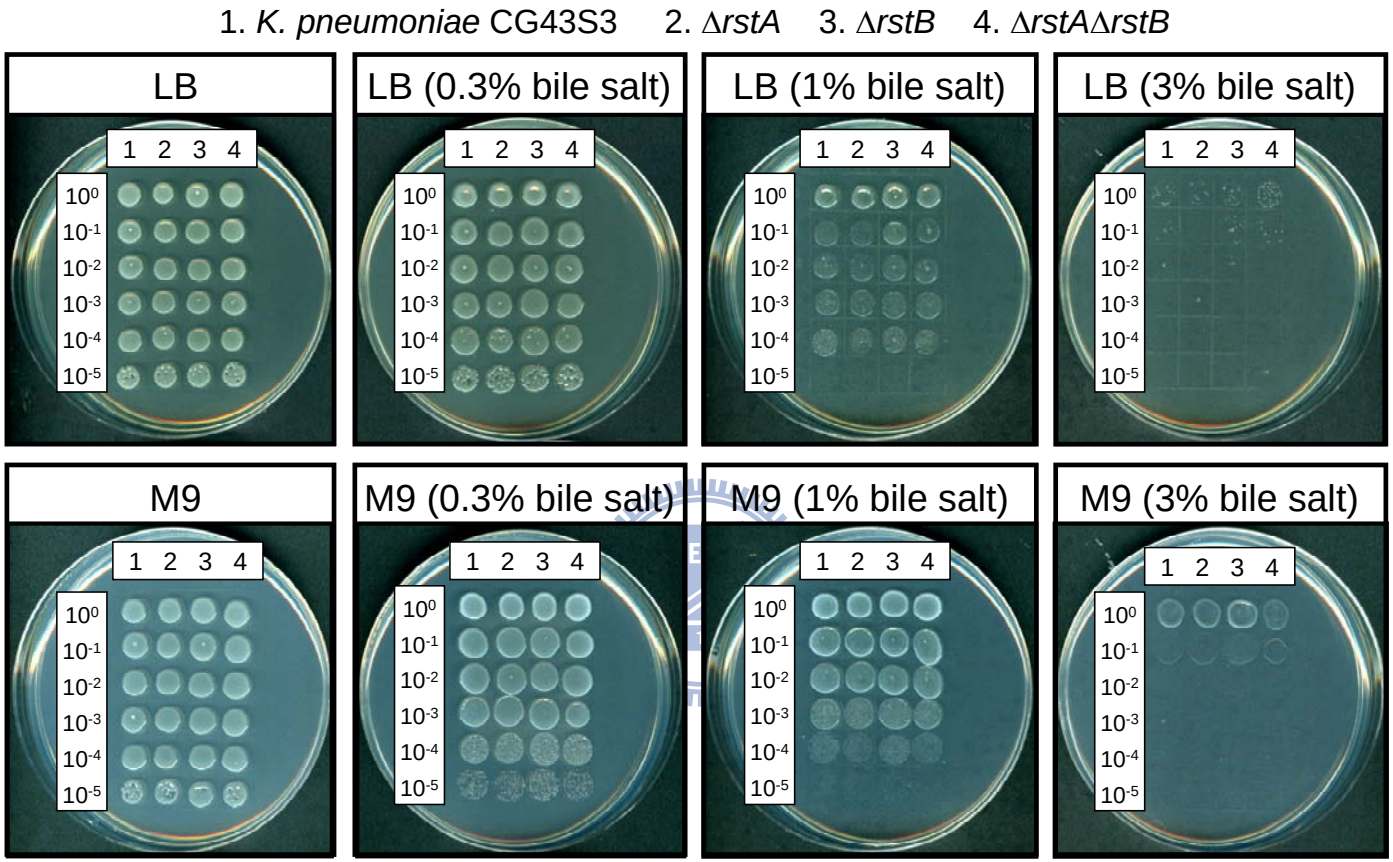

Fig. 3.7. Growth of *K. pneumoniae* strains on bile salt-containing medium

Overnight cultures of *K. pneumoniae* strains, as indicated above the figure, were serially diluted and spotted onto LB or M9 agar plates supplemented without or with different concentrations of bile salts. Bacterial growth after overnight incubation at 37°C was shown.

CHAPTER 4

RmpA Regulation of Capsular Polysaccharide Biosynthesis in *Klebsiella pneumoniae* CG43

4.1 Abstract

Sequence analysis of the large virulence plasmid pLVPK in *Klebsiella pneumoniae* CG43 revealed the presence of another mucoid factor encoding gene *rmpA* besides *rmpA2*. Promoter activity measurement indicated that the deletion of *rmpA* reduced K2 capsular polysaccharide (CPS) biosynthesis resulting in decreased colony mucoidy and virulence in mice. Introduction of a multicopy plasmid carrying *rmpA* restored CPS production in the *rmpA* or *rmpA2* mutant but not in the *rcsB* mutant. Transformation of the *rmpA* deletion mutant with an *rcsB*-carrying plasmid also failed to enhance CPS production, suggesting that a cooperation of RmpA with RcsB is required for regulatory activity. This was further corroborated by the demonstration of *in vivo* interaction between RmpA and RcsB using bacterial two-hybrid analysis and co-immunoprecipitation analysis. A putative Fur binding box was only found at the 5' non-coding region of *rmpA*. The promoter activity analysis indicated that the deletion of *fur* increased the *rmpA* promoter activity. Using EMSA, we further demonstrated that Fur exerts its regulatory activity by binding directly to the promoter. As a result, the *fur* deletion mutant exhibited an increase in colony mucoidy, CPS production, and virulence in mice. In summary, our results suggested that RmpA activates CPS biosynthesis in *K. pneumoniae* CG43 via an RcsB-dependent manner. The expression of *rmpA* is regulated by the availability of iron and is negatively controlled by Fur.[a]

[a] A part of this chapter has been published:

Cheng, H. Y., Y. S. Chen, C. Y. Wu, H. Y. Chang, Y. C. Lai, and H. L. Peng. 2010. RmpA regulation of capsular polysaccharide biosynthesis in *Klebsiella pneumoniae* CG43. *J Bacteriol* 192:3144-58.

4.2 Introduction

Klebsiella pneumoniae, an important nosocomial pathogen, causes a wide range of infections, including pneumonia, bacteremia, urinary tract infection, and life-threatening septic shock (196). Clinically isolated *K. pneumoniae* strains usually produce a large amount of capsular polysaccharide (CPS), which confers not only a mucoid phenotype to the bacteria but also resistance to engulfment by professional phagocytes or to serum bactericidal factors (143, 203). CPS also plays a role in hindering fimbrial binding (209) and bactericidal effects resulting from antimicrobial peptides (30). The degree of mucoidy has been positively correlated with successful establishment of infection (176, 177). Most recently, the hypermucoviscosity of *K. pneumoniae* isolates has also been associated with the development of invasive syndrome (137). Among the identified serotypes, *K. pneumoniae* strains of K1 or K2 CPS are highly virulent in the mouse peritonitis model (167).

Klebsiella CPS resembles the *E. coli* group I CPS in primary structure and the mechanisms of biosynthesis (254). The chemical composition of *Klebsiella* K2 CPS, which contains uronic acid as the major component, has been determined as $[\rightarrow 4\text{-Glc-}(1\rightarrow 3)\text{-}\alpha\text{-Glc-}(1\rightarrow 4)\text{-}\beta\text{-Man-}(3\leftarrow 1)\text{-}\alpha\text{-GlcA})\text{-}(1\rightarrow]_n$ (246). Sequencing of the region responsible for K2 CPS biosynthesis in the *K. pneumoniae* Chedid strain revealed a total of 17 open reading frames organized into three transcriptional units (5). The two-component system (2CS) RcsCDB, which is the key regulatory system for *E. coli* colonic acid synthesis, often serves as a model for group I CPS biosynthesis (106, 155). Upon receiving environmental stimuli, the transmembrane sensor kinase RcsC undergoes autophosphorylation, the signal is subsequently relayed to the inner membrane Hpt (histidine-containing phosphotransfer) module RcsD and eventually to the cytoplasmic response regulator RcsB. The phosphorylated RcsB then interacts with RcsA, an auxiliary transcriptional regulator, and the heterodimer binds to the *cps* promoters, which in turn activates the biosynthesis of colanic acid capsule. RcsA is highly susceptible to degradation by the Lon protease; hence, *lon* mutation often leads to the accumulation of colanic acid (87). However, the introduction of multicopy *rcsB* has been shown to suppress the *rcsA*-negative phenotype (23).

K. pneumoniae CG43, with a LD_{50} of 10 CFU for laboratory mice, is a highly mucoid clinical isolate of K2 serotype (36). Its mucoid phenotype has been correlated with the presence of the large virulence plasmid pLVPK; curing of this plasmid has rendered an

approximately 1000-fold decrease in mice virulence (12). We have also shown that *rmpA2* on pLVPK encodes a transcriptional activator for the *cps* expression by binding directly to the putative promoters, $P_{orf1\text{-}2}$ and $P_{orf3\text{-}15}$ (130). Interestingly, sequencing of the large virulence plasmid pLVPK revealed an *rmpA* gene 29 kb away from *rmpA2* (37). Excluding the extended 15 amino acids at the N-terminus of RmpA2, the deduced RmpA sequence shares an overall 71.4% identity and a conserved C-terminal DNA binding motif with the RmpA2 protein.

An *rmpA* gene on the 180-kb virulence plasmid pKP100 of *K. pneumoniae* 52145 has been reported twenty years ago (29). The encoding protein RmpA was subsequently demonstrated to be able to enhance colonic acid biosynthesis in *E. coli* HB101 (176). Later, the *rmpA2* gene, carrying an extended 5' sequences of the *rmpA*, was isolated and shown to be able to activate K2 capsule production in the recombinant *E. coli* K-12 harboring *Klebsiella* K2 *cps* genes (246). Herein, we report the characterization of RmpA in K2 CPS biosynthesis and comparative analysis of the expression of the two mucoid factor encoding genes. We have demonstrated the interaction between RmpA and RcsB on the regulation of the CPS biosynthesis and the involvement of Fur on the expression of *rmpA* has also been studied.

4.3 Results

4.3.1 Comparison of *rmpA/rmpA2* containing regions in *K. pneumoniae* CG43

On the basis of the sequence analysis, the DNA fragment containing the *rmpA2* gene with upstream *vagC* and *vagD* and downstream *iucABCDiutA* genes was labeled as PAI (pathogenicity island)-1, while the *rmpA*-, *fecIRA*- and *iroBCD*-containing region was named PAI-2 (Fig. 4.1). It was noted that both regulator genes were located downstream of the siderophore biosynthesis genes flanked by insertion sequences. The positive regulatory role of RmpA2 in the expression of the major virulence factor, CPS, has been demonstrated (20). As a result, whether RmpA plays a role in the regulation of CPS biosynthesis was investigated.

4.3.2 Deletion of *rmpA* reduced CPS production and virulence

To assess the functional role of RmpA, the *rmpA* deletion mutant was generated using the allelic-exchange strategy. The colony of Δ*rmpA* mutant on the LB agar plate was found to be smaller than its parental strain, and the degree of mucoidy was reduced significantly as determined by a string test (130), which refers to the ability to form a string when the bacterial colony was picked with toothpick. As shown in the sedimentation test in Fig. 4.2A, the Δ*rmpA* mutant as well as the Δ*rcsB* mutant could be rapidly precipitated by low-speed centrifugation. The loss of mucoid phenotype in Δ*rmpA* mutant could be complemented with the transformation of pRK415-RmpA, or pRK415-RmpA2. Interestingly, the mucoid phenotype could not be restored by introducing the *rcsB*-expression plasmid pRK415-RcsB. The sedimentation analysis also revealed that the introduction of pRK415-RmpA or pRK415-RmpA2 was able to increase the mucoviscosity of the *rmpArmpA2* double mutant (Fig. 4.2A), indicating the independent regulatory activity of RmpA and RmpA2. The effect of *rcsB* deletion could only be complemented by transformation of the Δ*rcsB* mutant with pRK415-RcsB but not pRK415-RmpA. As assessed by measuring the glucuronic acid content, which served as an indicator for *Klebsiella* K2 CPS (187), deletion of *rmpA* or *rcsB* caused approximately 25% reduction in the amount of CPS compared with that of CG43S3 (Fig. 4.2B). The effect of *rmpA* or *rcsB* deletion could only be restored by transformation of Δ*rmpA* with pRK415-RmpA or transformation of Δ*rcsB* with pRK415-RcsB (Fig. 4.2C), which is consistent with the findings in Fig. 4.2A. Furthermore, the *rmpA* deletion appeared to increase LD_{50} from 1×10^4 CFU to 5×10^5 CFU in the mouse peritonitis model and

reduced the resistance to human serum from > 95% to > 70% (Table 4.1). The deficiency in serum resistance could be reverted by the introduction of pRK415-RmpA, suggesting a role of RmpA in bacterial virulence.

4.3.3 RmpA acted as an activator of *cps* expression

To investigate whether the CPS-deficient phenotype of Δ*rmpA* mutant was a result of altered expression of the *cps* genes, three reporter plasmids pOrf12 ($P_{orf1\text{-}2}$::*lacZ*), pOrf315 ($P_{orf3\text{-}15}$::*lacZ*) and pOrf1617 ($P_{orf16\text{-}17}$::*lacZ*), each carrying a *lacZ* reporter gene transcriptionally fused to the putative promoter region of the K2 *cps* gene cluster (142), were used to transform *K. pneumoniae* strains CG43S3Δ*lacZ*, Δ*rmpA*Δ*lacZ*, Δ*rmpA2*Δ*lacZ* or Δ*rcsB*Δ*lacZ* individually. The promoter activity measurements shown in Fig. 4.3A reveal that the deletion of *rmpA* reduced the activity of $P_{orf1\text{-}2}$::*lacZ* and $P_{orf16\text{-}17}$::*lacZ*. A reduction in the activity $P_{orf1\text{-}2}$::*lacZ* or $P_{orf16\text{-}17}$::*lacZ* was also observed in the Δ*rcsB* mutant. Interestingly, the deletion of *rmpA2* had less effect on the activity of $P_{orf16\text{-}17}$::*lacZ* compared with the *rmpA* deletion. As shown in Fig. 4.3B, the deleting effect of *rmpA*, *rmpA2* or *rcsB* on $P_{orf3\text{-}15}$::*lacZ* activity was only apparent when the strains were grown in M9-glocuse minimal medium. Compared with that of *rmpA2*, the deletion of *rmpA* resulted in a more drastic reduction in the activity of $P_{orf1\text{-}2}$::*lacZ* and $P_{orf16\text{-}17}$::*lacZ* implying a differential regulation of RmpA and RmpA2 on the *cps* promoters. Nevertheless, the results suggested that the expression of RmpA, RcsB, and RmpA2 is required for *cps* expression.

4.3.4 Effect of poly(G) tract variation on *rmpA/rmpA2* expression

A close inspection of the *rmpA* and *rmpA2* nucleotide sequences has revealed a poly(G) tract in both genes. Previously it has been reported that different *K. pneumoniae* clinical isolates harbored *rmpA2* genes with various length of poly(G) tract encoding either a full-length or a truncated form of RmpA2, which lost its DNA-binding ability as well as its trans-activation on K2 *cps* expression (130). Similarly, only the 10-Gs version of the poly(G) tract in *rmpA* would allow the synthesis of full-length RmpA while other lengths of the poly(G) tract would result in the occurrence of an ochre stop codon and render the synthesis of a truncated RmpA (Fig. 4.4AB). It remained unknown, however, whether the length of poly(G) tracts in *rmpA* and *rmpA2* would be altered in a different rate during bacterial growth. To address this, a modified assay from the insertional restoration of LacZα-complementation (46) was designed. Firstly, the DNA fragments encompassing the translational start site and the latter stop codon encoding region in *rmpA* and *rmpA2* genes were cloned in-frame with

the *lacZ*α gene in yT&A to generate pHY291 and pHY306. Since the *rmpA* and *rmpA2* genes harboring respectively the 10-Gs and 11-Gs versions of poly(G) tracts were introduced, *E. coli* JM109 transformants harboring either pHY291 or pHY306 would form blue colonies on LB agar plates supplemented with IPTG and X-gal if the association between the recombinant LacZα peptides and the ω peptides synthesized from the chromosomal *lacZ*ω gene was successful. As a control, the same DNA fragments were cloned in the opposite direction to *lacZ*α to generate pHY290 and pHY305. Transformants carrying pHY290 or pHY305 would fail to synthesize full-length LacZα peptides due to the presence of multiple stop codons in the inserted sequences. It was later found that transformants carrying pHY291 or pHY306 could form pale blue colonies on LB agar plates supplemented with IPTG and X-gal while strains harboring pHY290 or pHY305 formed white colonies. As a result, cultures of *E. coli* JM109 transformants harboring yT&A or each of the recombinant plasmids were either grown overnight and spotted onto LB agar plates supplemented with IPTG and X-gal or grown to log phase, diluted serially and plated onto the same plates.

As shown in Fig. 4.4C, strains carrying yT&A (no. 1 and 4) formed blue colonies while those carrying pHY290 (no. 2) or pHY305 (no. 5) formed white colonies as expected. Interestingly, *E. coli* cells harboring pHY291 (no. 3) or pHY306 (no. 6) formed blue colonies during the initial period of incubation, and several white colonies were subsequently observed after a longer incubation duration. The white colonies were also found in the refreshed cultures carrying pHY291 or pHY306 as shown in Fig. 4.4D, although in approximately the same frequency (about 1 per 300 colonies in both transformants). Sequence analysis of these white colonies has revealed various lengths of poly(G) tracts in the inserted sequence, implying the event of slip-strand synthesis during DNA replication. The results indicated the presence of the similar mechanism governing the variation of RmpA and RmpA2 coding sequences.

4.3.5 RmpA regulates *cps* expression in an RcsB-dependent manner

To investigate the possibility of an interaction between RmpA and RcsB for *cps* expression, the *lacZ* reporter cassette on pOrf12 was cloned into a suicide vector, and the plasmid was mobilized into *K. pneumoniae* CG43S3Δ*lacZ* and its isogenic Δ*rmpA* and Δ*rcsB* mutant. The resulting strain harboring a chromosomally integrated $P_{orf1\text{-}2}$::*lacZ* cassette was then transformed with different complementation plasmids, and the β-galactosidase activities were determined. As shown in Fig. 4.5, the introduction of pRK415-RmpA or pRK415-RcsB could enhance $P_{orf1\text{-}2}$::*lacZ* activity in the parental strain, suggesting the functional activity of

RmpA or RcsB. Functional RmpA could enhance *cps* expression in the *rmpA* deletion strain but not the *rcsB* deletion strain. Consistent with the phenotype observed in Fig. 4.2B, the functional RcsB carried by pRK415-RcsB could not restore *cps* expression in the *rmpA* deletion strain. The introduction of pRK415-RmpAN, which encoded a truncated RmpA without the carboxyl terminal DNA binding region, into the *rmpA* deletion strain also failed to restore *cps* expression. The results suggest that RmpA activates *cps* expression in an RcsB-dependent manner and that its DNA binding motif is required for regulation.

4.3.6 Interaction between RmpA and RcsB using two-hybrid analysis

Since the cooperation of RcsA and RcsB for regulation on K2 *cps* expression has been demonstrated (250), we thought of using EMSA to investigate if the RmpA exerts RcsA-like activity to interact with RcsB in order to bind to the $P_{orf1\text{-}2}$ region cooperatively. However, the overproduction of RmpA using the pET expression system appeared to impair cell growth significantly; hence, the bacterial two-hybrid assay was employed instead. Therefore plasmids pTRG-RcsA, pTRG-RmpA, pTRG-RmpA2, pTRG-RmpAN and pBT-RcsB which harbored λ-cI-RcsA, λ-cI-RmpA, λ-cI-RmpA2, λ-cI-RmpAN and α-RNAP-RcsB coding sequences were constructed. The interaction between α-RNAP and λ-cI fusion proteins would allow binding of λ-cI to the operator sequence and recruitment of α-RNAP to initiate the transcription of *ampR* as well as *lacZ* genes in the reporter cassette harbored in the *E. coli* reporter strain. The interaction between the recombinant proteins could be verified by bacterial growth on the X-gal indicator plate supplemented with carbenicillin and the level of interaction could be quantified by measuring the activation of the LacZ reporter. As shown in Fig. 4.6A, the strain carrying pBT-RcsB/pTRG-RcsA or the positive control plasmids grew well on the indicator plate. Substitution of pBT-RcsB and pTRG-RcsA with pBT or pTRG resulted in poor or no growth. Those strains carrying pBT-RcsB/ pTRG-RmpA, pBT-RcsB/ pTRG-RmpA2, or pBT-RcsB/ pTRG-RmpAN also grew on the indicator plate. As shown in Fig. 4.6B, the strain pBT-RcsB/pTRG-RcsA exhibited relatively higher activity than the bacteria carrying pBT-RcsB/pTRG-RmpA, pTRG-RmpA2 or pTRG-RmpAN. The transformants harboring pBT-RcsB and pTRG-RmpA, pTRG-RmpA2 or pTRG-RmpAN also exhibited higher activity compared with strains of which pBT-RcsB was replaced by pBT (Fig. 4.6B, right panel). The results suggested an *in vivo* interaction between RcsB and RmpA, and the N-terminal peptide (residues 1 to 84) of RmpA may play an important role in the interaction.

4.3.7 Co-immunoprecipitation analysis of the interaction between RmpA and RcsB

To confirm the results from the two-hybrid analysis, co-IP was also performed. The full-length RcsA, RmpA, RmpA2 and RmpAN coding regions were cloned into pGEX-5X-1 to generate plasmids pGEX-RcsA, pGEX-RmpA, pGEX-RmpA2 and pGEX-RmpAN, respectively. The plasmid pACYC184-RcsB, which is compatible with pGEX-5X-1, was also constructed. Using anti-GST or anti-His monoclonal antibody, the amounts of the recombinant GST fusion proteins and the recombinant RcsB in the pre-immunoprecipitation (Pre-IP) samples were determined (Fig. 4.7A). As shown in Fig. 4.7B, the immunoprecipitates of cells harbored the combinations of pACYC184-RcsB plus pGEX-RcsA, pGEX-RmpA, pGEX-RmpAN, or pGEX-RmpA2 pulled down with the Glutathione Sepharose all contained the RcsB-His as determined by anti-His monoclonal antibody or anti-RcsB polyclonal antibody. The amounts of recombinant RcsB protein precipitated by GST-RcsA and GST-RmpA were much lower than those pulled down by GST-RmpAN and GST-RmpA2 (Fig. 4.7B). This could be resulted from instability of the GST-RcsA and GST-RmpA fusion proteins, as reflected by very low amounts of both proteins detected by anti-GST monoclonal antibody after IP (Fig. 4.7B). The results further supported a role of RmpA or RmpA2 as an auxiliary factor, like RcsA, for RcsB in regulating the CPS biosynthesis.

4.3.8 The expression of *rmpA* is subjected to negative regulation by Fur

Differential control likely explains the co-existence of the two functional mucoid factors, RmpA and RmpA2, in the *cps* expression in the bacteria. To verify this, the DNA fragments encompassing the putative promoter region of *rmpA* or *rmpA2* was cloned in front of the promoter-less *lacZ* to generate placZ15-PrmpA and placZ15-PrmpA2. The resulting plasmids were then transformed individually into *K. pneumoniae* CG43S3Δ*lacZ* for promoter activity measurements. In contrast to the negative autoregulation for *rmpA2* expression demonstrated previously (130) and in our analysis (Fig. 4.8B), the *rmpA* expression appeared to be independent of such negative autoregulation as reflected by a steady increase of P_{rmpA}::*lacZ* activity in response to bacterial growth whether in LB (Fig. 5,8A) or M9 medium (Fig. 4.8B).

Since *rmpA* and *rmpA2* are respectively located next to the iron acquisition genes *iucABCDiutA* and *iroBCDN* (Fig. 4.1), it is of interest to know if any iron uptake regulator is involved in their expression. A close inspection of the *rmpA* and *rmpA2* upstream regions revealed a Fur box-like sequence (10, 61) on P_{rmpA} but not on P_{rmpA2}. This element was also identified in front of a set of Fur-regulated genes including *iucABCD* and *iroBCD*. To

investigate if Fur, the global regulator for iron uptake regulation, participated in the control of the gene expression, the expression levels of P_{rmpA}::*lacZ* and P_{rmpA2}::*lacZ* were measured in the wild-type strain and the *fur* deletion mutant. As shown in Fig. 4.9A, *fur* deletion resulted in a higher level of activity for the Fur-dependent promoters P_{iucA} and P_{iroB} in LB. An increased level of P_{rmpA}::*lacZ* expression in the Δ*fur* mutant was even more profound when the bacterial culture was switched from LB to the M9-glucose medium (Fig. 4.9B). In the presence of iron scavenger 2,2-dipyridyl, the activity of P_{iucA}::*lacZ*, P_{iro}::*lacZ* or P_{rmpA}::*lacZ* was higher in M9-glucose medium but less affected by Fur. On the other hand, the deletion of *fur* or addition of iron scavenger had no apparent effect on the expression of P_{rmpA2}::*lacZ* in either medium (Fig. 4.9). The results suggest that Fur negatively regulate the expression of P_{rmpA} but does not participate in the regulation of *rmpA2* expression.

4.3.9 The recombinant Fur was able to bind specifically to P_{rmpA}

The Fur box-like sequence could be predicted upstream of *iucA*, *iroB* and *rmpA* as shown in Fig. 4.10A. To further ascertain the effect of Fur on *rmpA* expression, an EMSA was performed. The DNA fragments encompassing P_{iucA} (P1), P_{iroB} (P2), and P_{rmpA} (P3) and the truncated forms P4, P5, P6 as depicted in Fig. 4.10A were isolated and isotope-labeled for the analysis. As shown in Fig. 4.10B, the purified recombinant His-Fur protein was able to bind to the DNA probes P1, P2, and P3. By using different lengths of P_{rmpA}, the binding of His-Fur could be observed for P3, P4, and P5 but not for P6 (Fig. 4.10C). This suggested that the His-Fur binding site may be located between -226 to -184 relative to the RmpA start codon (Fig. 4.10A). As shown in Fig. 4.10D, the formation of the P_{rmpA}/Fur complex could be observed as the amount of His-Fur increased, and the binding specificity was demonstrated as the complex diminished in the presence of excess non-labeled P3 or P5 acting as specific competitor DNA. The binding of His-Fur on P_{rmpA} remained unaffected by the addition of excess amounts of pT7-7 (227), a plasmid without Fur box-containing sequence, pUC19 DNA, *rmpA* gene or P6 DNA fragment. The results support the conclusion that the recombinant Fur protein could specifically interact with P_{rmpA} DNA.

4.3.10 Identification of *rmpA* transcriptional start site

As shown in Fig. 4.11A, single DNA band has been obtained from the 5'-RACE analysis using either primer pair. Sequence analysis of a total of 31 clones revealed the transcription start site at the G nucleotide at position -80 relative to the translational start site of RmpA. As shown in Fig. 4.11B, a conserved -10 and -35 promoter sequence of σ^{70} could

be readily identified. Limiting-dilution RT-PCR was subsequently carried out to determine whether the *rmpA* transcription would be affected by Fur. As shown in Fig. 4.11C, a stronger signal for *rmpA* transcript in the *fur* mutant than in the parental strain also supports a negative regulatory role of Fur on the *rmpA* expression.

4.3.11 Deletion of *fur* led to overproduction of CPS

If *rmpA* expression is negatively regulated by Fur, then the CPS level in the *fur* deletion mutant should increase. As shown in Fig. 4.12A, the Δ*fur* mutant formed more mucoid and glistening colonies when compared with the parental strain. In a string test, the Δ*fur* mutant could form a string at least three-fold longer than its parental strain (data not shown). Introduction of pRK415-Fur carrying a functional *fur* allele in Δ*fur* mutant resulted in small colonies (Fig. 4.12A) and readily precipitated phenotype (Fig. 4.12B). The changes in CPS production were also evident in the glucuronic acid content measurement. As shown in Fig. 4.12C, the *fur* mutant exhibited more than two-fold increase in the glucuronic acid production while transformation with pRK415-Fur resulted in an approximately 50% reduction of the glucuronic acid.

4.4 Discussion

The presence of *rmpA* and *rmpA2* on pLVPK as two independent loci 29 kb apart has been demonstrated (37). As shown in Fig. 4.1, the DNA fragments containing *rmpA2* and *rmpA* also harbored an iron-acquisition gene cluster and insertion sequence, which are characteristics of a pathogenicity island, and hence named PAI-1 and PAI-2, respectively. Why and how the evolutionary convergence of the similar gene organization occured remained to be explained. In this study, we show that *rmpA* and *rmpA2* genes are present in one bacterial strain and both encode a mucoid factor contributing to K2 CPS biosynthesis. Presumably, differential control on the expression of these two mucoid factors is required for an efficient regulatory function with no redundant activity in the bacteria.

Sequence analysis revealed that RmpA and RmpA2 belong to the UhpA-LuxR family of transcription factors, which also include RcsA and RcsB (224). The involvement of RcsB in *Klebsiella* K2 capsule biosynthesis of the recombinant *E. coli* K-12 has been demonstrated (245). Previous studies have found that RcsB must interact with RcsA to form a heterodimer in order to bind specifically to the *cps* promoter for transcription initiation (122). In *E. coli*, the cellular level of RcsA was limited at 37°C due to its degradation by the Lon protease, and thus the colonic acid capsule was overproduced only at lower temperatures (87). In *K. pneumoniae* CG43, however, a profound production of CPS was observed at 37°C. We assumed that RmpA or RmpA2 could take the place of RcsA to regulate the *cps* expression at 37°C. This hypothesis was supported by the fact that the deletion of *rcsA* in *K. pneumoniae* CG43 did not affect the mucoid phenotype or the CPS amount at 37°C (data not shown). Moreover, the two-hybrid analysis and co-immunoprecipitation assay further demonstrated that RmpA or RmpA2, in addition to RcsA, was able to interact with RcsB. Therefore in *K. pneumoniae*, multiple accessory factors may be employed in order to increase the CPS biosynthesis in response to different environmental stimuli.

Though bacterial two-hybrid analysis has clearly indicated an interaction between RcsB and its auxiliary factors, the bacterial growth on the indicator plate was similar between the positive control strain and the strain carrying pBT-RcsB and pTRG-RcsA while the results from the β-galactosidase activity measurements showed that the level of reporter gene expression in the positive control strain was approximately four times as the strain carrying pBT-RcsB and pTRG-RcsA. The discrepancy may be due to the concentration of antibiotics administrated in the indicator plate, in which all the bacteria strains expressing the resistance

gene above a threshold level could grow on the plate. The hypothesis was supported by the relatively weaker growth of the strains carrying pBT-RcsB along with pTRG-RmpA, pTRG-RmpA2 or pTRG-RmpAN, which also revealed a lower level of β-galactosidase activity, in comparison with the positive control strain or the strain harboring pBT-RcsB and pTRG-RcsA. Nevertheless, the levels of bacterial growth could be further quantified as the relative survival of strains challenged with different doses of antibiotics, in order to correlate the phenotype observations to the expression levels of the reporter gene and to differentiate between weak interactions.

Previously over-expression of *rmpA* by pET30 system resulted in a significant reduction of bacterial growth after IPTG induction, and most of the protein produced was found in the insoluble fraction, which could not be solubilized by 6N or 8N urea after prolonged incubations (16 to 24 h). The over-expression by using pET32 system in combination with *E. coli* strain carrying a *trxB* mutation also failed to produce soluble recombinant RmpA proteins though the growth retardation after IPTG induction was reduced. As a result, the pGEX system with a GST fusion tag was utilized. Although the growth retardation was no longer observed after IPTG induction, the majority of GST-RmpA remained insoluble and rapidly degraded during purification processes. To improve the solubility of the recombinant RmpA protein, strategies including addition of ion cofactors, using a larger fusion tag such as mannose-binding protein or co-expression with a chaperone protein or with an interaction partner such as RcsB could be considered.

In a typical 2CS, the response regulator could undergo a conformational change to form a homo-dimer upon phosphorylation. In the case of RcsB, which interacted with more than one factor, it remained unclear if phosphorylation state of RcsB would be in favor of homo-dimerization. Since we have shown that RcsB protein could bind specifically to RcsA, RmpA or RmpA2, whether RcsB proteins with alterations on the Aspartic acid at position 56 to Alanine or Glutamate mimicking un-phosphorylated or constitutively-phosphorylated status respectively would require further analysis.

A conserved RcsAB box sequence has been identified in *Klebsiella* K2 *cps* $P_{orf1\text{-}2}$ (250), and analysis of the $P_{orf16\text{-}17}$ sequence also revealed a semi-conserved RcsAB box. This suggested that the decrease of the CPS production in the Δ*rmpA* mutant may have been due to a reduction in the expression of *cps-orf1-2* and *cps-orf16-17*. The existence of an *rmpA* gene has been correlated to the hypermucoviscosity phenotype in *K. pneumoniae* clinical isolates (273). It is interesting to note that no *rmpA* homologue in any other bacterial genomes could

be identified. The BLAST (http://www.ncbi.nlm.nih.gov) search in the released genome sequences of *K. pneumoniae* NTUH-K2044 (262), MGH78578 (http://genome.wustl.edu/), and 342 (74) revealed the presence of *rmpA* only in NTUH-K2044, which is a heavy encapsulated clinical isolate of K1 serotype (65, 273). We have also observed that *rmpA* was more prevalent in the strains belonging to K1/K2 serotypes (36 out of 36 isolates, 100%) than in the non-K1/K2 clinical isolates (28 out of 83 isolates, 33.73%) collected in our laboratory. The presence of *rmpA* in *K. pneumoniae* K1 or K2 isolates has also been associated with virulence in mice (24). These findings suggest that the profound expression of *K. pneumoniae* CPS, which is a major virulence factor, could be attributed to the regulation by RmpA or its homologue.

Similar to *rmpA2*, *rmpA* harbored a poly(G) tract in the coding sequence. The occurrence of DNA slip-strand synthesis may result in a truncated RmpA of abnormal function. Conceivably, the frequency of the mutation caused by DNA slip-strand synthesis in *rmpA* or *rmpA2* may play a role in the differential expression of the two regulatory genes. Although the modified LacZα-complementation assay in this study was feasible in detecting the variation of poly(G) tract, no significant differences in the rate of change in the poly(G) tracts of *rmpA* and *rmpA2* during bacterial replication was noted. However, it remained to be clarified if the rate of change would differ when bacterial replication took place in a different growth medium or when cells were grown under environmental stress. Moreover, changes in the poly(G) tract would result in the biosynthesis of either a full-length/functional or a truncated/non-functional RmpA and RmpA2 protein. Since bacterial growth would be impaired upon the accumulation of RmpA, it would be more appropriate and practical to investigate phase variation of the poly(G) tract when the full-length coding region of *rmpA* and *rmpA2* were taken into consideration.

It was noted that the white colony retrieved in the modified LacZα-complementation assay did not turn to blue compared with the blue-to-white frequency investigated in this study, which was approximately 0.3% in both *rmpA* and *rmpA2* poly(G). The possible explanation could be that the once the poly(G) tract was altered to result in a stop codon, the chance to restore the correct reading frame was at least one-thirds lower given the same probability of adding/deleting a guanidine during DNA replications.

The importance of the poly(G) tract would be more apparent in clinical surveillance of *rmpA*/*rmpA2* genes as not all *rmpA* or *rmpA2* gene detected by using PCR would inevitably encode a functional/full-length protein. We have also found that the presence of a poly(G)

tract would severely interfere the validity of DNA sequencing, and thus the sequencing process could only be completed by using a primer complementary to the non-coding region of *rmpA* or *rmpA2*. It is therefore strongly recommended that the reading frames of the poly(G) tract be determined by DNA sequencing analysis in clinical prevalence studies of *rmpA*/*rmpA2* gene.

A Fur-box like sequence was identified within -146 and -104 upstream of the transcription start site (Fig. 4.11B). This site was not uncommon compared with a genome-wide study in *Yersinia pestis* (77), in which 17 out of 34 predicted Fur binding sites were located at -100 relative to each transcriptional start site. Also as shown in Fig. 4.11C, the *rmpA* transcript was increased upon the deletion of *fur* indicating a negative regulation of Fur on *rmpA* expression in *K. pneumoniae*.

Fur governs iron uptake by repressing the transcription of the genes involved in the biosynthesis of siderophore, iron storage, iron sparing and respiration (10, 139, 244). In addition , it is also involved in virulence properties (247, 263), acid stress response (73), osmotic shock (104) and chemotaxis (60). In this study, a negative role of Fur in CPS biosynthesis that is achieved by the reduction of the RmpA expression is reported for the first time. The findings imply that some *K. pneumoniae* strains may face iron shortage during infection; accordingly, the genes involved in both the biosynthesis of the iron acquisition system and the production of CPS are up-regulated. Therefore, coordination between CPS production and iron uptake may play an important role in the pathogenesis of the bacteria. Nevertheless, *cps* expression was also subjected to regulation by the 2CS response regulators KvgA, KvhA, and KvhR (142). How the interplay between Fur, RmpA and the 2CS determines the control of the *cps* expression remains to be elucidated.

In summary, the overall scene could be depicted as shown in Fig. 4.13. In *K. pneumoniae* CG43, the mucoid factor RmpA exerts a regulatory role on *cps* expression in an RcsB-dependent manner. The interaction between RcsB and its auxiliary factors RcsA, RmpA or RmpA2 leads to the elevated biosynthesis of K2 CPS. A differential regulation of *rmpA* and *rmpA2* expression is also noted as *fur* deletion increased *rmpA* expression but had no effect on *rmpA2* expression through a direct binding of Fur to the putative promoter of *rmpA* in addition to the promoters of siderophore biosynthetic genes. The findings not only connect iron uptake to capsule biosynthesis but also report the first time that the *Klebsiella* Fur is involved in the regulation of K2 CPS biosynthesis.

4.5 Table

Table 4.1. Virulence properties of *K. pneumoniae* strains.

Strain	LD50 (CFU)	Survival rate in human serum (%)[a]
CG43S3	1×10^4	95.6 ± 3.6
CG43S3Δ*rmpA*	5×10^5	71.2 ± 5.6
CG43S3Δ*rmpA*[pRK415-RmpA]	ND[b]	> 99
CG43S3Δ*galU* (control)	1×10^6	0

[a] Percent survival rate in human serum is expressed as 100 × (the number of viable bacteria after treatment with human serum/ the number of viable bacteria after treatment with PBS).

[b] ND, not determined.

4.6 Figure

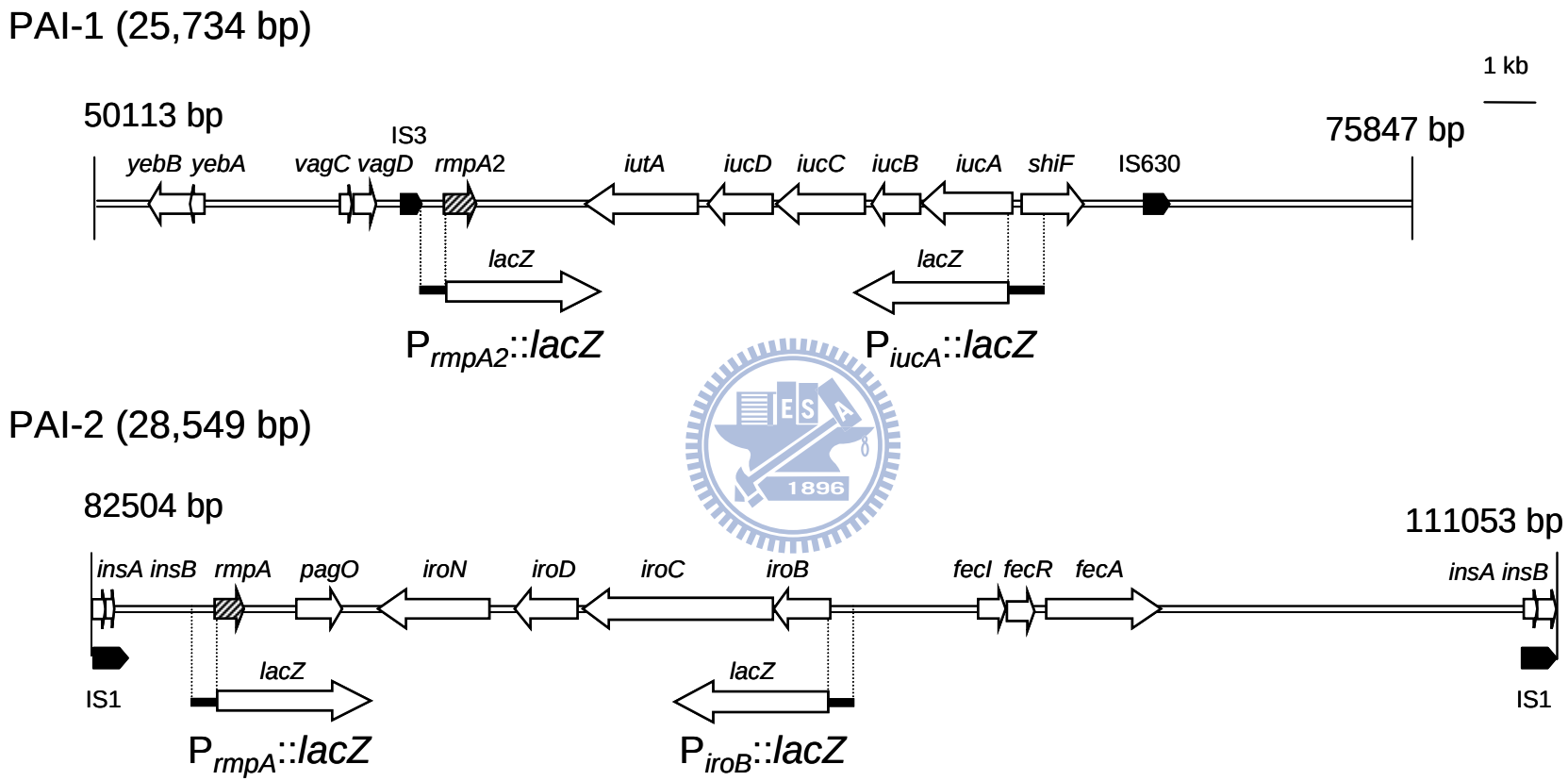

Fig. 4.1. Comparison of *rmpA* and *rmpA2* containing PAI-like regions

The arrows indicate predicted open reading frames and insertion sequences. The reporter constructs used for promoter activity measurement are shown below.

(A)

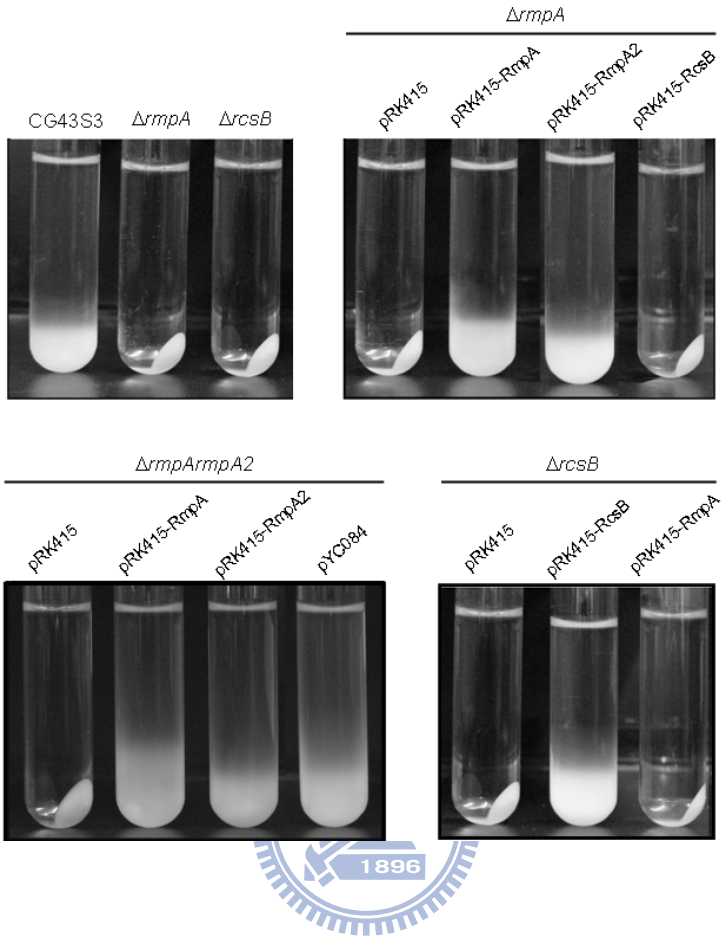
ΔrmpA
CG43S3
ΔrmpA
ΔrcsB
pRK415
pRK415-RmpA
pRK415-RmpA2
pRK415-RcsB
ΔrmpArmpA2
pRK415
pRK415-RmpA
pRK415-RmpA2
pYC084
ΔrcsB
pRK415
pRK415-RcsB
pRK415-RmpA

(B)

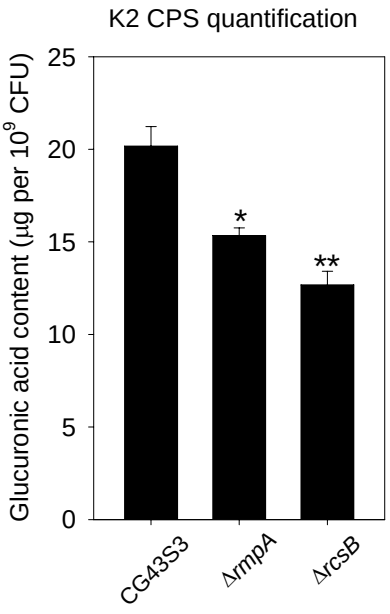
K2 CPS quantification
Glucuronic acid content (μg per 10^9 CFU)
25
20
15
10
5
0
*
**
CG43S3
ΔrmpA
ΔrcsB

(C)

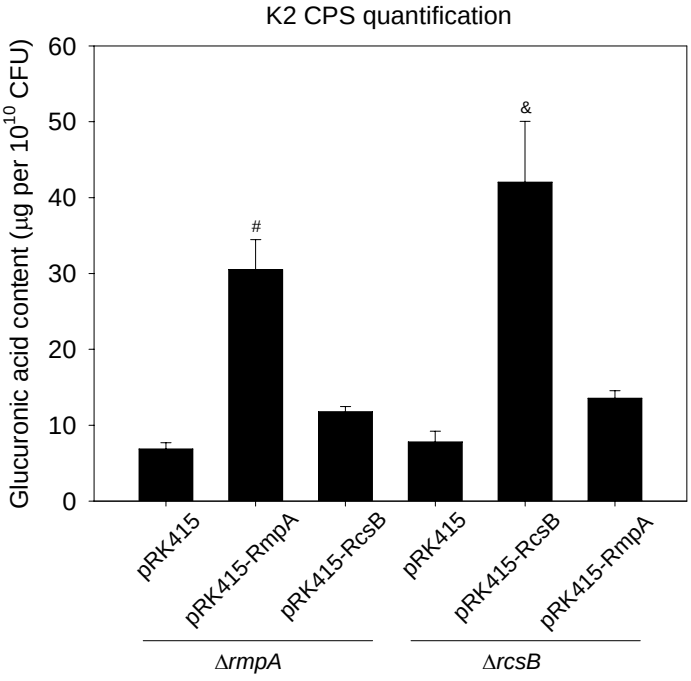
K2 CPS quantification
Glucuronic acid content (μg per 10^10 CFU)
60
50
40
30
20
10
0
#
&
pRK415
pRK415-RmpA
pRK415-RcsB
pRK415
pRK415-RcsB
pRK415-RmpA
ΔrmpA
ΔrcsB

Fig. 4.2. Comparison of precipitation speeds and K2 CPS production in *K. pneumoniae* strains

(A) The strains tested were grown overnight in LB broth at 37°C and subjected to centrifugation at 4,000 ×*g* for 5 min. (B) The glucuronic acid content, which served as an indicator of K2 CPS, was determined from overnight *K. pneumoniae* cultures. The results are expressed as the average of the triplicate samples. Error bars indicate standard deviations. *, $P < 0.01$ compared with CG43S3. **, $P < 0.001$ compared with CG43S3. (C) Quantification of *Klebsiella* K2 CPS production. The results are expressed as an average of triplicate samples. Error bars indicate standard deviations. #, $P < 0.001$ compared with Δ*rmpA* mutant carrying pRK415 or pRK415-RcsB. &, $P < 0.001$ compared with Δ*rcsB* mutant carrying pRK415 or pRK415-RmpA.

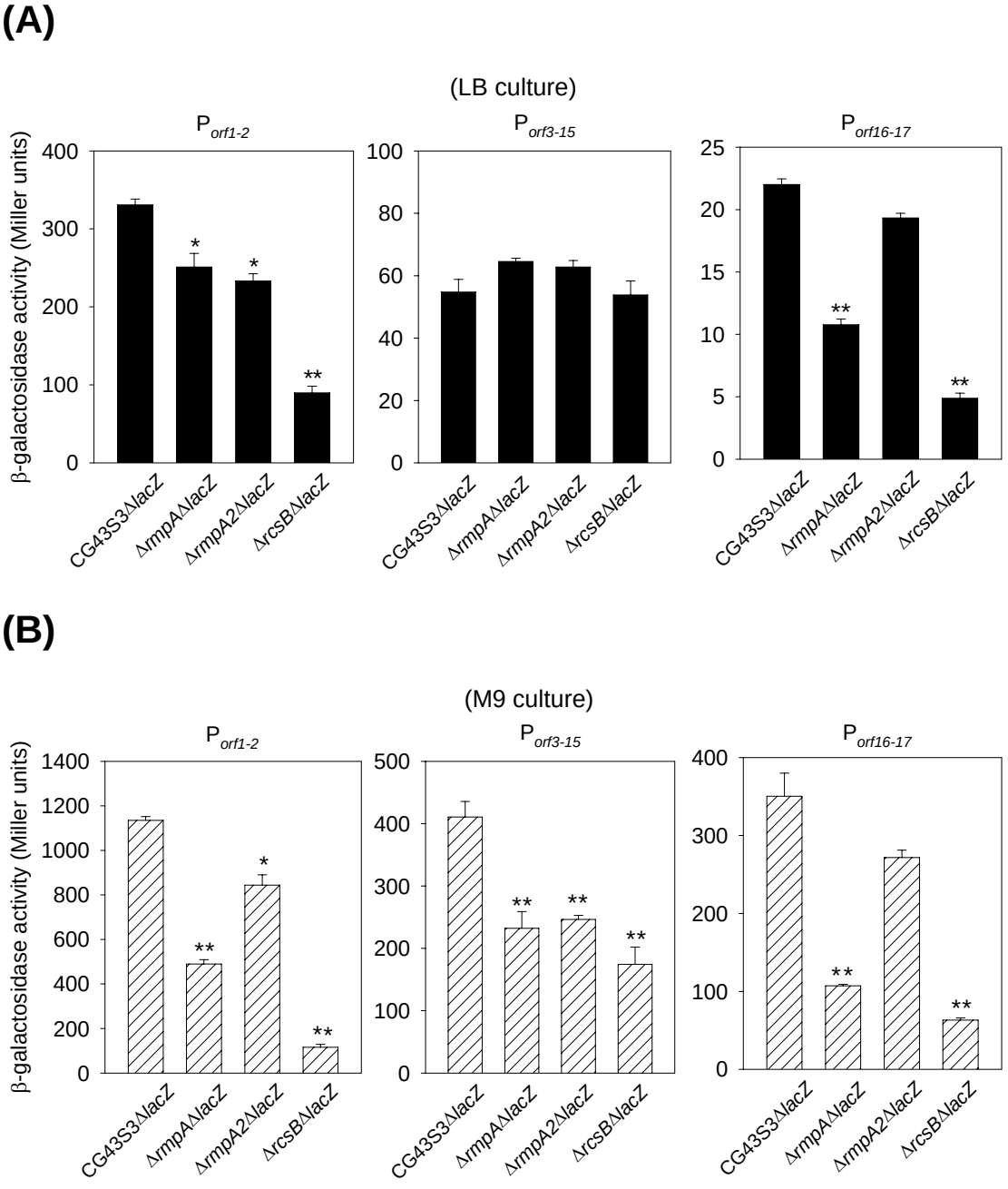

Fig. 4.3. Expression of K2 *cps* genes in various genetic backgrounds

The β-galactosidase activities of K2 *cps* P_{orf1-2}::*lacZ*, $P_{orf3-15}$::*lacZ* and $P_{orf16-17}$::*lacZ* in *K. pneumoniae* CG43S3Δ*lacZ* (wild-type) and its isogenic strains (Δ*rmpA*Δ*lacZ*, Δ*rmpA2*Δ*lacZ*, and Δ*rcsB*Δ*lacZ*) harboring each of the reporter plasmids pOrf12, pOrf315 or pOrf1617 were determined from log-phased cultures grown in LB broth (A) or M9-glucose medium (B). The results are shown as an average of triplicate samples. Error bars indicate standard deviations. *, $P < 0.01$ compared with CG43S3Δ*lacZ*. **, $P < 0.001$ compared with CG43S3Δ*lacZ*.

(A)


Val Ser Gly Gly Gly Arg Phe Tyr Pro Lys Gly Cys Asp Tyr Asp Ile Tyr Val Asn Met Gln Gly Asn Val
poly(G) tract
226
298
rmpA-10Gs GTTTCGGGGGGGGGG-CGGTTTTATCCTAAAGGGTGTGATTATGACATCTATGTTAACATGCAAGGAAATGTAA
rmpA-11Gs GTTTCGGGGGGGGGGGCGGTTTTATCCTAAAGGGTGTGATTATGACATCTATGTTAACATGCAAGGAAATGTAA
rmpA-9Gs GTTTCGGGGGGGGG--CGGTTTTATCCTAAAGGGTGTGATTATGACATCTATGTTAACATGCAAGGAAATGTAA

(B)


Ile Ser Gly Gly Gly Glu Lys Phe Tyr Pro Gln Gly Cys Asp Tyr Asp Ile Tyr Val Asn Met Gln Gly Asn Leu
poly(G) tract
270
345
rmpA2-11Gs ATTTCGGGGGGGGGGGAGAAGTTTTATCCTCAAGGGTGTGATTATGACATCTATGTCAACATGCAAGGAAATTTAA
rmpA2-10Gs ATTTCGGGGGGGGGG-AGAAGTTTTATCCTCAAGGGTGTGATTATGACATCTATGTCAACATGCAAGGAAATTTAA
rmpA2-9Gs ATTTCGGGGGGGGG--AGAAGTTTTATCCTCAAGGGTGTGATTATGACATCTATGTCAACATGCAAGGAAATTTAA

(C)

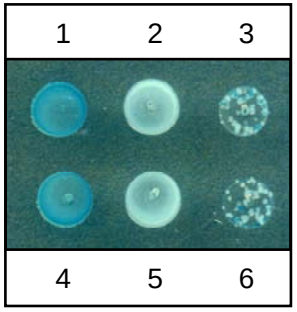
1 2 3
4 5 6

(D)

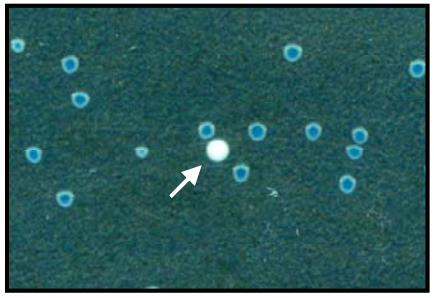

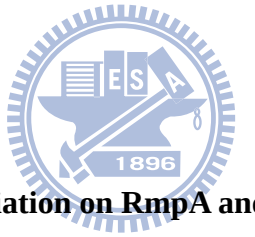

Fig. 4.4. Effect of poly(G) tract variation on RmpA and RmpA2 coding sequence

The DNA sequences and the encoded amino acids encompassing the poly(G) tract (boxed guanidine sequences) in *rmpA* (A) and *rmpA2* (B) genes are shown. The numbers denote the nucleotide position relative to the tri-nucleotide encoding the first amino acid in full-length RmpA or RmpA2. Different numbers of guanidine resulted in the translation of full-length RmpA (*rmpA-10Gs*) and RmpA2 (*rmpA2-11Gs*) or the truncated forms of RmpA (*rmpA-11Gs* and *rmpA-9Gs*) and RmpA2 (*rmpA2-10Gs* and *rmpA2-9Gs*) due to the occurrence of an ochre or an opal stop codon, which are boxed and indicated by an arrow. (C) Overnight cultures of *E. coli* JM109 transformants carrying yT&A (1 and 4), pHY290 (2), pHY291 (3), pHY305 (5) or pHY306 (6) were spotted onto an LB agar plate supplemented with ampicillin, IPTG and X-gal. After incubation at 37°C for 24 h, the plate was photographed. (D) Log-phased culture of *E. coli* JM109 harboring pHY291 was diluted serially and plated onto LB agar plates supplemented with ampicillin, IPTG and X-gal. After incubation at 37°C for 24 h, the plate was photographed. The arrow indicated a white bacterial colony, which harbored a pHY291 carrying alteration in the poly(G) tract, which is confirmed by DNA sequencing.

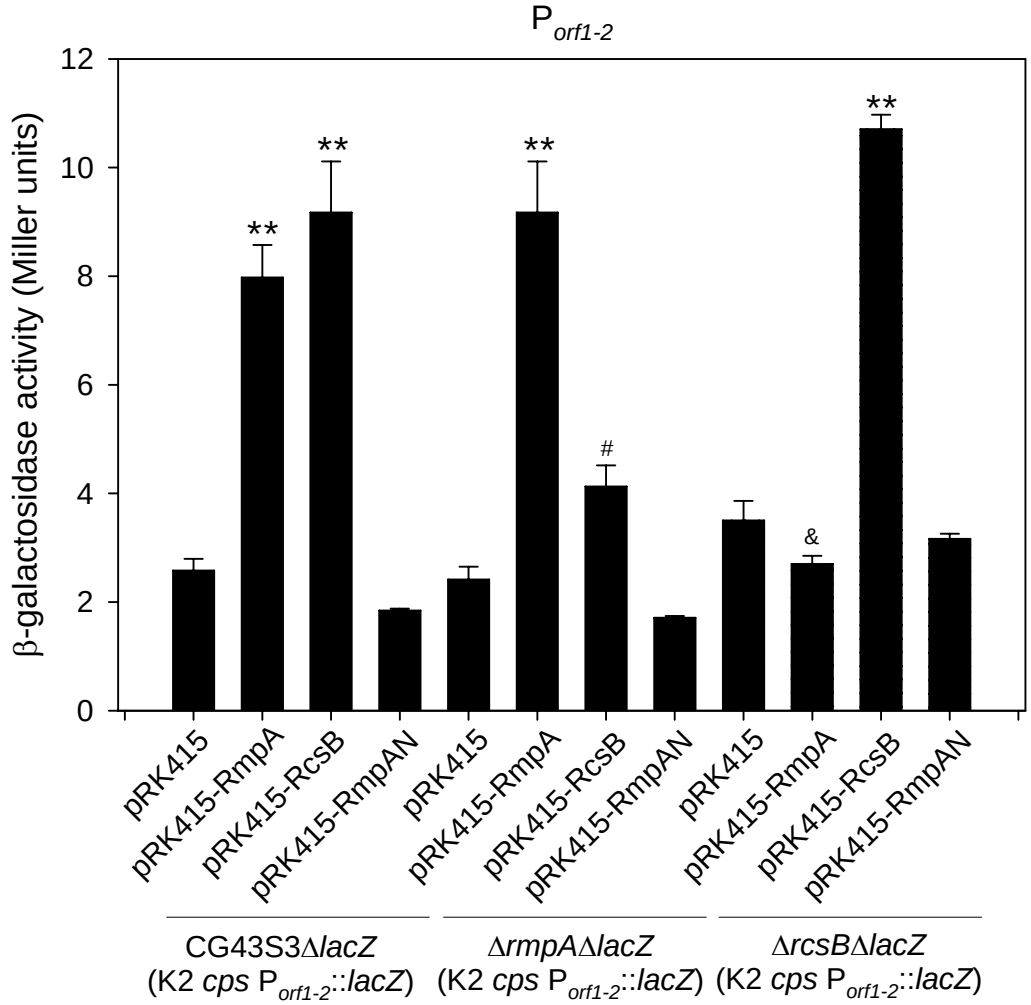

Fig. 4.5. RmpA and RcsB activated the expression of K2 *cps* genes in a coordinated manner

The *K. pneumoniae* CG43S3Δ*lacZ* (wild-type) and its isogenic strains (Δ*rmpA*Δ*lacZ* and Δ*rcsB*Δ*lacZ*), each carrying a chromosomally-integrated K2 *cps* $P_{orf1\text{-}2}$::*lacZ* cassette, were transformed individually with pRK415 and its derived plasmids. The β-galactosidase activities were determined from log-phased (OD_{600} of 0.7) cultures grown in LB broth. The results are shown as the average of the triplicate samples. Error bars indicate standard deviations. **, $P < 0.001$ compared with each strain carrying pRK415 or pRK415-RmpAN. #, $P < 0.001$ compared with Δ*rmpA*Δ*lacZ*[pRK415-RmpA]. &, $P < 0.001$ compared with Δ*rcsB*Δ*lacZ*[pRK415-RcsB].

(A)

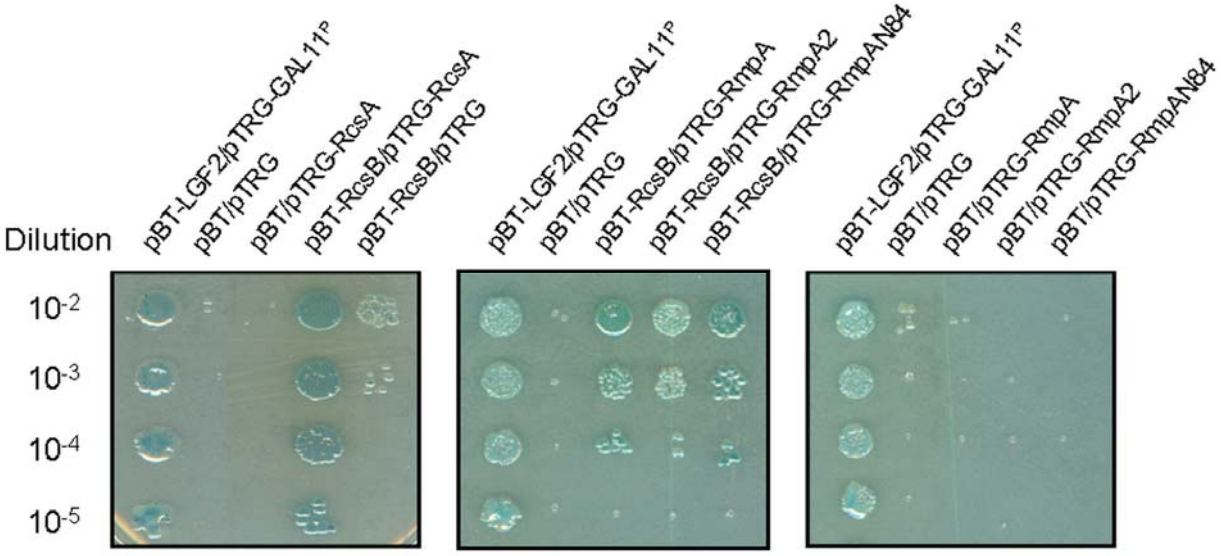
Dilution
pBT-LGF2/pTRG-GAL11P
pBT/pTRG
pBT/pTRG-RcsA
pBT-RcsB/pTRG-RcsA
pBT-RcsB/pTRG
pBT-LGF2/pTRG-GAL11P
pBT/pTRG
pBT-RcsB/pTRG-RmpA
pBT-RcsB/pTRG-RmpA2
pBT-RcsB/pTRG-RmpAN84
pBT-LGF2/pTRG-GAL11P
pBT/pTRG
pBT/pTRG-RmpA
pBT/pTRG-RmpA2
pBT/pTRG-RmpAN84
10-2
10-3
10-4
10-5

(B)

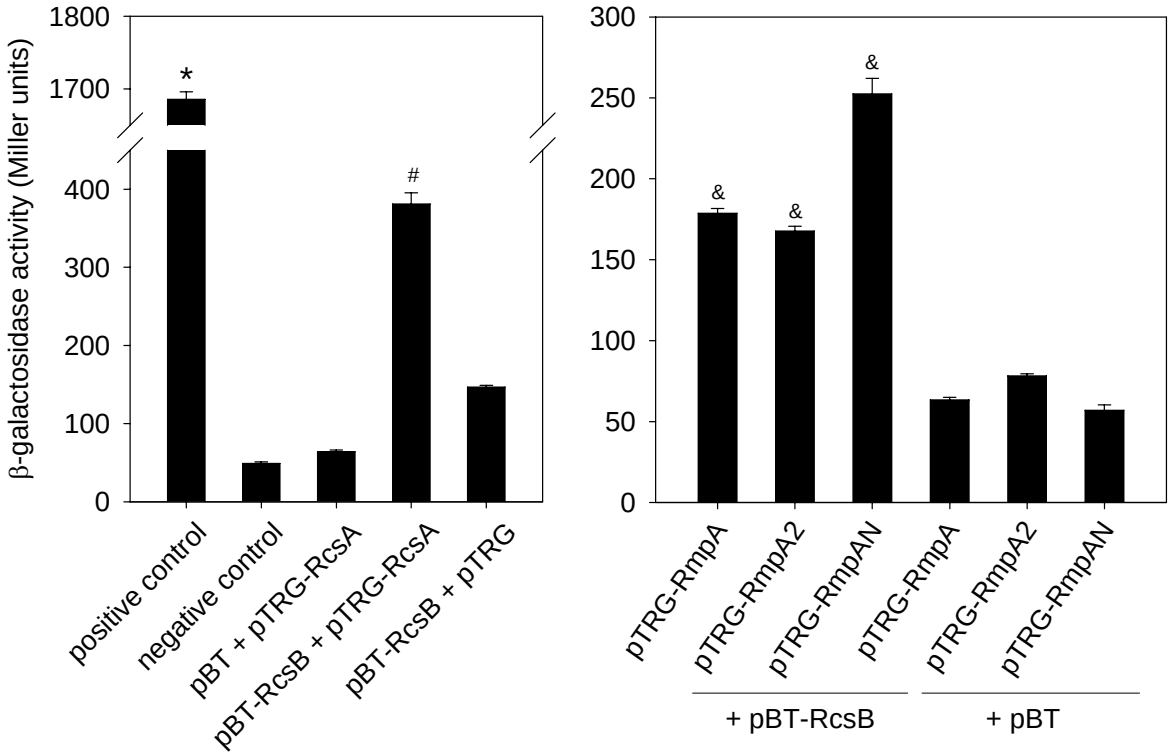
β-galactosidase activity (Miller units)
1800
1700
400
300
200
100
0
300
250
200
150
100
50
0
*
#
&
&
&
positive control
negative control
pBT + pTRG-RcsA
pBT-RcsB + pTRG-RcsA
pBT-RcsB + pTRG
pTRG-RmpA
pTRG-RmpA2
pTRG-RmpAN
pTRG-RmpA
pTRG-RmpA2
pTRG-RmpAN
+ pBT-RcsB
+ pBT

Fig. 4.6. Bacterial two-hybrid analysis of the interaction between RcsA/RcsB, RcsB/RmpA, and RcsB/RmpA2 proteins

(A) The growth of serially-diluted cultures of *E. coli* reporter strains co-transformed with pTRG and pBT or the derived plasmids was investigated on the indicator plate. (B) The *E. coli* reporter strains co-transformed with pTRG and pBT or the derived plasmids were grown to log-phase (OD_{600} of 0.5) in LB broth, induced with IPTG, and the β-galactosidase activities were determined. The results are shown as the average of the triplicate samples. Error bars indicate standard deviations. *, $P < 0.001$ compared with negative control strain carrying the pBT and pTRG. #, $P < 0.001$ compared with the reporter strain carrying either pBT/pTRG-RcsA or pBT-RcsB/pTRG. &, $P < 0.001$ compared with the reporter strain carrying the same pTRG-derived plasmid and the bait vector pBT.

(A)

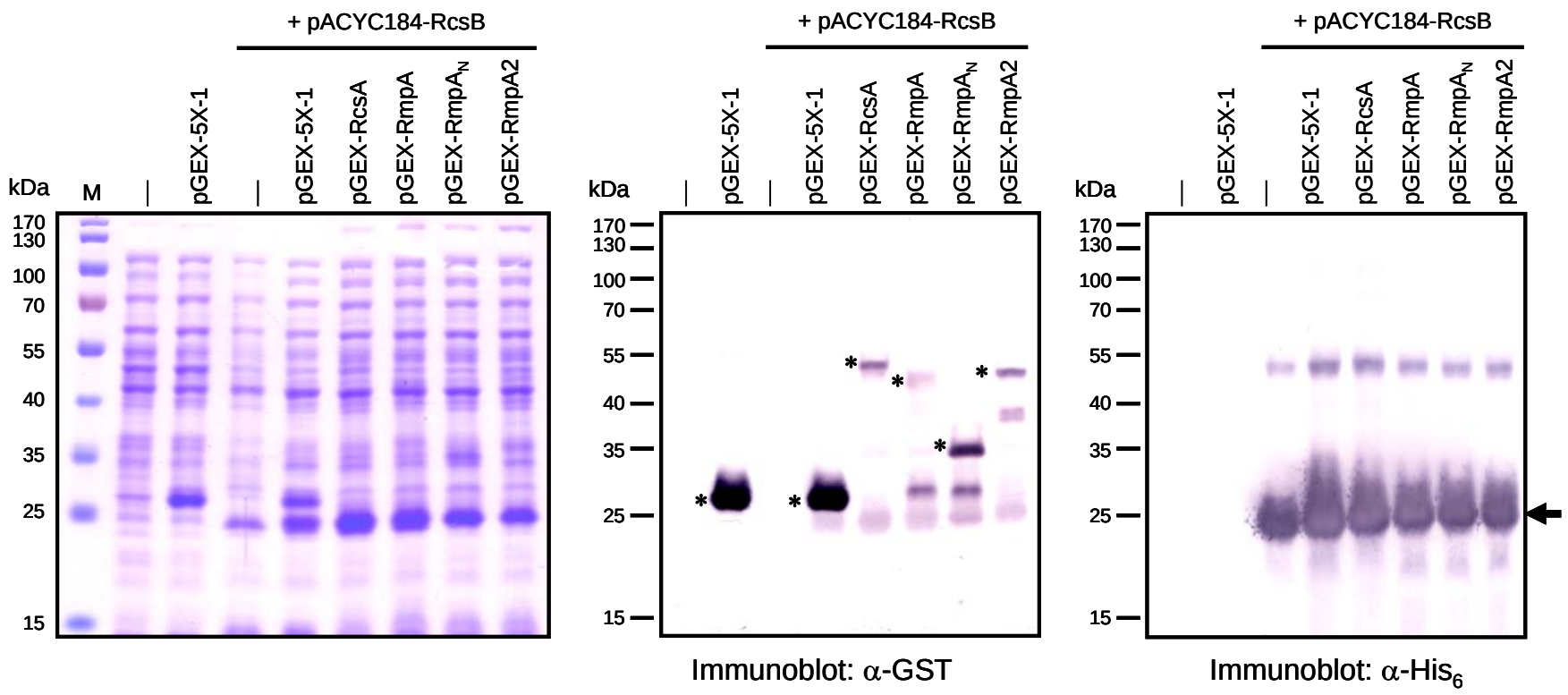
+ pACYC184-RcsB
kDa
M
—
pGEX-5X-1
pGEX-RcsA
pGEX-RmpA
pGEX-RmpA$_N$
pGEX-RmpA2
170
130
100
70
55
40
35
25
15
Immunoblot: α-GST
Immunoblot: α-His$_6$

(B)

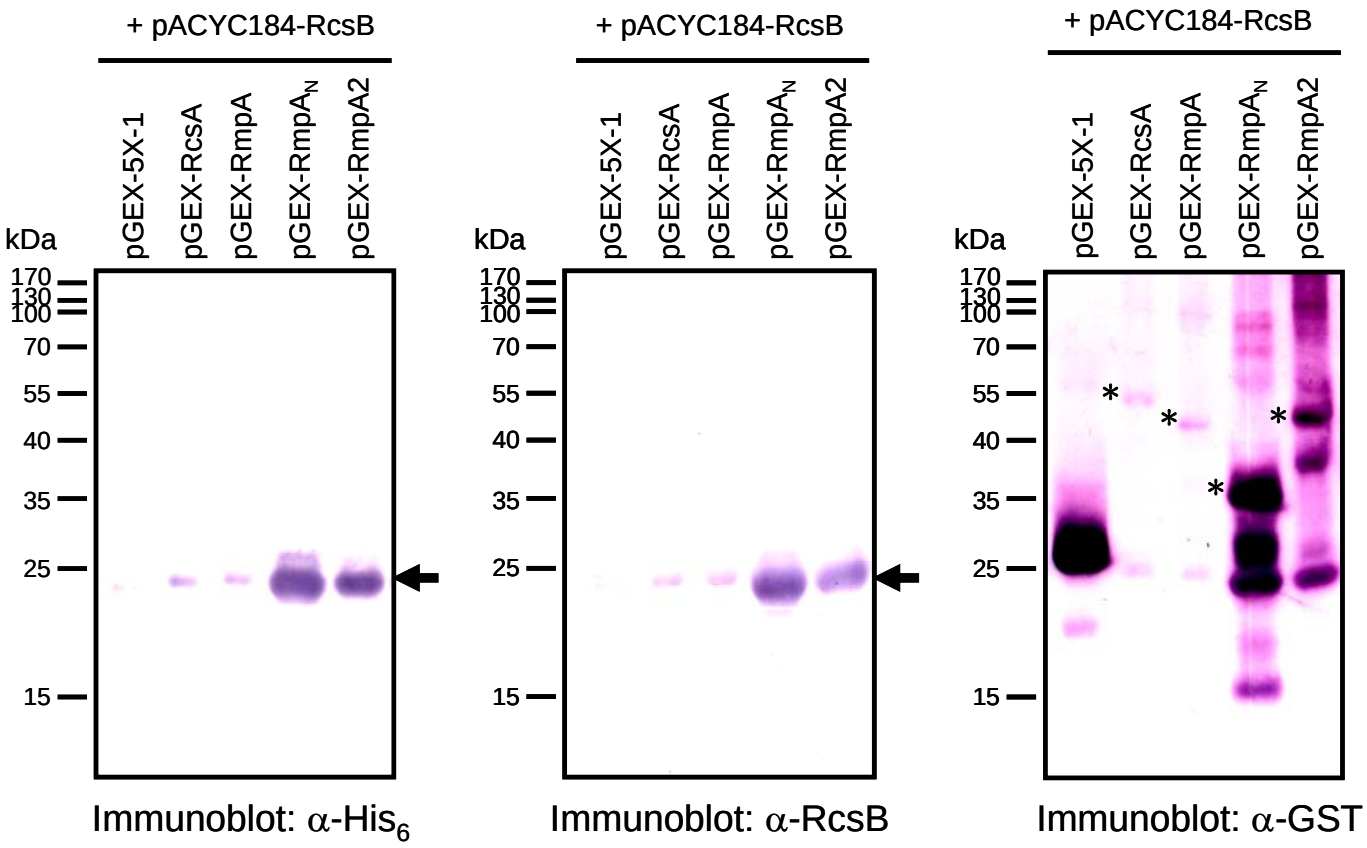
+ pACYC184-RcsB
pGEX-5X-1
pGEX-RcsA
pGEX-RmpA
pGEX-RmpA$_N$
pGEX-RmpA2
kDa
170
130
100
70
55
40
35
25
15
Immunoblot: α-His$_6$
Immunoblot: α-RcsB
Immunoblot: α-GST

84

Fig. 4.7. Co-immunoprecipitation analysis of the interaction between RcsA/RcsB RcsB/RmpA, and RcsB/RmpA2 proteins

(A) Results of SDS PAGE and immunoblot analysis of Pre-IP samples using anti-GST (α-GST) or anti-His_6 (α-His_6) monoclonal antibodies, showing respectively the expression of GST fusion proteins and RcsB-His. Samples were supernatants of induced bacterial cell lysates prepared from *E. coli* BL21(DE3) with or without (—) different combinations of expression vectors as indicated above the figure, and 10 μg of total protein was loaded in each well. The asterisks indicate the expected size of GST and GST fusion proteins. The arrow indicates the expected size of RcsB-His. M, protein ladder. (B) Results of immunoblot analysis of IP samples showing the interaction between the recombinant proteins. Protein complexes were precipitated with glutathione-Sepharose beads, separated by SDS-PAGE and immunoblotted using anti-His_6 (α-His_6) monoclonal antibody, anti-RcsB-His (α-RcsB) polyclonal antiserum or anti-GST (α-GST) monoclonal antibody. The arrows indicate the expected size of RcsB-His.

(A)

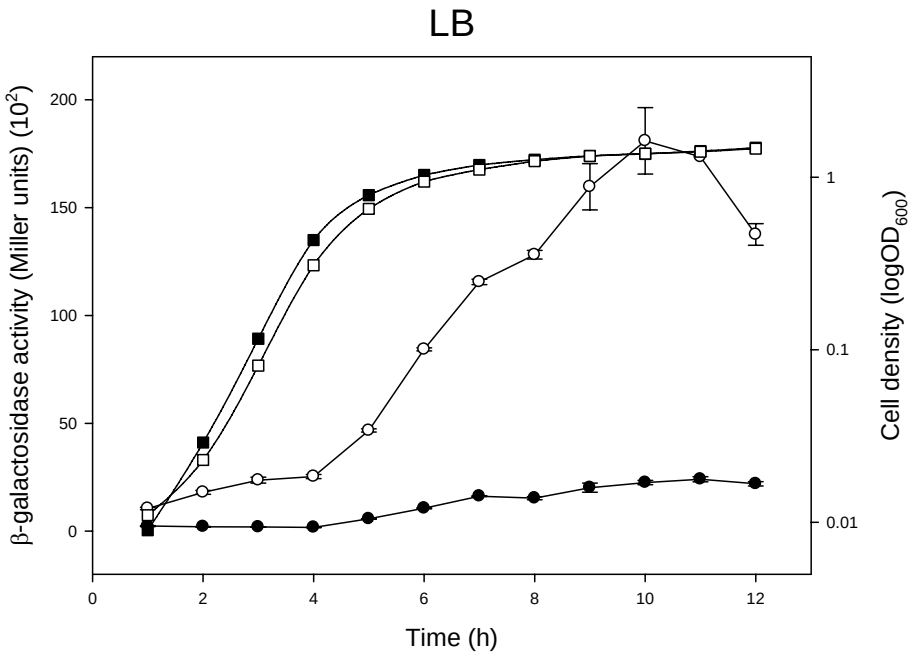

(B)

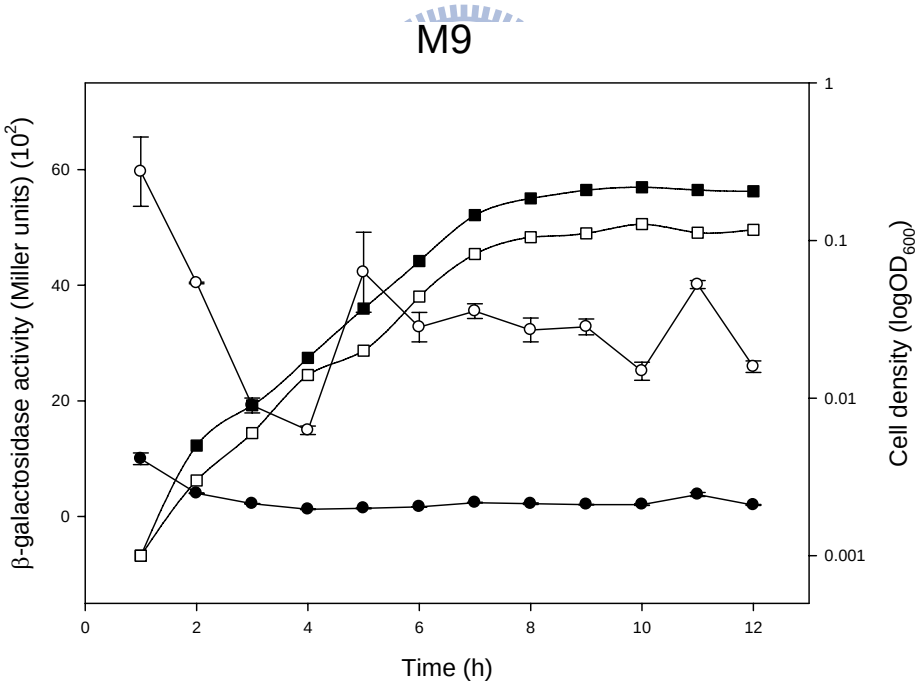

Fig. 4.8. Time course analysis of P_{rmpA}::*lacZ* and P_{rmpA2}::*lacZ* expression

The β-galactosidase activities of *K. pneumoniae* CG43S3Δ*lacZ* carrying respectively placZ15-PrmpA (P_{rmpA}::*lacZ*), placZ15-PrmpA2 (P_{rmpA2}::*lacZ*) were determined from LB (A) or M9-glucose (B) grown cultures. The results are shown as the average of the triplicate samples. Error bars, standard deviations.

(A)

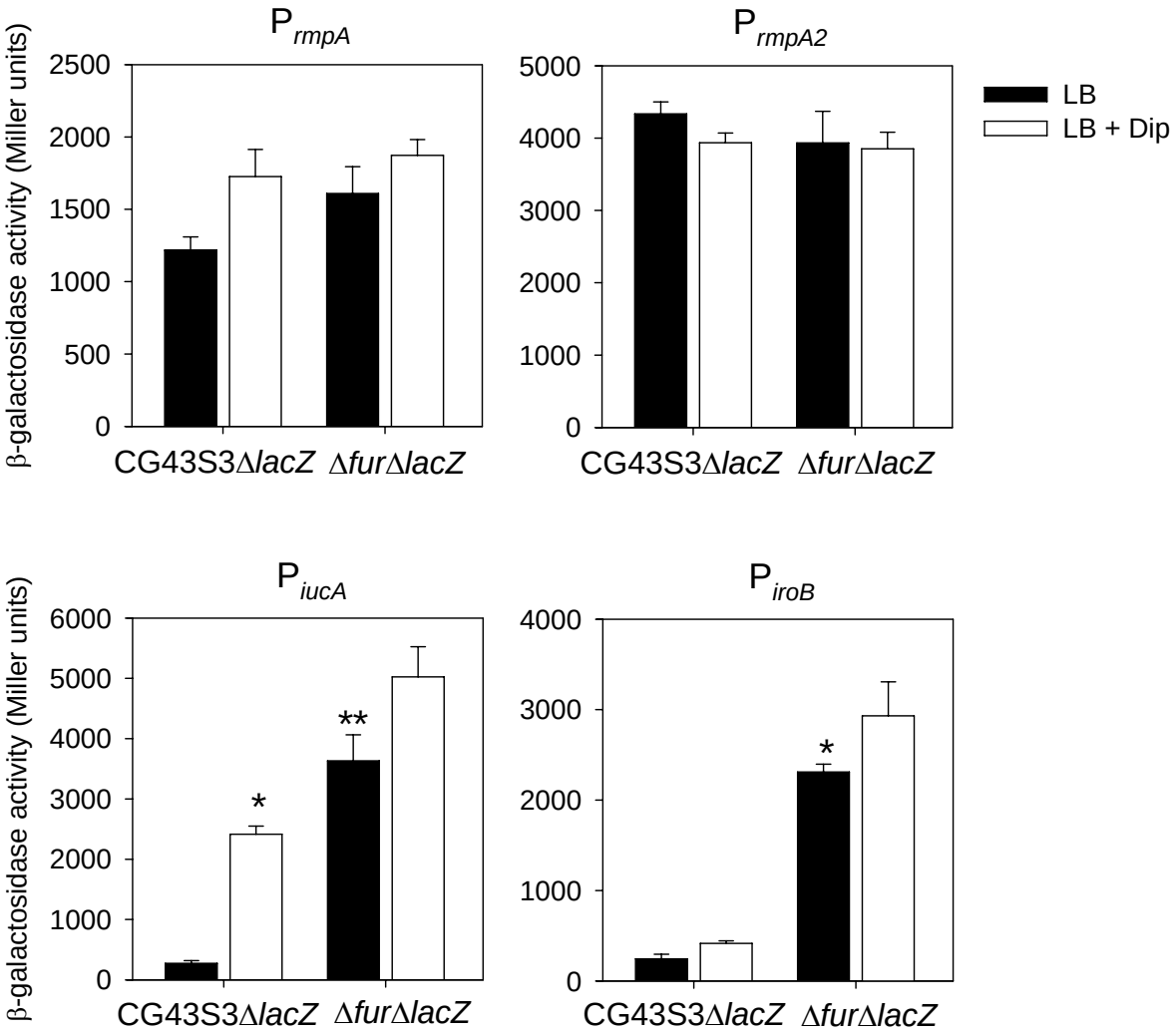
P rmpA
P rmpA2
P iucA
P iroB
β-galactosidase activity (Miller units)
LB
LB + Dip
CG43S3ΔlacZ
ΔfurΔlacZ
*
**

(B)

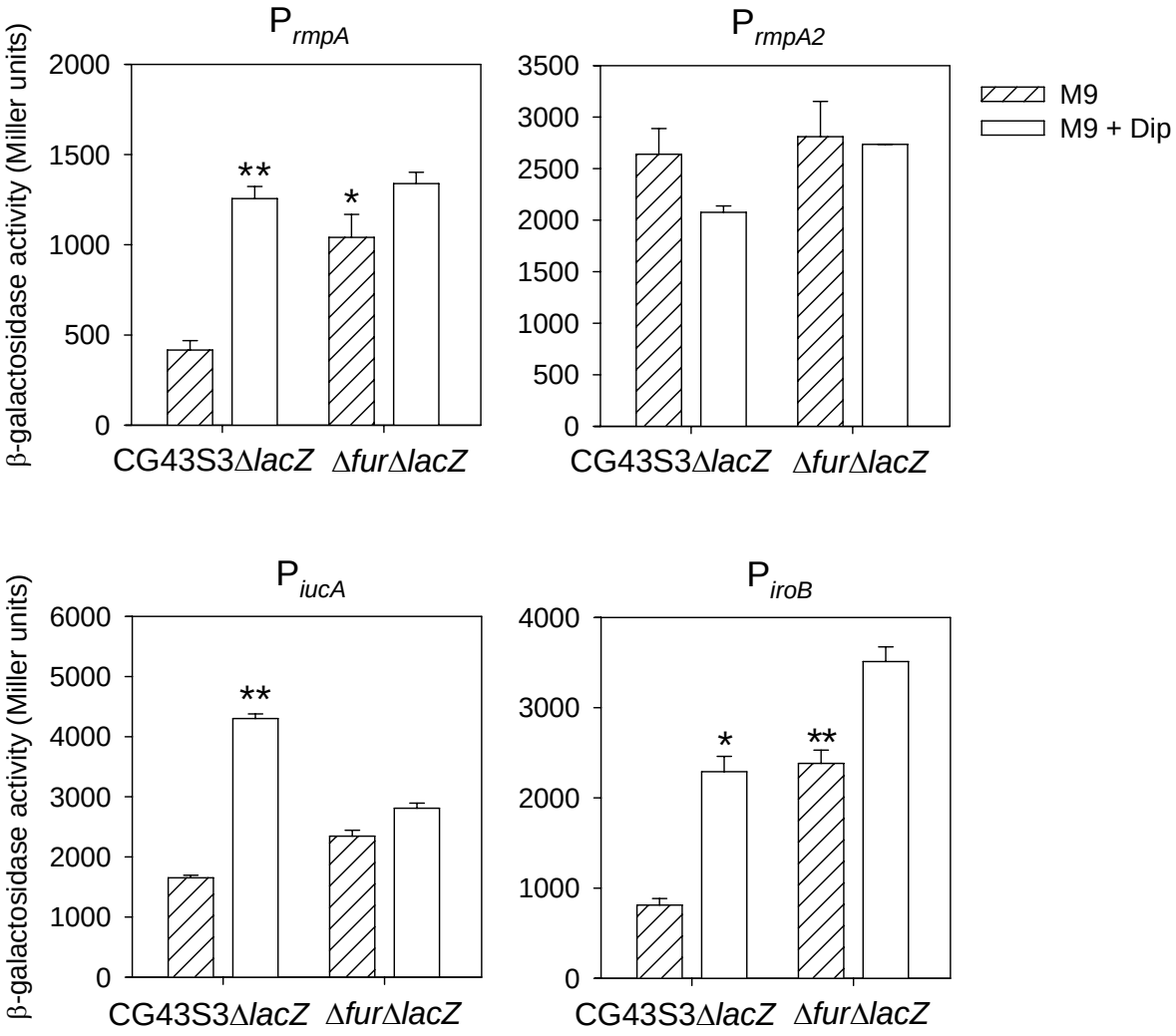
P rmpA
P rmpA2
β-galactosidase activity (Miller units)
2000
1500
1000
500
0
3500
3000
2500
2000
1500
1000
500
0
**
*
CG43S3ΔlacZ
ΔfurΔlacZ
M9
M9 + Dip
P iucA
P iroB
6000
5000
4000
3000
2000
1000
0
4000
3000
2000
1000
0

Fig. 4.9. Effect of *fur* deletion or iron depletion on the activity of P_{rmpA}::*lacZ*, P_{rmpA2}::*lacZ*, P_{iucA}::*lacZ*, and P_{iroB}::*lacZ*

The β-galactosidase activities of *K. pneumoniae* CG43S3Δ*lacZ* (wild-type) or its isogenic *fur* deletion mutant (Δ*fur*) carrying respectively placZ15-PrmpA (P_{rmpA}::*lacZ*), placZ15-PrmpA2 (P_{rmpA2}::*lacZ*), placZ15-PiucA (P_{iucA}::*lacZ*) or placZ15-PiroB (P_{iroB}::*lacZ*) were determined from LB (A) or M9-glucose (B) grown cultures. Media were supplemented with (open bars) or without (filled bars) 200 μM iron chelator 2,2-dipyridyl (+Dip). The results are shown as the average of the triplicate samples. Error bars, standard deviations. *, $P < 0.01$; **, $P < 0.001$ compared with CG43S3Δ*lacZ* grown in the same medium without supplements.

(A)

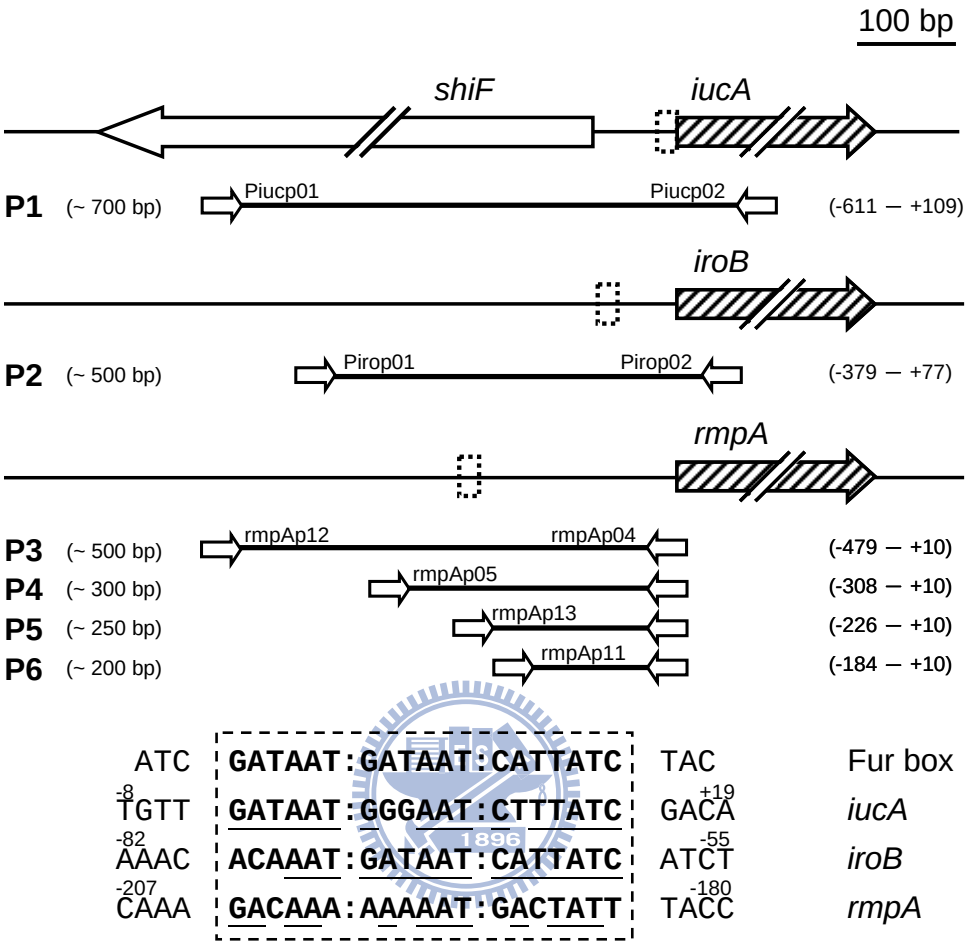
100 bp
shiF
iucA
P1 (~ 700 bp)
Piucp01
Piucp02
(-611 – +109)
iroB
P2 (~ 500 bp)
Pirop01
Pirop02
(-379 – +77)
rmpA
P3 (~ 500 bp)
rmpAp12
rmpAp04
(-479 – +10)
P4 (~ 300 bp)
rmpAp05
(-308 – +10)
P5 (~ 250 bp)
rmpAp13
(-226 – +10)
P6 (~ 200 bp)
rmpAp11
(-184 – +10)
ATC GATAAT : GATAAT : CATTATC TAC Fur box
-8 +19
TGTT GATAAT : GGGAAT : CTTTATC GACA iucA
-82 -55
AAAC ACAAAT : GATAAT : CATTATC ATCT iroB
-207 -180
CAAA GACAAA : AAAAAT : GACTATT TACC rmpA

(B)

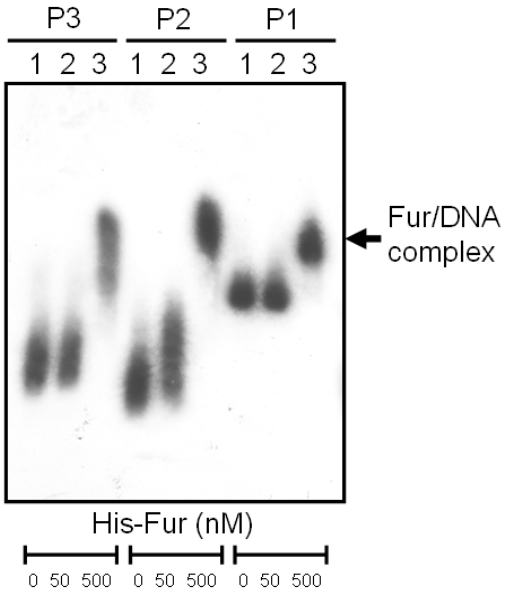
P3
P2
P1
1 2 3 1 2 3 1 2 3
Fur/DNA complex
His-Fur (nM)
0 50 500 0 50 500 0 50 500

(C)

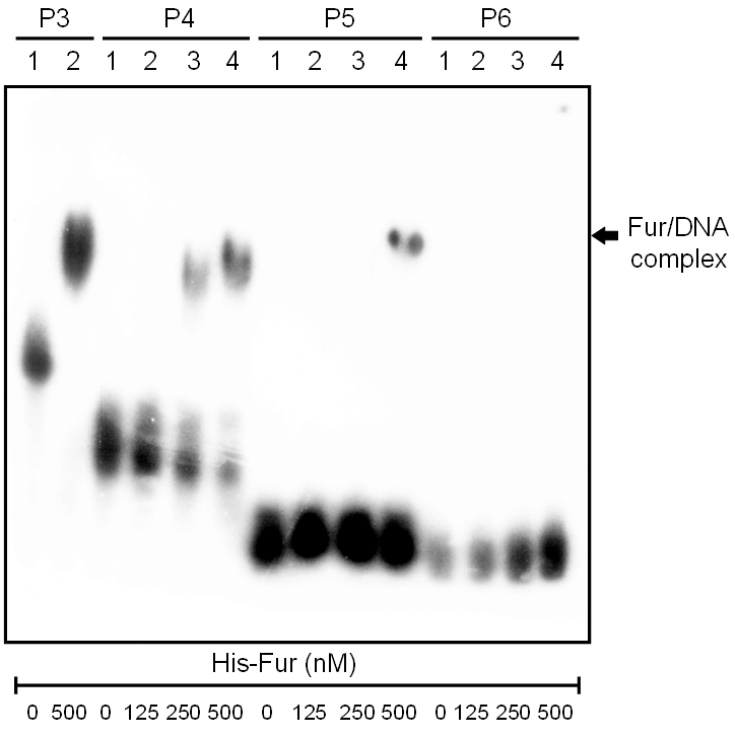
P3
P4
P5
P6
1 2 1 2 3 4 1 2 3 4 1 2 3 4
Fur/DNA complex
His-Fur (nM)
0 500 0 125 250 500 0 125 250 500 0 125 250 500

(D)

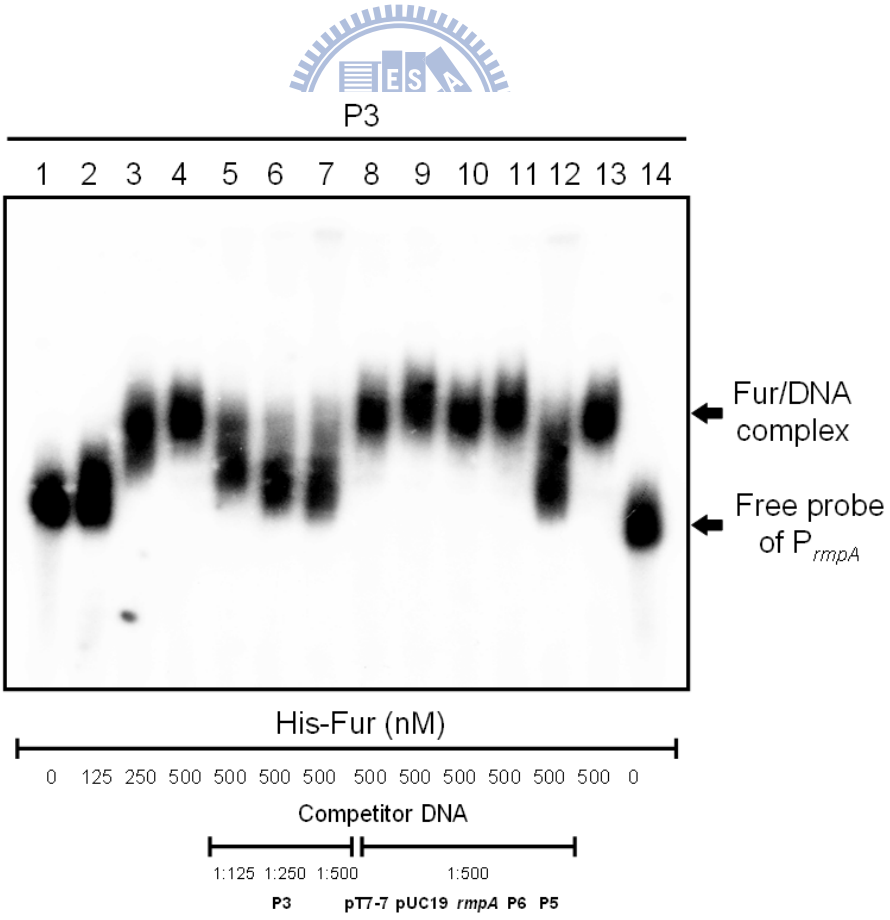
P3
1 2 3 4 5 6 7 8 9 10 11 12 13 14
Fur/DNA complex
Free probe of P_{rmpA}
His-Fur (nM)
0 125 250 500 500 500 500 500 500 500 500 500 500 0
Competitor DNA
1:125 1:250 1:500 1:500
P3 pT7-7 pUC19 rmpA P6 P5

Fig. 4.10. EMSA of the recombinant His-Fur and its target promoters

(A) Diagrammatic representation of the *iucA*, *iroB* and *rmpA* loci. The large arrows represent the open reading frames. The relative positions of the primer sets used in PCR-amplification of the DNA probes are respectively indicated, and the numbers denote the relative positions to the translational start site. Names and sizes of the DNA probes are shown on the left. The dashed boxes indicate the predicted Fur binding sequences and the alignment result is shown below. (B) Binding of His-Fur to its target promoters. The ^{32}P-labeled DNA probes of P_{iucA} (P1), P_{iroB} (P2) and P_{rmpA} (P3) were incubated with increasing amounts of recombinant His-Fur protein as indicated. (C) Binding of His-Fur to P_{rmpA}. The ^{32}P-labeled DNA probes of P_{rmpA} (P3, P4, P5 and P6) were incubated with increasing amounts of recombinant His-Fur protein as indicated. (D) Binding specificity of His-Fur to P_{rmpA}. The ^{32}P-labeled DNA probe of P_{rmpA} (P3) was incubated with varying amounts of His-Fur as indicated. Binding specificity was investigated by adding indicated amounts of unlabeled specific (P3 and P5, lane 5 to7 and lane 12) or non-specific (pT7-7, pUC19 plasmid DNA, *rmpA* gene and P6, lane 8 to 11) competitor DNA fragments.

(A)

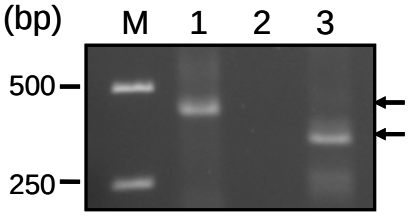
(bp)
M 1 2 3
500
250

(B)

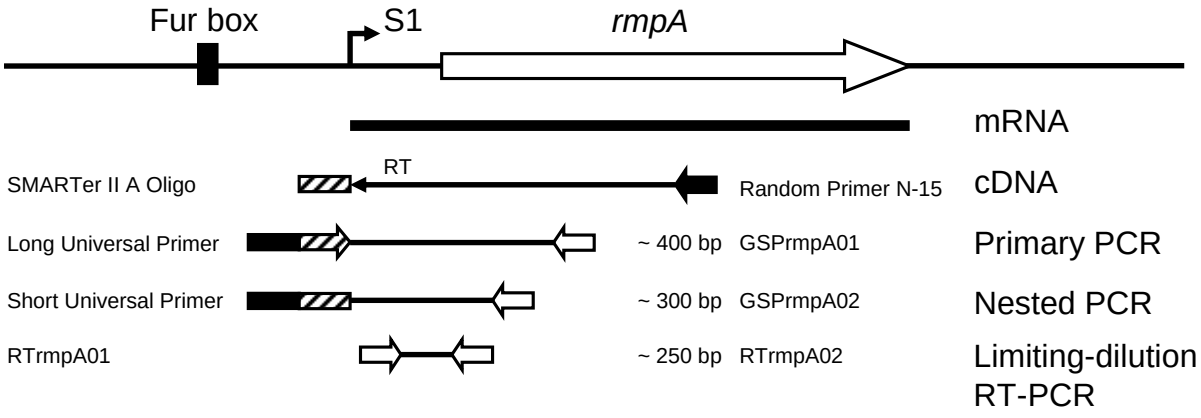
Fur box
S1
rmpA
mRNA
SMARTer II A Oligo
RT
Random Primer N-15
cDNA
Long Universal Primer
~ 400 bp
GSPrmpA01
Primary PCR
Short Universal Primer
~ 300 bp
GSPrmpA02
Nested PCR
RTrmpA01
~ 250 bp
RTrmpA02
Limiting-dilution RT-PCR

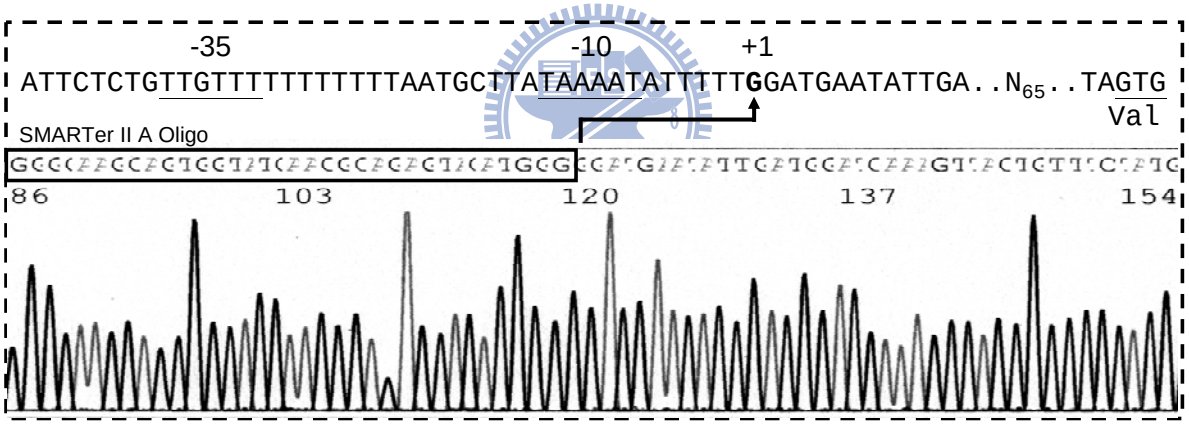
-35
-10
+1
ATTCTCTGTTGTTTTTTTTTTTAATGCTTATAAAATATTTTTGGATGAATATTGA..N65..TAGTG
Val
SMARTer II A Oligo
86
103
120
137
154

(C)

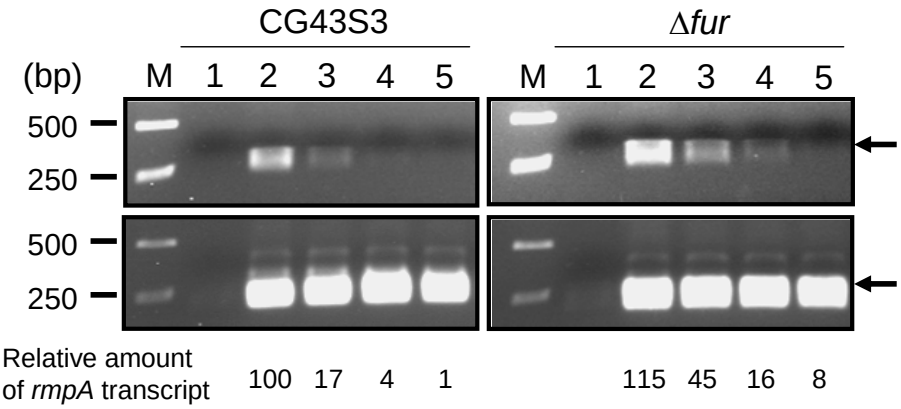
CG43S3
Δfur
(bp)
M 1 2 3 4 5
M 1 2 3 4 5
500
250
500
250
Relative amount of rmpA transcript
100 17 4 1
115 45 16 8

Fig. 4.11. Identification of *rmpA* transcription start site by 5'-RACE

(A) Electrophoresis of the 5'-RACE PCR products. M, DNA ladder. The templates used in each PCR reaction include the cDNA from *K. pneumoniae* CG43S3 (Primary PCR) (lane 1), reverse transcription reaction mixture without transcriptase as a negative control (lane 2), or one hundred-fold diluted primary PCR mixture (Nested PCR) (lane 3). The arrows indicate the expected sizes of the PCR products. (B) Schematic representation of the *rmpA* loci and the 5'-RACE experimental design. The large arrow represents RmpA open reading frame. Relative position of the primers and expected sizes of the products in Primary and Nested PCR are indicated. The *rmpA* transcriptional start site is marked as S1. The potential -10, -35 sites and the translational start site are underlined. (C) Assessment of *rmpA* transcription by limiting-dilution RT-PCR. The templates used in each reaction include total RNA (lane 1) and the four-fold serially-diluted cDNA (lanes 2 to 5 are respectively 1-, 1/4-, 1/16 and 1/64-fold dilution) from *K. pneumoniae* CG43S3 or its isogenic *fur* mutant. Upper panel represents electrophoresis of the RT-PCR products amplified with primers RTrmpA01/RTrmpA02. The RT-PCR products using 23S rRNA gene primers are shown in the lower panel. The expression levels of *rmpA* were quantified and normalized with 23S rRNA using ImageJ software (NIH) as shown below. The *rmpA* expression level of the undiluted cDNA from *K. pneumoniae* CG43S3 was set as 100. The arrows indicate the expected size of the PCR products. M, DNA ladder.

(A)

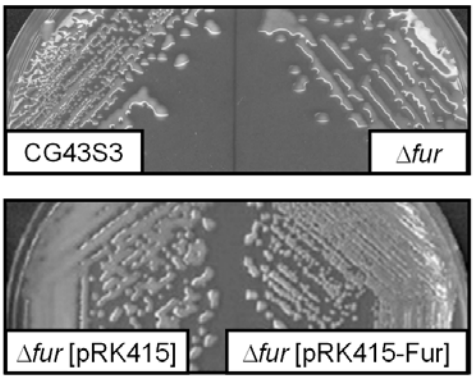
CG43S3
Δfur
Δfur [pRK415]
Δfur [pRK415-Fur]

(B)

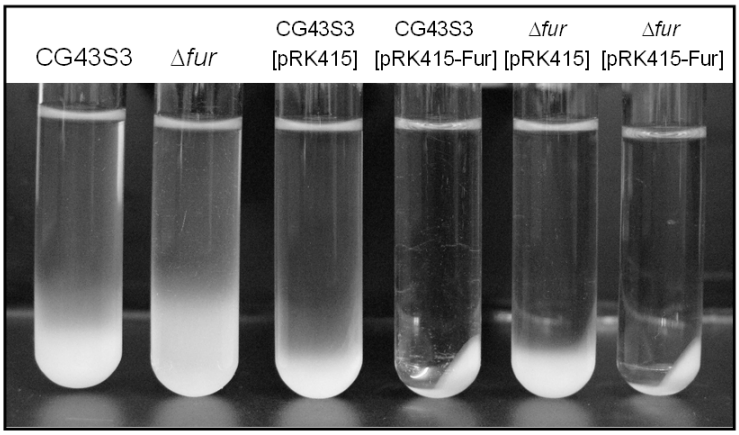
CG43S3
Δfur
CG43S3 [pRK415]
CG43S3 [pRK415-Fur]
Δfur [pRK415]
Δfur [pRK415-Fur]

(C)

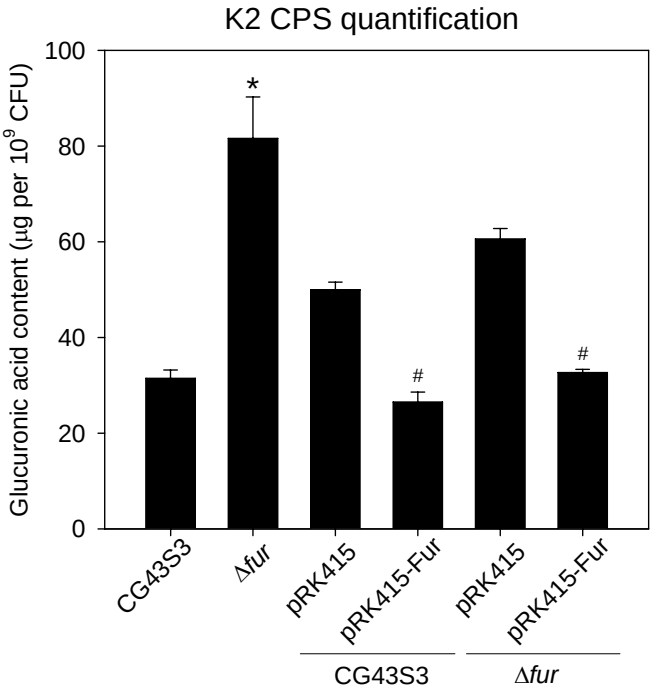
K2 CPS quantification
Glucuronic acid content (μg per 10^9 CFU)
100
80
60
40
20
0
*
#
#
CG43S3
Δfur
pRK415
pRK415-Fur
pRK415
pRK415-Fur
CG43S3
Δfur

Fig. 4.12. Phenotype comparison of *K. pneumoniae* CG43S3, *fur* deletion mutant, and the complemented strain

(A) The bacterial strains on LB agar plates incubated at 37°C for 48 h. (B) Sedimentation test and quantification of K2 CPS for strains grown overnight in LB broth at 37°C and subjected to centrifugation at 4,000 ×*g* for 5 min. (C) The glucuronic acid contents (μg/10^9 CFU) determined from overnight *K. pneumoniae* cultures, expressed as the average of the triplicate samples ± standard deviations. *, $P < 0.001$ compared with CG43S3. **, $P < 0.001$ compared with the same strain carrying pRK415.

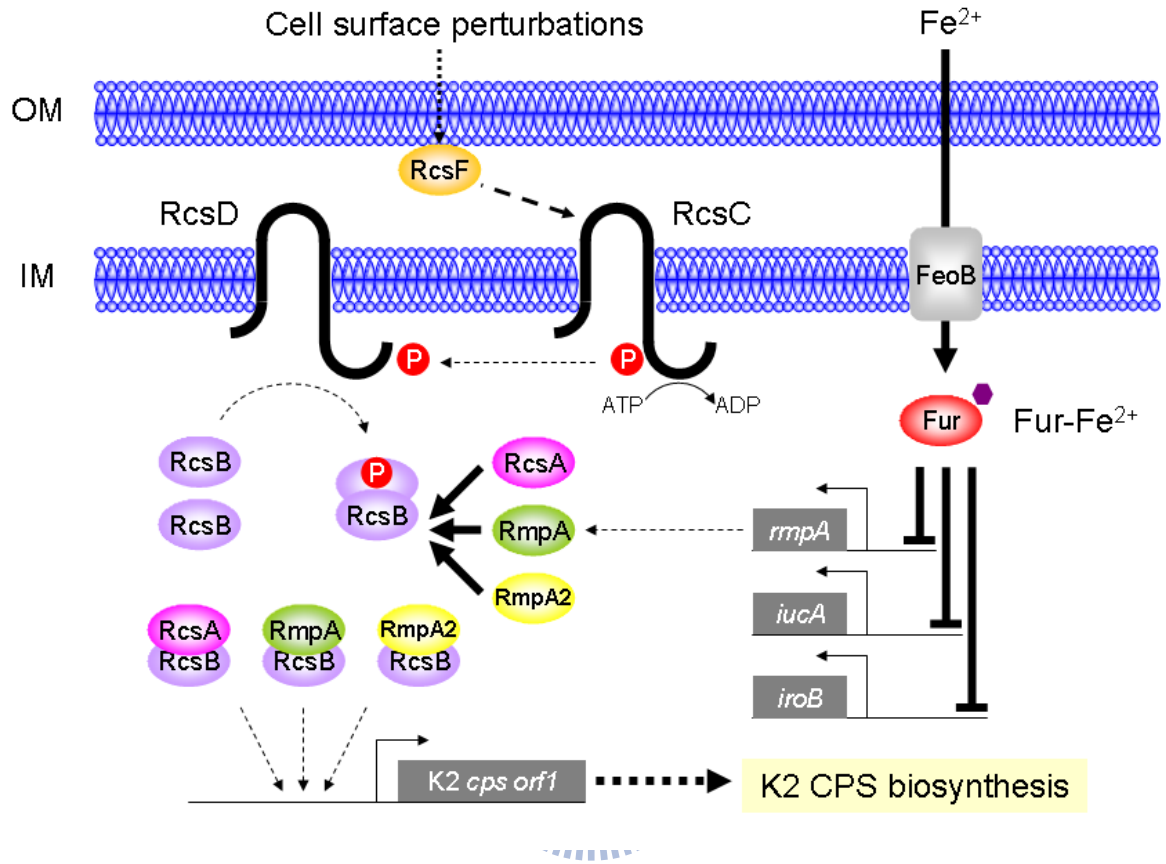

Fig. 4.13. A model illustrating the regulation of *Klebsiella* K2 CPS biosynthesis by RcsB and its auxiliary factors RcsA, RmpA and RmpA2 and the regulation of *rmpA* expression by Fur

The Rcs phosphorelay is initiated from the cell surface perturbations sensed by the membrane protein RcsF, which subsequently activates the sensor kinase RcsC. The phosphate group is then transferred from RcsC to the Hpt protein RcsD and finally to the response regulator RcsB. Apart from the formation of a homo-dimer, RcsB could also form a hetero-dimer with auxiliary factors RcsA, RmpA or RmpA2 to activate the expression of *Klebsiella* K2 *cps* genes. The global regulator Fur, when bound with ferrous ion (shown as a hexagon), represses the expression of *rmpA*, *iuc* and *iro* genes through a direct binding to the respective upstream regions. Consequently, deletion of *fur* results in a de-repression on *rmpA* expression, yielding a more profound K2 CPS biosynthesis.

CHAPTER 5

Conclusion and Perspectives

In this dissertation, we have characterized the regulatory circuits built around 2CSs PhoP/PhoQ, PmrA/PmrB, RstA/RstB and the RcsCDB phosphorelay in *K. pneumoniae* CG43. Though our findings have highlighted a versatile mode of action exerted by bacterial 2CS response regulators, the influence of the sensor kinase could not be underestimated since the integration of multiple environmental clues was a prerequisite of the subsequent phosphorylation cascade. A more complicated regulatory scheme could be expected if the interplay of more than one sensor kinase on a target gene was considered, as some of the cellular functions influenced by different systems may overlap. As described recently, PhoP/PhoQ could also regulate iron uptake via the activation by different signals (41). This also indicated that a subset of virulence genes could be expressed in response to multiple signals, whether they were encountered at the same time or not.

An important issue regarding the regulation of 2CS would be the level and the dynamics of the phosphorylation of each response regulator. We have clearly shown that the phosphorylation and dephosphorylation of PmrA could be finely modulated by PmrB and PmrD *in vitro*. It is unknown; however, if another sensor protein also affects the phosphorylation state of PmrA at a condition yet to be verified. A systematic approach using *in vitro* phosphorylation of PmrA by all the 29 sensor proteins predicted in the *K. pneumoniae* genome, as described previously in *E. coli* (264), would help the identification of the involvement of another 2CS. Alternatively, a comparative analysis of the expression of the PmrA/PmrB downstream targets, such as the *pmr* genes, in the wild-type and each of the 29 sensor kinase gene deletion mutants could be performed. The decreased levels of gene activation in each sensor mutant would indicate the interplay of another sensor kinase. Most recently, the sensor kinase RstB was shown to affect the expression of PhoP-regulated genes by acting on the PhoP sensor (174). Though the precise mechanisms involved in the RstB/PhoQ interaction remained to be demonstrated, it could be inferred that the mode of action exerted by multiple sensors was not restricted to their cognate response regulator.

Although our results indicated that PmrD could interact with the phosphorylated form of PmrA, it remained unknown whether PmrA could interact with PmrD before its phosphorylation. It would also be of importance to investigate the influence of PmrD on the PmrB-mediated phosphorylation and subsequent dimerization of PmrA at the molecular level. In addition, since PmrA could activate the expression of its target genes by a direct binding to the promoter region, how the dimerized PmrA interacts with its DNA target upon PmrD binding would also require further investigation. To resolve the co-structure of PmrA/PmrD complex or even with its DNA binding sequence may help explore the molecular basis of and

the consequences upon PmrD binding to PmrA.

The finding that RcsA/RcsB could cooperatively bind to *K. pneumoniae* K2 *cps* promoter and that RmpA and RmpA2 could both act as alternative accessory factors for RcsB have implied that at least three types of protein complexes could activate K2 *cps* expression. Although the levels of interaction of RcsB with RcsA, RmpA or RmpA2 were determined by two-hybrid analysis, the DNA binding properties of these protein complexes remained to be demonstrated. For example, it remained to be verified if the binding sites of the three complexes would be located on K2 *cps* promoter regions and if they would overlap. Whether the binding of one complex would physically hinder the binding of other complexes or if individual complexes would exhibit differential affinity to each K2 *cps* promoter also required further verification. Strategies such as an EMSA in which excess amounts of an auxiliary factor was added to compete for the DNA/heterodimer complex pre-formed by RcsB and another auxiliary factor could be performed, and the altered mobility of the DNA/protein complex would be indicative of the formation of heterodimer between RcsB and the competitor protein administrated. In addition, the stability of the RmpA or RcsA recombinant protein was relatively low, and to solve this, larger fusion tags such as mannose-binding protein or Nus tag could be utilized. As an alternative approach, co-expression with interaction partner such as RcsB or a chaperone could be considered.

To date, none of the structure of RcsA, RmpA or RmpA2 has been resolved except that the DNA binding portion of RcsB and its interaction with RcsAB box sequence has been reported (200). The complex structure of RcsB with its auxiliary protein and even with their target DNA sequences, such as *Klebsiella* K2 *cps* $P_{orf1\text{-}2}$, would provide a deeper insight into the mode of DNA recognition and complex formation. It must also be taken into account that the expression of each accessory factor-encoding gene may take place in a specific condition; for example, *rmpA* was expressed at a higher level when the environmental level of ferrous ion was scarce. Therefore it is likely that only one complex would predominate in response to one physiological condition.

Accessory factors other than RcsA, RmpA and RmpA2 could also play a role in the expression of RcsCDB downstream genes, as exemplified most recently by the co-binding of GadE/RcsB complex to *gadA* promoter region to initiate the expression of glutamate-dependent acid resistance genes (31). A genome-wide search, such as the co-immunoprecipitation using recombinant RcsB protein or screening of the co-transformants harboring pBT-RcsB and a genomic library constructed on pTRG, would contribute to the identification of other likely accessory factor encoding genes of RcsB. The linkage between

RcsCDB with other regulatory systems not only expends the spectrum of Rcs regulon but also provide additional clues in the regulation of *K. pneumoniae* CPS biosynthesis.

CHAPTER 6

Experimental Section

6.1 Materials

6.1.1 Plasmids, bacterial strains, primers and growth conditions

Bacterial strains and plasmids used in this study are listed in Table 6.1 and Table 6.2, and the primers used are listed in Table 6.3. *E. coli*, *K. pneumoniae* CG43 (36, 192) and its derivatives were propagated at 37°C in Luria-Bertani (LB) broth or M9 minimal medium. Bacterial growth was assessed by measuring the absorbance of optical density at 600 nm (OD_{600}). Otherwise indicated, the antibiotics used include ampicillin (100 μg/mL), chloramphenicol (35 μg/mL), kanamycin (25 μg/mL), tetracycline (12.5 μg/mL) and streptomycin (500 μg/mL). Polymyxin B sulfate salt (8210 USP units per mg) (Sigma-Aldrich) was prepared as 1 unit/μL stock solution in PBS and stored at 4°C before use.

6.2 General Experimental Procedures

6.2.1 Construction of specific gene-deletion mutants

Specific gene deletion was individually introduced into the chromosome of *K. pneumoniae* CG43S3 by allelic exchange strategy (130). In brief, two approximately 1000-bp DNA fragments flanking both sides of the deleted region were cloned into the suicide vector pKAS46 (218), a suicide vector containing *rpsL*, which allows positive selection with streptomycin for vector loss. The resulting plasmid was then mobilized from *E. coli* S17-1 λ*pir* (218) to *K. pneumoniae* CG43S3, *K. pneumoniae* CG43S3Δ*lacZ* (142), *K. pneumoniae* CG43S3Δ*rcsB* (130) or CG43S3-derived strains, by conjugation. The transconjugants, with the plasmid integrated into the chromosome via homologous recombination, were selected with ampicillin and kanamycin on M9 agar plates. Several of the colonies were grown in LB broth supplemented with 500 μg/mL of streptomycin to log phase at 37°C and then spread onto an LB agar plate containing 500 μg/mL of streptomycin. The streptomycin-resistant and kanamycin-sensitive colonies were selected, and the deletion was verified by PCR. The resulting *K. pneumoniae* mutants are listed Table 6.1. To obtain the complementation plasmids, DNA fragments containing the coding sequence of *pmrA*, *phoP*, *pmrF*, *pmrD*, *rmpA*, *rmpA2*, *rcsB* and *fur* were individually PCR-amplified with primer pairs pmrAp03/pmrA06, phoP01/phoP02, ppmrF01/ppmrF02, pmrDp01/pmrDe02, Yu05/Yu06, rmpA2p06/rmpA2p07, rcsBc01/rcsBc02, and CY007/CY008 (Table 6.3) and cloned into the shuttle vector pRK415 (121) to generate pRK415-PmrA, pRK415-PhoP, pRK415-PmrF, pRK415-PmrD, pRK415-RmpA, pRK415-RmpA2, pRK415-RcsB and pRK415-Fur (Table 6.2), respectively. Plasmid pRK415-RmpAN carries an *rmpA* allele with a poly(G) tract of 11-Gs, encoding a truncated form of RmpA (RmpAN) of residues 1 to 84 (Table 6.2).

6.2.2 Extraction and quantification of CPS

Bacterial CPS was extracted using the method described (54). Briefly, 500 μL of overnight grown bacteria was mixed with 100 μL of 1% Zwittergent 3-14 (Sigma-Aldrich, Milwaukee, WI, USA) in 100 mM citric acid (pH 2.0) and incubated at 50°C for 20 min. After centrifugation, 250 μL of the supernatant was transferred to a new tube, and the CPS was precipitated with 1 mL of absolute ethanol. The pellet was dried, dissolved in 200 μL distilled water, and then 1,200 μL of 12.5 mM borax in H_2SO_4 was added. The mixture was vigorously mixed, boiled for 5 min, cooled, and then 20 μL 0.15% 3-hydroxydiphenol

(Sigma-Aldrich, Milwaukee, WI, USA) was added. The absorbance at 520 nm was measured, and the uronic acid content was determined from a standard curve of glucuronic acid and expressed as μg per 10^9 CFU or 10^{10} CFU.

6.2.3 Polymyxin B resistance assay

Polymyxin B resistance assay was performed essentially as described (30) with some modifications. In brief, the overnight-grown *K. pneumoniae* strains were washed twice with saline (0.85% NaCl solution, w/v) and subcultured in LB broth alone or supplemented with 1 mM $FeCl_3$ or with 10 mM $MgCl_2$ at 37°C. The log-phased (OD_{600} of 0.7) bacterial culture was then washed twice and a suspension containing ca. 2.5×10^4 CFU/mL in LB was prepared. Then, 100 μL of the suspension was placed in each well of a 96-well micro-titer plate and 100 μL PBS or PBS-diluted polymyxin B was added to each well to final concentrations of 0, 1, 2, or 4 units/mL of polymyxin B. The plate was incubated at 37°C for 1 h with vigorous shaking. Subsequently, 100 μL of the suspension was directly plated on LB agar plates and incubated at 37°C overnight to determine the number of viable bacteria. The survival rates were expressed as colony counts divided by the number of the same culture treated with PBS and multiplied by 100. The assays were performed thrice, and the results were shown as the average ± standard deviation from triplicate samples.

6.2.4 Cell line, cell culture and phagocytosis assay

The mouse macrophage cell line RAW264.7 was cultivated in Dulbecco's Modified Eagle Medium (DMEM) (Gibco) supplemented with 10% fetal bovine serum (Gibco), 100 units/mL of penicillin and 100 μg/mL of streptomycin (Gibco) at 37°C under 5% CO_2. The evaluation of bacterial phagocytosis was carried out as described with some modifications (45). In brief, cells were washed, resuspended in DMEM containing 10% FBS, and approximately 10^6 cells per well were seeded in a 24 well tissue culture plate and incubated at 37°C for 16 h. Then 100 μL of the bacterial suspension (approximately 3×10^8 CFU/mL in PBS) was used to infect each well to obtain a ratio of ca. 30 bacteria per macrophage. After incubation for 2 h, the cells were washed thrice, then 1 mL of DMEM containing 100 μg/mL of gentamycin was added and incubated for another 2 h to kill the extracellular bacteria. Cells were washed thrice, 1 mL of 0.1% Triton X-100 was added and incubated at room temperature for 10 min with gentle shaking to disrupt the cell membrane. The cell lysate was diluted serially with PBS, plated onto LB agar plates and incubated overnight for determining viable bacteria count. The relative survival rates after phagocytosis were expressed as the

colony counts of viable bacteria divided by those of the original inoculums and multiplied by 100. Three independent trials were performed, and the data shown were the average ± standard deviation from five replicas.

6.2.5 Construction of reporter fusion plasmids and the measurement of promoter activity

The approximately 450, 200, 150, 350 or 500-bp DNA fragments containing the upstream region of the *K. pneumoniae rstA, pmrD* or *pmrHFIJKLM* gene cluster were PCR-amplified with primers rstAp01/rstAp02, rstAp03/rstAp02, rstAp04/rstAp02, pmrDp01/pmrDp02 or pmrHp01/pmrHp02 (Table 6.3), respectively and cloned in front of a promoter-less *lacZ* gene of the promoter selection plasmid placZ15 (142). The resulting plasmids, pHY048, pHY050, pHY053, placZ15-PpmrD and placZ15-PpmrH were mobilized from *E. coli* S17-1 λ*pir* to *K. pneumoniae* strains by conjugation. β-galactosidase activity was determined as previously described (142). In brief, overnight cultures were washed twice with saline and sub-cultured in LB alone or supplemented with 10 mM $MgCl_2$, 0.1 mM $FeCl_3$, or 0.1 mM $FeCl_3$ plus 0.3 mM ferric iron scavenger deferoxamine (Sigma-Aldrich) to mid-log phase (OD_{600} of 0.7). Then 100 μL of the culture was mixed with 900 μL of Z buffer (60 mM Na_2HPO_4, 40 mM NaH_2PO_4, 10 mM KCl, 1 mM $MgSO_4$, 50 mM β-mercaptoethanol), 17 μL of 0.1% SDS, and 35 μL of chloroform and the mixture was shaken vigorously. After incubation at 30°C for 10 min, the reaction was initiated by adding 200 μL of 4 mg/mL ONPG (o-nitrophenyl-β-D-galactopyranoside) (Sigma-Aldrich). Upon the appearance of yellow color, the reaction was stopped by adding 500 μL 1 M Na_2CO_3. OD_{420} was recorded and the β-galactosidase activity was expressed as Miller units (163). Each sample was assayed in triplicate, and at least three independent experiments were carried out. The data shown were calculated from one representative experiment and shown as the means and standard deviation from triplicate samples.

6.2.6 Cloning, expression and purification of recombinant proteins

The DNA fragment of PhoP coding region was PCR amplified from the genomic DNA of *K. pneumoniae* CG43S3 with primers phoP05/phoP06 (Table 6.3). The amplified PCR products were cloned into the PCR cloning vector yT&A (Yeastern Biotech, Taiwan). The *Eco*RI/*Bam*HI and *Sal*I fragments from the resulting plasmid were then cloned individually into pET30b (Novagen, Madison, Wis, USA) to generate pET30b-PhoP and pET30b-PhoPN (Table 6.2) to allow the in-frame fusion to the amino-terminal His-tag. Plasmid pET30b-PmrBC was constructed by cloning DNA fragments PCR-amplified with

pmrBe03/pmrBe04 (Table 6.3) into a *Bam*HI/*Hin*dIII site on pET30b. Plasmids pET-PmrA and pET-PmrD (courtesy of Dr. Chinpan Chen, Academia Sinica, Taipei, Taiwan) were constructed by cloning DNA fragments PCR-amplified with KP1760-1/KP1760-2 and KP3573-1/KP3573-2 (Table 6.3) into an *Nde*I/*Xho*I site, respectively into pET29b. The coding region of *rcsB* or *fur* was PCR amplified with primer sets rcsBe01/rcsBe02 or CY0010/CY0011 (Table 6.3) and cloned into the *Nde*I/*Xho*I site in pET30b or the *Bam*HI/*Hin*dIII site in pET30c, respectively. This generates pET30b-RcsB with a carboxyl terminus His-tag (RcsB-His) or pET30c-Fur with an amino-terminus His-tag (His-Fur). The resulting plasmids were transformed into *E. coli* BL21(DE3) or *E. coli* BL21(DE3)[pLysS] (Invitrogen, USA), and the recombinant proteins were over-produced from the mid-log phased culture (OD_{600} ~ 0.4 to 0.5) by induction with 0.5 mM IPTG (isopropyl 1-thio-β-$_D$-galactopyranoside) for 4 h at 37°C. The proteins were then purified from total cell lysate by affinity chromatography using His-Bind resin (Novagen, Madison, Wis). After purification, the eluent was dialyzed against 1× protein storage buffer (10 mM Tris-HCl pH 7.5, 138 mM NaCl, 2.7 mM KCl, and 10% glycerol) at 4°C overnight, followed by condensation with PEG20000, and the purity was determined by SDS-PAGE analysis.

6.2.7 DNA electrophoretic mobility shift assay (EMSA)

EMSA was performed as previously described (130). In brief, the DNA fragments encompassing the putative *pmrD* promoter region or P1 to P6 were obtained by PCR amplification with primer pairs pmrDp01/pmrDp02, piucp01/piucp02, pirop01/pirop02, rmpAp04/rmpAp12, rmpAp04/rmpAc01, rmpAp04/rmpAp13 and rmpAp04/rmpAp11 (Table 6.3) respectively and end-labeled with [γ-^{32}P]ATP using T4 polynucleotide kinase. The purified His-PhoP or His-PhoP$_{N149}$ protein was mixed with the P_{pmrD} DNA probe in a 50-μL reaction mixture containing 20 mM Tris-HCl pH 8.0, 50 mM KCl, 1 mM $MgCl_2$, 1 mM dithiothreitol, and 7.5 mM acetyl phosphate. The purified His-Fur protein was mixed with labeled probes P1 to P6 (approximately 0.1 ng) in a 50-μL reaction mixture containing 50 mM Tris-HCl pH 7.5, 100 mM NaCl, 0.1 mM EDTA, 10 mM dithiothreitol, and 0.5 μg/μL BSA. The mixture was incubated at room temperature for 30 min, mixed with 0.1 volume of DNA loading dye, and then loaded onto a 5% nondenaturing polyacrylamide gel containing 5% glycerol in 0.5× TBE buffer (45 mM Tris-HCl pH 8.0, 45 mM boric acid, 1.0 mM EDTA) (for His-PhoP and His-PhoP$_{N149}$) or 0.5× TB buffer (45 mM Tris-HCl pH 8.0, 45 mM boric acid) containing 100 μM of $MnCl_2$ (for His-Fur). After electrophoresis at a constant current

of 20 mA at 4°C for 1 to 2 h, the results were detected by autoradiography.

6.2.8 Bacterial two-hybrid assay

The bacterial two-hybrid assay was performed as described previously (105, 129). To obtain the recombinant plasmids, the DNA fragments encoding full-length PmrA and PmrD were PCR-amplified with primer sets pmrA10/pmrA11 and pmrDe15/pmrDe16 (Table 6.3), respectively, and cloned into the 3' end of genes encoding the α subunit of RNA polymerase (RNAPα) domain in pBT and λ-cI repressor protein domain in pTRG to generate pBT-PmrA and pTRG-PmrD. The DNA fragments encoding full-length RcsA, RmpA, RmpAN, or RmpA2 were PCR-amplified with primer sets rcsAe04/rcsAe07, rmpAe04/rmpAe05 or rmpA2p08/rmpA2p14 (Table 6.3) and cloned to the 3' end of the gene encoding λ-cI repressor protein domain in pTRG to generate pTRG-RcsA, pTRG-RmpA, pTRG-RmpAN or pTRG-RmpA2, respectively. The DNA fragments encoding the full-length RcsB were PCR-amplified with primers rcsBe02/rcsBe04 (Table 6.3) and cloned to the 3' end of the gene encoding the α subunit of RNA polymerase (RNAPα) domain in pBT to generate pBT-RcsB. The resulting plasmids were confirmed by DNA sequencing. The positive control plasmids used were pTRG-Gal11^{P} and pBT-LGF2 (Stratagene). The pBT and pTRG derived plasmids were co-transformed into *E. coli* XL1-Blue MRF' Kan cells and selected on LB agar plates supplemented with 12.5 μg/mL tetracycline, 25 μg/mL chloramphenicol, and 50 μg/mL kanamycin. To investigate the protein-protein interaction *in vivo*, cells were grown until the OD_{600} reached 0.3 at 30°C and then diluted serially (10^{-1}, 10^{-2}, 10^{-3}, and 10^{-4}). Two-microliters of the bacterial culture were spotted onto LB agar plates supplemented with 350 μg/mL carbenicillin, 25 μg/mL chloramphenicol, 50 μg/mL kanamycin, 12.5 μg/mL tetracycline, 50 μg/mL X-gal (5-bromo-4-chloro-3-indolyl-β-$_{D}$-galactopyranoside), and 20 μM IPTG. Growth of the bacterial cells was observed after incubation at 30°C for 36 to 48 h and photographed. For the measurement of β-galactosidase activities, *E. coli* strains carrying different combinations of the recombinant plasmids were grown for 48 h at 30°C. After washing with LB, the bacteria were grown at 30°C to an OD_{600} of 0.5. IPTG was then added to a final concentration of 20 μM, and the cultures were incubated at 30°C for another 16 h. Finally, the β-galactosidase activity was determined and calculated as described above.

6.2.9 *In vitro* phosphotransfer assay

The *in vitro* phosphotransfer assay was performed essentially as described (117). The phospho-PmrB$_{C276}$ protein was obtained by pre-incubation of His-PmrB$_{C276}$ protein (5 μM)

with 40 μCi of [γ-^{32}P]ATP in 80 μL of 1× phosphorylation buffer (10 mM Tris-HCl, pH 7.5; 138 mM NaCl; 2.7 mM KCl; 1 mM $MgCl_2$; 1 mM DTT) for 1 h at room temperature. The reaction mixture was then chilled on ice, and 5 μL of the mixture was removed and mixed with 2.5 μL of 5× SDS sample buffer as a reference sample. The phospho-$PmrB_{C276}$ protein mixture (30 μL) was then mixed with equal volumes of 1× phosphorylation buffer containing either PmrA (10 μM) or PmrA with PmrD (each at 10 μM) to initiate the phosphotransfer reaction. A 10-μL aliquot was removed at specific time points, mixed with 2.5 μL of 5× SDS sample buffer to stop the reaction, and the samples were kept on ice until the performance of SDS-PAGE. After electrophoresis at 4°C, the signal was detected by autoradiography.

6.2.10 Kinase/phosphatase and autokinase assay

The assays were performed essentially as described (117). The recombinant protein His-$PmrB_{C276}$ (2.5 μM) was incubated with His-PmrA (5 μM) alone or with His-PmrD (5 μM) for kinase/phosphatase assay or incubated with His-PmrD (5 μM) alone for autokinase assay. The reactions were carried out in 30 μL of 1× phosphorylation buffer with 3.75 μCi [γ-^{32}P]ATP at room temperature and started with the addition of His-$PmrB_{C276}$. An aliquot of 10-μL was removed at specific time points, mixed with 5 × SDS sample buffer to stop the reaction, and the samples were kept on ice until the performance of SDS-PAGE. After electrophoresis at 4°C, the signal was detected by autoradiography.

6.2.11 Construction of complementation plasmids encoding PmrD with point mutations

The *pmrD* complementation plasmids carrying mutant *pmrD* alleles were constructed by either inverse-PCR or by overlap-PCR method. In inverse-PCR strategy, 10 ng of pHY115 was used as the template for PCR-amplification with the complementary primer sets encompassing the mutation site by using Phusion DNA polymerase (Finnzymes, Espoo, Finland). The PCR product was resolved on agarose gel, recovered, treated with *Dpn*I for 3 h to remove the template plasmid and transformed into *E. coli* JM109. The plasmids carrying each mutation allele were individually prepared from each transformant colony and confirmed by sequence analysis. Then the DNA fragments carrying each mutant *pmrD* allele preceded by a native *pmrD* promoter region were cloned into pRK415 to generate the complementation plasmids. For the overlap-PCR method, two DNA fragments were first PCR-amplified from pHY115 template: one with the primer set designed complementary to *pmrD* upstream 278-bp region (pmrDp01) (Table 6.3) and to the mutation site; the other with the primer set designed complementary to the mutation site and the 3'-end of *pmrD* gene

(pmrDe02) (Table 6.3). The PCR products were mixed, diluted hundredfold individually and used as the template for a second PCR amplification with the primer set pmrDp01/pmrDe02 (Table 6.3). The resulting DNA fragments, each harboring a mutant *pmrD* allele preceded by a native *pmrD* promoter region, were cloned into pRK415 to generate the complementation plasmids (Table 6.2) which were confirmed by sequence analysis.

6.2.12 Subtractive cDNA hybridization

To identify genes specifically expressed in *K. pneumoniae* wild type strain and Δ*rstA* mutant, cDNA PCR amplicon was obtained by using Clontech PCR-Select™ cDNA Subtraction Kit (Clontech, Palo Alto, CA). Total RNA was isolated from mid-log phased M9 cultures of *K. pneumoniae* CG43S3U9451 and its isogenic Δ*rstA* mutant strain by extraction with TRI reagent (Molecular Research Center, Cincinnati, OH). Contaminating DNA was eliminated from the RNA samples with RQ1 RNase-Free DNase (Promega, Madison, WI, USA). Two micrograms of total RNA were used in the first-strand cDNA synthesis and the subsequent second-strand cDNA synthesis by using the Avian Myeloblastosis Virus (AMV) Reverse Transcriptase provided in the kit. The cDNA samples from the parental strain and isogenic Δ*rstA* mutant were then digested by *Rsa*I, ligated to two different adaptors to produce separate tester and driver cDNA pools. Subtraction of cDNA was then performed by mixing the cDNA samples stoichiometrically in two rounds of hybridization followed by two rounds of PCR amplification to enrich the differentially expressed sequences, firstly with the primers based on the adaptor sequence and then with the primers designed with sequences nested into the adaptors. The PCR products were then cloned into yT&A and then were sequenced. The retrieved DNA sequences were used to search in the released genome sequences of *K. pneumoniae* NTUH-K2044 (262), MGH78578 (http://genome.wustl.edu/), and 342 (74) by BLAST (http://www.ncbi.nlm.nih.gov).

6.2.13 Measurement of bacterial growth in iron depletion/repletion conditions

Cultures of the parental strain *K. pneumoniae* CG43S3, along with deletion mutant strains Δ*rstA*, Δ*rstB*, and Δ*rstA*Δ*rstB* were grown overnight in LB or M9 medium. For the growth curve measurement in LB medium, iron depletion was created by adding 2,2-dipyridyl to a final concentration of 200 μM as described previously (111). Twenty microliters of overnight LB cultures of *K. pneumoniae* strains was used to inoculate 4 mL of either LB or LB supplemented with 2,2-dipyridyl. For the growth curve measurement in M9 medium, ferrous sulfate was added to a final concentration of 20 μM for iron-repletion

conditions (111). Thirty microliters of overnight M9 cultures of *K. pneumoniae* strains was used to inoculate 2 mL of either M9 or M9 supplemented with ferrous sulfate. The cultures were incubated at 37°C with shaking, and the optical density was recorded as the absorbance at 600nm (OD_{600}) at the indicated time points. Values were the average and standard deviation from triplicate samples from one of the three independent trials.

6.2.14 Growth inhibition assay

As described previously, growth inhibition assays was performed to investigate the bacterial resistance to lead with some modifications (108). In brief, *K. pneumoniae* strains were grown overnight in M9 minimal medium, washed twice with heavy metal MOPS (HMM) medium (132) and diluted 100-fold into fresh HMM medium. Then, 100 μL of each *K. pneumoniae* culture was used to inoculate each well of a 96-well microtiter plate preloaded with 100 μL HMM medium or HMM medium supplemented with increasing concentrations of lead nitrate to reach final concentrations ranging from 80 to 0.15625 μM in a two-fold serial dilution. The top and bottom 12-well rows contained only HMM medium without bacteria for the duration of the experiment in order to minimize error from evaporation of the medium. Assays were performed with triplicate samples, and the plates were incubated at 37°C and shaken for 24 hours before measuring OD_{595} using a BIO-TEK ELx800 Universal Microplate Reader (Cole-Parmer, Vernon Hills, IL). The average OD_{595} of the 12 wells containing only medium was subtracted from the average OD_{595} of triplicate samples to obtain the OD reading used in relative growth calculations. Relative growth values were determined by dividing the average OD_{595} of each strain at each concentration with the average OD_{595} in wells with the lowest concentration of Pb^{2+} (0.15625μM) in the same strain. Relative growth values of one and zero corresponded to no growth inhibition and to no bacterial growth, respectively.

6.2.15 Preparation of CAS agar plates

Chrome azurol S (CAS) agar plates were prepared according to a previous report (162) with some modifications. First, Solution A was created with 0.53 g NaOH and 3.24 g piperazine-N,N'-bis(2-ethanesulfonic acid) (PIPES) dissolved in 75 mL of water with 1.5 g agar power added last, which was autoclaved with a salt solution consisting of 0.3 g KH_2PO_4, 0.5 g NaCl, and 1.0 g NH_4Cl dissolved in water, 0.121 g CAS dissolved in 100 mL water, and 72.9 mg hexadecyltrimethylammonium bromide (HDTMA) dissolved in 40 mL water. Next, 10 mL salt solution, 3 mL 10% casamino acid (filter-sterilized), 1 mL 20% glucose

(filter-sterilized), 100 mL 1M $MgCl_2$, 10 mL 1M $CaCl_2$, 5 mL 2 mM CAS stock solution, 1 mL Fe stock solution (1 mM $FeCl_3$ in 10 mM HCl), and 4 mL HDTMA solution were sequentially added to an approximate 60°C Solution A. The resulting solution was mixed well, carefully poured in sterile culture plates and allowed to solidify. After solidification, 1 μL of the overnight cultures of *K. pneumoniae* strains was individually spotted onto the CAS agar plate, allowed to dry, incubated at 30°C for 24 hours and photographed.

6.2.16 Acid tolerance response

Bacterial resistance to acid challenge was determined essentially as previously described (94). To investigate the effect of pre-adaptation in different growth conditions, the parental strain CG43S3 was grown separately in LB and M9 medium, and the log-phased cultures were further divided into two groups. One group (approximately 1×10^8 CFU/mL) was first centrifuged and resuspended in LB or M9 medium (pH 4.5) for a 30 min adaption period before the acid challenge, while the other group (approximately 2×10^8 CFU/mL) was directly acid challenged by re-suspending bacterial cultures in M9 medium (pH 3.0). Upon acid challenge, 100 μL of each culture was immediately removed for serial tenfold dilution in PBS, and 100 μL of each culture to the 10^{-5} dilution was plated onto LB agar plates at what was considered to be the initial time point (t_0). The strains were incubated at 37°C for 30 min (t_{30}), when 100 μL was again removed and immediately serially diluted. Ten microliters of the undiluted and diluted culture was then spotted onto LB agar plates with five replications. The remainder of the cultures were promptly returned to incubation at 37°C after the portion necessary for dilution was removed. The same procedure was carried out at 60 min (t_{60}) and 90 min (t_{90}). The bacterial survival was expressed as the CFU of each strain after acid challenge divided by the CFU of each strain at t_0. For the comparison of acid tolerance response between *K. pneumoniae* strains, M9 overnight cultures of CG43S3, Δ*rstA,* Δ*rstB,* and Δ*rstA*Δ*rstB* mutant strains were used to inoculate fresh M9 medium, and strains were grown to log-phase (OD_{600} 0.4-0.5) at 37°C. Then the bacterial cultures were subjected to pre-adaptation at pH 4.5, acid challenged, and the survival rates at 30, 60 and 90 min were determined as described above. Three independent assays were performed, and data shown were the average and standard deviation of five samples from one of the trials.

6.2.17 Bile salt resistance

The LB or M9 overnight cultures of *K. pneumoniae* strains were serially diluted in PBS, and 5 μL was spotted onto LB or M9 agar plates without or with 0.3%, 1% or 3% bile salt

(Sigma). The plates were incubated at 37°C overnight and photographed.

6.2.18 Mouse lethality assay

The virulence in mice was determined as previously described (130). Female BALB/c mice (4 to 5 weeks old) were obtained from the National Laboratory Animal Center (NLAC) (Taipei, Taiwan) and acclimatized in an animal house for 7 days. The tested bacterial strains were cultured in LB medium at 37°C overnight. Four mice of a group were injected intraperitoneally with 0.2 mL of bacterial suspension in saline in 10-fold graded doses. Based on the number of survivors after 14 days, LD_{50} was calculated using Reed and Muench's method (202) and expressed as a colony forming unit (CFU).

6.2.19 Bacterial survival in serum

Bacterial survival in serum was determined with minor modifications (130). First, 100 μL of bacterial suspension in saline was mixed with 100 μL of pooled serum from three healthy volunteers, and the mixture was incubated at 37°C for 30 min. The number of viable bacteria was then determined by plate counting. The survival rate was expressed as the number of viable bacteria treated with human serum compared with the number of those incubated with PBS. The assay was performed twice, each with triplicate samples. The data from one of the representative experiments are shown and expressed as the mean and standard deviation from the three samples. The 0% survival of *K. pneumoniae* CG43S3Δ*galU* (130) served as a negative control.

6.2.20 Construction of the plasmid for K2 *cps* $P_{orf1\text{-}2}$::*lacZ* chromosomal fusion

The $P_{orf1\text{-}2}$::*lacZ* cassette from pOrf12 (142) was sub-cloned into pKAS46; the resulting plasmid was mobilized into *K. pneumoniae* CG43S3Δ*lacZ*, Δ*rcsB*Δ*lacZ* or Δ*rmpA*Δ*lacZ* via conjugation from *E. coli* S17-1 λ*pir*. The transconjugants were screened by counter-selection on M9 agar plate supplemented with kanamycin and X-gal. After overnight incubation at 37°C, blue colonies, in which the reporter cassette was integrated into the chromosomal *cps* region via the $P_{orf1\text{-}2}$ by homologous recombination, were isolated. The integration of the reporter cassette in the resulting strains was further confirmed by PCR with the primers CH009/CH010 (Table 6.3).

6.2.21 Preparation of RcsB-His antiserum

The RcsB-His antiserum was prepared by immunizing five-week-old female BALB/c mice purchased from the Laboratory Animal Center of National Taiwan University (Taipei,

Taiwan) intraperitoneally with 10 mg of purified RcsB-His. Ten days later, the mice were immunized again with 10 mg of the same protein, and the antiserum was obtained by intracardiac puncture.

6.2.22 Construction of GST fusion plasmids and co-immunoprecipitation

To obtain the GST fusion plasmids, the DNA fragments encoding full-length RcsA, RmpA, RmpAN or RmpA2 were PCR-amplified with primer sets rcsAe04/rcsAe08, rmpAe04/rmpAe07 or rmpA2p08/rmpA2p17 (Table 6.3) and cloned, into the *Bam*HI/*Xho*I site in pGEX-5X-1 (GE Healthcare) to generate pGEX-RcsA, pGEX-RmpA, pGEX-RmpAN or pGEX-RmpA2 (Table 6.2), respectively. To construct an RcsB-His expression plasmid compatible with pGEX-5X-1, the DNA fragment containing the entire RcsB-His coding sequence and the upstream T7 promoter region was PCR amplified with primers pET30f2/pET30r2 (Table 6.3) and cloned into an *Eco*RI site on pACYC184 to generate pACYC184-RcsB. To perform co-immunoprecipitation, different combinations of the expression plasmids were co-transformed into *E. coli* BL21(DE3). The transformants were grown overnight in LB medium at 37°C and grown in refreshed LB medium at 37°C to an OD_{600} of 0.5. IPTG was then added to a final concentration of 1 mM, and the cultures were incubated at 25°C for another 16 h. The cells were recovered by centrifugation, resuspended in 500 μL IP buffer (1 × TBS pH 7.4, 0.1% (w/v) BSA, 1 × protease inhibitor cocktail set VII (Calbiochem, La Jolla, CA, USA)) and disrupted by sonication on ice. After centrifugation at 4°C, the supernatant was collected as Pre-IP samples. Ten micrograms of each Pre-IP sample were subjected to SDS-PAGE and immunoblotted with anti-GST or anti-His_6 monoclonal antibody to ensure the expression of the recombinant proteins. For IP analysis, 500 μg of total protein for each sample was incubated with approximately 50 μL of Glutathione Sepharose 4 Fast Flow (GE Healthcare) in a final volume of 500 μL. After incubation at 4°C for 3 h with end-over-end mixing, the beads were collected by centrifugation, washed three times with 500 μL ice-cold IP buffer containing 1% (v/v) Triton X-100 and washed once with 500 μL ice-cold IP buffer containing 1% (v/v) Triton X-100 and 1 M NaCl. Finally, the beads were washed with 500 μL ice-cold IP buffer containing 1% (v/v) Triton X-100 to remove the residual salts and mixed with 50 μL of 5 × SDS-PAGE sample buffer. The samples were boiled at 95°C for 10 min and subjected to SDS-PAGE and immunoblot analysis with anti-His_6 monoclonal antibody, anti-GST monoclonal antibody or anti-RcsB-His polyclonal antiserum. The presence of proteins was visualized by an alkaline phosphatase-mediated chromogenic substrate reaction.

6.2.23 Identification of *rmpA* transcriptional start site

For the determination of *rmpA* 5'-mRNA ends, a 5'-RACE PCR was performed using 5'-RACE kit (Clontech, Mountain View, CA) according to the manufacturer's instruction. In brief, total RNA was isolated from log-phased *K. pneumoniae* CG43S3 and Δ*fur* mutant grown in LB medium using High Pure RNA Isolation Kit (Roche, Mannheim, Germany). One microgram of total RNA was treated with RNase-free DNase I (Roche, Mannheim, Germany) and recovered by phenol-chloroform extraction. For the first-strand cDNA synthesis, a 3.75-μL reaction mixture containing 1 μg of DNase-treated RNA and Random Primer Mix (N-15) was incubated at 72°C for 3 min and then reduced to room temperature for 5 min before the addition of 5X First-Strand buffer, deionized water, DTT, dNTP mix, RNase inhibitor, SMARTer II A Oligonucleotide and SMARTScribe^{TM} reverse transcriptase to a final volume of 10 μL. The reaction mixture was incubated at room temperature for 10 min, 42°C for 90min and 72°C for 10 min to terminate the reaction, diluted with 20 μL Tricine-EDTA buffer and then stored at -20°C. For the primary PCR, a 50-μL reaction mixture containing diluted cDNA templates, gene-specific primer, Universal Primer Mix, dNTP mix, PCR buffer, deionized water and DNA polymerase was prepared. The reaction mixture without reverse transcriptase served as a negative control template. The PCR program was 5 cycles of 30 s at 94°C, 3 min at 72°C, 5 cycles of 30 s at 94°C, 30 s at 70°C, 3 min at 72°C, and 25 cycles of 30 s at 94°C, 30 s at 68°C, 3 min at 72°C. For the nested PCR, the reaction mixture was essentially the same as the primary PCR mixture except 100-fold diluted primary PCR product as the template, gene-specific primer, and Nested Universal Primer were used. The PCR program was 25 cycles of 30 s at 94°C, 30 s at 60°C, 3 min at 72°C. The PCR products were resolved on an agarose gel by electrophoresis, and the DNA fragments were recovered and cloned into the PCR cloning vector yT&A. A total of 31 clones were subjected to sequence analysis, and the transcriptional start site of *rmpA* was determined from the longest inserted DNA fragments from 18 of the 31 samples.

6.2.24 Limiting-dilution RT-PCR

The reaction mixtures include primer sets RTrmpA01/RTrmpA02 or 23SR/23SF (Table 6.3) and the diluted cDNA templates from the first-strand synthesis in 5'-RACE PCR. The PCR program was 30 cycles of 30 s at 94°C, 30 s at 50°C, 20 s at 72°C. For a quantitative comparison of the *rmpA* expression levels, the intensity of the band resolved on agarose gel was analyzed and normalized with 23S rRNA gene using ImageJ software (NIH). The

expression level of *rmpA* from the undiluted cDNA of CG43S3 was set as 100.

6.2.25 Statistical analysis

Two-tailed Student's *t* test was used to determine the significance of the differences between the survivals in polymyxin B assay/phagocytosis, the levels of β-galactosidase activity and CPS amounts. *P* values less than 0.01 were considered statistically significant.

6.3 Table

Table 6.1. Bacterial strains used in this study

Strain	Description	Reference or source
K. pneumoniae		
CG43	Clinical isolate	(36)
CG43-101	CG43-101	(37)
CG43S3	CG43 Sm^r	(130)
Δ*lacZ*	CG43S3Δ*lacZ* Sm^r	(142)
Δ*rcsB* (B2202)	CG43S3Δ*rcsB* Sm^r	(130)
Δ*rmpA2* (R2035)	CG43S3Δ*rmpA2* Sm^r	(130)
Δ*galU* (U9451)	CG43S3Δ*galU* Sm^r	Laboratory stock
Δ*fur*	CG43S3Δ*fur* Sm^r	This study
Δ*phoP*	CG43S3Δ*phoP* Sm^r	This study
Δ*pmrA*	CG43S3Δ*pmrA* Sm^r	This study
Δ*pmrD*	CG43S3Δ*pmrD* Sm^r	This study
Δ*pmrF*	CG43S3Δ*pmrF* Sm^r	This study
Δ*rmpA*	CG43S3Δ*rmpA* Sm^r	This study
Δ*rstA*	CG43S3Δ*rstA* Sm^r	This study
Δ*rstB*	CG43S3Δ*rstB* Sm^r	This study
Δ*ugd*	CG43S3Δ*ugd* Sm^r	This study
Δ*wza*	CG43S3Δ*wza* Sm^r	This study
Δ*lacZ*Δ*fur*	CG43S3Δ*lacZ*Δ*fur* Sm^r	This study

117

Table 6.1. (continued)

Strain	Description	Reference or source
Δ*lacZ*Δ*phoP*	CG43S3Δ*lacZ*Δ*phoP* Sm^r	This study
Δ*lacZ*Δ*pmrA*	CG43S3Δ*lacZ*Δ*pmrA* Sm^r	This study
Δ*lacZ*Δ*pmrD*	CG43S3Δ*lacZ*Δ*pmrD* Sm^r	This study
Δ*lacZ*Δ*rmpA*	CG43S3Δ*lacZ*Δ*rmpA* Sm^r	This study
Δ*lacZ*Δ*rmpA2*	CG43S3Δ*lacZ*Δ*rmpA2* Sm^r	This study
Δ*pmrA*Δ*phoP*	CG43S3Δ*pmrA*Δ*phoP* Sm^r	This study
Δ*rcsB*Δ*phoP*	CG43S3Δ*rcsB*Δ*phoP* Sm^r	This study
Δ*rcsB*Δ*pmrA*	CG43S3Δ*rcsB*Δ*pmrA* Sm^r	This study
Δ*rcsB*Δ*pmrD*	CG43S3Δ*rcsB*Δ*pmrD* Sm^r	This study
Δ*rcsB*Δ*pmrF*	CG43S3Δ*rcsB*Δ*pmrF* Sm^r	This study
Δ*rmpA*Δ*rmpA2*	CG43S3Δ*rmpA*Δ*rmpA2* Sm^r	This study
Δ*rstA*Δ*galU*	CG43S3Δ*rstA*Δ*galU* Sm^r	This study
Δ*rstA*Δ*rstB*	CG43S3Δ*rstA*Δ*rstB* Sm^r	This study
E. coli		
BL21(DE3)	F$^-$ *ompT hsdS$_B$*($r_B^-m_B^-$) *gal dcm trxB*15::*kan* (DE3)	Novagen
BL21(DE3) [pLysS]	F$^-$ *ompT hsdS$_B$*($r_B^-m_B^-$) *gal dcm trxB*15::*kan* (DE3) [pLysS]	Novagen
JM109	*endA1 glnV44 thi-1 relA1 gyrA96 recA1 mcrB*$^+$ Δ*(lac-proAB) e14-* [F' *traD36 proAB*$^+$ *lacI*^{q} *lacZ*Δ*M15*] *hsdR17*($r_K^-m_K^+$)	New England Biolabs
S17-1λ*pir*	*hsdR recA pro* RP4-2 (Tc::Mu; Km::Tn*7*)(λ*pir*)	(218)
XL1-Blue MRF' Kan	Δ(*mcrA*)*183* Δ(*mcrCB-hsdSMR-mrr*)*173 endA1 supE44 thi-1 recA1 gyrA96 relA1 lac* [F' *proAB lacI*^{q}Z Δ*M15* Tn*5* (Kan^r)]	Stratagene

118

Table 6.2. Plasmids used in this study

Plasmid	Description	Reference or source
yT&A	Ap^r, T/A-type PCR cloning vector,	Yeastern
pBT	Cm^r, bait plasmid, *p15A* origin of replication, *lac-UV5* promoter, λ-cI open reading frame	Stratagene
pTRG	Tc^r, target plasmid, *ColE1* origin of replication, *lac-UV5* promoter, *RNAPα* open reading frame	Stratagene
pET30a-c	Km^r, His-tagged protein expression vector	Novagen
pBT-LGF2	Cm^r, control plasmid containing a fragment encoding the yeast transcriptional activator Gal4 fused with λ-cI	Stratagene
pTRG-GAL11^P	Tc^r, control plasmid containing a fragment encoding a mutant form of Gal11 protein, called Gal11^P, fused with RNAPα	Stratagene
pGEX-5X-1	Ap^r, GST-tagged protein expression vector	GH Hleathcare
pACYC184	Cm^r, Tc^r, plasmid with *p15A* origin of replication	(35)
pKAS46	Ap^r, Km^r, suicide vector, *rpsL*	(218)
pRK415	Tc^r, shuttle vector, *mob*$^+$	(121)
pYC084	Tc^r, 2.1-kb *Hin*dIII/*Bam*HI fragment containing the entire *rmpA2* locus cloned into pRK415	(130)
placZ15	Cm^r, promoter selection vector, *lacZ*$^+$	(142)
pOrf12	Cm^r, 500-bp fragment containing the region upstream of *Klebsiella* K2 *cps orf1-orf2* cloned into placZ15	(142)
pOrf315	Cm^r, 900-bp fragment containing the region upstream of *Klebsiella* K2 *cps orf3-orf15* cloned into placZ15	(142)
pOrf1617	Cm^r, 300-bp fragment containing the region upstream of *Klebsiella* K2 *cps orf16-orf17* cloned into placZ15	(142)

119

Table 6.2. (continued)

Plasmid	Description	Reference or source
pHY048	Cm^r, 450-bp fragment containing the upstream region of the *K. pneumoniae rstA* gene cloned into placZ15	This study
pHY050	Cm^r, 200-bp fragment containing the upstream region of the *K. pneumoniae rstA* gene cloned into placZ15	This study
pHY053	Cm^r, 150-bp fragment containing the upstream region of the *K. pneumoniae rstA* gene cloned into placZ15	This study
pHY083	Km^r, Ap^r, the $P_{orf1\text{-}2}$::*lacZ* reporter cassette cloned into pKAS46	This study
pHY115	Ap^r, 550-bp fragment containing a *pmrD* allele cloned intoyT&A	This study
pHY118	Ap^r, 300-bp fragment containing the upstream region of the *K. pneumoniae pmrD* gene cloned in the same direction to *lacZα* in yT&A,	This study
pHY290	Ap^r, 299-bp fragment encoding residues 1-100 of RmpA cloned in-frame with *lacZα* into yT&A	This study
pHY291	Ap^r, 299-bp fragment encoding residues 1-100 of RmpA cloned in the opposite direction to *lacZα* into yT&A	This study
pHY305	Ap^r, 347-bp fragment encoding residues 1-116 of RmpA2 cloned in-frame with *lacZα* into yT&A	This study
pHY306	Ap^r, 347-bp fragment encoding residues 1-116 of RmpA2 cloned in the opposite direction to *lacZα* into yT&A	This study
pACYC184-RcsB	Tc^r, 1.1-kb *Eco*RI fragment containing full-length RcsB-His and the upstream T7 promoter region from pET30b-RcsB cloned into pACYC184	This study
pBT-PmrA	Cm^r, 669-bp fragment encoding full-length PmrA cloned into pBT	This study
pBT-RcsB	Cm^r, 648-bp fragment encoding full-length RcsB cloned into pBT	This study
pET30b-PhoP	Km^r, 711-bp fragment encoding full-length PhoP cloned into pET30b	This study
pET30b-PhoPN	Km^r, 447-bp fragment encoding residues 1-149 of PhoP cloned into pET30b	This study
pET30b-PmrBC	Km^r, 828-bp fragment encoding residues 90-365 of PmrB cloned into pET30b	This study

120

Table 6.2. (continued)

Plasmid	Description	Reference or source
pET-PmrA	Km^r, 669-bp fragment encoding full-length PmrA cloned into pET29b	Courtesy of Dr. Chinpan Chen
pET-PmrD	Km^r, 243-bp fragment encoding full-length PmrD cloned into pET29b	Courtesy of Dr. Chinpan Chen
pET30b-RcsB	Km^r, 648-bp fragment encoding full-length RcsB cloned into pET30b	This study
pET30c-Fur	Km^r, 450-bp fragment encoding full-length Fur cloned into pET30c	This study
pGEX-RcsA	Ap^r, 621-bp fragment encoding full-length RcsA cloned into pGEX-5X-1	This study
pGEX-RmpA	Ap^r, 585-bp fragment encoding full-length RmpA cloned into pGEX-5X-1	This study
pGEX-RmpAN	Ap^r, 252-bp fragment encoding residues 1-84 of RmpA cloned into pGEX-5X-1	This study
pGEX-RmpA2	Ap^r, 636-bp fragment encoding full-length RmpA2 cloned into pGEX-5X-1	This study
placZ15-PiroB	Cm^r, 450-bp fragment containing the upstream region of the *K. pneumoniae iroBCD* genes cloned into placZ15	This study
placZ15-PiucA	Cm^r, 700-bp fragment containing the upstream region of the *K. pneumoniae iucABCD* genes cloned into placZ15	This study
placZ15-PpmrD	Cm^r, 350-bp fragment containing the upstream region of the *K. pneumoniae pmrD* gene cloned into placZ15	This study
placZ15-PpmrH	Cm^r, 500-bp fragment containing the upstream region of the *K. pneumoniae pbgP* genes cloned into placZ15	This study
placZ15-PrmpA	Cm^r, 500-bp fragment containing the upstream region of the *K. pneumoniae rmpA* gene cloned into placZ15	This study
placZ15-PrmpA2	Cm^r, 500-bp fragment containing the upstream region of the *K. pneumoniae rmpA2* gene cloned into placZ15	This study
pRK415-Fur	Tc^r , 0.8-kb fragment containing a *fur* allele cloned into pRK415	This study

121

Table 6.2. (continued)

Plasmid	Description	Reference or source
pRK415-PhoP	Tc^r , 900-bp fragment containing a *phoP* allele cloned into pRK415	This study
pRK415-PmrA	Tc^r , 1.1-kb fragment containing a *pmrA* allele cloned into pRK415	This study
pRK415-PmrD	Tc^r , 550-bp fragment containing a *pmrD* allele cloned into pRK415	This study
pRK415-PmrDK6A	Tc^r , 550-bp fragment containing a *pmrD* allele encoding PmrDK6A cloned into pRK415	This study
pRK415-PmrDV8A	Tc^r , 550-bp fragment containing a *pmrD* allele encoding PmrDK6A cloned into pRK415	This study
pRK415-PmrDQ9A	Tc^r , 550-bp fragment containing a *pmrD* allele encoding PmrDK6A cloned into pRK415	This study
pRK415-PmrDD10A	Tc^r , 550-bp fragment containing a *pmrD* allele encoding PmrDK6A cloned into pRK415	This study
pRK415-PmrDS23A	Tc^r , 550-bp fragment containing a *pmrD* allele encoding PmrDK6A cloned into pRK415	This study
pRK415-PmrDG24A	Tc^r , 550-bp fragment containing a *pmrD* allele encoding PmrDK6A cloned into pRK415	This study
pRK415-PmrDL26A	Tc^r , 550-bp fragment containing a *pmrD* allele encoding PmrDK6A cloned into pRK415	This study
pRK415-PmrDM28A	Tc^r , 550-bp fragment containing a *pmrD* allele encoding PmrDK6A cloned into pRK415	This study
pRK415-PmrDE31A	Tc^r , 550-bp fragment containing a *pmrD* allele encoding PmrDK6A cloned into pRK415	This study
pRK415-PmrDT46A	Tc^r , 550-bp fragment containing a *pmrD* allele encoding PmrDK6A cloned into pRK415	This study
pRK415-PmrDY53A	Tc^r , 550-bp fragment containing a *pmrD* allele encoding PmrDK6A cloned into pRK415	This study
pRK415-PmrDT69A	Tc^r , 550-bp fragment containing a *pmrD* allele encoding PmrDK6A cloned into pRK415	This study
pRK415-PmrDY71A	Tc^r , 550-bp fragment containing a *pmrD* allele encoding PmrDK6A cloned into pRK415	This study
pRK415-PmrDW76A	Tc^r , 550-bp fragment containing a *pmrD* allele encoding PmrDK6A cloned into pRK415	This study
pRK415-PmrDT77A	Tc^r , 550-bp fragment containing a *pmrD* allele encoding PmrDK6A cloned into pRK415	This study
pRK415-PmrDN78A	Tc^r , 550-bp fragment containing a *pmrD* allele encoding PmrDK6A cloned into pRK415	This study
pRK415-PmrDD80A	Tc^r , 550-bp fragment containing a *pmrD* allele encoding PmrDK6A cloned into pRK415	This study
pRK415-PmrF	Tc^r , 1.3-kb fragment containing a *pmrF* allele cloned into pRK415	This study

122

Table 6.2. (continued)

Plasmid	Description	Reference or source
pRK415-RcsB	Tc^r , 1.2-kb fragment containing an *rcsB* allele cloned into pRK415	This study
pRK415-RmpA	Tc^r , 1.1-kb fragment containing an *rmpA* allele cloned into pRK415	This study
pRK415-RmpAN	Tc^r , 1.1-kb fragment containing the *rmpA* locus encoding residues 1-84 of RmpA cloned into pRK415	This study
pRK415-RmpA2	Tc^r , 1.2-kb fragment containing an *rmpA2* allele cloned into pRK415	This study
pTRG-PmrD	Tc^r, 243-bp fragment encoding full-length PmrD cloned into pTRG	This study
pTRG-RcsA	Tc^r, 621-bp fragment encoding full-length RcsA cloned into pTRG	This study
pTRG-RmpAN	Tc^r, 252-bp fragment encoding residues 1-84 of RmpA cloned into pTRG	This study
pTRG-RmpA2	Tc^r, 636-bp fragment encoding full-length RmpA2 cloned into pTRG	This study

123

Table 6.3. Oligonucleotide primers used in this study

Primer	Sequence[a]	Enzyme cleaved	Complementary position
CH009	5'-AGCGTGACGAGACCTGCCCA-3'	None	-802 relative to the K2 *cps orf1* start codon
CH010	5'-GGCTGCGGGCGTAAGAGAAC-3'	None	+217 relative to the *lacZ* start codon
CY007	5'-TCTAGAGGCAGGTTGGCTCTTCAGTC-3'	*Xba*I	+489 relative to the *fur* start codon
CY008	5'-GGATCCATGAAGACAGCCAGCCGGA-3'	*Bam*HI	-389 relative to the *fur* start codon
CY0010	5'-GGATCCGATTCCGCATGACTGACAAC-3'	*Bam*HI	-8 relative to the *fur* start codon
CY0011	5'-AAGCTTGGCAGGTTGGCTCTTCAGTC-3'	*Hin*dIII	+489 relative to the *fur* start codon
GSPrmpA01	5'-TTAGGATAAAACCGCCCCCCCCCCGAAAC-3'	None	+254 relative to the *rmpA* start codon
GSPrmpA02	5'-CATTTTGTACCCTCCCCATTTCCCTGA-3'	None	+180 relative to the *rmpA* start codon
KP1760-1	5'-GGAATTCCATATGAAAATCTTAGTCATTGAA-3'	*Nde*I	+1 relative to the *pmrA* start codon
KP1760-2	5'-CCGCTCGAGCTATTCCGTGTCGATGTTGTT-3'	*Xho*I	+672 relative to the *pmrA* start codon
KP3573-1	5'-GGAATTCCATATGGAGTGGTGGGTAAAAAAA-3'	*Nde*I	+1 relative to the *pmrD* start codon
KP3573-2	5'-CCGCTCGAGTTTGTCGGCGTTTGTCCAACG-3'	*Xho*I	+243 relative to the *pmrD* start codon
pET30f2	5'-TTGAATTCTAGGTTGAGGCCGTTGAGCA-3'	*Eco*RI	+673 to +692 region on pET30a
pET30r2	5'-CAAGAATTCAAACCCCTCAAGACCCGT-3'	*Eco*RI	+31 to +47 region on pET30a
phoP01	5'-CGCTCGCCGTTCGGATCCTG-3'	*Bam*HI	-171 relative to the *phoP* start codon
phoP02	5'-GCAACGGTACCTTCATCAGCGC-3'	*Kpn*I	+729 relative to the *phoP* start codon
phoP05	5'-GTAATGACAGCGGGAAGATATG-3'	None	+753 relative to the *phoP* start codon
phoP06	5'-CAGCCGTTTATATTTTGCGT-3'	None	-25 relative to the *phoP* start codon
pirop01	5'-GGATCCGATTTCAGTACGGCATGGAC-3'	*Bam*HI	-379 relative to the *iroB* start codon
pirop02	5'-AGATCTACGGGAAACGCCTGTGCCA-3'	*Bgl*II	+77 relative to the *iroB* start codon

124

Table 6.3. (continued)

Primer	Sequence[a]	Enzyme cleaved	Complementary position
piucp01	5'-GGATCCAGAGGGTGATTTGCCAGCAT-3'	*Bam*HI	-611 relative to the *iucA* start codon
piucp02	5'-AGATCTGGAAGCACTGAGCAGCCACA-3'	*Bgl*II	+109 relative to the *iucA* start codon
pmrA06	5’-GAGCCATGGTCTATTCCGTG-3’	*Nco*I	+682 relative to the *pmrA* start codon
pmrA10	5’-ACTCGAGCCATGGTCTATTCCGTG-3’	*Xho*I	+1 relative to the *pmrA* start codon
pmrA11	5’-AATGCGGCCGCAATGAAAATCTTAGTC-3’	*Not*I	+672 relative to the *pmrA* start codon
pmrAp03	5’-CAATTGGATCCAGGGCTGTAC-3’	*Bam*HI	-424 relative to the *pmrA* start codon
pmrBe03	5’-TGGATCCTCGCAAGATCACCCGCC-3’	*Bam*HI	+283 relative to the *pmrB* start codon
pmrBe04	5’-CAAGCTTATGGGTGCTGACGTTCTGAC-3’	*Hin*dIII	+1095 relative to the *pmrB* start codon
pmrDe02	5’-CGAGCTCGTGTTATTTGTCGGCGTTTGTC-3’	*Sac*I	+250 relative to the *pmrD* start codon
pmrDe15	5’-AAAGCGGCCGCGATGGAGTGGTGGGTAAAAAAAGTA-3’	*Not*I	+1 relative to the *pmrD* start codon
pmrDe16	5’-TTTCTCGAGTGTGTTATTTGCCGGCGTTT-3’	*Xho*I	+243 relative to the *pmrD* start codon
pmrDp01	5’-TGGATCCTTCATGACGCTCTCTC-3’	*Bam*HI	-278 relative to the *pmrD* start codon
pmrDp02	5’-CGCACAGATCTGAAGCACGAC-3’	*Bgl*II	+75 relative to the *pmrD* start codon
pmrDp05	5’-TTACCCACCACTCCATATGTTTTTTA-3’	*Nde*I	+10 relative to the *pmrD* start codon
pmrDK6Af	5’-ACAGATGGAGTGGTGGGTA**GC**AAAAGTACAGGACAACGCT-3’	None	-4 to +36 relative to the *pmrD* start codon
pmrDK6Ar	5’-AGCGTTGTCCTGTACTTTT**GC**TACCCACCACTCCATCTGT-3’	None	-4 to +36 relative to the *pmrD* start codon
pmrDQ9Af	5’-GGAGTGGTGGGTAAAAAAAGTA**GC**GGACAACGCTTCGGC-3’	None	+2 to +41 relative to the *pmrD* start codon
pmrDQ9Ar	5’-GCCGAAGCGTTGTCC**GC**TACTTTTTTTACCCACCACTCC-3’	None	+2 to +41 relative to the *pmrD* start codon
pmrDD10Af	5'-GGGTAAAAAAAGTACAGG**C**CAACGCTTCGGCCAGCC-3'	None	+11 to +47 relative to the *pmrD* start codon
pmrDD10Ar	5'- GGCTGGCCGAAGCGTTG**G**CCTGTACTTTTTTTACCC-3'	None	+11 to +47 relative to the *pmrD* start codon
pmrDS23Af1	5’-CGTCGTGCTTCAG**GC**CGGTGCGCT-3’	None	+54 to +78 relative to the *pmrD* start codon

125

Table 6.3. (continued)

Primer	Sequence[a]	Enzyme cleaved	Complementary position
pmrDS23Ar1	5’-AGCGCACCG**GC**CTGAAGCACGACG-3’	None	+54 to +78 relative to the *pmrD* start codon
pmrDG24Af	5’-GTGCTTCAGAGCG**C**TGCGCTGGAGATG-3’	None	+58 to + 85 relative to the *pmrD* start codon
pmrDG24Ar	5’-CATCTCCAGCGCA**G**CGCTCTGAAGCAC-3’	None	+58 to + 85 relative to the *pmrD* start codon
pmrDL26Af1	5’-CAGAGCGGTGCG**GC**GGAGATGATCG-3’	None	+64 to +89 relative to the *pmrD* start codon
pmrDL26Ar1	5’-CGATCATCTCC**GC**CGCACCGCTCTG-3’	None	+64 to +89 relative to the *pmrD* start codon
pmrDM28Af1	5’-CGGTGCGCTGGAG**GC**GATCGCAGAGATTGAA-3’	None	+69 to +100 relative to the *pmrD* start codon
pmrDM28Ar1	5’-TTCAATCTCTGCGATC**GC**CTCCAGCGCACCG-3’	None	+69 to +100 relative to the *pmrD* start codon
pmrDE31Af	5’-CTGGAGATGATCGCAG**C**GATTGAAGCCTGTCGC-3’	None	+76 to +109 relative to the *pmrD* start codon
pmrDE31Ar	5’-GCGACAGGCTTCAATC**G**CTGCGATCATCTCCAG-3’	None	+76 to +109 relative to the *pmrD* start codon
pmrDT46Af	5’-GAAGGGGATAAACTC**G**CTCCGCTGGCCG-3’	None	+121 to +149 relative to the *pmrD* start codon
pmrDT46Ar	5’-CGGCCAGCGGAG**C**GAGTTTATCCCCTTC-3’	None	+121 to +149 relative to the *pmrD* start codon
pmrDY53Af	5’-CGCTGGCCGATGCGCGC**GC**TTGTCTGAATAATAATCC-3’	None	+140 to +177 relative to the *pmrD* start codon
pmrDY53Ar	5’-GGATTATTATTCAGACAA**GC**GCGCGCATCGGCCAGCG-3’	None	+140 to +177 relative to the *pmrD* start codon
pmrDT69Af1	5’-GAAGATCCGCAACGCC**G**CTCATTATAG-3’	None	+189 to +216 relative to the *pmrD* start codon
pmrDT69Ar1	5’-CTATAATGAG**C**GGCGTTGCGGATCTTC-3’	None	+189 to +216 relative to the *pmrD* start codon
pmrDY71Af	5’-GAAGATCCGCAACGCCACTCAT**GC**TAGCAGCGAGCG-3’	None	+189 to +225 relative to the *pmrD* start codon
pmrDY71Ar	5’-CGCTCGCTGCTA**GC**ATGAGTGGCGTTGCGGATCTTC-3’	None	+189 to +225 relative to the *pmrD* start codon
pmrDT77Af	5’-GCAGCGAGCGTTGG**G**CAAACGCCGACAAA-3’	None	+215 to +244 relative to the *pmrD* start codon
pmrDT77Ar	5’-TTTGTCGGCGTTTG**C**CCAACGCTCGCTGC-3’	None	+215 to +244 relative to the *pmrD* start codon
pmrDN78Af1	5’-GCAGCGAGCGTTGGACA**GC**CGCCGGCAAATAA-3’	None	+215 to +247 relative to the *pmrD* start codon
pmrDN78Ar1	5’-TTATTTGCCGGCG**GC**TGTCCAACGCTCGCTGC-3’	None	+215 to +247 relative to the *pmrD* start codon

126

Table 6.3. (continued)

Primer	Sequence[a]	Enzyme cleaved	Complementary position
pmrDD80Af	5’-GCGTTGGACAAACGCCG**C**CAAATAACACAGATCTG-3’	None	+222 to +257 relative to the *pmrD* start codon
pmrDD80Ar	5’-CAGATCTGTGTTATTTG**G**CGGCGTTTGTCCAACGC-3’	None	+222 to +257 relative to the *pmrD* start codon
pmrHp01	5’-TCTGGATCCTGGTCATTAATTGCCCGGC-3’	*Bam*HI	-425 relative to the *pmrH* start codon
pmrHp02	5’-CTTAGATCTCGCTCATCATCATCCTGTTC-3’	*Bgl*II	+34 relative to the *pmrH* start codon
ppmrF01	5’-GATGGAAAAGCTGAAGGCGATGG-3’	None	-161 relative to the *pmrF* start codon
ppmrF02	5’-CAGCGATATCATACCCGGCGTC-3’	*Eco*RV	+1116 relative to the *pmrF* start codon
rcsAe04	5'-GTTTGTTTCACTCGAGGCGCATATTTACC-3'	*Xho*I	+631 relative to the *rcsA* start codon
rcsAe07	5’-CTAGCGGCCGCGATGTCAACGATGATTATGGATT-3’	*Not*I	+1 relative to the *rcsA* start codon
rcsAe08	5’-CTAGGATCCCCATGTCAACGATGATTATGGATT-3’	*Bam*HI	+1 relative to the *rcsA* start codon
rcsBc01	5’-CCCGGATCCAACTGCGGGTCAACTTT-3’	*Bam*HI	-398 relative to the *rcsB* start codon
rcsBc02	5’-CCCGGATCCTTGTCTGTCCAAGCCGGTCA-3’	*Bam*HI	+781 relative to the *rcsB* start codon
rcsBe01	5’-GGCCGCCTTATACCATATGAACACTA-3’	*Nde*I	+1 relative to the *rcsB* start codon
rcsBe02	5’-CCCTCGAGCTCTTTGTCCGTCGCGCTC-3’	*Xho*I	+648 relative to the *rcsB* start codon
rcsBe04	5’-CTCGCGGCCGCGATGAACACTATGAACGTAATTAT-3’	*Not*I	-1 relative to the *rcsB* start codon
rmpA06	5’-TTACCTAAATACTTGGCATGAGC-3’	None	+592 relative to the *rmpA* start codon
rmpA07	5’-CAAGGATCCAAAGCATAGTGTT-3’	*Bam*HI	-17 relative to the *rmpA* start codon
rmpAc01	5’-CCCGGATCCAGAAACAGACAGTATTACTAAGCGAA-3’	*Bam*HI	-384 relative to the *rmpA* start codon
rmpAe04	5’-CCCTTTTTTACCTCGAGAATACTTGGCATGA-3’	*Xho*I	+585 relative to the *rmpA* start codon
rmpAe05	5’-CTTGCGGCCG**C**GGTGTTGACTGATGATTATTTTTTTTA-3’	*Not*I	+1 relative to the *rmpA* start codon
rmpAe07	5’-CTTGGATCCCCGTGTTGACTGATGATTATTTTTTTTA-3’	*Bam*HI	-2 relative to the *rmpA* start codon
rmpAg05	5’-TTGTGTTGACTGATGATTATTTT-3’	None	+1 relative to the *rmpA* start codon

127

Table 6.3. (continued)

Primer	Sequence[a]	Enzyme cleaved	Complementary position
rmpAg06	5’-TTTACATTTCCTTGCAT-3’	None	+299 relative to the *rmpA* start codon
rmpAp04	5'-CCCAGATCTCAGTCAACACGGTGCTTTAC-3'	*Bgl*II	+10 relative to the *rmpA* start codon
rmpAp05	5’-CCCGGATCCAACTCGCCCCTCCCCACAC-3’	*Bam*HI	-308 relative to the *rmpA* start codon
rmpAp11	5’-CCAGGATCCTACCGTGATTGATTGAATTTTTA-3’	*Bam*HI	-184 relative to the *rmpA* start codon
rmpAp12	5’-GTCGGATCCATCGCCAAATAACTC-3’	*Bam*HI	-479 relative to the *rmpA* start codon
rmpAp13	5’-TCAATTAATTGCAAACACGC-3’	None	-226 relative to the *rmpA* start codon
rmpAt01	5’-ACAGAGGTAGTCCAGTTAACA-3’	None	+61 relative to the *rmpA* start codon
rmpA2g01	5’-TTATGGAAAAATATATTTACTT-3’	None	+1 relative to the *rmpA2* start codon
rmpA2g02	5’-TTTAAATTTCCTTGCATGTT-3’	None	+347 relative to the *rmpA2* start codon
rmpA2p06	5’-CCCGGATCCCACTTAGTCCTGTGTC-3’	*Bam*HI	-391 relative to the *rmpA2* start codon
rmpA2p07	5’-GATGGATCCCTAGGTATTTGATGTGCAC-3'	*Bam*HI	+639 relative to the *rmpA2* start codon
rmpA2p08	5’-GATCTCGAGGGTATTTGATGTGCAC-3’	*Xho*I	+639 relative to the *rmpA2* start codon
rmpA2p14	5’-CCCGCGGCCGCGATGGAAAAATATATTTACTT-3’	*Not*I	-1 relative to the *rmpA2* start codon
rmpA2p17	5’-CCCGGATCCCCATGGAAAAATATATTTACTT-3’	*Bam*HI	+1 relative to the *rmpA2* start codon
rstAp01	5’-GCAGGATCCCGGTGAAATAC-3’	*Bam*HI	-378 relative to the *rstA* start codon
rstAp02	5’-CCAGATCTTGCTTGCCGAG-3’	*Bgl*II	+79 relative to the *rstA* start codon
rstAp03	5’-CCCGGATCCCTTAACAGTGA-3’	*Bam*HI	-127 relative to the *rstA* start codon
rstAp04	5’-GAGTAATGGCGGGTAAAATAAGTG-3’	None	-61 relative to the *rstA* start codon
RTrmpA01	5’-TGATGGATCAAAGTTACTGT-3’	None	-70 relative to the *rmpA* start codon
RTrmpA02	5’-TCCCTGAATAAAAAATCCTGCTGTC-3’	None	+160 relative to the *rmpA* start codon
Yu05	5’-CCTTCACATCCCCTCCCCTT-3’	None	+614 relative to the *rmpA* start codon

128

Table 6.3. (continued)

Primer	Sequence[a]	Enzyme cleaved	Complementary position
Yu06	5’-GTCGGATCCATCGCCAAATAA-3’	None	-479 relative to the *rmpA* start codon
23SF	5’-AGCGACTAAGCGTACACGGTGG-3’	None	+4 relative to the *rrnB* start codon
23SR	5’-GATGTTTCAGTTCCCCCGGTTC-3’	None	+200 relative to the *rrnB* start codon

[a] The nucleotide sequence recognized by each restriction enzyme listed are underlined; the boldface sequences indicate the altered nucleotides for the generation of point mutation in the PmrD coding sequence.

129

References

1. **Allali, N., H. Afif, M. Couturier, and L. Van Melderen.** 2002. The highly conserved TldD and TldE proteins of *Escherichia coli* are involved in microcin B17 processing and in CcdA degradation. *J Bacteriol* **184:**3224-31.
2. **Alpuche Aranda, C. M., J. A. Swanson, W. P. Loomis, and S. I. Miller.** 1992. *Salmonella typhimurium* activates virulence gene transcription within acidified macrophage phagosomes. *Proc Natl Acad Sci* U S A **89:**10079-83.
3. **Anderson, G. G., T. L. Yahr, R. R. Lovewell, and G. A. O'Toole.** The *Pseudomonas aeruginosa* magnesium transporter MgtE inhibits transcription of the type III secretion system. *Infect Immun* **78:**1239-49.
4. **Ansaldi, M., C. Jourlin-Castelli, M. Lepelletier, L. Theraulaz, and V. Mejean.** 2001. Rapid dephosphorylation of the TorR response regulator by the TorS unorthodox sensor in *Escherichia coli. J Bacteriol* **183:**2691-5.
5. **Arakawa, Y., R. Wacharotayankun, T. Nagatsuka, H. Ito, N. Kato, and M. Ohta.** 1995. Genomic organization of the *Klebsiella pneumoniae cps* region responsible for serotype K2 capsular polysaccharide synthesis in the virulent strain Chedid. *J Bacteriol* **177:**1788-96.
6. **Asensio, A., A. Oliver, P. Gonzalez-Diego, F. Baquero, J. C. Perez-Diaz, P. Ros, J. Cobo, M. Palacios, D. Lasheras, and R. Canton.** 2000. Outbreak of a multiresistant *Klebsiella pneumoniae* strain in an intensive care unit: antibiotic use as risk factor for colonization and infection. *Clin Infect Dis* **30:**55-60.
7. **Ayers, R. A., and K. Moffat.** 2008. Changes in quaternary structure in the signaling mechanisms of PAS domains. *Biochemistry* **47:**12078-86.
8. **Bader, M. W., W. W. Navarre, W. Shiau, H. Nikaido, J. G. Frye, M. McClelland, F. C. Fang, and S. I. Miller.** 2003. Regulation of *Salmonella typhimurium* virulence gene expression by cationic antimicrobial peptides. *Mol Microbiol* **50:**219-30.
9. **Bagley, S. T., R. J. Seidler, H. W. Talbot, Jr., and J. E. Morrow.** 1978. Isolation of *Klebsielleae* from within living wood. *Appl Environ Microbiol* **36:**178-85.
10. **Baichoo, N., and J. D. Helmann.** 2002. Recognition of DNA by Fur: a reinterpretation of the Fur box consensus sequence. *J Bacteriol* **184:**5826-32.
11. **Batchelor, E., and M. Goulian.** 2003. Robustness and the cycle of phosphorylation and dephosphorylation in a two-component regulatory system. *Proc Natl Acad Sci* U S A **100:**691-6.
12. **Beier, D., and R. Gross.** 2006. Regulation of bacterial virulence by two-component systems. *Curr Opin Microbiol* **9:**143-52.
13. **Belden, W. J., and S. I. Miller.** 1994. Further characterization of the PhoP regulon: identification of new PhoP-activated virulence loci. *Infect Immun* **62:**5095-101.
14. **Benincasa, M., M. Mattiuzzo, Y. Herasimenka, P. Cescutti, R. Rizzo, and R. Gennaro.** 2009. Activity of antimicrobial peptides in the presence of polysaccharides produced by pulmonary pathogens. *J Pept Sci* **15:**595-600.

15. **Bennett, C. J., M. N. Young, and H. Darrington.** 1995. Differences in urinary tract infections in male and female spinal cord injury patients on intermittent catheterization. *Paraplegia* **33:**69-72.

16. **Borremans, B., J. L. Hobman, A. Provoost, N. L. Brown, and D. van Der Lelie.** 2001. Cloning and functional analysis of the *pbr* lead resistance determinant of *Ralstonia metallidurans* CH34. *J Bacteriol* **183:**5651-8.

17. **Bou, G., M. Cartelle, M. Tomas, D. Canle, F. Molina, R. Moure, J. M. Eiros, and A. Guerrero.** 2002. Identification and broad dissemination of the CTX-M-14 beta-lactamase in different *Escherichia coli* strains in the northwest area of Spain. *J Clin Microbiol* **40:**4030-6.

18. **Boulette, M. L., and S. M. Payne.** 2007. Anaerobic regulation of *Shigella flexneri* virulence: ArcA regulates Fur and iron acquisition genes. *J Bacteriol* **189:**6957-67.

19. **Braun, V., and C. Herrmann.** 2007. Docking of the periplasmic FecB binding protein to the FecCD transmembrane proteins in the ferric citrate transport system of *Escherichia coli. J Bacteriol* **189:**6913-8.

20. **Breazeale, S. D., A. A. Ribeiro, A. L. McClerren, and C. R. Raetz.** 2005. A formyltransferase required for polymyxin resistance in *Escherichia coli* and the modification of lipid A with 4-Amino-4-deoxy-L-arabinose. Identification and function oF UDP-4-deoxy-4-formamido-L-arabinose. *J Biol Chem* **280:**14154-67.

21. **Brechtel, C. E., L. Hu, and S. C. King.** 1996. Substrate specificity of the *Escherichia coli* 4-aminobutyrate carrier encoded by *gabP*. Uptake and counterflow of structurally diverse molecules. *J Biol Chem* **271:**783-8.

22. **Brenwald, N. P., G. Jevons, J. M. Andrews, J. H. Xiong, P. M. Hawkey, and R. Wise.** 2003. An outbreak of a CTX-M-type beta-lactamase-producing *Klebsiella pneumoniae*: the importance of using cefpodoxime to detect extended-spectrum beta-lactamases. *J Antimicrob Chemother* **51:**195-6.

23. **Brill, J. A., C. Quinlan-Walshe, and S. Gottesman.** 1988. Fine-structure mapping and identification of two regulators of capsule synthesis in *Escherichia coli* K-12. *J Bacteriol* **170:**2599-611.

24. **Brisse, S., C. Fevre, V. Passet, S. Issenhuth-Jeanjean, R. Tournebize, L. Diancourt, and P. Grimont.** 2009. Virulent clones of *Klebsiella pneumoniae*: identification and evolutionary scenario based on genomic and phenotypic characterization. *PLoS ONE* **4:**e4982.

25. **Brown, C., and R. J. Seidler.** 1973. Potential pathogens in the environment: *Klebsiella pneumoniae*, a taxonomic and ecological enigma. *Appl Microbiol* **25:**900-4.

26. **Brown, M. R., and A. Kornberg.** 2008. The long and short of it - polyphosphate, PPK and bacterial survival. *Trends Biochem Sci* **33:**284-90.

27. **Buelow, D. R., and T. L. Raivio.** Three (and more) component regulatory systems - auxiliary regulators of bacterial histidine kinases. *Mol Microbiol* **75:**547-66.

28. **Cabeza, M. L., A. Aguirre, F. C. Soncini, and E. G. Vescovi.** 2007. Induction of RpoS degradation by the two-component system regulator RstA in *Salmonella enterica. J Bacteriol* **189:**7335-42.

29. **Campbell, T. L., C. S. Ederer, A. Allali-Hassani, and E. D. Brown.** 2007. Isolation of the *rstA* gene as a multicopy suppressor of YjeE, an essential ATPase of unknown function in *Escherichia coli*. *J Bacteriol* **189:**3318-21.

30. **Campos, M. A., M. A. Vargas, V. Regueiro, C. M. Llompart, S. Alberti, and J. A. Bengoechea.** 2004. Capsule polysaccharide mediates bacterial resistance to antimicrobial peptides. *Infect Immun* **72:**7107-14.

31. **Castanie-Cornet, M. P., K. Cam, B. Bastiat, A. Cros, P. Bordes, and C. Gutierrez.** Acid stress response in *Escherichia coli*: mechanism of regulation of *gadA* transcription by RcsB and GadE. *Nucleic Acids Res* **38:**3546-54.

32. **Castanie-Cornet, M. P., H. Treffandier, A. Francez-Charlot, C. Gutierrez, and K. Cam.** 2007. The glutamate-dependent acid resistance system in *Escherichia coli*: essential and dual role of the His-Asp phosphorelay RcsCDB/AF. *Microbiology* **153:**238-46.

33. **Caza, M., F. Lepine, S. Milot, and C. M. Dozois.** 2008. Specific roles of the *iroBCDEN* genes in virulence of an avian pathogenic *Escherichia coli* O78 strain and in production of salmochelins. *Infect Immun* **76:**3539-49.

34. **Cerwenka, H.** Pyogenic liver abscess: differences in etiology and treatment in Southeast Asia and Central Europe. *World J Gastroenterol* **16:**2458-62.

35. **Chang, A. C., and S. N. Cohen.** 1978. Construction and characterization of amplifiable multicopy DNA cloning vehicles derived from the P15A cryptic miniplasmid. *J Bacteriol* **134:**1141-56.

36. **Chang, H. Y., J. H. Lee, W. L. Deng, T. F. Fu, and H. L. Peng.** 1996. Virulence and outer membrane properties of a *galU* mutant of *Klebsiella pneumoniae* CG43. *Microb Pathog* **20:**255-61.

37. **Chen, Y. T., H. Y. Chang, Y. C. Lai, C. C. Pan, S. F. Tsai, and H. L. Peng.** 2004. Sequencing and analysis of the large virulence plasmid pLVPK of *Klebsiella pneumoniae* CG43. *Gene* **337:**189-98.

38. **Cheng, H. Y., Y. S. Chen, C. Y. Wu, H. Y. Chang, Y. C. Lai, and H. L. Peng.** RmpA regulation of capsular polysaccharide biosynthesis in *Klebsiella pneumoniae* CG43. *J Bacteriol* **192:**3144-58.

39. **Cheung, J., C. A. Bingman, M. Reyngold, W. A. Hendrickson, and C. D. Waldburger.** 2008. Crystal structure of a functional dimer of the PhoQ sensor domain. *J Biol Chem* **283:**13762-70.

40. **Cheung, J., and W. A. Hendrickson.** 2008. Crystal structures of C4-dicarboxylate ligand complexes with sensor domains of histidine kinases DcuS and DctB. *J Biol Chem* **283:**30256-65.

41. **Choi, E., E. A. Groisman, and D. Shin.** 2009. Activated by different signals, the PhoP/PhoQ two-component system differentially regulates metal uptake. *J Bacteriol* **191:**7174-81.

42. **Chuang, Y. P., C. T. Fang, S. Y. Lai, S. C. Chang, and J. T. Wang.** 2006. Genetic determinants of capsular serotype K1 of *Klebsiella pneumoniae* causing primary pyogenic liver abscess. *J Infect Dis* **193:**645-54.

43. **Chung, D. R., S. S. Lee, H. R. Lee, H. B. Kim, H. J. Choi, J. S. Eom, J. S. Kim, Y. H. Choi, J. S. Lee, M. H. Chung, Y. S. Kim, H. Lee, M. S. Lee, and C. K. Park.** 2007. Emerging invasive liver abscess caused by K1 serotype *Klebsiella pneumoniae* in Korea. *J Infect* **54:**578-83.

44. **Colodner, R., W. Rock, B. Chazan, N. Keller, N. Guy, W. Sakran, and R. Raz.** 2004. Risk factors for the development of extended-spectrum beta-lactamase-producing bacteria in nonhospitalized patients. *Eur J Clin Microbiol Infect Dis* **23:**163-7.

45. **Cortes, G., N. Borrell, B. de Astorza, C. Gomez, J. Sauleda, and S. Alberti.** 2002. Molecular analysis of the contribution of the capsular polysaccharide and the lipopolysaccharide O side chain to the virulence of *Klebsiella pneumoniae* in a murine model of pneumonia. *Infect Immun* **70:**2583-90.

46. **Cronan, J. E., Jr., M. L. Narasimhan, and M. Rawlings.** 1988. Insertional restoration of beta-galactosidase alpha-complementation (white-to-blue colony screening) facilitates assembly of synthetic genes. *Gene* **70:**161-70.

47. **Davis, T. J., and J. M. Matsen.** 1974. Prevalence and characteristics of *Klebsiella* species: relation to association with a hospital environment. *J Infect Dis* **130:**402-405.

48. **de Lorenzo, V., and J. L. Martinez.** 1988. Aerobactin production as a virulence factor: a reevaluation. *Eur J Clin Microbiol Infect Dis* **7:**621-9.

49. **Derzelle, S., E. Turlin, E. Duchaud, S. Pages, F. Kunst, A. Givaudan, and A. Danchin.** 2004. The PhoP-PhoQ two-component regulatory system of *Photorhabdus luminescens* is essential for virulence in insects. *J Bacteriol* **186:**1270-9.

50. **Di Martino, P., Y. Bertin, J. P. Girardeau, V. Livrelli, B. Joly, and A. Darfeuille-Michaud.** 1995. Molecular characterization and adhesive properties of CF29K, an adhesin of *Klebsiella pneumoniae* strains involved in nosocomial infections. *Infect Immun* **63:**4336-44.

51. **Di Martino, P., V. Livrelli, D. Sirot, B. Joly, and A. Darfeuille-Michaud.** 1996. A new fimbrial antigen harbored by CAZ-5/SHV-4-producing *Klebsiella pneumoniae* strains involved in nosocomial infections. *Infect Immun* **64:**2266-73.

52. **Di Martino, P., D. Sirot, B. Joly, C. Rich, and A. Darfeuille-Michaud.** 1997. Relationship between adhesion to intestinal Caco-2 cells and multidrug resistance in *Klebsiella pneumoniae* clinical isolates. *J Clin Microbiol* **35:**1499-503.

53. **Domenico, P., R. J. Salo, A. S. Cross, and B. A. Cunha.** 1994. Polysaccharide capsule-mediated resistance to opsonophagocytosis in *Klebsiella pneumoniae*. *Infect Immun* **62:**4495-9.

54. **Domenico, P., S. Schwartz, and B. A. Cunha.** 1989. Reduction of capsular polysaccharide production in *Klebsiella pneumoniae* by sodium salicylate. *Infect Immun* **57:**3778-82.

55. **Drummelsmith, J., and C. Whitfield.** 2000. Translocation of group 1 capsular polysaccharide to the surface of *Escherichia coli* requires a multimeric complex in the outer membrane. *EMBO J* **19:**57-66.

56. **Dubey, G. P., A. Narayan, A. R. Mattoo, G. P. Singh, R. K. Kurupati, M. S. Zaman, A. Aggarwal, R. B. Baweja, S. Basu-Modak, and Y. Singh.** 2009. Comparative genomic study of *spo0E* family genes and elucidation of the role of Spo0E in *Bacillus anthracis*. *Arch Microbiol* **191:**241-53.

57. **Dutta, R., L. Qin, and M. Inouye.** 1999. Histidine kinases: diversity of domain organization. *Mol Microbiol* **34:**633-40.

58. **Edberg, S. C., V. Piscitelli, and M. Cartter.** 1986. Phenotypic characteristics of coliform and noncoliform bacteria from a public water supply compared with regional and national clinical species. *Appl Environ Microbiol* **52:**474-8.

59. **Eguchi, Y., and R. Utsumi.** 2005. A novel mechanism for connecting bacterial two-component signal-transduction systems. *Trends Biochem Sci* **30:**70-2.

60. **Ernst, F. D., S. Bereswill, B. Waidner, J. Stoof, U. Mader, J. G. Kusters, E. J. Kuipers, M. Kist, A. H. van Vliet, and G. Homuth.** 2005. Transcriptional profiling of *Helicobacter pylori* Fur- and iron-regulated gene expression. *Microbiology* **151:**533-46.

61. **Escolar, L., J. Perez-Martin, and V. de Lorenzo.** 1999. Opening the iron box: transcriptional metalloregulation by the Fur protein. *J Bacteriol* **181:**6223-9.

62. **Evrard, B., D. Balestrino, A. Dosgilbert, J. L. Bouya-Gachancard, N. Charbonnel, C. Forestier, and A. Tridon.** 2010. Roles of capsule and lipopolysaccharide O antigen in interactions of human monocyte-derived dendritic cells and *Klebsiella pneumoniae*. *Infect Immun* **78:**210-9.

63. **Falagas, M. E., and I. A. Bliziotis.** 2007. Pandrug-resistant Gram-negative bacteria: the dawn of the post-antibiotic era? *Int J Antimicrob Agents* **29:**630-6.

64. **Falagas, M. E., and P. Kopterides.** 2007. Old antibiotics for infections in critically ill patients. *Curr Opin Crit Care* **13:**592-7.

65. **Fang, C. T., Y. P. Chuang, C. T. Shun, S. C. Chang, and J. T. Wang.** 2004. A novel virulence gene in *Klebsiella pneumoniae* strains causing primary liver abscess and septic metastatic complications. *J Exp Med* **199:**697-705.

66. **Fang, C. T., S. Y. Lai, W. C. Yi, P. R. Hsueh, and K. L. Liu.** The function of wzy_{K1} (*magA*), the serotype K1 polymerase gene in *Klebsiella pneumoniae cps* gene cluster. *J Infect Dis* **201:**1268-9.

67. **Fang, C. T., S. Y. Lai, W. C. Yi, P. R. Hsueh, K. L. Liu, and S. C. Chang.** 2007. *Klebsiella pneumoniae* genotype K1: an emerging pathogen that causes septic ocular or central nervous system complications from pyogenic liver abscess. *Clin Infect Dis* **45:**284-93.

68. **Fang, F. C., N. Sandler, and S. J. Libby.** 2005. Liver abscess caused by $magA^{+}$ *Klebsiella pneumoniae* in North America. *J Clin Microbiol* **43:**991-2.

69. **Flamez, C., I. Ricard, S. Arafah, M. Simonet, and M. Marceau.** 2008. Phenotypic analysis of *Yersinia pseudotuberculosis* 32777 response regulator mutants: new insights into two-component system regulon plasticity in bacteria. *Int J Med Microbiol* **298:**193-207.

70. **Flannagan, R. S., G. Cosio, and S. Grinstein.** 2009. Antimicrobial mechanisms of phagocytes and bacterial evasion strategies. *Nat Rev Microbiol* **7:**355-66.

71. **Flidel-Rimon, O., E. Leibovitz, A. Juster-Reicher, M. Amitay, A. Miskin, Y. Barak, and B. Mogilner.** 1996. An outbreak of antibiotic multiresistant *Klebsiella* at the Neonatal Intensive Care Unit, Kaplan Hospital, Rehovot, Israel, November 1991 to April 1992. *Am J Perinatol* **13:**99-102.

72. **Foster, J. W.** 2004. *Escherichia coli* acid resistance: tales of an amateur acidophile. *Nat Rev Microbiol* **2:**898-907.

73. **Foster, J. W., and H. K. Hall.** 1992. Effect of *Salmonella typhimurium* ferric uptake regulator (*fur*) mutations on iron- and pH-regulated protein synthesis. *J Bacteriol* **174:**4317-23.

74. **Fouts, D. E., H. L. Tyler, R. T. DeBoy, S. Daugherty, Q. Ren, J. H. Badger, A. S. Durkin, H. Huot, S. Shrivastava, S. Kothari, R. J. Dodson, Y. Mohamoud, H. Khouri, L. F. Roesch, K. A. Krogfelt, C. Struve, E. W. Triplett, and B. A. Methe.** 2008. Complete genome sequence of the N_2-fixing broad host range endophyte *Klebsiella pneumoniae* 342 and virulence predictions verified in mice. *PLoS Genet* **4:**e1000141.

75. **French, G. L., K. P. Shannon, and N. Simmons.** 1996. Hospital outbreak of *Klebsiella pneumoniae* resistant to broad-spectrum cephalosporins and beta-lactam-beta-lactamase inhibitor combinations by hyperproduction of SHV-5 beta-lactamase. *J Clin Microbiol* **34:**358-63.

76. **Galperin, M. Y.** Diversity of structure and function of response regulator output domains. *Curr Opin Microbiol* **13:**150-9.

77. **Gao, H., D. Zhou, Y. Li, Z. Guo, Y. Han, Y. Song, J. Zhai, Z. Du, X. Wang, J. Lu, and R. Yang.** 2008. The iron-responsive Fur regulon in *Yersinia pestis. J Bacteriol* **190:**3063-75.

78. **Garcia Vescovi, E., F. C. Soncini, and E. A. Groisman.** 1994. The role of the PhoP/PhoQ regulon in *Salmonella* virulence. *Res Microbiol* **145:**473-80.

79. **Genevaux, P., C. Georgopoulos, and W. L. Kelley.** 2007. The Hsp70 chaperone machines of *Escherichia coli*: a paradigm for the repartition of chaperone functions. *Mol Microbiol* **66:**840-57.

80. **Georgellis, D., O. Kwon, P. De Wulf, and E. C. Lin.** 1998. Signal decay through a reverse phosphorelay in the Arc two-component signal transduction system. *J Biol Chem* **273:**32864-9.

81. **Gniadkowski, M., A. Palucha, P. Grzesiowski, and W. Hryniewicz.** 1998. Outbreak of ceftazidime-resistant *Klebsiella pneumoniae* in a pediatric hospital in Warsaw, Poland: clonal spread of the TEM-47 extended-spectrum beta-lactamase (ESBL)-producing strain and transfer of a plasmid carrying the SHV-5-like ESBL-encoding gene. *Antimicrob Agents Chemother* **42:**3079-85.

82. **Gooderham, W. J., S. L. Gellatly, F. Sanschagrin, J. B. McPhee, M. Bains, C. Cosseau, R. C. Levesque, and R. E. Hancock.** 2009. The sensor kinase PhoQ mediates virulence in *Pseudomonas aeruginosa. Microbiology* **155:**699-711.

83. **Gooderham, W. J., and R. E. Hancock.** 2009. Regulation of virulence and antibiotic resistance by two-component regulatory systems in *Pseudomonas aeruginosa. FEMS Microbiol Rev* **33:**279-94.

84. **Gordeliy, V. I., J. Labahn, R. Moukhametzianov, R. Efremov, J. Granzin, R. Schlesinger, G. Buldt, T. Savopol, A. J. Scheidig, J. P. Klare, and M. Engelhard.** 2002. Molecular basis of transmembrane signalling by sensory rhodopsin II-transducer complex. *Nature* **419:**484-7.

85. **Gotoh, Y., A. Doi, E. Furuta, S. Dubrac, Y. Ishizaki, M. Okada, M. Igarashi, N. Misawa, H. Yoshikawa, T. Okajima, T. Msadek, and R. Utsumi.** Novel antibacterial compounds specifically targeting the essential WalR response regulator. *J Antibiot* (Tokyo) **63:**127-34.

86. **Gotoh, Y., Y. Eguchi, T. Watanabe, S. Okamoto, A. Doi, and R. Utsumi.** Two-component signal transduction as potential drug targets in pathogenic bacteria. *Curr Opin Microbiol* **13:**232-9.

87. **Gottesman, S., and V. Stout.** 1991. Regulation of capsular polysaccharide synthesis in *Escherichia coli* K12. *Mol Microbiol* **5:**1599-606.

88. **Grenha, R., N. J. Rzechorzek, J. A. Brannigan, R. N. de Jong, E. Ab, T. Diercks, V. Truffault, J. C. Ladds, M. J. Fogg, C. Bongiorni, M. Perego, R. Kaptein, K. S. Wilson, G. E. Folkers, and A. J. Wilkinson.** 2006. Structural characterization of Spo0E-like protein-aspartic acid phosphatases that regulate sporulation in bacilli. *J Biol Chem* **281:**37993-8003.

89. **Groisman, E. A.** 1998. The ins and outs of virulence gene expression: Mg^{2+} as a regulatory signal. *Bioessays* **20:**96-101.

90. **Groisman, E. A.** 2001. The pleiotropic two-component regulatory system PhoP-PhoQ. *J Bacteriol* **183:**1835-42.

91. **Gunn, J. S.** 2008. The *Salmonella* PmrAB regulon: lipopolysaccharide modifications, antimicrobial peptide resistance and more. *Trends Microbiol* **16:**284-90.

92. **Gunn, J. S., S. S. Ryan, J. C. Van Velkinburgh, R. K. Ernst, and S. I. Miller.** 2000. Genetic and functional analysis of a PmrA-PmrB-regulated locus necessary for lipopolysaccharide modification, antimicrobial peptide resistance, and oral virulence of *Salmonella enterica* serovar typhimurium. *Infect Immun* **68:**6139-46.

93. **Gusa, A. A., and J. R. Scott.** 2005. The CovR response regulator of group A streptococcus (GAS) acts directly to repress its own promoter. *Mol Microbiol* **56:**1195-207.

94. **Hall, H. K., and J. W. Foster.** 1996. The role of *fur* in the acid tolerance response of *Salmonella typhimurium* is physiologically and genetically separable from its role in iron acquisition. *J Bacteriol* **178:**5683-91.

95. **Hancock, R. E.** 1997. Peptide antibiotics. *Lancet* **349:**418-22.

96. **Handford, J. I., B. Ize, G. Buchanan, G. P. Butland, J. Greenblatt, A. Emili, and T. Palmer.** 2009. Conserved network of proteins essential for bacterial viability. *J Bacteriol* **191:**4732-49.

97. **Hattori, M., and O. Nureki.** 2008. Structural basis for the mechanism of Mg^{2+} homeostasis by MgtE transporter. *Tanpakushitsu Kakusan Koso* **53:**242-8.

98. **Hengge, R.** 2009. Principles of c-di-GMP signalling in bacteria. *Nat Rev Microbiol* **7:**263-73.

99. **Hirakawa, H., K. Nishino, T. Hirata, and A. Yamaguchi.** 2003. Comprehensive studies of drug resistance mediated by overexpression of response regulators of two-component signal transduction systems in *Escherichia coli. J Bacteriol* **185:**1851-6.

100. **Hirakawa, H., K. Nishino, J. Yamada, T. Hirata, and A. Yamaguchi.** 2003. Beta-lactam resistance modulated by the overexpression of response regulators of two-component signal transduction systems in *Escherichia coli. J Antimicrob Chemother* **52:**576-82.

101. **Hitchen, P. G., J. L. Prior, P. C. Oyston, M. Panico, B. W. Wren, R. W. Titball, H. R. Morris, and A. Dell.** 2002. Structural characterization of lipo-oligosaccharide (LOS) from *Yersinia pestis*: regulation of LOS structure by the PhoPQ system. *Mol Microbiol* **44:**1637-50.

102. **Ho, Y. S., L. M. Burden, and J. H. Hurley.** 2000. Structure of the GAF domain, a ubiquitous signaling motif and a new class of cyclic GMP receptor. *EMBO J* **19:**5288-99.

103. **Hoffer, S. M., H. V. Westerhoff, K. J. Hellingwerf, P. W. Postma, and J. Tommassen.** 2001. Autoamplification of a two-component regulatory system results in "learning" behavior. *J Bacteriol* **183:**4914-7.

104. **Hoffmann, T., A. Schutz, M. Brosius, A. Volker, U. Volker, and E. Bremer.** 2002. High-salinity-induced iron limitation in *Bacillus subtilis. J Bacteriol* **184:**718-27.

105. **Hsu, J. L., H. C. Chen, H. L. Peng, and H. Y. Chang.** 2008. Characterization of the histidine-containing phosphotransfer protein B-mediated multistep phosphorelay system in *Pseudomonas aeruginosa* PAO1. *J Biol Chem* **283:**9933-44.

106. **Huang, Y. H., L. Ferrieres, and D. J. Clarke.** 2006. The role of the Rcs phosphorelay in *Enterobacteriaceae*. *Res Microbiol* **157:**206-12.

107. **Huang, Y. J., H. W. Liao, C. C. Wu, and H. L. Peng.** 2009. MrkF is a component of type 3 fimbriae in *Klebsiella pneumoniae. Res Microbiol* **160:**71-9.

108. **Hynninen, A., T. Touze, L. Pitkanen, D. Mengin-Lecreulx, and M. Virta.** 2009. An efflux transporter PbrA and a phosphatase PbrB cooperate in a lead-resistance mechanism in bacteria. *Mol Microbiol* **74:**384-94.

109. **Ibanez-Ruiz, M., V. Robbe-Saule, D. Hermant, S. Labrude, and F. Norel.** 2000. Identification of RpoS (sigma(S))-regulated genes in *Salmonella enterica* serovar typhimurium. *J Bacteriol* **182:**5749-56.

110. **Ishitani, R., Y. Sugita, N. Dohmae, N. Furuya, M. Hattori, and O. Nureki.** 2008. Mg^{2+}-sensing mechanism of Mg^{2+} transporter MgtE probed by molecular dynamics study. *Proc Natl Acad Sci* U S A **105:**15393-8.

111. **Jeon, J., H. Kim, J. Yun, S. Ryu, E. A. Groisman, and D. Shin.** 2008. RstA-promoted expression of the ferrous iron transporter FeoB under iron-replete conditions enhances Fur activity in *Salmonella enterica. J Bacteriol* **190:**7326-34.

112. **Julian, D. J., C. J. Kershaw, N. L. Brown, and J. L. Hobman.** 2009. Transcriptional activation of MerR family promoters in *Cupriavidus metallidurans* CH34. *Antonie Van Leeuwenhoek* **96:**149-59.

113. **Kabha, K., L. Nissimov, A. Athamna, Y. Keisari, H. Parolis, L. A. Parolis, R. M. Grue, J. Schlepper-Schafer, A. R. Ezekowitz, D. E. Ohman, and et al.** 1995. Relationships among capsular structure, phagocytosis, and mouse virulence in *Klebsiella pneumoniae. Infect Immun* **63:**847-52.

114. **Kambampati, R., and C. T. Lauhon.** 2003. MnmA and IscS are required for *in vitro* 2-thiouridine biosynthesis in *Escherichia coli. Biochemistry* **42:**1109-17.

115. **Karama, E. M., F. Willermain, X. Janssens, M. Claus, S. Van den Wijngaert, J. T. Wang, C. Verougstraete, and L. Caspers.** 2008. Endogenous endophthalmitis complicating *Klebsiella pneumoniae* liver abscess in Europe: case report. *Int Ophthalmol* **28:**111-3.

116. **Kasiakou, S. K., A. Michalopoulos, E. S. Soteriades, G. Samonis, G. J. Sermaides, and M. E. Falagas.** 2005. Combination therapy with intravenous colistin for management of infections due to multidrug-resistant Gram-negative bacteria in patients without cystic fibrosis. *Antimicrob Agents Chemother* **49:**3136-46.

117. **Kato, A., and E. A. Groisman.** 2004. Connecting two-component regulatory systems by a protein that protects a response regulator from dephosphorylation by its cognate sensor. *Genes Dev* **18:**2302-13.

118. **Kato, A., T. Latifi, and E. A. Groisman.** 2003. Closing the loop: the PmrA/PmrB two-component system negatively controls expression of its posttranscriptional activator PmrD. *Proc Natl Acad Sci* U S A **100:**4706-11.

119. **Kato, A., A. Y. Mitrophanov, and E. A. Groisman.** 2007. A connector of two-component regulatory systems promotes signal amplification and persistence of expression. *Proc Natl Acad Sci* U S A **104:**12063-8.

120. **Kato, A., H. Tanabe, and R. Utsumi.** 1999. Molecular characterization of the PhoP-PhoQ two-component system in *Escherichia coli* K-12: identification of extracellular Mg^{2+}-responsive promoters. *J Bacteriol* **181:**5516-20.

121. **Keen, N. T., S. Tamaki, D. Kobayashi, and D. Trollinger.** 1988. Improved broad-host-range plasmids for DNA cloning in gram-negative bacteria. *Gene* **70:**191-7.

122. **Kelm, O., C. Kiecker, K. Geider, and F. Bernhard.** 1997. Interaction of the regulator proteins RcsA and RcsB with the promoter of the operon for amylovoran biosynthesis in *Erwinia amylovora. Mol Gen Genet* **256:**72-83.

123. **Key, J., V. Srajer, R. Pahl, and K. Moffat.** 2007. Time-resolved crystallographic studies of the heme domain of the oxygen sensor FixL: structural dynamics of ligand rebinding and their relation to signal transduction. *Biochemistry* **46:**4706-15.

124. **Keynan, Y., and E. Rubinstein.** 2007. The changing face of *Klebsiella pneumoniae* infections in the community. *Int J Antimicrob Agents* **30:**385-9.

125. **Kim, S. H., W. Jia, V. R. Parreira, R. E. Bishop, and C. L. Gyles.** 2006. Phosphoethanolamine substitution in the lipid A of *Escherichia coli* O157 : H7 and its association with PmrC. *Microbiology* **152:**657-66.

126. **Kirby, J. R.** 2009. Chemotaxis-like regulatory systems: unique roles in diverse bacteria. *Annu Rev Microbiol* **63:**45-59.

127. **Kox, L. F., M. M. Wosten, and E. A. Groisman.** 2000. A small protein that mediates the activation of a two-component system by another two-component system. *EMBO J* **19:**1861-72.

128. **Lacour, S., E. Bechet, A. J. Cozzone, I. Mijakovic, and C. Grangeasse.** 2008. Tyrosine phosphorylation of the UDP-glucose dehydrogenase of *Escherichia coli* is at the crossroads of colanic acid synthesis and polymyxin resistance. *PLoS One* **3:**e3053.

129. **Lahiri, S., L. Pulakat, and N. Gavini.** 2005. Functional NifD-K fusion protein in *Azotobacter vinelandii* is a homodimeric complex equivalent to the native heterotetrameric MoFe protein. *Biochem Biophys Res Commun* **337:**677-84.

130. **Lai, Y. C., H. L. Peng, and H. Y. Chang.** 2003. RmpA2, an activator of capsule biosynthesis in *Klebsiella pneumoniae* CG43, regulates K2 *cps* gene expression at the transcriptional level. *J Bacteriol* **185:**788-800.

131. **Langstraat, J., M. Bohse, and S. Clegg.** 2001. Type 3 fimbrial shaft (MrkA) of *Klebsiella pneumoniae*, but not the fimbrial adhesin (MrkD), facilitates biofilm formation. *Infect Immun* **69:**5805-12.

132. **LaRossa, R. A., D. R. Smulski, and T. K. Van Dyk.** 1995. Interaction of lead nitrate and cadmium chloride with *Escherichia coli* K-12 and *Salmonella typhimurium* global regulatory mutants. *J Ind Microbiol* **14:**252-8.

133. **Lederman, E. R., and N. F. Crum.** 2005. Pyogenic liver abscess with a focus on *Klebsiella pneumoniae* as a primary pathogen: an emerging disease with unique clinical characteristics. *Am J Gastroenterol* **100:**322-31.

134. **Lee, C. H., T. H. Hu, and J. W. Liu.** 2005. Splenic abscess caused by *Klebsiella pneumoniae* and non-*Klebsiella pneumoniae* in Taiwan: emphasizing risk factors for acquisition of *Klebsiella pneumoniae* splenic abscess. *Scand J Infect Dis* **37:**905-9.

135. **Lee, C. H., H. S. Leu, T. S. Wu, L. H. Su, and J. W. Liu.** 2005. Risk factors for spontaneous rupture of liver abscess caused by *Klebsiella pneumoniae*. *Diagn Microbiol Infect Dis* **52:**79-84.

136. **Lee, C. H., J. W. Liu, L. H. Su, C. C. Chien, C. C. Li, and K. D. Yang.** Hypermucoviscosity associated with *Klebsiella pneumoniae*-mediated invasive syndrome: a prospective cross-sectional study in Taiwan. *Int J Infect Dis* **14:**e688-92.

137. **Lee, H. C., Y. C. Chuang, W. L. Yu, N. Y. Lee, C. M. Chang, N. Y. Ko, L. R. Wang, and W. C. Ko.** 2006. Clinical implications of hypermucoviscosity phenotype in *Klebsiella pneumoniae* isolates: association with invasive syndrome in patients with community-acquired bacteraemia. *J Intern Med* **259:**606-14.

138. **Lee, J., G. Patel, S. Huprikar, D. P. Calfee, and S. G. Jenkins.** 2009. Decreased susceptibility to polymyxin B during treatment for carbapenem-resistant *Klebsiella pneumoniae* infection. *J Clin Microbiol* **47:**1611-2.

139. **Lee, J. W., and J. D. Helmann.** 2007. Functional specialization within the Fur family of metalloregulators. *Biometals* **20:**485-99.

140. **Lejona, S., A. Aguirre, M. L. Cabeza, E. Garcia Vescovi, and F. C. Soncini.** 2003. Molecular characterization of the Mg^{2+}-responsive PhoP-PhoQ regulon in *Salmonella enterica*. *J Bacteriol* **185:**6287-94.

141. **Li, Y., G. Wei, and J. Chen.** 2004. Glutathione: a review on biotechnological production. *Appl Microbiol Biotechnol* **66:**233-42.

142. **Lin, C. T., T. Y. Huang, W. C. Liang, and H. L. Peng.** 2006. Homologous response regulators KvgA, KvhA and KvhR regulate the synthesis of capsular polysaccharide in *Klebsiella pneumoniae* CG43 in a coordinated manner. *J Biochem* (Tokyo) **140:**429-38.

143. **Lin, J. C., F. Y. Chang, C. P. Fung, J. Z. Xu, H. P. Cheng, J. J. Wang, L. Y. Huang, and L. K. Siu.** 2004. High prevalence of phagocytic-resistant capsular serotypes of *Klebsiella pneumoniae* in liver abscess. *Microbes Infect* **6:**1191-8.

144. **Lin, J. C., L. K. Siu, C. P. Fung, H. H. Tsou, J. J. Wang, C. T. Chen, S. C. Wang, and F. Y. Chang.** 2006. Impaired phagocytosis of capsular serotypes K1 or K2 *Klebsiella pneumoniae* in type 2 diabetes mellitus patients with poor glycemic control. *J Clin Endocrinol Metab* **91:**3084-7.

145. **Lin, T. L., C. Z. Lee, P. F. Hsieh, S. F. Tsai, and J. T. Wang.** 2008. Characterization of integrative and conjugative element ICEKp1-associated genomic heterogeneity in a *Klebsiella pneumoniae* strain isolated from a primary liver abscess. *J Bacteriol* **190:**515-26.

146. **Lin, W. H., M. C. Wang, C. C. Tseng, W. C. Ko, A. B. Wu, P. X. Zheng, and J. J. Wu.** 2010. Clinical and microbiological characteristics of *Klebsiella pneumoniae* isolates causing community-acquired urinary tract infections. *Infection*. (In press)

147. **Lindstrom, S. T., P. R. Healey, and S. C. Chen.** 1997. Metastatic septic endophthalmitis complicating pyogenic liver abscess caused by *Klebsiella pneumoniae. Aust N Z J Med* **27:**77-8.

148. **Ling, T. K., J. Xiong, Y. Yu, C. C. Lee, H. Ye, and P. M. Hawkey.** 2006. Multicenter antimicrobial susceptibility survey of gram-negative bacteria isolated from patients with community-acquired infections in the People's Republic of China. *Antimicrob Agents Chemother* **50:**374-8.

149. **Llama-Palacios, A., E. Lopez-Solanilla, and P. Rodriguez-Palenzuela.** 2005. Role of the PhoP-PhoQ system in the virulence of *Erwinia chrysanthemi* strain 3937: involvement in sensitivity to plant antimicrobial peptides, survival at acid Hh, and regulation of pectolytic enzymes. *J Bacteriol* **187:**2157-62.

150. **Llobet, E., J. M. Tomas, and J. A. Bengoechea.** 2008. Capsule polysaccharide is a bacterial decoy for antimicrobial peptides. *Microbiology* **154:**3877-86.

151. **Long, T., K. C. Tu, Y. Wang, P. Mehta, N. P. Ong, B. L. Bassler, and N. S. Wingreen.** 2009. Quantifying the integration of quorum-sensing signals with single-cell resolution. *PLoS Biol* **7:**e68.

152.**Luzzaro, F., M. Mezzatesta, C. Mugnaioli, M. Perilli, S. Stefani, G. Amicosante, G. M. Rossolini, and A. Toniolo.** 2006. Trends in production of extended-spectrum beta-lactamases among enterobacteria of medical interest: report of the second Italian nationwide survey. *J Clin Microbiol* **44:**1659-64.

153. **Lye, W. C., R. K. Chan, E. J. Lee, and G. Kumarasinghe.** 1992. Urinary tract infections in patients with diabetes mellitus. *J Infect* **24:**169-74.

154. **Ma, L. C., C. T. Fang, C. Z. Lee, C. T. Shun, and J. T. Wang.** 2005. Genomic heterogeneity in *Klebsiella pneumoniae* strains is associated with primary pyogenic liver abscess and metastatic infection. *J Infect Dis* **192:**117-28.

155. **Majdalani, N., and S. Gottesman.** 2005. The Rcs phosphorelay: a complex signal transduction system. *Annu Rev Microbiol* **59:**379-405.

156. **Marceau, M., F. Sebbane, F. Ewann, F. Collyn, B. Lindner, M. A. Campos, J. A. Bengoechea, and M. Simonet.** 2004. The *pmrF* polymyxin-resistance operon of *Yersinia pseudotuberculosis* is upregulated by the PhoP-PhoQ two-component system but not by PmrA-PmrB, and is not required for virulence. *Microbiology* **150:**3947-57.

157. **Matsen, J. M., J. A. Spindler, and R. O. Blosser.** 1974. Characterization of *Klebsiella* isolates from natural receiving waters and comparison with human isolates. *Appl Microbiol* **28:**672-8.

158. **McDonald, M. I.** 1984. Pyogenic liver abscess: diagnosis, bacteriology and treatment. *Eur J Clin Microbiol* **3:**506-9.

159. **Medeiros, A. A.** 1993. Nosocomial outbreaks of multiresistant bacteria: extended-spectrum beta-lactamases have arrived in North America. *Ann Intern Med* **119:**428-30.

160. **Merino, S., S. Camprubi, S. Alberti, V. J. Benedi, and J. M. Tomas.** 1992. Mechanisms of *Klebsiella pneumoniae* resistance to complement-mediated killing. *Infect Immun* **60:**2529-35.

161. **Meyer, K. S., C. Urban, J. A. Eagan, B. J. Berger, and J. J. Rahal.** 1993. Nosocomial outbreak of *Klebsiella infection* resistant to late-generation cephalosporins. *Ann Intern Med* **119:**353-8.

162. **Milagres, A. M., A. Machuca, and D. Napoleao.** 1999. Detection of siderophore production from several fungi and bacteria by a modification of chrome azurol S (CAS) agar plate assay. *J Microbiol Methods* **37:**1-6.

163. **Miller, J. H.** 1972. *Experiments in Molecular Genetics.* Cold Spring Harbor Laboratory Press, Cold Spring Harbor, N.Y.

164. **Minagawa, S., H. Ogasawara, A. Kato, K. Yamamoto, Y. Eguchi, T. Oshima, H. Mori, A. Ishihama, and R. Utsumi.** 2003. Identification and molecular characterization of the Mg^{2+} stimulon of *Escherichia coli. J Bacteriol* **185:**3696-702.

165. **Mitrophanov, A. Y., M. W. Jewett, T. J. Hadley, and E. A. Groisman.** 2008. Evolution and dynamics of regulatory architectures controlling polymyxin B resistance in enteric bacteria. *PLoS Genet* **4:**e1000233.

166. **Miyashiro, T., and M. Goulian.** 2008. High stimulus unmasks positive feedback in an autoregulated bacterial signaling circuit. *Proc Natl Acad Sci* U S A **105:**17457-62.

167. **Mizuta, K., M. Ohta, M. Mori, T. Hasegawa, I. Nakashima, and N. Kato.** 1983. Virulence for mice of *Klebsiella* strains belonging to the O1 group: relationship to their capsular (K) types. *Infect Immun* **40:**56-61.

168. **Monteiro, J., A. F. Santos, M. D. Asensi, G. Peirano, and A. C. Gales.** 2009. First report of KPC-2-producing *Klebsiella pneumoniae* strains in Brazil. *Antimicrob Agents Chemother* **53:**333-4.

169. **Moskowitz, S. M., R. K. Ernst, and S. I. Miller.** 2004. PmrAB, a two-component regulatory system of *Pseudomonas aeruginosa* that modulates resistance to cationic antimicrobial peptides and addition of aminoarabinose to lipid A. *J Bacteriol* **186:**575-9.

170. **Mouslim, C., and E. A. Groisman.** 2003. Control of the *Salmonella ugd* gene by three two-component regulatory systems. *Mol Microbiol* **47:**335-44.

171. **Muller, S. I., M. Valdebenito, and K. Hantke.** 2009. Salmochelin, the long-overlooked catecholate siderophore of *Salmonella*. *Biometals* **22:**691-5.

172. **Munday, C. J., J. Xiong, C. Li, D. Shen, and P. M. Hawkey.** 2004. Dissemination of CTX-M type beta-lactamases in *Enterobacteriaceae* isolates in the People's Republic of China. *Int J Antimicrob Agents* **23:**175-80.

173. **Murayama, N., H. Shimizu, S. Takiguchi, Y. Baba, H. Amino, T. Horiuchi, K. Sekimizu, and T. Miki.** 1996. Evidence for involvement of *Escherichia coli* genes *pmbA*, *csrA* and a previously unrecognized gene *tldD*, in the control of DNA gyrase by *letD* (*ccdB*) of sex factor F. *J Mol Biol* **256:**483-502.

174. **Nam, D., E. Choi, D. H. Kweon, and D. Shin.** 2010. The RstB sensor acts on the PhoQ sensor to control expression of PhoP-regulated genes. *Mol Cells.* (In press)

175. **Nassif, X., J. M. Fournier, J. Arondel, and P. J. Sansonetti.** 1989. Mucoid phenotype of *Klebsiella pneumoniae* is a plasmid-encoded virulence factor. *Infect Immun* **57:**546-52.

176. **Nassif, X., N. Honore, T. Vasselon, S. T. Cole, and P. J. Sansonetti.** 1989. Positive control of colanic acid synthesis in *Escherichia coli* by *rmpA* and *rmpB*, two virulence-plasmid genes of *Klebsiella pneumoniae*. *Mol Microbiol* **3:**1349-59.

177. **Nassif, X., and P. J. Sansonetti.** 1986. Correlation of the virulence of *Klebsiella pneumoniae* K1 and K2 with the presence of a plasmid encoding aerobactin. *Infect Immun* **54:**603-8.

178. **Navon-Venezia, S., A. Leavitt, M. J. Schwaber, J. K. Rasheed, A. Srinivasan, J. B. Patel, and Y. Carmeli.** 2009. First report on a hyperepidemic clone of KPC-3-producing *Klebsiella pneumoniae* in Israel genetically related to a strain causing outbreaks in the United States. *Antimicrob Agents Chemother* **53:**818-20.

179. **Newcombe, J., J. C. Jeynes, E. Mendoza, J. Hinds, G. L. Marsden, R. A. Stabler, M. Marti, and J. J. McFadden.** 2005. Phenotypic and transcriptional characterization of the meningococcal PhoPQ system, a magnesium-sensing two-component regulatory system that controls genes involved in remodeling the meningococcal cell surface. *J Bacteriol* **187:**4967-75.

180. **Nguele, J. C., P. Eswaramoorthy, M. Bhattacharya, E. Ngou-Milama, and M. Fujita.** Genetic and biochemical analyses of sensor kinase A in *Bacillus subtilis* sporulation. *Genet Mol Res* **9:**573-90.

181. **Nordmann, P., and L. Poirel.** 2005. Emergence of plasmid-mediated resistance to quinolones in *Enterobacteriaceae*. *J Antimicrob Chemother* **56:**463-9.

182. **Numata, T., Y. Ikeuchi, S. Fukai, H. Adachi, H. Matsumura, K. Takano, S. Murakami, T. Inoue, Y. Mori, T. Sasaki, T. Suzuki, and O. Nureki.** 2006. Crystallization and preliminary X-ray analysis of the tRNA thiolation enzyme MnmA from *Escherichia coli* complexed with tRNA(Glu). *Acta Crystallogr Sect F Struct Biol Cryst Commun* **62:**368-71.

183. **Ogasawara, H., A. Hasegawa, E. Kanda, T. Miki, K. Yamamoto, and A. Ishihama.** 2007. Genomic SELEX search for target promoters under the control of the PhoQP-RstBA signal relay cascade. *J Bacteriol* **189:**4791-9.

184. **Okumura, N., K. Masamoto, and H. Wada.** 1997. The *gshB* gene in the cyanobacterium *Synechococcus* sp. PCC 7942 encodes a functional glutathione synthetase. *Microbiology* **143 (Pt 9):**2883-90.

185. **Otto, M.** 2009. Bacterial sensing of antimicrobial peptides. *Contrib Microbiol* **16:**136-49.

186. **Pan, Y. J., H. C. Fang, H. C. Yang, T. L. Lin, P. F. Hsieh, F. C. Tsai, Y. Keynan, and J. T. Wang.** 2008. Capsular polysaccharide synthesis regions in *Klebsiella pneumoniae* serotype K57 and a new capsular serotype. *J Clin Microbiol* **46:**2231-40.

187. **Park, S. H., J. Eriksen, and S. D. Henriksen.** 1967. Structure of the capsular polysaccharide of *Klebsiella pneumoniae* type 2 (B). *Acta Pathol. Microbiol. Scand.* **69:**431-6.

188. **Park, S. Y., X. Chao, G. Gonzalez-Bonet, B. D. Beel, A. M. Bilwes, and B. R. Crane.** 2004. Structure and function of an unusual family of protein phosphatases: the bacterial chemotaxis proteins CheC and CheX. *Mol Cell* **16:**563-74.

189. **Paterson, D. L., W. C. Ko, A. Von Gottberg, S. Mohapatra, J. M. Casellas, H. Goossens, L. Mulazimoglu, G. Trenholme, K. P. Klugman, R. A. Bonomo, L. B. Rice, M. M. Wagener, J. G. McCormack, and V. L. Yu.** 2004. Antibiotic therapy for *Klebsiella pneumoniae* bacteremia: implications of production of extended-spectrum beta-lactamases. *Clin Infect Dis* **39:**31-7.

190. **Patzer, S. I., M. R. Baquero, D. Bravo, F. Moreno, and K. Hantke.** 2003. The colicin G, H and X determinants encode microcins M and H47, which might utilize the catecholate siderophore receptors FepA, Cir, Fiu and IroN. *Microbiology* **149:**2557-70.

191. **Pazy, Y., M. A. Motaleb, M. T. Guarnieri, N. W. Charon, R. Zhao, and R. E. Silversmith.** Identical phosphatase mechanisms achieved through distinct modes of binding phosphoprotein substrate. *Proc Natl Acad Sci* U S A **107:**1924-9.

192. **Peng, H. L., P. Y. Wang, J. L. Wu, C. T. Chiu, and H. Y. Chang.** 1991. Molecular epidemiology of *Klebsiella pneumoniae. Zhonghua Min Guo Wei Sheng Wu Ji Mian Yi Xue Za Zhi* **24:**264-71.

193. **Perez, J. C., and E. A. Groisman.** 2007. Acid pH activation of the PmrA/PmrB two-component regulatory system of *Salmonella enterica*. *Mol Microbiol* **63:**283-93.

194. **Permina, E. A., A. E. Kazakov, O. V. Kalinina, and M. S. Gelfand.** 2006. Comparative genomics of regulation of heavy metal resistance in *Eubacteria*. *BMC Microbiol* **6:**49.

195. **Pitout, J. D., P. Nordmann, K. B. Laupland, and L. Poirel.** 2005. Emergence of *Enterobacteriaceae* producing extended-spectrum beta-lactamases (ESBLs) in the community. *J Antimicrob Chemother* **56:**52-9.

196. **Podschun, R., and U. Ullmann.** 1998. *Klebsiella* spp. as nosocomial pathogens: epidemiology, taxonomy, typing methods, and pathogenicity factors. *Clin Microbiol Rev* **11:**589-603.

197. **Poirel, L., M. Gniadkowski, and P. Nordmann.** 2002. Biochemical analysis of the ceftazidime-hydrolysing extended-spectrum beta-lactamase CTX-M-15 and of its structurally related beta-lactamase CTX-M-3. *J Antimicrob Chemother* **50:**1031-4.

198. **Pollack, M., P. Charache, R. E. Nieman, M. P. Jett, J. A. Reimhardt, and P. H. Hardy, Jr.** 1972. Factors influencing colonisation and antibiotic-resistance patterns of gram-negative bacteria in hospital patients. *Lancet* **2:**668-71.

199. **Pope, J. V., D. L. Teich, P. Clardy, and D. C. McGillicuddy.** 2008. *Klebsiella* Pneumoniae Liver Abscess: An Emerging Problem in North America. *J Emerg Med.* (In press)

200. **Pristovsek, P., K. Sengupta, F. Lohr, B. Schafer, M. W. von Trebra, H. Ruterjans, and F. Bernhard.** 2003. Structural analysis of the DNA-binding domain of the *Erwinia amylovora* RcsB protein and its interaction with the RcsAB box. *J Biol Chem* **278:**17752-9.

201. **Radice, M., P. Power, J. Di Conza, and G. Gutkind.** 2002. Early dissemination of CTX-M-derived enzymes in South America. *Antimicrob Agents Chemother* **46:**602-4.

202. **Reed, L. J., and H. Muench.** 1938. A simple method of estimating fifty percent endpoints. *Am J Hyg* **27:**493-7.

203. **Regueiro, V., M. A. Campos, J. Pons, S. Alberti, and J. A. Bengoechea.** 2006. The uptake of a *Klebsiella pneumoniae* capsule polysaccharide mutant triggers an inflammatory response by human airway epithelial cells. *Microbiology* **152:**555-66.

204. **Rodrigue, A., Y. Quentin, A. Lazdunski, V. Mejean, and M. Foglino.** 2000. Two-component systems in *Pseudomonas aeruginosa*: why so many? *Trends Microbiol* **8:**498-504.

205. **Roland, K. L., L. E. Martin, C. R. Esther, and J. K. Spitznagel.** 1993. Spontaneous *pmrA* mutants of *Salmonella typhimurium* LT2 define a new two-component regulatory system with a possible role in virulence. *J Bacteriol* **175:**4154-64.

206. **Romling, U., and R. Simm.** 2009. Prevailing concepts of c-di-GMP signaling. *Contrib Microbiol* **16:**161-81.

207. **Rose, H. D., and J. Schreier.** 1968. The effect of hospitalization and antibiotic therapy on the gram-negative fecal flora. *Am J Med Sci* **255:**228-36.

208. **Schellhorn, H. E., J. P. Audia, L. I. Wei, and L. Chang.** 1998. Identification of conserved, RpoS-dependent stationary-phase genes of *Escherichia coli. J Bacteriol* **180:**6283-91.

209. **Schembri, M. A., J. Blom, K. A. Krogfelt, and P. Klemm.** 2005. Capsule and fimbria interaction in *Klebsiella pneumoniae. Infect Immun* **73:**4626-33.

210. **Schirmer, T., and U. Jenal.** 2009. Structural and mechanistic determinants of c-di-GMP signalling. *Nat Rev Microbiol* **7:**724-35.

211. **Schultz-Hauser, G., B. Van Hove, and V. Braun.** 1992. 8-Azido-ATP labelling of the FecE protein of the *Escherichia coli* iron citrate transport system. *FEMS Microbiol Lett* **74:**231-4.

212. **Seidler, R. J., M. D. Knittel, and C. Brown.** 1975. Potential pathogens in the environment: cultural reactions and nucleic acid studies on *Klebsiella pneumoniae* from clinical and environmental sources. *Appl Microbiol* **29:**819-25.

213. **Selden, R., S. Lee, W. L. Wang, J. V. Bennett, and T. C. Eickhoff.** 1971. Nosocomial *Klebsiella* infections: intestinal colonization as a reservoir. *Ann Intern Med* **74:**657-64.

214. **Seputiene, V., D. Motiejunas, K. Suziedelis, H. Tomenius, S. Normark, O. Melefors, and E. Suziedeliene.** 2003. Molecular characterization of the acid-inducible *asr* gene of *Escherichia coli* and its role in acid stress response. *J Bacteriol* **185:**2475-84.

215. **Sevvana, M., V. Vijayan, M. Zweckstetter, S. Reinelt, D. R. Madden, R. Herbst-Irmer, G. M. Sheldrick, M. Bott, C. Griesinger, and S. Becker.** 2008. A ligand-induced switch in the periplasmic domain of sensor histidine kinase CitA. *J Mol Biol* **377:**512-23.

216. **Simpson, W., T. Olczak, and C. A. Genco.** 2000. Characterization and expression of HmuR, a TonB-dependent hemoglobin receptor of *Porphyromonas gingivalis. J Bacteriol* **182:**5737-48.

217. **Siryaporn, A., and M. Goulian.** 2008. Cross-talk suppression between the CpxA-CpxR and EnvZ-OmpR two-component systems in *E. coli. Mol Microbiol* **70:**494-506.

218. **Skorupski, K., and R. K. Taylor.** 1996. Positive selection vectors for allelic exchange. *Gene* **169:**47-52.

219. **Smits, W. K., C. Bongiorni, J. W. Veening, L. W. Hamoen, O. P. Kuipers, and M. Perego.** 2007. Temporal separation of distinct differentiation pathways by a dual specificity Rap-Phr system in *Bacillus subtilis. Mol Microbiol* **65:**103-20.

220. **Soncini, F. C., E. Garcia Vescovi, F. Solomon, and E. A. Groisman.** 1996. Molecular basis of the magnesium deprivation response in *Salmonella typhimurium*: identification of PhoP-regulated genes. *J Bacteriol* **178:**5092-9.

221. **Sorsa, L. J., S. Dufke, J. Heesemann, and S. Schubert.** 2003. Characterization of an *iroBCDEN* gene cluster on a transmissible plasmid of uropathogenic *Escherichia coli*: evidence for horizontal transfer of a chromosomal virulence factor. *Infect Immun* **71:**3285-93.

222.**Stahlhut, S. G., S. Chattopadhyay, C. Struve, S. J. Weissman, P. Aprikian, S. J. Libby, F. C. Fang, K. A. Krogfelt, and E. V. Sokurenko.** 2009. Population variability of the FimH type 1 fimbrial adhesin in *Klebsiella pneumoniae*. *J Bacteriol* **191:**1941-50.

223. **Stahlhut, S. G., V. Tchesnokova, C. Struve, S. J. Weissman, S. Chattopadhyay, O. Yakovenko, P. Aprikian, E. V. Sokurenko, and K. A. Krogfelt.** 2009. Comparative structure-function analysis of mannose-specific FimH adhesins from *Klebsiella pneumoniae* and *Escherichia coli. J Bacteriol* **191:**6592-601.

224. **Stout, V., A. Torres-Cabassa, M. R. Maurizi, D. Gutnick, and S. Gottesman.** 1991. RcsA, an unstable positive regulator of capsular polysaccharide synthesis. *J Bacteriol* **173:**1738-47.

225. **Struve, C., M. Bojer, and K. A. Krogfelt.** 2008. Characterization of *Klebsiella pneumoniae* type 1 fimbriae by detection of phase variation during colonization and infection and impact on virulence. *Infect Immun* **76:**4055-65.

226. **Struve, C., M. Bojer, and K. A. Krogfelt.** 2009. Identification of a conserved chromosomal region encoding *Klebsiella pneumoniae* type 1 and type 3 fimbriae and assessment of the role of fimbriae in pathogenicity. *Infect Immun* **77:**5016-24.

227. **Studier, F. W., A. H. Rosenberg, J. J. Dunn, and J. W. Dubendorff.** 1990. Use of T7 RNA polymerase to direct expression of cloned genes. *Methods Enzymol* **185:**60-89.

228. **Suziedeliene, E., K. Suziedelis, V. Garbenciute, and S. Normark.** 1999. The acid-inducible asr gene in *Escherichia coli*: transcriptional control by the *phoBR* operon. *J Bacteriol* **181:**2084-93.

229. **Suzuki, K., T. Tanabe, Y. H. Moon, T. Funahashi, H. Nakao, S. Narimatsu, and S. Yamamoto.** 2006. Identification and transcriptional organization of aerobactin transport and biosynthesis cluster genes of *Vibrio hollisae. Res Microbiol* **157:**730-40.

230. **Szurmant, H., T. J. Muff, and G. W. Ordal.** 2004. *Bacillus subtilis* CheC and FliY are members of a novel class of CheY-P-hydrolyzing proteins in the chemotactic signal transduction cascade. *J Biol Chem* **279:**21787-92.

231. **Tabei, Y., K. Okada, and M. Tsuzuki.** 2007. Sll1330 controls the expression of glycolytic genes in *Synechocystis* sp. PCC 6803. *Biochem Biophys Res Commun* **355:**1045-50.

232. **Taghavi, S., C. Lesaulnier, S. Monchy, R. Wattiez, M. Mergeay, and D. van der Lelie.** 2009. Lead(II) resistance in *Cupriavidus metallidurans* CH34: interplay between plasmid and chromosomally-located functions. *Antonie Van Leeuwenhoek* **96:**171-82.

233. **Tagourti, J., A. Landoulsi, and G. Richarme.** 2008. Cloning, expression, purification and characterization of the stress kinase YeaG from *Escherichia coli. Protein Expr Purif* **59:**79-85.

234. **Tamayo, R., J. T. Pratt, and A. Camilli.** 2007. Roles of cyclic diguanylate in the regulation of bacterial pathogenesis. *Annu Rev Microbiol* **61:**131-48.

235. **Tamayo, R., S. S. Ryan, A. J. McCoy, and J. S. Gunn.** 2002. Identification and genetic characterization of PmrA-regulated genes and genes involved in polymyxin B resistance in *Salmonella enterica* serovar typhimurium. *Infect Immun* **70:**6770-8.

236. **Tan, Y. M., S. P. Chee, K. C. Soo, and P. Chow.** 2004. Ocular manifestations and complications of pyogenic liver abscess. *World J Surg* **28:**38-42.

237. **Tang, H. L., M. K. Chiang, W. J. Liou, Y. T. Chen, H. L. Peng, C. S. Chiou, K. S. Liu, M. C. Lu, K. C. Tung, and Y. C. Lai.** Correlation between *Klebsiella pneumoniae* carrying pLVPK-derived loci and abscess formation. *Eur J Clin Microbiol Infect Dis* **29:**689-98.

238. **Thompson, J. M., H. A. Jones, and R. D. Perry.** 1999. Molecular characterization of the hemin uptake locus (*hmu*) from *Yersinia pestis* and analysis of hmu mutants for hemin and hemoprotein utilization. *Infect Immun* **67:**3879-92.

239. **Tsai, F. C., Y. T. Huang, L. Y. Chang, and J. T. Wang.** 2008. Pyogenic liver abscess as endemic disease, Taiwan. *Emerg Infect Dis* **14:**1592-600.

240. **Tsakris, A., I. Kristo, A. Poulou, F. Markou, A. Ikonomidis, and S. Pournaras.** 2008. First occurrence of KPC-2-possessing *Klebsiella pneumoniae* in a Greek hospital and recommendation for detection with boronic acid disc tests. *J Antimicrob Chemother* **62:**1257-60.

241. **Tu, Y. C., M. C. Lu, M. K. Chiang, S. P. Huang, H. L. Peng, H. Y. Chang, M. S. Jan, and Y. C. Lai.** 2009. Genetic requirements for *Klebsiella pneumoniae*-induced liver abscess in an oral infection model. *Infect Immun* **77:**2657-71.

242. **Tullus, K., B. Berglund, B. Fryklund, I. Kuhn, and L. G. Burman.** 1988. Epidemiology of fecal strains of the family *Enterobacteriaceae* in 22 neonatal wards and influence of antibiotic policy. *J Clin Microbiol* **26:**1166-70.

243. **Turton, J. F., H. Englender, S. N. Gabriel, S. E. Turton, M. E. Kaufmann, and T. L. Pitt.** 2007. Genetically similar isolates of *Klebsiella pneumoniae* serotype K1 causing liver abscesses in three continents. *J Med Microbiol* **56:**593-7.

244. **Vasil, M. L.** 2007. How we learnt about iron acquisition in *Pseudomonas aeruginosa*: a series of very fortunate events. *Biometals* **20:**587-601.

245.**Wacharotayankun, R., Y. Arakawa, M. Ohta, T. Hasegawa, M. Mori, T. Horii, and N. Kato.** 1992. Involvement of *rcsB* in *Klebsiella* K2 capsule synthesis in *Escherichia coli* K-12. *J Bacteriol* **174:**1063-7.

246. **Wacharotayankun, R., Y. Arakawa, M. Ohta, K. Tanaka, T. Akashi, M. Mori, and N. Kato.** 1993. Enhancement of extracapsular polysaccharide synthesis in *Klebsiella pneumoniae* by RmpA2, which shows homology to NtrC and FixJ. *Infect Immun* **61:**3164-74.

247. **Wang, F., S. Cheng, K. Sun, and L. Sun.** 2008. Molecular analysis of the *fur* (ferric uptake regulator) gene of a pathogenic *Edwardsiella tarda* strain. *J Microbiol* **46:**350-5.

248. **Wang, J. H., Y. C. Liu, S. S. Lee, M. Y. Yen, Y. S. Chen, S. R. Wann, and H. H. Lin.** 1998. Primary liver abscess due to *Klebsiella pneumoniae* in Taiwan. *Clin Infect Dis* **26:**1434-8.

249. **Weber, H., T. Polen, J. Heuveling, V. F. Wendisch, and R. Hengge.** 2005. Genome-wide analysis of the general stress response network in *Escherichia coli*: sigmaS-dependent genes, promoters, and sigma factor selectivity. *J Bacteriol* **187:**1591-603.

250. **Wehland, M., and F. Bernhard.** 2000. The RcsAB box. Characterization of a new operator essential for the regulation of exopolysaccharide biosynthesis in enteric bacteria. *J Biol Chem* **275:**7013-20.

251. **Wehland, M., C. Kiecker, D. L. Coplin, O. Kelm, W. Saenger, and F. Bernhard.** 1999. Identification of an RcsA/RcsB recognition motif in the promoters of exopolysaccharide biosynthetic operons from *Erwinia amylovora* and *Pantoea stewartii* subspecies stewartii. *J Biol Chem* **274:**3300-7.

252. **Weller, T. M., F. M. MacKenzie, and K. J. Forbes.** 1997. Molecular epidemiology of a large outbreak of multiresistant *Klebsiella pneumoniae. J Med Microbiol* **46:**921-6.

253. **Whitfield, C., and A. Paiment.** 2003. Biosynthesis and assembly of Group 1 capsular polysaccharides in *Escherichia coli* and related extracellular polysaccharides in other bacteria. *Carbohydr Res* **338:**2491-502.

254. **Whitfield, C., and I. S. Roberts.** 1999. Structure, assembly and regulation of expression of capsules in *Escherichia coli. Mol Microbiol* **31:**1307-19.

255. **Williams, C. L., and P. A. Cotter.** 2007. Autoregulation is essential for precise temporal and steady-state regulation by the *Bordetella* BvgAS phosphorelay. *J Bacteriol* **189:**1974-82.

256. **Winfield, M. D., and E. A. Groisman.** 2004. Phenotypic differences between *Salmonella* and *Escherichia coli* resulting from the disparate regulation of homologous genes. *Proc Natl Acad Sci* U S A **101:**17162-7.

257. **Winfield, M. D., T. Latifi, and E. A. Groisman.** 2005. Transcriptional regulation of the 4-amino-4-deoxy-L-arabinose biosynthetic genes in *Yersinia pestis. J Biol Chem* **280:**14765-72.

258. **Wolfe, A. J.** Physiologically relevant small phosphodonors link metabolism to signal transduction. *Curr Opin Microbiol* **13:**204-9.

259. **Woodford, N., J. Zhang, M. Warner, M. E. Kaufmann, J. Matos, A. Macdonald, D. Brudney, D. Sompolinsky, S. Navon-Venezia, and D. M. Livermore.** 2008. Arrival of *Klebsiella pneumoniae* producing KPC carbapenemase in the United Kingdom. *J Antimicrob Chemother* **62:**1261-4.

260. **Wosten, M. M., and E. A. Groisman.** 1999. Molecular characterization of the PmrA regulon. *J Biol Chem* **274:**27185-90.

261. **Wosten, M. M., L. F. Kox, S. Chamnongpol, F. C. Soncini, and E. A. Groisman.** 2000. A signal transduction system that responds to extracellular iron. *Cell* **103:**113-25.

262. **Wu, K. M., L. H. Li, J. J. Yan, N. Tsao, T. L. Liao, H. C. Tsai, C. P. Fung, H. J. Chen, Y. M. Liu, J. T. Wang, C. T. Fang, S. C. Chang, H. Y. Shu, T. T. Liu, Y. T. Chen, Y. R. Shiau, T. L. Lauderdale, I. J. Su, R. Kirby, and S. F. Tsai.** 2009. Genome sequencing and comparative analysis of *Klebsiella pneumoniae* NTUH-K2044, a strain causing liver abscess and meningitis. *J Bacteriol* **191:**4492-501.

263. **Wu, M. F., C. Y. Yang, T. L. Lin, J. T. Wang, F. L. Yang, S. H. Wu, B. S. Hu, T. Y. Chou, M. D. Tsai, C. H. Lin, and S. L. Hsieh.** 2009. Humoral immunity against capsule polysaccharide protects the host from *magA*$^{+}$ *Klebsiella pneumoniae*-induced lethal disease by evading Toll-like receptor 4 signaling. *Infect Immun* **77:**615-21.

264. **Yamamoto, K., K. Hirao, T. Oshima, H. Aiba, R. Utsumi, and A. Ishihama.** 2005. Functional characterization in vitro of all two-component signal transduction systems from *Escherichia coli. J Biol Chem* **280:**1448-56.

265. **Yan, A., Z. Guan, and C. R. Raetz.** 2007. An undecaprenyl phosphate-aminoarabinose flippase required for polymyxin resistance in *Escherichia coli. J Biol Chem* **282:**36077-89.

266. **Yang, X., J. Kuk, and K. Moffat.** 2009. Conformational differences between the Pfr and Pr states in *Pseudomonas aeruginosa* bacteriophytochrome. *Proc Natl Acad Sci* U S A **106:**15639-44.

267. **Yang, Y. S., L. K. Siu, K. M. Yeh, C. P. Fung, S. J. Huang, H. C. Hung, J. C. Lin, and F. Y. Chang.** 2009. Recurrent *Klebsiella pneumoniae* liver abscess: clinical and microbiological characteristics. *J Clin Microbiol* **47:**3336-9.

268. **Yeh, K. M., A. Kurup, L. K. Siu, Y. L. Koh, C. P. Fung, J. C. Lin, T. L. Chen, F. Y. Chang, and T. H. Koh.** 2007. Capsular serotype K1 or K2, rather than *magA* and *rmpA*, is a major virulence determinant for *Klebsiella pneumoniae* liver abscess in Singapore and Taiwan. *J Clin Microbiol* **45:**466-71.

269. **Yeh, K. M., J. C. Lin, F. Y. Yin, C. P. Fung, H. C. Hung, L. K. Siu, and F. Y. Chang.** Revisiting the importance of virulence determinant *magA* and its surrounding genes in *Klebsiella pneumoniae* causing pyogenic liver abscesses: exact role in serotype K1 capsule formation. *J Infect Dis* **201:**1259-67.

270. **Yinnon, A. M., A. Butnaru, D. Raveh, Z. Jerassy, and B. Rudensky.** 1996. *Klebsiella* bacteraemia: community versus nosocomial infection. *QJM* **89:**933-41.

271. **Yu, V. L., D. S. Hansen, W. C. Ko, A. Sagnimeni, K. P. Klugman, A. von Gottberg, H. Goossens, M. M. Wagener, and V. J. Benedi.** 2007. Virulence characteristics of Klebsiella and clinical manifestations of *K. pneumoniae* bloodstream infections. *Emerg Infect Dis* **13:**986-93.

272. **Yu, W. L., W. C. Ko, K. C. Cheng, C. C. Lee, C. C. Lai, and Y. C. Chuang.** 2008. Comparison of prevalence of virulence factors for *Klebsiella pneumoniae* liver abscesses between isolates with capsular K1/K2 and non-K1/K2 serotypes. *Diagn Microbiol Infect Dis* **62:**1-6.

273. **Yu, W. L., W. C. Ko, K. C. Cheng, H. C. Lee, D. S. Ke, C. C. Lee, C. P. Fung, and Y. C. Chuang.** 2006. Association between *rmpA* and *magA* genes and clinical syndromes caused by *Klebsiella pneumoniae* in Taiwan. *Clin Infect Dis* **42:**1351-8.

274. **Zavascki, A. P., L. Z. Goldani, J. Li, and R. L. Nation.** 2007. Polymyxin B for the treatment of multidrug-resistant pathogens: a critical review. *J Antimicrob Chemother* **60:**1206-15.

275. **Zhao, R., E. J. Collins, R. B. Bourret, and R. E. Silversmith.** 2002. Structure and catalytic mechanism of the *E. coli* chemotaxis phosphatase CheZ. *Nat Struct Biol* **9:**570-5.

Publication

1. **Cheng, H. Y., Y. F. Chen, and H. L. Peng.** 2010. Molecular characterization of the PhoPQ-PmrD-PmrAB mediated pathway regulating polymyxin B resistance in *Klebsiella pneumoniae* CG43. *J Biomed Sci* **17:**60-75.
2. **Luo, S. C., Y. C. Lou, H. Y. Cheng, Y. R. Pan, H. L. Peng, and C. Chen.** 2010. Solution structure and phospho-PmrA recognition mode of PmrD from *Klebsiella pneumoniae*. *J Struct Biol.* (In press)
3. **Cheng, H. Y., Y. S. Chen, C. Y. Wu, H. Y. Chang, Y. C. Lai, and H. L. Peng.** 2010. RmpA regulation of capsular polysaccharide biosynthesis in *Klebsiella pneumoniae* CG43. *J Bacteriol* **192:**3144-58.

Vita

Hsin-Yao Cheng attended Taipei Municipal Jianguo High School, Taipei, Taiwan. In 1999, he entered National Chiao-Tung University, Hsinchu, Taiwan and received his degree of Bachelor of Science from Department of Biological Science and Technology in 2003. Then he started his graduate studies at Institute of Biochemical Engineering in the same school as a Master student, under the supervision of Professor Hwei-Ling Peng in the Laboratory of Molecular Regulation. In 2004, he decided to enter the Ph. D. program at Department of Biological Science and Technology and continued his study in the same laboratory. During the years, he focused on the regulatory mechanisms of two-component signal transduction systems in the polymyxin B resistance and capsular polysaccharide biosynthesis in *K. pneumoniae*. He is working towards the degree of Doctor of Philosophy and will receive it this summer. He is interested in the molecular regulation of virulence determinants in pathogenic bacteria, and he is also interested in the field of molecular biology and microbiology. He is curious to explore the molecular basis of the phenotypic traits in microbes by means of various tools from molecular biology.